2021

Power network and smart grids analysis from a graph theoretic perspective

Hossein Parast Vand
Edith Cowan University

Edith Cowan University

Copyright Warning

Power Network and Smart Grids Analysis from a Graph Theoretic Perspective

This thesis is submitted in partial fulfillment for the award of degree of

Doctor of Phylosophy

in

Electrical Engineering

Hossein PARAST VAND

Under the supervision of

Principle supervisor: Dr. Octavian BASS
Coo-supervisor: Dr. Stefan W. LACHOWICZ
Adjunct supervisor: Dr. Airlie CHAPMAN

School of Engineering
Edith Cowan University

2021

Copyright and Access Declaration

I certify that this thesis does not, to the best of my knowledge and belief: (i) incorporate without acknowledgment any material previously submitted for a degree or diploma in any institution of higher education; (ii) contain any material previously published or written by another person except where due reference is made in the text; or (iii) contain any defamatory material
Signed...Hossein PARAST VAND.....
Dated....20/04/2021.....

Acknowledgement

I would like to express my special thanks to my principle supervisor, Dr. Octavian Bass, not only for his continuous support and suggestions but also for his trust in what I am doing in my venturous research journey. This study is inspired by the great works of Dr. Airlie Chapman who kindly accepted to be my adjunct supervisor. I am grateful for her comments specially during the early stages of this research. I also express my deep and sincere gratitude to Dr. Stefan W. Lachowicz for his suggestions and support in many occasions.

This study is also benefited from the insightful guidance of Prof. Mohammad A.S. Masoum. His role on the developing of the theoretical results of the study to the network of electric vehicles can not be ignored. I would like to also thank Dr. Valeh Moghaddam for her collaboration on two of the published results.

My achievements are beholden on my great family and friends. My wife joined me in the middle of my study and I can not thank her enough for being always there for me. Finally, I dedicate this accomplishment to the soul of my parents who did more than they could to see me at this stage.

Abstract

The growing size and complexity of power systems has given raise to the use of complex network theory in their modelling, analysis, and synthesis. Though most of the previous studies in this area have focused on distributed control through well established protocols like synchronization and consensus, recently, a few fundamental concepts from graph theory have also been applied, for example in symmetry-based cluster synchronization. Among the existing notions of graph theory, graph symmetry is the focus of this proposal. However, there are other development around some concepts from complex network theory such as graph clustering in the study.

In spite of the widespread applications of symmetry concepts in many real world complex networks, one can rarely find an article exploiting the symmetry in power systems. In addition, no study has been conducted in analysing controllability and robustness for a power network employing graph symmetry. It has been verified that graph symmetry promotes robustness but impedes controllability. A largely absent work, even in other fields outside power systems, is the simultaneous investigation of the symmetry effect on controllability and robustness.

The thesis can be divided into two section. The first section, including Chapters 2-3, establishes the major theoretical development around the applications of graph symmetry in power networks. A few important topics in power systems and smart grids such as controllability and robustness are addressed using the symmetry concept. These topics are directed toward solving specific problems in complex power networks. The controllability analysis will lead to new algorithms elaborating current controllability benchmarks such as the maximum matching and the minimum dominant set. The resulting algorithms will optimize the number of required driver nodes indicated as FACTS devices in power networks. The second topic, robustness, will be tackled by the symmetry analysis of the network to investigate three aspects of network robustness: robustness of controllability, disturbance decoupling, and fault tolerance against failure in a network element.

In the second section, including Chapters 4-8, in addition to theoretical development, a few novel applications are proposed for the theoretical development proposed in both sections one and two. In Chapter 4, an application for the proposed approaches is introduced and developed. The placement of flexible AC transmission systems (FACTS) is investigated where the cybersecurity of the associated data exchange under the wide area power networks is also considered. A new notion of security, i.e. moderated-k-symmetry, is introduced to leverage on the symmetry characteristics of the network to obscure the network data from the adversary perspective. In

chapters 5-8, the use of graph theory, and in particular, graph symmetry and centrality, are adapted for the complex network of charging stations. In Chapter 5, the placement and sizing of charging stations (CSs) of the network of electric vehicles are addressed by proposing a novel complex network model of the charging stations. The problems of placement and sizing are then reformulated in a control framework and the impact of symmetry on the number and locations of charging stations is also investigated. These results are developed in Chapters 6-7 to "robust" placement and sizing of charging stations for the Tesla network of Sydney where the problem of extending the capacity having a set of pre-existing CSs are addressed. The role of centrality in placement of CSs is investigated in Chapter 8. Finally, concluding remarks and future works are presented in Chapter 9.

The results of this study are published in five Q1 journals. Chapters 2-6 are published papers in Journal of The Franklin Institute, Control Engineering Practice, IEEE Access, IEEE Transaction in Smart Grids, and IEEE Access, respectively. Chapter 7 is currently under review in IEEE Transaction in Smart Grids. Chapter 8 is a paper presented in Intermountain Engineering, Technology and Computing Conference (I-ETC) , Utah Valey University, UT, 2020. The list of publications is as follows.

- H. Parastvand, A. Chapman, O. Bass, and S. Lachowicz, "Complex Network Controllability from a Topological Perspective," Journal of The Franklin Institute, Vol. 358, no. 7, 2020 (Chapter 2).

- H. Parastvand, A. Chapman, O. Bass, and S. Lachowicz, "Graph Automorphic Approaches to the Robustness of Complex Networks," Control Engineering Practice, vol. 108, Mar 2021 (Chapter 3).

- H. Parastvand, O. Bass, M.A.S. Masoum, A. Chapman, and S. Lachowicz, "Cyber-Security Constrained Placement of FACTS Devices in Power Networks from a Novel Topological Perspective," IEEE Access, vol. 8, pp. 108201 - 108215, Jun 2020 (Chapter 4).

- H. Parastvand, Z. Moghaddam, O. Bass, M.A.S. Masoum, A. Chapman, and S. Lachowicz, "A Graph Automorphic Approach for Placement and Sizing of Charging Stations in EV Network Considering Traffic," IEEE Transaction on Smart Grids, (Early Access) DOI: 10.1109/TSG.2020.2984037, 2020 (Chapter 5).

- H. Parastvand, O. Bass, M.A.S. Masoum, A. Chapman, and S. Lachowicz, "Robust Placement and Sizing of Charging Stations from a Novel Graph Theoretic Perspective," IEEE Access, vol. 8, pp. 118593 - 118602, 2020, DOI: 10.1109/ACCESS.2020.3005677 (Chapter 6).

- H. Parastvand, O. Bass, M.A.S. Masoum, A. Chapman, and S. Lachowicz, "Robust Graph-Theoretic Placement and Sizing of Charging Stations to Extend Capacity of Existing EV Networks Considering Controllability and Dynamic Traffic Flow," IEEE Transaction on Smart Grid, 2020 (Chapter 7).

- H. Parastvand, O. Bass, M.A.S. Masoum, Z. Moghaddam, S. Lachowicz, and A. Chapman, “Placement and Sizing of EV Charging Stations According to Centrality of the Underlying Network,” Intermountain Engineering, Technology and Computing Conference (i-ETC) Conference,” Orem, UT, US, 2020 (Chapter 8).

Contents

List of Figures

List of Tables

Chapter 1

Introduction

1.1 Overview

In this chapter, first, the motivation for this study is explained. It is stressed what is absent in other techniques that could be potentially applied to the network by analysing its complex network characteristics such as symmetry. It will be clarified that for each target of this study, what features or performance measures of interest might be presented using the symmetry perspective which could not be guaranteed by other existing methods. Then, a review of the applications of graph theory and its concepts is presented. Finally, the research objectives will be presented.

Since this study is prepared as a thesis by publication, the majority of literature review on each topic is presented in the related chapter. Thus, I have avoided repeating the literature review in this chapter. However, a brief review is provided in this chapter and readers are referred to the targeted chapter for in-dept review of the existing works.

1.2 Motivation

The growth of population and the expansion of cities and industries have increased the power demand. Meanwhile, the structure of power networks has become more complex. Moreover, the integration of renewable energy resources with power systems has made it even more complicated to use the traditional management and control strategies. On the other hand, complex network theory has emerged as a powerful tool in the design/analysis of large networks. Symmetry is an inherent feature of large networks which has been the focus of study for many years in graph theory. During the last decade, some interesting applications of the graph symmetry have been revealed in engineering and , in particular, power systems. However, many areas such as the impacts of symmetry analysis/modification on the network resilience, restoration, and the energy cost of control are still enigmatic. This study will try to narrow down the unknown about the symmetry impact on the behavior of complex power networks.

Control is the main issue in a dynamic system such as a complex power network. However, little is known about how to analytically control a complex network. The rank of Kalman filter is computationally prohibitive in a network consisting of several nodes, which limits its application to the small networks ([1], [2], and [3]). The lack of a general controllability criterion has driven the use of some tools from graph theory, mainly maximum matching principle (MMP) and the minimum dominating set (MDS), to analyze the controllability of complex networks. However, these tools have some drawbacks. Though, it is theoretically feasible to fully control a network using MMP or MDS, without a balance between energy cost and the number of driver nodes, realizing the physical control is not cost effective. This issue has not been addressed neither by the maximum matching nor by the minimum dominant set. It will be shown that the symmetry analysis could provide a quantitative tool to stress the degree of controllability. The flexible structure of microgrids makes it possible to manipulate the network symmetry so that the modified network has different degree of controllability, leading to lower number of required driver nodes, which in turn, will result in low energy cost of control. In addition, outside microgrid area, this analysis could be useful in the planning phase of power systems.

The robustness of complex power network could also be investigated using the symmetry analysis. It will be shown that robustness against line failure and disturbance could be improved using graph symmetry. Also, current restoration techniques such as those implemented in [4], [5], [45], and [44], and [6] do not investigate the changes in the symmetry strength of the network in the post fault topology. Possibility of considering the symmetry strength as a constraint in the optimization problem is another unique feature which could provide a framework for retaining the controllability and robustness of the post fault topology. The approach could be implemented to microgrid where a flexible power topology is available. It could also be used in the planning phase or whenever there is the need to expand the power system. As explained in the Chapter 1.5, it is expected that the resulted optimization formulation will lead to better controllability and robustness.

1.3 Background

The concepts of complex networks (CN) and multi agent systems (MAS) have been employed in many scientific areas including biology, physics, economy, mathematics, and engineering. Like all implemented theories in engineering, the CN and MAS theories are rooted in mathematics, and in particular, graph theory. Through this chapter, a review of CN applications in a broader context is presented and then, in Section 1.5, the focus will be on literature review of CN applications in power systems and microgrids.

The widespread application of graph theory has stimulated the advance in many new graph-theoretical concepts and has resulted in lots of challenges. It is predictable that the increasing trend in interplay between graph theory and other fields will ground significant developments in future. Recently, there have been efforts in developing new tools from graph theory for network study. Among those tools, graph partitioning and graph symmetry have been the focus of many studies during the last decade. Symmetry in power systems is an inherent characteristic of the network and usually can not be easily captured without some mathematical analysis. It is not either intentionally developed in the network. Graph automorphism is the main tool to capture the symmetry in complex networks.

The graph theory has provided a solid ground for developing new tools for analysis and synthesis of complex networks. Many of those tools have already been implemented in other branches of science while leaving a huge potential to be implemented in power systems as well. Some applications of graph theory in other scientific areas are (i), graph coloring in channel assignment ([7]), traffic phasing ([8]), fleet maintenance ([9]), task assignment ([10]), and mobile radio frequency assignment ([15]), (ii), the intersection graph in following problem ([11]), a molecular genetic problem known as Benzer's problem ([12]), locating the certain sites on a specific DNA ([13]), the study of preference and indifference in economics and psychology ([14]), seriation or sequence dating in archaeology ([16]), and seriation in developmental psychology ([17]), (iii) competition graph in ecology ([18]), communication over a noisy channel ([22]), channel assignment ([19]), modeling of complex systems ([20]), and phylogenetic tree reconstruction ([21]). A review on the graph applications is shown in Table 1.1. [1]. Figure 1.1 shows the chronological development of graph theory from early control engineering applications to the areas that will be covered by this study.

[1] Some of the information in Table 1.1 is taken from [**?**]

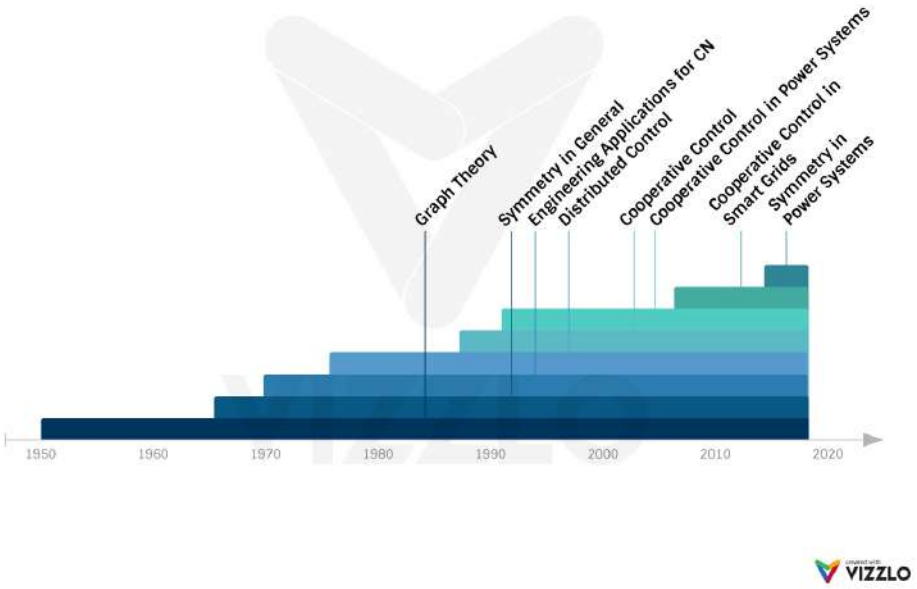

Figure 1.1: The chronological development of graph theory into control applications

Table 1.1: Applications of graph theory in science and engineering

Application field	**Property and concepts of graph theory**	**Applications area**	**Uses**
Database designing	Index-free adjacency	Graph database	Analyzing interconnection, Direct mapping and Natural scaling to large data sets.
Archaeology	Intersection graph	seriation or sequence dating	Seriation from abundance matrices, in f.r. hodson, et al. (eds.),mathematics in the archaeological and historical sciences ([16])
Ecology	Competition graph		Food webs and niche spaces ([18])
developmental psychology	Intersection graph	seriation	Detection of structures in attitudes and developmental processes ([17])
Communication	Graph coloring	Mobile radio frequency assignment	Traffic light phasing problem ([10])

Application field	**Property and concepts of graph theory**	**Applications area**	**Uses**
Communication	Competition graph	communication over a noisy channel	Associative graph products and their independence, domination, and coloring numbers ([22])
Software engineering	Connectivity and Data flow, Directed graph, and cyclomatic complexity	DFD, Control flow graph, ER-diagram, process sequencing and software quality	Transformations, Capturing requirements, Describing relations among modules, Designing system and in testing process
Communication	Competition graph	Channel assignment	Characterization of graphs with interval squares ([19])
Applied mathematics - Linear Algebra	Intersection graph	Following problem	([11])
Computer hardware	Graph coloring and Matrix representation	Coloring algorithms Fine-grain parallelism analysis , Data dependence matrix	Compilers uses graph coloring algorithms for Register allocation to variables , Calculate parallelism degree, Very useful in analytical modeling, Addressing the sequence of instruction execution , Resource allocation and Economizing the memory space(file organization).
Mathematics	Competition graph	Modeling of complex systems	Inverting signed graphs ([20])
Applied mathematics	Intersection graph	molecular genetic problem known as Benzer's problem	The fine structure of the gene([12])
Applied mathematics	Graph coloring	Channel assignment	Polynomial arrangements ([7])

Application field	**Property and concepts of graph theory**	**Applications area**	**Uses**
Network design	Connectivity, Traversing, Adjacency, Vertex cover algorithms and Different graph representation	Topological control and Weighted graph, Butterfly network and $2-D$ array	Finding shortest path, Searching and Arrangement of nodes in network designing, Modeling communication networks [7], Traffic analysis and in Network security.
Computer science	Intersection graph	locating the certain sites on a specific DNA	computational biology([13])
Applied mathematics	Graph coloring	Traffic phasing	Optimal i-intersection ([8])
Data Structure	Directed graphs , Matrices and Matrices operation	Array, Tree, Linked list, Pointers , Stacks, and Queues	Efficient organization of data, Finding minimum cost tree, Minimizing data retrieval times , Minimizing page swapping in data structure paging system and Provides link structure in websites
economics and psychology	Intersection graph	The study of preference and indifference	Measurement theory, with applications to decision-making, utility,and the social sciences ([14])
Applied mathematics	Graph coloring	fleet maintenance	Perfect graphs ([9])
Image processing	Edge connectivity, Regions, Spanning tree	Edge boundaries, Entropy, Shortest path algorithms and Search algorithms	Segmentation and registration, Distance transform and Center line extraction
Data mining	Sub graphs, isomorphism	graph mining	Sub-structure matching, Reducing search space.

Application field	**Property and concepts of graph theory**	**Applications area**	**Uses**
Operation system	Graph coloring, Directed graph	Job scheduling problems and Simultaneous execution of job	Provide feasible solution to job scheduling and Efficient resource(processor) allocation in solving simultaneous job execution problems and In process representation
Mathematics	Competition graph	phylogenetic tree reconstruction	Phylogeny numbers for graphs with two triangles ([21])
Web site designing	Directed graph, Undirected graph, In degree and out degree, Search algorithms and Bipartite graph	Web graph, Web pages and Hyperlinks	Community discovery , Searching and Website evaluation
Communication	Graph coloring	Mobile radio frequency assignment	Traffic light phasing problem ([10])
Applied mathematics	Graph coloring	Task assignment	Applied combinatorics ([10])

Figure 1.2 shows the number of published papers in IEEE Explore and Sciencedirect in the area of CN-based smart grids during the last decade, indicating a trend in applying CN theories in smart grids. This trend is mostly concerned with either modelling the grid using Laplacian matrix or controlling the grid using the established protocols like synchronization, consensus, and pinning control (for example see [24], [25], and [26]). However, there have been efforts in developing an important concept from graph theory in engineering, graph symmetry. This study will focus in developing this concept in the design and analysis of power systems. There are some mathematical tools, mainly graph automorphism and equitable partitions, to describe the network symmetry.

1.4 Aims

Through this study, a few important problems in power networks and renewable energy systems such as controllability and robustness will be addressed using the graph symmetry. In fact, a

Figure 1.2: Number of publications concerning MAS in smart grids([23]).

quantified description of graph symmetry, graph automorphism, will be employed to compute the symmetry level in the power grid. The established rules in graph theories about controllability and robustness of complex networks will be investigated in power systems. A common network protocol in power grid, pinning control, is considered as the underlying network protocol upon which the controllability will be investigated. It is well accepted that symmetry renders uncontrollability in complex networks while a symmetric system is in general more robust than an asymmetric system. This conflict raises an important question that how one can integrate both controllability and robustness in a complex symmetric (or asymmetric) network simultaneously.

The potential outcome of this research can be used in the planning of complex power networks and microgrids. The expectation is that the results could demonstrate their effectiveness when there are needs for expansion in power transmission, planning of generation, investment decision making, integrated resource planning, and stimulation of energy systems and testing the energy policies.

The objectives of the thesis are as follows:

- Clarifying the impacts of graph symmetry in the controllability of complex power networks;
- Establishing a theoretical framework for the relation between the number of required driver nodes for controllability and the network's symmetry level;
- Revealing the role of graph symmetry in improving the network robustness against disturbance;
- Using graph symmetry in improving the network cyber security via the concept of "security by obscurity";
- Implementing the findings of the thesis on graph of EV charging stations and reducing the waiting times;

- Placement and sizing of EV charging stations using the symmetry implications for the network

1.5 Literature Review

The focus of this study is on employing the symmetry concept to address a few important problems in power systems such as controllabity and robustness. Though various control protocols could be used, this study will focus on a particular network protocol, namely pinning control, as the controllability of the network must be investigated under a specific network protocol. The formulation of pinning control is presented in Section 1.5.1. Also, the robustness of the network will be investigated under the line failure and disturbance. The effects of symmetry on controllability and robustness have been investigated outside power systems. To justify the feasibility of extending the existing results to power grids, Sections 1.5.2 and 1.5.3 provide the literature review on specific applications of graph symmetry in controllability and robustness of complex networks in general. Section 1.5.4 provides a few sample studies on real power networks exploiting the symmetry. Finally, the research questions are presented in Section **??** based on the open areas discussed in Section 1.6.

1.5.1 Pinning control formulation

The control structure of distributed generation systems can be represented by the below dynamical equations.

$$\begin{aligned} \dot{x}_i &= f_i(x_i) + k_i(x_i)D_i + g_i(x_i)u_i \\ y_i &= h_i(x_i) \end{aligned} \tag{1.1}$$

where u_i is the control input, x_i is the state vector of i^{th} unit, D_i, f_i, k_i, h_i, and g_i can be extracted from the internal dynamics of the distributed units ([27]). For the purpose of voltage control, after feedback linearization, the dynamic model of each node can be written as

$$\dot{v}_i = Av_i + Bu_i + d_i \tag{1.2}$$

where d_i is the disturbance on y_i caused by other nodes. Then the error is

$$e_i = Ae_i + Bu_i + d_i \tag{1.3}$$

where $e_i = v_i - v_{ref}$. To find a control signal such that the error converges to zero in the presence of disturbance d_i, the pinning control approach will be used in this study. The general dynamic equation of pinning control can be written as

$$\dot{x}_i = F(x_i) - \sigma \sum_{j=1}^{N} l_{ij} H x_j \tag{1.4}$$

where x_i is the state vector, F is the individual systems' dynamical equation which is considered identical for all nodes, σ is the coupling strength, l_{ij} is the $(i,j)^{th}$ element of the Laplacian matrix. The IEEE 30 bus system with pinned nodes is shown in Figure 1.3. The objective is to synchronize all nodes to the desired state which can be defined as

$$\dot{s} = F(s(t)). \tag{1.5}$$

Then the control signal should be designed for the following equation:

$$\dot{x}_i = F(x_i) - \sigma \sum_{j=1}^{N} l_{ij} H x_j + \sigma b_{ii} u_i, \quad i = 1, 2, ..., N \tag{1.6}$$

where non-zero elements of H determine the coupled states of nodes in the network. b_{ii} is equal to one for the pinned nodes and is zero for other nodes. The objective of pinning control is to design control signals for driver nodes so that all states converge to the desired trajectory specified by $s(t)$ in a finite time.

Figure 1.3: IEEE 30-Bus system (A) the model; (B) graph-based representation with pinned nodes([28]).

1.5.2 Controllability: the impact of graph symmetry

Different tools from graph theory have been implemented to reveal the symmetry in a complex network. Among them, graph automorphism and equitable partitions are the most frequently used notions. The graph symmetry has been analyzed when the underlying dynamics are represented by the adjacency matrix, Laplacian matrix, and nonlinear systems.

Recently, the controllability of complex network has been a hot topic in literature (for example see [29], [30], and [31]). Kalman's rank provide the necessary and sufficient condition for controllability. However, it is not possible to check that rank for every complex network containing unknown parameters and exposed to variable topology. To target this drawback, the

classic controllability criterion has been replaced by structural controllability (STC) criteria, where system parameters, elements in A matrix representing the inter-agent interactions are not precisely known, only the zero-nonzero pattern of A is known. Though network topology and intrinsic dynamics of individual nodes can influence controllability, most chapters have only considered the effect of network topology through analyzing the number and position of control nodes.

Mathematically speaking, a system is controllable if the rank of corresponding controllability matrix is full. In general, symmetric graphs are not controllable from one or more input nodes. In fact, they have two or more linearly dependent eigenvectors. However, symmetry is not a necessary condition for uncontrollability. Breaking the symmetry by appropriate selection of control input nodes, i.e. by modifying the B matrix in state space structure, is the major approach to make a symmetric system controllable (see [32]).

In [33], based on symmetries in the structure of the grid eigenvectors and multiplicity of each eigenvalue, suitable graph decomposition, and some rules from number theory, the problem of observability and reachability (controllability) has been studied. The set of all and only the unobservable nodes is identified. Also, a simple approach is proposed to determine the set of observation nodes that guarantee observability. Using the existence of duality, all the results on observability hold for controllability.

In [34], the link between symmetry and controllability of complex network is projected on the relation between symmetry and multiplicity of the graph eigenvalues. Hence, controllability analysis is defined as analyzing the eigenvalue multiplicity using Popov-Belevitch-Hautus (PBH) test and Cauchy-Binet formula to reduce the controllability to examine non-singularity of sub-matrices of its Laplacian eigenvectors.

In [35], it is illustrated how the symmetry structure of the system, in the context of automorphisms, can negatively affect the controllability of multi-agent systems. Furthermore, it is shown that the automorphism can be replaced by another graph theoretic tool, named equitable partition, when the node selection as control input is involved in the consensus problem.

[32] have established a relation between graph symmetry and determining a set of a graph and eigenvalue multiplicity from which, one can realize how the symmetry structure of the network affects input nodes selection. Generalizing the graph automorphism to signed fractional graph automorphisms using a semi-definite programming relaxation has led to a relationship between graph automorphisms and uncontrollability to signed fractional graph automorphisms. It has been shown that the symmetries that exactly correspond to controllability are in fact characterized by signed fractional automorphism. Finally, the necessary and sufficient conditions for controllability are presented. In fact, the paper has shown that symmetry is just a sufficient condition for uncontrollability; and under certain mathematical graph property, i.e. k-regular concept, a necessary condition for controllability has been obtained. In [36], it is illustrated that the determining number of the graph (the minimum number of nodes that must be fixed to break all graph symmetry) can be used to formalize the cardinality requirements on the number of inputs into the graph. Their results have been extended to output controllabity and stabilizability

in [37]. They have shown that the symmetry perspective on system theoretic properties can be extended to network outputs. The paper also extends the results on the network controllability to stabilizability. A necessary and sufficient condition on input, output, non-output and leader symmetry to make a system controllable and/or stabilizable is also presented.

To address the controllability of a consensus problem in a leader-follower setup using graph theoretic approaches, most of the papers have focused on obtaining the sufficient condition for uncontrollability while in [38] the necessary conditions for three classes of graph controllability, namely, the classes of essentially controllable, completely uncontrollable, and conditionally controllable graphs for Laplacian leader-follower system have been introduced. It is shown that both topology of graph and control vectors influence the controllability. Essentially controllable graphs are controllable for any choice of nontrivial control vectors. It is proven that asymmetry is not a necessary condition for the class of essentially controllable graphs, but essentially controllable graphs are necessarily asymmetric. Completely uncontrollable graphs are uncontrollable for any choice of control vectors. Finally, conditionally controllable graphs are controllable only for a strict set of the control vectors. Though based on the results of this paper, there are a class of asymmetric uncontrollable graphs but this class covers a very small class of graphs namely the class of large block graphs of Steiner triple systems. The authors have also developed their work to multi-leaders symmetry with weighted digraphs in [29]. They have obtained a new necessary condition for controllability using the almost equitable partitions. It is shown that uncontrollability does not always arise from symmetry. Indeed, the number-theoretic properties of the communities is responsible for uncontrollability of some complex networks. While they have considered only linear time invariant dynamics for the agents, there is a potential to generalize their approaches to nonlinear systems. Another development on symmetric-based analysis of controllability is examined by [39] which uses a similar concept, the relaxed equitable partitions. [40] addresses the relation between network symmetries (or automorphism) and cluster formation with an emphasis on power grids. It is shown that some clusters lose synchronism without disturbing the others. Using computational group theory the hidden symmetries of networks are revealed and possible patterns of synchronization are predicted. The stability of clusters are predicted using irreducible group representation to find a block diagonalization of the variational equations that can predict the stability of the clusters. Then a symmetry breaking bifurcation, isolated desynchronization, is implemented in which one or more clusters lose synchronism while the remaining clusters stay synchronized. As discussed above, symmetry is in general an obstruction to controllability. System designer should try to avoid symmetry by appropriate choose of matrix B in state space model of network. However, controllability is not the only criterion that can be influenced by symmetry. Network robustness against disturbance, line failure, and parameter uncertainties is also characterized by symmetry; and surprisingly, symmetry has positive effect on robustness. As presented in the next section, in general, a symmetric system is more robust than asymmetric one. This is, to some extent, because of redundant couplings provided by the automorphism groups.

1.5.3 Robustness: the impact of graph symmetry

In [20], it is shown that many real world systems such as US power grid are highly symmetric. The robustness of complex network is realized through the redundancy in alternative ways for information exchange. To demonstrate how the symmetry can affect the redundancy and robustness, at first, the essential network symmetries have been identified. Considering the size and structure of automorphism groups, they are decomposed into irreducible factors such as a symmetric clique or a symmetric biclique (some sorts of symmetry factors in US power grid are shown in Figure 1.4). Then a symmetric subgraph is associated to each factor and the generic structure of symmetric subgraph is investigated. Finally, using automorphism group orbit, the relation between symmetry and redundancy (robustness) is analyzed.

Figure 1.4: Symmetric sub-graphs in the US power grid. Vertices in white correspond to those in the symmetric sub-graphs. Vertices in black are those adjacent to those in the symmetric subgraph, and are shown to clarify subgraph structure ([20]).

The main result of [42] is that an approximate symmetry is enough for a complex system to be robust against perturbation. In fact, the underlying system can be a symmetric consensus protocol with additional terms as perturbation on system dynamics, control vector fields or on the control inputs. If an exactly symmetric structure has a very stable dynamics, then the bounded perturbed terms result in deviation from asymptotically stable behavior by an amount determined by the perturbation terms. In such cases, the perturbation may prevent asymptotic stability but the solutions with unbounded growth will not be produced. An interesting result of the paper is that one only needs to check one system in the whole class to ensure the stable performance of the entire class of systems. While a special class of symmetry is considered in that paper, a more general and realistic type of perturbation will be considered as one of the directions of this thesis.

A graph theoretic-based definition for approximate graph symmetry is presented in [42] upon which a Lyapunov stability criterion is developed to address the network robustness. In fact, the paper is an extension of authors' previous work ([43]) on stability of a network with identical nodes to an important case where not all agents are identical. The underlying control protocol is a nonlinear consensus dynamics. The main result of the paper is that if an exactly symmetric system has very stable dynamics, then the bounded perturbed terms result

in solutions which deviate from asymptotically stable behavior by an amount determined by the perturbation terms. In addition, this result holds for the whole equivalent class of systems. Hence, one only needs to check a system in the entire class to ensure the stable operation of the whole class of systems.

1.5.4 Literature review on existence of symmetry in power systems

Symmetry in power grids is neither created intentionally nor detectable easily. In fact, to capture symmetry, some notions like graph automorphism and equitable partitions must be implemented. Recently, graph symmetry in power grid is addressed by two studies. The relation between graph symmetry and cluster formation (graph partitioning) is analyzed by [40]. After identifying symmetry in the grid, the network nodes can be partitioned into clusters. It is verified that if the symmetry induced clusters exist, cluster synchronization and global synchronization are the solution of the equations of motion.

Figure 1.5: Geographical diagram of the Nepal power grid network. Colours are used to indicate the computed cluster structure. The matrix (inset) shows the structure of the diagonalized coupling matrix. The diagonal colours indicate which cluster is associated with each column. ([40])

The small size power grid of Nepal and its block diagonalization of coupling matrix is shown in Figure 1.5 in which all power stations and their bidirectional couplings are identical. The Nepal power grid has 86,400 symmetries, three non-trivial clusters (two trivial ones) and three subgroups (one for each nontrivial cluster). The grid is divided into three sets of synchronized clusters. Based on dynamics, the parameters and the stability of global and cluster states, the global and cluster states may provide a route to desynchronization of Nepal grid. The network and cluster structure of the Mesa del Sol electric grid is shown in Figure 1.6 ([40]). The network size is 132 nodes and it has 4,096 symmetries, 20 non-trivial clusters and 10 subgroups. The

Figure 1.6: Network and cluster structure of the Mesa del Sol electric grid. Colours are used to denote clusters. Nodes coloured white are trivial clusters, containing only one element. ([40])

Figure 1.7: A typical arrangement of symmetric sub-graphs in US power grid ([20]).

network has three intertwined clusters, two with four clusters and one with five clusters. As indicated by [40] the future analysis about symmetry considers only the topology without the dynamics of real power networks.

In [20], it is mentioned that many real world complex networks such as US power grid are richly symmetric. Complex symmetric sub-graphs of US power grid is shown in Figure 1.4 which shows that in complex real world power grids a certain degree of symmetry exists. Figure 1.7, illustrates how different symmetric sub-graphs compose an automorphism. In [20], these

symmetries in the context of graph automorphism have been linked with graph redundancy (robustness).

1.6 Open areas

In this section, based on the arguments presented in Sections 1.5.2, 1.5.3, and 9.2.1, some open areas will be summarized to further develop the concept of graph symmetry into power systems. In fact, two problems will be addressed by symmetry: controllability and robustness.

1.6.1 Controllability and robustness of power grids: symmetry context

Symmetry plays an important role in complex networks. In particular, controllability and robustness analysis and synthesis are two closely related issues to control that have been addressed using graph symmetry. The investigation will be conducted under specific power network protocols such as pinning control. Surprisingly, symmetry has completely different effects on controllability and robustness. Briefly explaining, in eigenvector decomposition of symmetric system, there are one or more base vectors that have linear dependency. That, in turn, makes the rank of controllability matrix be deficient (not being full rank). On the other side, symmetry provides coupling redundancy in the network. This redundancy can be interpreted as robustness since it establishes redundant paths for interaction among agents. That, in turn, makes room for analysing the robustness against line failure in power networks. Also, through a comprehensive symmetry analysis on the effect of failure in each line, the critical lines could be identified and more protective strategies could be recommended for those lines. There is the potential to relate the symmetry (or redundancy) strength of the power grid to its robustness. Robustness could also be investigated under the pinning control protocol as presented by Equation 1.3 or Equation 1.6. In that case, the robustness will be investigated against the disturbance. Except for some special graphs, in general, one can say:

- A symmetric network is not controllable;
- A symmetric network is more robust than asymmetric network.

There is a gap here since no paper has ever analyzed both controllability and robustness in the network using graph theory (particularly using the symmetry feature). Motivated by this lack of investigation, this study will try to find a solution for that problem.

Analyzing line failure impact on restoration strategy and robustness exploiting the graph symmetry of the power grid could also be accompanied by investigating those failures that may result in cascading failure leading to the whole grid failure. A very interesting result might be obtained after comparing the critical lines obtained from symmetry analysis and those lines for which failure could result in cascading failure. Having near equal results in both strategies is an educated guess. Also, the symmetry based approach does not require knowing the weight of each link or transmission line which is the case in the existing studies ([17]).

Table 1.2 shows which of the areas covered by this thesis have already been investigated in literature and which parts will be targeted by this study.

Table 1.2: The open topics and applications related to this study and those which have already been addressed in literature.

Topic	**Application**	**In general**	**In power systems**
Existence of Symmetry in complex networks		Done	Done
The effect of symmetry on controllability	The energy cost of control	Done	Open
Symmetry impact on robustness	Robustness against cascading failure	Done	Open
Symmetry impact on Controllability and Robustness		Open	Open

1.7 Conclusion

Motivated by the widespread symmetric structures in complex power networks, this study will contribute to the application of graph-theoretic tools such as graph symmetry to the design and analysis of power systems and microgrids. The existing results on controllability and robustness of complex networks will be examined in power grids from the symmetry perspective. In particular, the energy cost of control will be optimized using symmetry analysis. In addition, the line failure impact on symmetry strength will present a new framework to the analysis/design of network's robustness. Also, the conflict between the effects of symmetry on the network behavior will be examined aiming at a trade off between the controllability and robustness.

To the best of the author's knowledge, there is no study exploiting the symmetry characteristics of the network, even outside of power systems, which has investigated controllability and robustness simultaneously. Also, the problem of restoration under the symmetry related constraint has never been addressed. This is also the case for the energy cost of control and finding the critical lines. Pursuing these issues will result in better understanding of the topology effects on the behavior of complex power network.

Bibliography

1.8 References

[1] B. Liu, T. CHu. L. Wang, and G. Xie, "Controllability of a leader–follower dynamic network with switching topology," *IEEE Transactions on Automatic Control*, vol. 53, 2008.

[2] A. Lombardi and M. Hornquist, "Controllability analysis of networks," *Physical Review E*, vol. 75, 2007.

[3] H. G. Tanner, "On the controllability of nearest neighbor interconnections," 43rd IEEE Conf. Decision Contr.In Proc., vol. 3, 2004.

[4] T. Ding, Y. Lin, Z. Bie, and C. Chen, "A resilient microgrid formation strategy for load restoration considering master-slave distributed generators and topology reconfiguration," *Applied Energy*, vol. 199, 2017.

[5] S. Fukunagaa and T. Nagata, "A Decentralized Power System Restoration by means of Multi-agent Approach," *Energy Procedia*, vol. 14, 2012.

[6] R. Sampaio, L. Silveira-Melo, R. P. S. Leao, G. C. Barroso, and J. R. Bezerra, "Automatic restoration system for power distribution networks based on multi-agent systems," *IET Generation, Transmission & Distribution*, vol. 11, 2017.

[7] D. J. A. Welsh and G. P. Whittle, "Arrangements, channel assignments, and associated polynomials," *Advances in Applied Math*, vol. 23, 1999.

[8] R. J. Opsut and F. S. Roberts, "Optimal I-intersection assignments for graphs: A linear programming approach," *Networks*, vol. 13, 1983.

[9] M. C. Golumbic, "Algorithmic Graph Theory and Perfect Graphs," Academic Press, New York, 1980, vol. 16, 1980.

[10] F. S. Roberts, "Applied Combinatorics," Prentice-Hall, Englewood Cliffs, NJ, 1984.

[11] S. R. Kim, T. McKee, F. McMorris, and F. S. Roberts, "p-competition graphs," *Linear Alg. Applications*, vol. 217, 1995.

[12] S. Benzer, "The fine structure of the gene," *Sci. Amer.*, vol. 206, 1962.

[13] D. Gusfield, "Algorithms on Strings, Trees, and Sequences: Computer Science and Computational Biology," Cambridge University Press, Cambridge, UK, 1997.

[14] F. S. Roberts, "Measurement Theory, with Applications to Decisionmaking, Utility, and the Social Sciences," Addison-Wesley, Reading, MA, 1979.

[15] F. S. Roberts, "On the mobile radio frequency assignment problem and the traffic light phasing problem," *Annals, NY Acad. Sci*, vol. 319, 1979.

[16] D. G. Kendall, "Seriation from abundance matrices, in F.R. Hodson, et al. (eds.), Mathematics in the Archaeological and Historical Sciences," Edinburgh University Press, Edinburgh, 1971.

[17] C. H. Coombs and J. E. K. Smith, "On the detection of structures in attitudes and developmental processe," *Psych. Rev*, vol. 80, 1973.

[18] J. E. Cohn, "Food Webs and Niche Space,"Princeton University Press, Princeton, NJ, 1978.

[19] J. R. Lundgren, S. K. Merz, and C. W. Rasmussen, "A characterization of graphs with interval squares," *Congr. Numer.*, vol. 98, 1993.

[20] H. J. Greenberg, J. R. Lundgren, and J. S. Maybee, "Inverting signed graphs," *SIAM J. Alg. & Discr. Meth.*, vol. 5, 1984.

[21] F. S. Roberts and L. Sheng, "Phylogeny numbers for graphs with two triangles," *Discrete Appl. Math.*, vol. 103, 2000.

[22] R. J. Nowakowski and D. F. Rall, "Associative graph products and their independence, domination, and coloring numbers," *Discussiones Math. Graph Theory*, vol. 16, 1996.

[23] A. H. Moradi, and S. Razini, and S. M. Hosseinian, "State of art of multiagent systems in power engineering: A review," *Renewable and Sustainable Energy Reviews*, vol. 58, 2016.

[24] Chu, Chia-Chi, H. Iu, and Cho-Ching, "Complex Networks Theory For Modern Smart Grid Applications: A Survey," *IEEE JOURNAL ON EMERGING AND SELECTED TOPICS IN CIRCUITS AND SYSTEMS*, vol. 17, 2017.

[25] F. Dorfler and F. Bullo, "Synchronization in complex networks of phase oscillators: A survey," *Automatica*, vol. 50, 2014.

[26] A. Bidram, A. Davoudi, F. L. Lewis, and J. M. Guerrero, "Distributed cooperative secondary control of microgrids using feedback linearization," *IEEE Trans. Power Syst*, vol. 28, 2013.

[27] A. Bidram, F. L. Lewis, and A. Davoudi, "Distributed control systems for small-scale power networks," *IEEE Control Syst. Mag.*, vol. 34, 2014.

[28] A. Morasi-Amani, N. Gaeini, M. Jalili, and X. Yu, "Voltage control in distributed generation systems based on comple xnetwork approach," 1st International Conference on Energy and Power, ICEP2016, 14-16 December 2016, RMITUniversity, Melbourne, Australia.

[29] C. O. Aguilar and B. Gharesifard, "Almost equitable partitions and new necessary conditions for network controllability," *Automatica*, vol. 80, 2017.

[30] J. Ruths and D. Ruths, "Control Profiles of Complex Networks," *Science*, vol. 343, 2014.

[31] Y. Y. Liy, J. J. Slotine, and A. L. Barabasi, "Controllability of complex networks," *Nature*, vol. 473, 2011.

[32] A. Chapman and M. Mesbahi, "On Symmetry and Controllability of Multi-Agent Systems," 53rd IEEE Conference on Decision and Control December 15-17, 2014. Los Angeles, California, USA.

[33] G. Notarsteano and G. Parlangeli, "Observability and reachability of grid graphs via reduction and symmetries," 2011 50th IEEE Conference on Decision and Control and European Control Conference (CDC-ECC) Orlando, FL, USA.

[34] M. Nabi-Abdolyousefi and M. Mesbahi, "On the Controllability Properties of Circulant Networks," *IEEE TRANSACTIONS ON AUTOMATIC CONTROL*, vol. 58, 2013.

[35] A. Rahmani, M. Ji, M. Mesbahi, and M. Eagerstedt, "CONTROLLABILITY OF MULTI-AGENT SYSTEMS FROM A GRAPH-THEORETIC PERSPECTIVE," *SIAM J. CONTROL OPTI*, vol. 48, 2009.

[36] A. Chapman, M. Nabi-Abdolyousefi, and M. Mesbahi, "Controllability and observability of networks-of-networks via Cartesian products," *IEEE Transactions on Automatic Control*, vol. 59, 2011.

[37] A. Chapman, and M. Mesbahi, "State Controllability, Output Controllability and Stabilizability of Networks: A Symmetry Perspective," 2015 IEEE 54th Annual Conference on Decision and Control (CDC) December 15-18, 2015. Osaka, Japan.

[38] C. O. Aguilar and B. Gharesifard, "A graph-theoretic classification for the controllability of the Laplacian leader-follower dynamics," 53rd IEEE Conference on Decision and Control December 15-17, 2014. Los Angeles, California, USA.

[39] S. Martini, M. Eagerstedt, and A. Bicchi, "Controllability analysis of multi-agent systems using relaxed equitable partitions," *Int. J. Systems, Control and Communications*, vol. 2, 2010.

[40] L. M. Pecora, F. Sorrentinio, A. M. Hagerstrom, T. E. Murphy, and R. Roy, "Cluster synchronization and isolated desynchronization in complex networks with symmetries," *Nature, Communication*, 2014.

[41] B. D. MacArthur, R. J. Sanchez-Garcia, and J. W. Anderson, "Symmetry in complex networks," *Discrete Applied Mathematics*, vol. 156, 2008.

[42] B. Goodwine, "Nonlinear Stability and Boundedness of Approximately Symmetric Large-Scale Systems,"Symmetry in complex networks," Proceedings of the 19th World Congress The International Federation of Automatic Control Cape Town, South Africa. August 24-29, 2014.

[43] B. Goodwine and G. P. Antsaklis, "Multi-agent compositional stability exploiting system symmetries," *Automatica*, vol. 49, 2013.

[44] W. Khampanchai, M. Pipattanasomporn, and S. Rahman, "A Multi-Agent System for Restoration of an Electric Power Distribution Network with Local Generation," Power and Energy Society General Meeting, 2012 IEEE, 2012.

[45] F. Ren, M. Zhang, D. Soetanto, and X. D. Su, "Conceptual Design of A Multi-Agent System for Interconnected Power Systems Restoration," *IEEE TRANSACTIONS ON POWER SYSTEMS*, vol. 27, 2012.

[46] Y.S. Li, D.Z. Ma, H.G. Zhang, and Q.Y. Sun, "Critical Nodes Identification of Power Systems Based on Controllability of Complex Networks", *Applied Sciencce*, vol. 5, pp. 622-636, 2015.

[47] Y. Y. Liu, J. J. Slotine, and A. L. Barabasi, "Controllability transition and non-locality in network control," Proc. Natl. Acad. Sci. USA, vol. 110, 2013.

[48] Z. Yuan and C. Zhao, Z. Di, W. X. Wang, and Y. C. Lai, "Exact controllability of complex networks," *Nature: Communincation*, vol. 4, no.2447, Sep. 2013, DOI: 10.1038/ncomms3447.

[49] The GAP Group, "GAP: Groups, Algorithms, and Programming," *GAP: Groups, Algorithms, and Programming*, 2005.

[50] W. Stein, "SAGE: Software for Algebra an Geometry Experimentation," http://www.sagemath.org/sage/; http://sage.scipy.org/, 2013.

[51] C. Zhao, W. X. Wang, Y. Y. Liu, amd J. Slotine, "Intrinsic dynamics induce global symmetry in network controllability," *Nature, Scientific Report*, vol. 5, no. 2015.

[52] A. J. Whalen, S. N. Brennan, T. D. Sauer, and S. J. Schiff, "Observability and Controllability of Nonlinear Networks: The Role of Symmetry," *PHYSICAL REVIEW X*, vol. 5, 2015.

[53] M. Mesbahi and M. Eagerstedt, "Graph Theoretic Methods in Multiagent Networks," Princeton University Press, 2010.

[54] F. Ball and A. Geyer-Schulz, "How Symmetric Are Real-World Graphs? A Large-Scale Study," *Symmetry*, 2018.

[55] D. Leitold, A. Vath-Fogarassy, and J. Abonyi, "Controllability and observability in complex networks – the effect of connection type," *Nature, Scientific Report*, 2017.

[56] J. L. Gross and J. Yellen, "Handbook of graph theory," CRC Press, 2000.

[57] D. M. Cardoso C. Delorme, P. Rama, "Laplacian eigenvectors and eigenvalues and almost equitable partitions," *European Journal of Combinatorics*, vol. 28, 2007.

[58] F. Chung, T. G> Dewey, and D. J. Galas, "Duplication models for biological networks," *J. Comput. Biol.*, vol. 10, 2003.

[59] M. Golubitsky and I. Stewart, "Nonlinear dynamics of networks: The groupiod formalisms," *Bull. Amer. Math. Soc.*, vol. 43, 2006.

[60] P. Holme, "Detecting degree symmetries in networks," *Phys. Rev. E*, vol. 74, 2006.

[61] I. Stewart, "Networking opportunity," *Nature*, vol. 427, 2004.

[62] L. Che, X. Zhang, and M. Shahidehpour, "Optimal Planning of Loop-Based Microgrid Topology," *IEEE TRANSACTIONS ON SMART GRID*, vol. 8, 2017.

[63] C. A. Cortes, S. F. Contreras, and M. Shahidehpour, "Microgrid Topology Planning for Enhancing the Reliability of Active Distribution Networks," *IEEE Transactions on Smart Grid*, 2018.

[64] S. Hassanvand, M. Nayeripour, E. Waffenschmidt, and H. Fallahzadeh-Abarghouei, "A new approach to transform an existing distribution network into a set of micro-grids for enhancing reliability and sustainability," *Applied Soft Computing*, vol, 52, 2017.

[65] R. Jovanovich, M. Tuba, and S. Vob, "An ant colony optimization algorithm for partitioning graphs with supply and demand," *Applied Soft Computing*, vol. 41, 2016.

[66] M. E. J. Newman, "Networks," Oxford university press, 2010.

Chapter 2

The Impact of Graph Symmetry on the Number of Driver Nodes in Complex Networks

2.1 Overview

This study investigates on a strong correlation between complex network (CN) controllability (characterized by the number of required driver nodes) and graph symmetry (described by automorphism groups) in undirected and unweighted networks. Based on the properties of permutation products of elementary automorphisms, novel necessary conditions for CN controllability are presented which are computationally more effective than previous method. In addition, a novel index of symmetry is proposed upon which a more meaningful understanding of symmetry impact on CN controllability can be comprehended. Based on this new index, a modification strategy is suggested aiming to satisfy CN controllability with a lower number of driver nodes. The study shows that the proposed modification approach can result in a minimal set of driver nodes with a reasonable computational complexity. Further, the critical components of complex networks, in terms of their impact on the number of required driver nodes, are identified. The results of the proposed methodologies have been verified for several synthetic and real test systems including small, medium, and large power networks[1].

[1]This chapter is published in *Journal of The Franklin Institute*

2.2 Introduction

The interplay between various concepts from graph theory and other fields has stimulated significant advances in resolving widespread engineering problems. The reliability and functionality of a network are highly dependent on the effectiveness of the external controls and reconfiguration strategies [1]. In spite of advances in control theory, some network emergent behaviors such as CN controllability can not be fully explained rendering network topology as a focal point of research (for example see [2]- [5]).

Structural controllability is a measure of CN controllability where system parameters representing inter-agent interactions are not precisely known. In fact, in most complex networks, only the zero-nonzero pattern of the system state matrix is known ([8]). In literature, the problem of CN controllability has been transformed to the problem of finding a set of driver nodes that can drive the system into the desired states ([2]- [6], and [9]). Better CN controllability is then attributed to the lower number of required driver nodes.

The dominant approaches for finding the set of driver nodes in CNs are maximum matching principle (MMP) [8] or minimum dominating set (MDS) ([10]). Maximum matching is equivalent to the maximum set of matched links that do not share any node in a graph. The set of nodes that are not an end point of a matched link are called unmatched nodes. It is verified in [8]- [10] that the network is controllable if one controls the set of unmatched nodes, also known as driver nodes or input nodes. This structural controllability framework is applicable to directed networks where all edges are independent free parameters [2]. In [4], the exact controllability method is proposed as an alternative method to structural controllability, one that is applicable to undirected networks as well.

Recently, the role of graph symmetry (described by automorphism groups) in controllability of CNs has been revealed [11]- [19]. It is verified that the family of asymmetric graphs are essentially controllable [11]. According to [12], the symmetry structure of the system, in the form of graph automorphisms, can negatively affect the controllability of multi-agent systems. Furthermore, equitable partition is an alternative concept for automorphism when the node selection as control input is involved in the consensus problem [12]. These results are extended in [13] to a more general condition based on equitable partitions of the underlying graph. Breaking the symmetry by appropriate selection of driver nodes, i.e. modifying the input matrix B in state space structure, is a common approach to make a symmetric system controllable ([14]). In fact, a relation between graph symmetry and determining a set of eigenvalue multiplicities has been established which shows how the symmetry structure of the network affects the selection of input nodes. In [15], the determining number of the graph (the minimum number of nodes that must be fixed to break all graph symmetries) is used to formalize the cardinality requirements on the number of inputs into the graph. The results have been extended to output controllability and stabilizability in [16], where the symmetry perspective on system theoretic properties is extended to network outputs. The connection between structural controllability and symmetry is established in [17] and is developed in [18] to the structural controllability

of neural networks. In [19], the role of symmetry in controlling network dynamics is revealed by decomposing the network into observable/controllable and unobservable/uncontrollable sub-networks. Equivalently, it is studied as symmetry-driven vs. asymmetry-driven sub-networks.

All previous works on relation between controllability and symmetry ([11]- [19]) have limitations related to computation of the set of automorphism groups. The typical size of automorphism group for a medium/large network is a gigantic number [20]. Computing and sweeping over this set (to find the determining set) is computationally prohibitive and limit the implementation of the proposed symmetry-based methods to small networks. Moreover, since the symmetry presence in network necessitates a higher number of driver nodes for CN controllability it is expected that modifying the network topology aiming at reduced number of automorphisms will reduce the number of required driver nodes. However, it will be shown that, in some cases, the trend in reduction of the number of driver nodes is not always consistent with reduction in the size of automorphism groups. This implies that relying on the size of automorphism group can not sufficiently characterize the CN symmetry strength and a more informative measure of symmetry is required. On the other hand, previous studies have shown that sparse networks are difficult to control ([21] and [22]) meaning a high number of driver nodes are required compared to other networks such as biologic networks. Also, the number of driver nodes attained based on maximum matching is highly dependent on the node degree distribution [2]. This makes it economically inefficient to modify the network since it necessitates modifying a large number of edges in order to impact on degree distribution. Moreover, in networks with symmetric adjacency matrices, with a fixed number of driver nodes, an exponential increase in energy cost of control occurs as network size increases ([6]). To enhance the CN controllability, the existing modification strategies mostly have relied on modifying the degree distribution of the network based on rather complicated algorithms ([2], [5] and [23]- [24]). According to [24], adding 5% of additional edges are needed for optimizing the controllability. On the other hand, the degree distribution can not sufficiently characterize the network controllability [24]. In addition, modifying a network's degree distribution essences many structural modifications ([5] and [23]) or many edges must be added/deleted or their directions must be reversed (for example see [25] and [26]). In many CNs such as power networks these modifications in the grid topology are not economically feasible. To address the above issues, this study leverages on the characteristics of permutation products of automorphisms in undirected and unweighted networks to propose new solutions to investigate CN controllability, introduce a new metric for symmetry, reduce the number of required driver nodes with minimal modifications, and identify the most critical nodes in terms of CN controllability.

The power networks are used as the simulation platforms for this study. The use of the term "driver node" is not new and has been used for investigation of the controllability of power networks (for example see [27]- [28]). In the context of power networks, the so called driver nodes are the well-known wide area controllers (WACs) [29]- [32] or flexible AC transmission systems (FACTS) devices [33]- [37]. A comprehensive review on various technologies of FACTS devices is presented in [38]. WACs or FACTS devices are crucial in damping the inter-area os-

cillations as the local controllers have only access to local measurements which can be used for damping the local modes [31]. These controllers are vital from CN perspective since, unlike the local and primary controller in power grids, they impact on emergent behaviour of the whole network. Finding the optimal locations of these devices are vital for power system stability and performance improvement against disturbances and has been a very recent line of research in literature [33]- [34].

This study is motivated by (i) the lack of a computationally effective approach in finding the number and locations of driver nodes based on symmetry, (ii) the increased cost and complexity of controlling CNs via a high number of driver nodes, (iii) the lack of a consistent symmetry index with the number of required driver nodes, and (iv) the high modification cost imposed by the existing approaches which are based on modifying the degree distribution. The novelties of this chapter are as follows:

- By investigating the properties of permutation products, novel necessary conditions for controllability are attained which are, unlike previous approaches, computationally effective.
- A new index of symmetry is proposed which is more consistent with the trend in reducing the number of driver nodes as the the network symmetry decreases.
- A new algorithm for reducing the number of required driver nodes based on the symmetry index is proposed which, unlike the previous modification strategy based on modifying the degree distribution, does not impose many modifications on the network topology.
- The network's critical components, in terms of their impact on symmetry, and in turn controllability, can be identified.

The organization of the chapter is as follows. The mathematical preliminaries on graph theory, symmetry, and controllability are presented in Section 2.3. Section 2.4 contains the main results of the chapter. Initially, new necessary conditions for controllability are attained. Then, a new metric of controllability is adapted based on a new proposed index of symmetry upon which an algorithm is proposed for modifying the network in order to reduce the number of required driver nodes. The symmetry impact on controllability of complex networks is verified on various power networks in Section 2.5. Concluding remarks and future works are presented in Section 2.6.

2.3 Preliminaries

2.3.1 Graph theory

Graph theory rooted in discrete mathematics is the bedrock of network analyses. An abstract model of a network with complex inter/intra agents dynamics can be represented by a finite graph $\mathcal{G} = (V, E)$ characterized by a set of nodes V and a set of edges E. An edge exists from

node i to j if $(i,j) \in E$. The $order$ of a graph $\mathcal{G}$ is the cardinality of its node set V, and the $size$ of a graph is the cardinality of its edge set E. For a simple graph, the adjacency matrix $\mathcal{A}$ is a square $|V| \times |V|$ matrix whose element $[\mathcal{A}_{ij}]$ is one when there is an edge from i to j, and zero when there is no edge. A $permutation$ σ on the set V translates through the act of node reordering which is a bijection from V to itself.

2.3.2 Graph symmetry

Symmetry, in general, is an inherent property of complex networks which is not intentionally built in the network and can not be intuitively captured. To reveal the network symmetry, a notion from discrete algebra known as automorphism is implemented. Automorphism is a node permutation that maps a graph to itself while preserving the graph structure. The set of mappings that preserve the graph structure can then be detected and realized as the graph symmetries.

Definition 2.3.1. *For a graph $\mathcal{G}(V,E)$ with edge set E and node set V, an automorphism of $\mathcal{G}$ is a permutation σ of nodes of $\mathcal{G}$ such that for any two nodes i and j in $V(\mathcal{G})$, $\{i,j\} \in E(\mathcal{G})$ if and only if $\{\sigma(i),\sigma(j)\} \in E(\mathcal{G})$.*

The automorphism group of $\mathcal{G}$ represented by $Aut(\mathcal{G})$ is a finite group under composition operator and its size, $|Aut(\mathcal{G})|$, characterizes the symmetry strength of the network. The permutation that fixes all nodes, i.e., $\sigma(i) = i$, is called identity I, also known as trivial automorphism. Identity is an automorphism for any simple graph. The symmetric group $Aut(\mathcal{G})$ is the group of permutations $\sigma : V \to V$. The cycle $(\rho, \rho+1, ..., \rho+r)$ of order r is the set of ordered nodes $V(\mathcal{G})$ for which $\sigma(i) = i+1$ for all $\rho \leq i \leq \rho+r-1$ and $\sigma(\rho+r) = \rho$.

Remark 2.3.1. *A sparse network usually has a gigantic number of automorphisms which can not be computed with conventional computation tools. In this study, the Python programming in Sage (System for Algebra and Geometry Experimentation) has been used for drawing the network topology and computing the symmetry related parameters such as automorphism. Although Sage is a prominent software for computing the symmetry it is unable to compute the very large sets of automorphisms. In most cases, Sage can only derive the size of automorphisms and is not able to generate the whole set of permutations within the automorphism group.*

If ζ and δ are two permutations in a symmetric group, then the composition (or product) of ζ and δ is the permutation $\zeta \circ \delta$ in the symmetry group so that $(\delta \circ \zeta)(i) = \delta(\zeta(i))$. Generally, the composition of permutations is not commutative, meaning that $\zeta \circ \delta$ may be different from $\delta \circ \zeta$.

Remark 2.3.2. *The set of automorphisms $Aut(\mathcal{G})$ can be constructed from a set of elementary factors called generators and represented by $Gen(\mathcal{G})$. Throughout the chapter, the terms elementary factors and generators convey the same meaning. The size of the generator set is denoted by $|Gen(\mathcal{G})|$. The standard algorithm for computing $Aut(\mathcal{G})$ is to generate a tree: the*

root is the identity element; and the nodes are elements of the group. If w is a node, it has as children the nodes $w \circ q$ (product in the group). For each generator q, if $w \circ q$ is already a node then $w \circ q$ is a leaf of the tree. If the group is finite, the algorithm stops and generates a finite tree whose internal nodes are exactly all the elements of the group. This algorithm is a built-in function of SAGE and can be easily implemented.

Definition 2.3.2. *Let $\sigma \in S$ be a permutation of set S. For $\{a, b\} \in S$, a and b are equivalent (denoted by $a \sim b$) if and only if $b = \sigma^n(a)$ for some $n \in Z$. The equivalence classes described are the orbits of S. Subsequently, the graph $\mathcal{G}$ can be partitioned into equivalence classes under the action of $Aut(\mathcal{G})$.*

Definition 2.3.3. *A permutation which belongs to the set $Aut(\mathcal{G})$ is a cycle if it has at most one orbit under the action of an automorphism group containing more than one element. The length of the cycle is the number of elements in its largest orbit.*

Definition 2.3.4. *A set of nodes S is a determining set for a graph $\mathcal{G}$ if every automorphism of $\mathcal{G}$ is uniquely determined by its action on S. Equivalently, a subset S of the nodes of a graph G is called a determining set if whenever $g, h \in Aut(\mathcal{G})$ so that $g(s) = h(s)$ for all $s \in S$, then $g = h$.*

2.3.3 Controllability and exact controllability method

For a continuous linear time invariant system as

$$\frac{d\boldsymbol{x}}{dt} = A\boldsymbol{x}(t) + B\boldsymbol{u}(t) \tag{2.1}$$

where $\boldsymbol{x}(t)$ is the state vector, $\boldsymbol{u}$ is the control vector, A is the $n \times n$ state matrix and B is the $n \times r$ input matrix, the state controllability means that states can be driven from any initial state to any final state in finite steps by a bounded control input injected to the selected nodes. The $n \times nr$ controllability matrix is given by

$$R = [B \quad AB \quad A^2B \quad ... \quad A^{n-1}B] \tag{2.2}$$

and the system is controllable if the controllability matrix has full rank, i.e.,

$$\text{Rank}\{R\} = n. \tag{2.3}$$

The dynamic equation (5.10) is controllable if the pair (A, B) is controllable, meaning the matrix B sets the control inputs that can fully control the network. However, testing the controllability of complex networks using Equation (7.3) is a challenging task since it involves a computationally expensive rank condition calculation and is not feasible when the state and control matrix have unknown nonzero. Hence the rank of controllability matrix is computationally prohibitive in a network consisting of many nodes which limits its application to the

small networks [39]. These stimulate employing the exact controllability method [4] which is based on finding the set of driver nodes that can fully control the network (CN controllability). Throughout this chapter, the exact controllability method [4] is used to calculate the number of driver nodes required for fully controlling the network. The method could be applied to undirected networks based on maximum geometric multiplicity of eigenvalues. For system (5.10), an equivalent to the controllability test in (7.3) is that the system is fully controllable if and only if

$$\text{rank}(cI_N - A, B) = N \tag{2.4}$$

is satisfied for any complex number c, where I_N is the identity matrix of dimension N. According to [4], the minimum number of driver nodes can be computed by the maximum geometric multiplicity $\mu(\lambda_i)$ of the eigenvalue λ_i of A, i.e.,

$$N_d = \text{max}_i\{\mu(\lambda_i)\} \tag{2.5}$$

where

$$\mu(\lambda_i) = N - \text{rank}(\lambda_i I_N - A) \tag{2.6}$$

and $\lambda_i (i = 1, ..., l)$ represents the eigenvalues of A. For undirected networks, the maximum algebraic multiplicity $\delta(\lambda_i)$ determines the number of driver nodes as

$$N_d = \text{max}_i\{\delta(\lambda_i)\} \tag{2.7}$$

where $\delta(\lambda_i)$ is also the eigenvalue degeneracy of matrix A [4]. According to the exact controllability method, the number of driver nodes can be determined from the maximum geometric multiplicity μ of the eigenvalue λ^M. Therefore the control input matrix B has to satisfy

$$\text{rank}\{\lambda^M I_N - A, B\} = N. \tag{2.8}$$

The exact controllability method in [4] implements elementary column transformation on the matrix $(\lambda^M I_N - A)$ to drive a reduced row echelon form of the adjacency matrix. Subsequently, the set of linearly dependent rows corresponds to the driver nodes which is equivalent to the maximum geometric multiplicity.

Before presenting the main results of the chapter, a few more terms shall be introduced. For a given network, "symmetry group" and "graph symmetry" refer to sets of quantified notion of symmetry such as the sets of automorphism, generators of automorphisms, or orbits of automorphism. Network "density" is the ratio of links to nodes within the network. The "node multiplicity" means the number of repetition of a given node within the symmetry group.

2.4 A more efficient method for investigating the controllability of complex networks

This section presents the main results of the chapter. All results are attained leveraging on graph symmetry and its characteristics. First, the difficulty of checking the existing necessary condition (based on automorphism groups) for controllability is verified. Then, novel necessary conditions for controllability are presented which resolve this computation issues. A new index of symmetry is then proposed upon which (i) the symmetry impact on controllability can be better captured, (ii) an algorithm is proposed for network modification (with minimal structural modification) to determine a lower number of required driver nodes and, in turn, lower cost and complexity of control task, (iii) and the network's critical elements can be identified.

2.4.1 The new necessary conditions for controllability

An adaption of the results in [12] on relation between controllability and symmetry is rewritten in [14] as the proposition below.

Proposition 2.4.1. *[14] The system of Equations (5.10) is uncontrollable if there exists a nontrivial automorphism of $\mathcal{G}$ which fixes all inputs in the set S.*

The condition of the Proposition 3.1 implies on breaking the symmetry structure of $\mathcal{G}$ to satisfy CN controllability. In [15], the above result is restated employing the concept of determining sets.

Lemma 2.4.1. *([15]) Assume that $A(\mathcal{G})$ is diagonalizable and symmetry preserving. Then the pair $\big(A(\mathcal{G}), B(S)\big)$ is uncontrollable if $\mathcal{G}$ admits a nontrivial automorphism σ which fixes the input set S, i.e., $\sigma(i) = i$ for all $i \in S$.*

In practice, checking the above condition for medium/large networks is not feasible. In particular, the size of automorphism group for sparse networks are gigantic ([21] and [22]). Although the conventional computing tools like Sage and GAP can calculate the cardinality of these groups they are unable to generate all permutations. For example, the size of the automorphism group of 1176-bus system is approximately 10^{259} [20]. Even if the whole set of automorphisms could be computed (which is not the case with current computation ability of Sage and existing processors) it is not possible to sweep over this huge number of permutations to find the determining set and node multiplicities in the symmetry group. This is in-line with the big number of driver nodes required to control these sparse networks discussed in [21] and [22]. To resolve this issue, another method is proposed based on generators of automorphisms which results in a minimal determining set in a finite time. First, some properties of the composition of permutations are introduced. Then, based on these properties, the finding of determining set based on generators of automorphisms (which are very smaller groups compared to Aut($\mathcal{G}$)) is established. Since Gen($\mathcal{G}$) is a very small group it is computationally efficient to compute and sweep over it.

Definition 2.4.1. *Let $\sigma : S \to S$ be a permutation of a set S. An element $s \in S$ is a fixed point of σ if $\sigma(s) = s$. That is, the fixed points of a permutation are the points not moved by the permutation. The permutation σ moves the point v if $\sigma(v) \neq v$. The fixed and moved points by the permutation σ are denoted by Fix(σ) and Move(σ), respectively. Also, the set of nodes permuted from node p by a permutation set $P = \{\zeta_1, \zeta_2, ..., \zeta_3\}$ is denoted by $Move(\zeta_1 \cup \zeta_2 \cup ... \cup \zeta_i)_p$ if p is permuted by one or multiple of permutations in P, and is denoted by $Move(\zeta_1 \cap \zeta_2 \cap ... \cap \zeta_i)_p$ if p is permuted by multiple permutation in P. The set of permutation matrix J associated with σ fixes the matrix $B(S)$, i.e., $JB(S) = B(S)$.*

Definition 2.4.2. *Two permutations ζ and δ are disjoint if they do not share a common node, that is $Move(\zeta) \cap Move(\delta) = \varnothing$, otherwise they are joint permutations.*

Using the above definition, a preliminary result on the properties of permutations is presented below.

Theorem 2.4.1. *[40] Every permutation in the symmetric group can be expressed as a composition of disjoint cycles uniquely up to a reordering of the cycles.*

The disjoint cycles determine a partition of $V(G)$ into orbits. The set of nodes in an orbit have the same degree. There is an m such that the repeated application of a permutation σ will lead back a node to itself, that means $\sigma(v) = v$. Now, based on the following properties of permutation product, new necessary conditions for controllability can be established.

Proposition 2.4.2. *If*

$$\big(Move(\zeta_1) \cap Move(\zeta_2) \cap ... \cap Move(\zeta_i)\big) = \varnothing$$

where i is the number of permutations, then

(i) $Move(\zeta_1^{n_1} \circ \zeta_2^{n_2} \circ ... \circ \zeta_i^{n_l})_p \neq \varnothing$ *if* $Move(\zeta_1 \cup \zeta_2 \cup ... \cup \zeta_i)_p \neq \varnothing$, *and*

(ii) $Move(\zeta_1^{n_1} \circ \zeta_2^{n_2} \circ ... \circ \zeta_i^{n_l}))_p = \varnothing$ *if* $Move(\zeta_1 \cup \zeta_2 \cup ... \cup \zeta_i)_p = \varnothing$

where l is the order of permutation up to generating non-repeated permutations in the products of permutations.

Proof. This proposition simply means if two or multiple permutations of a generator set are disjoint then their composition of any order (i) does not fix an already moved node by one of them, and (ii) does not move any node that is already fixed by multiple of them. Using an ad absurdum statement, if the composition of disjoint permutations fixes an already moved node, that node is essentially a joint node which contradicts the permutations being disjoint (proof of (i)). Similarly, if the composition of disjoint permutations $\zeta \circ \delta$ moves an already fixed node, that node has to be moved by one or some of the permutations. This contradicts the node being already fixed by multiple permutations (proof of (ii)). □

Proposition 2.4.3. *If there is at least one joint node between the set of permutations* $\{\zeta_1, \zeta_2, ..., \zeta_i\} \in Gen(\mathcal{G})$*, i.e.*

$$\big(Move(\zeta_1) \cap Move(\zeta_2) \cap ... \cap Move(\zeta_i)\big) \neq \varnothing$$

then $Move(\zeta_1^{n_1} \circ \zeta_2^{n_2} \circ ... \circ \zeta_i^{n_l})_p$ *may fix or move* p *if*

$$Move\big(\zeta_1 \cap \zeta_2 \cap ... \cap \zeta_i\big)_p \neq \varnothing.$$

Proof. This proposition implies that if two or multiple permutations have a common node then their compositions of any order may fix or move an unfixed node by multiple of them. The proof is rather straightforward. Consider the two permutations below with the joint nodes a and b:

$$\zeta_1 = (a \quad b), \quad \delta_1 = (a \quad c \quad b)$$

in which $\{a, b, c\}$ are the node numbers, and a and b are two joint nodes. The composition of these permutations can be written as

$$\zeta_1 \circ \delta_1 = (a \quad b) \circ (a \quad c \quad b) = (a \quad c)$$

by which a moved node by both permutations, i.e. node b, is now fixed. However, the other moved node, i.e. node a, is moved again. Hence, it is both possible that compositions of joint permutations of any order fix or move an unfixed node by all permutations. □

Proposition 2.4.4. *If* $Move(\zeta_1 \cup \zeta_2 \cup ... \cup \zeta_i)_p \neq \varnothing$ *where* $\{\zeta_1, \zeta_2, ..., \zeta_i\} \in Gen(\mathcal{G})$ *then* $Move(\zeta_1^{n_1} \circ \zeta_2^{n_2} \circ ... \circ \zeta_i^{n_l})_p$ *can fix* p*.*

Proof. This proposition implies that if a node is not fixed by one or multiple permutations of a generator set, it might be fixed by a function of their composition. The proof is straightforward using Proposition 2.4.2 and 2.4.3. □

Now a main result on new necessary conditions for controllability can be established using the properties of permutation products presented in Propositions 3.2, 3.3, and 3.4. The below lemma characterizes these necessary conditions for controllability which, unlike Lemma 5.4.1, can be computed effectively by only computing and sweeping over the generators of automorphisms.

Lemma 2.4.2. *Assume that* $A(\mathcal{G})$*, the adjacency matrix of the underlying network, is diagonalizable and symmetry preserving and* B *is the input matrix applied to set* S *of* N_d *driver nodes. Necessary conditions for controllability of the pair* $(A(\mathcal{G}), B(S))$ *are*

(i) $\sigma_{g_t}(i) \neq i$ *for all* $i \in S$ *and* $t = 1, 2, ..., k$*, where* $\sigma_{g_t}(i)$ *represents the set of generators and* $k = |Gen(\mathcal{G})|$*,*

(ii) $S(i) \neq j$ *for the set of pairwise joint generators with joint node* j *where* $i = 1, 2, ..., N_d$*,*

(iii) If all nodes of generators g_k *are joint nodes then all of its joint nodes are in* S*.*

Proof. According to Proposition 2.4.2, if two or multiple permutations are disjoint then their composition of any order does not fix any unfixed node by them, i.e., if

$$\sigma_t(i) \neq i \quad , t = 1, 2, ..., k$$

then

$$\sigma_{g_t}(i) \neq i \quad for \quad f\big(\prod(\sigma_{g_1}^{n_1} \circ \sigma_{g_2}^{n_2} \circ ... \circ \sigma_{g_k}^{n_h})\big)$$

where $n_1, n_2, ..., n_h$ are the order of permutations in composition and are up to generating the non-repeated automorphisms. This means that the determining set attained from a set of disjoint generators necessarily contains all nodes that can be attained by the corresponding automorphism group. This condition is satisfied by (i). Condition (i) also considers the set of joint generators which their compositions, according to Proposition 2.4.3, can result in two possible cases as follows:

First, it fixes an unfixed node: According to condition (i), the unfixed node may have already been selected as a node in S. According to Proposition 3.4, this node can be fixed after composition. Thus. it must not be included in the determining set attained from the corresponding automorphism group. Therefore, these joint nodes have to be excluded from the determining set in order to minimize N_d. Condition (ii) excludes the set of joint nodes from S by setting $S(i) \neq j$. This simply means that for the set of joint generators only disjoint nodes have to be selected as a driver node to be included in S.

Second, it moves an unfixed node: In this case, the unfixed node by generators will appear in the corresponding automorphism group. That means selecting that node as a driver node in S is a valid choice which is guaranteed by condition (i).

Therefore the determining set S attained from a set of disjoint and joint generators is a minimal determining set as long as all joint nodes are excluded from the set. However, if all nodes of a generator are joint nodes, then all nodes of that generator have to be included in S since there might be an automorphism that fixes all joint nodes of that generator (condition (iii)). □

Lemma 8.2 characterizes the necessary conditions for controllability which, unlike the previous results in [12] and [14]- [15], are computationally effective. This is because it needs to sweep over elementary factors of automorphism groups or generator sets which have very smaller sizes compared to the associated automorphism groups.

2.4.2 New controllability metric via a new measure of symmetry

In general, a lower number of automorphisms leads tolower number of driver nodes and, in turn, lower cost and complexity of control; see, e.g., [11]. However, using the number of driver nodes (attained by exact controllability method) as a controllability metric, N_d does not always perfectly correlates with the size of the automorphism group (This can be observed later in Figure 2.1.(a)-(e)). This motivates seeking other avenues for a more comprehensive criterion

for measuring symmetry strength which is more consistent with the associated number of driver nodes.

To quantify graph symmetry in a more informative way, Shannon's Entropy Formula is employed to capture the impacts of (i) orbits of automorphisms and (ii), multiplicity of nodes in $Gen(\mathcal{G})$ as well as the impact of $|\text{Aut}(\mathcal{G}|$. The entropy H of a discrete random variable $X \in \{x_1, x_2, ..., x_n\}$ is defined as

$$H(X) = \mathbb{E}[I(X)] = \mathbb{E}[-\ln(P(X))] \tag{2.9}$$

where $P(X)$ is the probability function. Then entropy can be written as

$$H(X) = \sum_{i=1}^{n} P(x_i)I(x_i) = -\sum_{i=1}^{n} P(x_i)\ln(P(x_i)) \tag{2.10}$$

and is often interpreted as a measure of disorder, uniformity, or randomness in system [41]. The impact of orbits of automorphisms on symmetry can be realized from

$$S_{\mathcal{O}}(\mathcal{G}) = \frac{\sum_{i=1}^{l} |\mathcal{O}_l|\ln|\mathcal{O}_l|}{n} \tag{2.11}$$

where $S_{\mathcal{O}}(\mathcal{G})$ is the impact of orbits of automorphisms on symmetry structure, $|\mathcal{O}_l|$ is the number of elements of l^{th} orbit, and n is the number of nodes. The bigger the orbits are, the more symmetric is the underlying graph. The below example reveals the importance of (3.22) when two networks have equal size of automorphism groups but realize different orbit structures.

Example IV.1: As a rather extreme example, consider two networks with the same size; one with only one orbit containing all nodes and the other with 5 orbits each containing only 2 nodes. The first network is clearly more symmetric for which (3.22) is equal to

$$S_{\mathcal{O}_1}(\mathcal{G}) = \frac{(10)\ln(10)}{n} = \frac{23.03}{n}$$

and for the second network, it can be written as

$$S_{\mathcal{O}_2}(\mathcal{G}) = \frac{(5)(2)\ln(2)}{n} = \frac{6.93}{n}$$

The difference between $S_{\mathcal{O}_1}(\mathcal{G})$ and $S_{\mathcal{O}_2}(\mathcal{G})$ could not be delivered by the traditional measure of symmetry, i.e., the size of automorphism group. We redefine the symmetry as

$$S_{\mathcal{R}}(\mathcal{G}) = \frac{\sum_{j=1}^{l} j.|\mathcal{N}_j|}{n} \tag{2.12}$$

where $S_{\mathcal{R}}(\mathcal{G})$ is the impact of multiplicity of nodes in $Gen(\mathcal{G})$ and $\mathcal{N}_j$ is the number of nodes with the multiplicity equal to j in generators. Equation (3.4.2) highlights the impact of multiplicity of each node in $Gen(\mathcal{G})$, that is, the higher the number of nodes with higher multiplicity

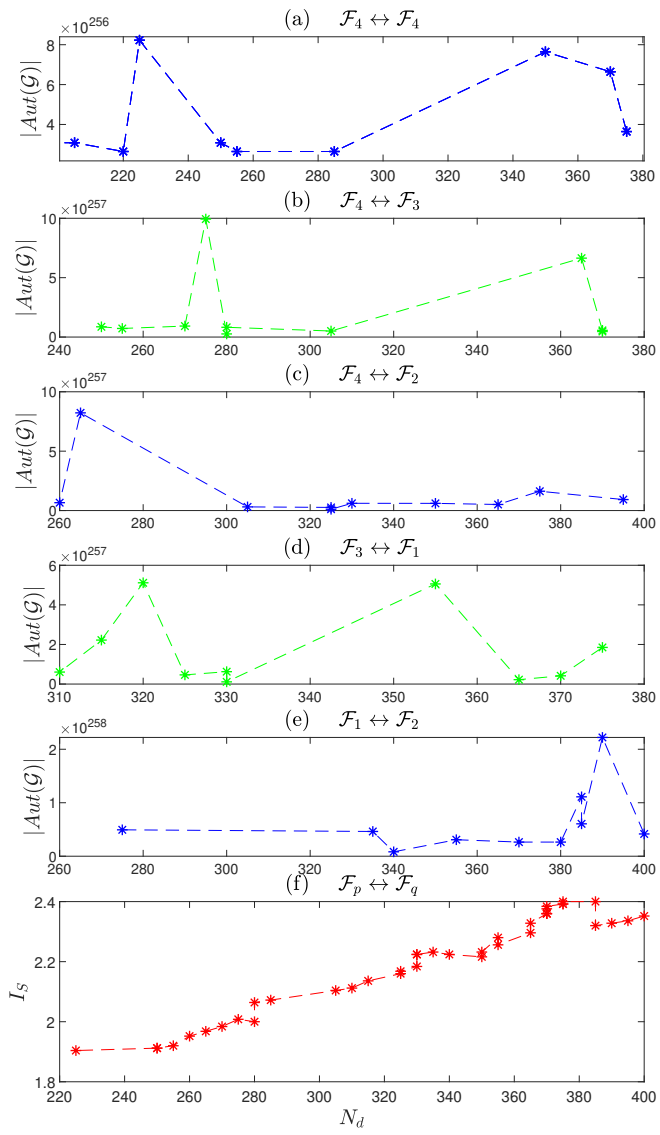

Figure 2.1: Symmetry impact on controllability of 1176-bus system: The number of driver nodes N_d versus the size of automorphism group $|Aut(\mathcal{G})|$ after adding (a) an edge between two nodes with multiplicities 4 in generator set ($\mathcal{F}_4 \leftrightarrow \mathcal{F}_4$), (b) an edge between two nodes with multiplicities 4 and 3 ($\mathcal{F}_4 \leftrightarrow \mathcal{F}_3$), (c) an edge between two nodes with multiplicities 4 and 2 ($\mathcal{F}_4 \leftrightarrow \mathcal{F}_2$), (d) an edge between two nodes with multiplicities 3 and 1 ($\mathcal{F}_3 \leftrightarrow \mathcal{F}_1$), (e) an edge between two nodes with multiplicities 1 and 2 ($\mathcal{F}_1 \leftrightarrow \mathcal{F}_2$), and (f) number of driver nodes n_d versus the new index of symmetry I_S after adding an edge between two nodes with multiplicities p and q in generator set ($\mathcal{F}_p \leftrightarrow \mathcal{F}_q$)

in $Gen(\mathcal{G})$, the higher is the symmetry index. Lastly, the traditional measure of symmetry, i.e., the size of automorphism groups, is reformulated as below

$$S_{\mathcal{A}}(\mathcal{G}) = \sqrt[n]{|Aut(\mathcal{G})|} \tag{2.13}$$

where $S_{\mathcal{A}}(\mathcal{G})$ is the impact of the size of automorphism group on the symmetry of the graph. Finally, all contributing factors to the symmetry profile of a network attained in (3.22)-(2.13)

are integrated into the below equation

$$S(\mathcal{G}) = S_{\mathcal{O}}(\mathcal{G}) + S_{\mathcal{R}}(\mathcal{G}) + S_{\mathcal{A}}(\mathcal{G}). \tag{2.14}$$

Example IV.2: Computing this new index for the 1176-bus system after several modifications results in a more logical trend in improving the controllability with decreasing symmetry index rendering a more reliable index for modifying the network. The number of driver nodes attained with this new index is compared with the original index, i.e. the number of automorphisms, in Figure 2.1. The 1176-bus system has approximately 10^{259} automorphisms and 402 driver nodes. Adding an edge to the nodes contributing to the generator set results in a reduced number of driver nodes and automorphisms as shown in Figure 2.1.(a)-(e). In the rest of the chapter, $\mathcal{F}_p \leftrightarrow \mathcal{F}_q$ resembles the network modification via adding an edge between two nodes with multiplicities p and q. Although there is no monotonic trend in N_d as $|Aut(\mathcal{G})|$ decreases, a trend can be realized in monotonically decreasing the $|Aut(\mathcal{G})|$ as an edge is added to those nodes with higher multiplicities in $Gen(\mathcal{G})$. The $|Aut(\mathcal{G})|$ after adding an edge between nodes with multiplicity 4 in $Gen(\mathcal{G})$ (i.e., $\mathcal{F}_4 \leftrightarrow \mathcal{F}_4$) is approximately equal to 10^{256}, while this parameter for $\mathcal{F}_4 \leftrightarrow \mathcal{F}_3$, $\mathcal{F}_4 \leftrightarrow \mathcal{F}_2$, and $\mathcal{F}_3 \leftrightarrow \mathcal{F}_1$ is $\approx 10^{257}$ and for $\mathcal{F}_1 \leftrightarrow \mathcal{F}_2$ it is equal to $\approx 10^{258}$. Figure 2.1.(f) demonstrates the number of driver nodes versus the new index of symmetry (2.14). This new index is computed each time after adding an edge between two nodes with multiplicities p and q. As can be seen, a monotonic decrease in N_d is realized as $\mathcal{S}(\mathcal{G})$ decreases.

The proposed symmetry metric in (2.14) contains three symmetry factors. However, it is not possible to conclude, as a general rule, which factor is more effective in the symmetry strength due to the complexity and diversity of symmetry sub-structures within the network. A given network can have a gigantic number of automorphisms but very small number of orbital index and vice versa. Thus, concluding which factor is more contributing is totally case specific meaning it only applies for the given network.

Based on findings of this section, algorithm 1 is proposed which summarizes the proposed approach for improving the controllability of complex networks by reducing the number of required driver nodes which, in turn, will lead to lower energy cost of control.

The cost of adding/removing a link between two nodes must be considered before selecting the two associated nodes for modification. Adding a link between two nodes with large distance is not practical as it impose huge infrastructure cost in physical networks such as power grids. Once the set of nodes with maximum multiplicities are identified, a nearby node to a node with maximum multiplicity can be selected for adding/removing a link. Also, by repeating this with other nearby nodes, we can choose the best results by comparing (2.14) before and after modification.

Algorithm 1 Improving the controllability (reducing the number of required driver nodes) of complex networks using the symmetry analysis and minimal network modification

Input: The adjacency matrix A of the underlying graph
Output: The modified structure of network aiming at lower number of driver nodes

1: Compute the number of automorphisms $|Aut(\mathcal{G})|$ using Sage.
2: Compute the generators set $Gen(\mathcal{G})$ in Sage.
3: Compute the orbits of automorphisms $\mathcal{O}(\mathcal{G})$ in Sage.
4: Using (2.14) compute the symmetry index of network $\mathcal{G}$.
5: Using exact controllability method, compute the number of required driver nodes N_d.
6: Cluster the nodes based on their multiplicities in generator set $Gen(\mathcal{G})$.
7: Begin modifying the network by adding an edge to those nodes with higher multiplicity in $Gen(\mathcal{G})$ aiming at a lower symmetry index of Equation (2.14).
8: Choose the modified graph corresponding to the lower symmetry and, in turn, lower number of required driver nodes.

2.5 Simulation results

In this section, the simulation is carried out on a few power grids modelled as complex networks. Initially, as a proof of symmetry concept in power networks, the prevalence of symmetry in these networks is verified. Then the impact of symmetry is investigated on controllability of a few power networks of various sizes.

2.5.1 Modeling the voltage control of power systems as a complex network controllability problem

The dynamics of i^{th} generation unit in the dq frame ([42]) is presented in [43] as

$$\begin{aligned} \dot{x}_i &= f_i(x_i) + k_i(x_i)D_i + g_i(x_i)u_i \\ y_i &= h_i(x_i) \end{aligned} \tag{2.15}$$

where f_i, k_i, and g_i are attained from the internal dynamics of generation unit, D_i is the disturbance at node ith, and u_i and x_i are the control signal and the state vector of the i^{th} unit. The detailed expression for these parameters can be extracted from []. Using feedback linearization, the nonlinear model of i^{th} generation unit can be written as

$$\dot{h} = Ah_i + Bu_i + d_i \tag{2.16}$$

in which $h_i = [\nu_{odi}\, \dot{\nu}_{odi}]$ and d_i is the disturbance on i^{th} unit caused by other generation units. Assuming ν_{ref} as the reference voltage, $e_i = h_i - h_{ref}$, and $h_{ref} = [v_{ref}, 0]$, the error dynamics of unit i, e_i, can be written as

$$\dot{e}_i = Ae_i + Bu_i + d_i \tag{2.17}$$

Since the reference voltage is constant we can write $\dot{\nu}_{ref} = 0$. The objective of control signal design is to approach $e_i = 0$ in the presence of disturbance d_i. The pinning control [44] can be implemented for this purpose. In pinning control, the control signal u_i should be designed for the system below:

$$\frac{dx_i}{dt} = F(x_i) - \rho \sum_{j=1}^{n} l_{ij} H x_j \tag{2.18}$$

where $x_i \in R^n$ is the state vector, $F : R^n \rightarrow R_n$ is the individual systems' dynamical equation (which is considered identical for all nodes), and ρ is the unified coupling strength. l_{ij} is the $(i,j)^{th}$ element of the Laplacian matrix $\mathcal{L}$, where $\mathcal{L} = \mathcal{D} - \mathcal{A}$. $\mathcal{D}$ represents the degrees of nodes in the network and $\mathcal{A}$ is the adjacency matrix. The couplings between nodes is represented by non-zero elements of H. The pinning control objective is to synchronize all system states to the desired state $s(t)$, i.e., $x_1(t) = x_2(t) = \ldots = x_n(t) = s(t)$. This implies that

$$\frac{d(s(t))}{dt} = F(s(t)). \tag{2.19}$$

To drive all nodes to the desired state, the control signal u_i must be appropriately designed for the equation below

$$\frac{dx_i}{dt} = F(x_i) - \rho \sum_{j=1}^{n} l_{ij} H x_j + \rho b_{ii} u_i, \quad i = 1, 2, ..., n \tag{2.20}$$

where for control node or driver node $b_{ii} = 1$, otherwise $b_{ii} = 0$. In power systems, the coupling matrix between nodes is usually denoted by the admittance matrix representing the power flow. From graph theory and Kirchhoff law, the coupling dynamics of power flow for a network containing n_g generation units can be written as below:

$$\begin{pmatrix} Y_{11} & -Y_{12} & \cdots & -Y_{1n} \\ -Y_{21} & Y_{22} & \cdots & -Y_{2n} \\ \vdots & \vdots & \ddots & \vdots \\ -Y_{n1} & -Y_{n2} & \cdots & Y_{nn} \end{pmatrix} . \begin{pmatrix} y_1 \\ y_2 \\ \vdots \\ y_n \end{pmatrix} = \begin{pmatrix} 0 \end{pmatrix} \tag{2.21}$$

From $e_i = y_i - y_{ref}$ one can write:

$$\begin{pmatrix} Y \end{pmatrix} . \begin{pmatrix} e_1 \\ e_2 \\ \vdots \\ e_n \end{pmatrix} = \begin{pmatrix} 0 \end{pmatrix} \tag{2.22}$$

where $Y_{ii} = \sum_j Y_{ij}$. Then the disturbance of other units that affect on the voltage error of unit i can be written as:

$$d_i = Y_{ii}^{-1} \sum_{j \neq i}^{N} Y_{ij} e_j \tag{2.23}$$

From (2.17) and (2.23) one can write:

$$\dot{e}_i = Ae_i + Bu_i + Y_{ii}^{-1} \sum_{j \neq i}^{N} Y_{ij} e_j = (A - I)e_i + Y_{ii}^{-1} \sum_{j=1}^{N} Y_{ij} e_j + Bu_i \tag{2.24}$$

Let $Y_{ii}^{-1} \sum_{j=1}^{N} Y_{ij} = A'$. Then (2.24) can be written as:

$$\dot{e}_i = (A - I)e_i + A'e_j + Bu_i \tag{2.25}$$

The combination of $(A - I)$ and A' represented by $[(A - I)|A'] = \mathcal{A}$ constitutes the adjacency matrix of the graph of system (5.4.1). Then

$$\dot{e} = \mathcal{A}e + Bu_i \tag{2.26}$$

represents a model of voltage control in power networks under pinning protocol.

2.5.2 Symmetry prevalence in power networks: a proof of the concept

Since this research represents the first study connecting symmetry and controllability in power networks, it is important to reveal the symmetry prevalence and its impact on the controllability of complex power networks. To this end, a set of 99 complex power networks from [45] have been examined. Each network contains a certain level of symmetry characterized by the size of its automorphism group. Table 2.1 contains the number of nodes N_V, number of edges N_E, density D, and symmetry level indicated by the size of the automorphism group $|\text{Aut}(\mathcal{G})|$ for 12 power networks. The graph automorphisms are computed in Sage. The bluesizes of $\text{Aut}(\mathcal{G})$ for that set of networks are between 4 and 10^{259}. This symmetry prevalence and its independence to network size, order, and degree distribution justifies applying new symmetry based results to power networks of various sizes. Apart from the high cardinality of the networks, the large number of automorphisms in most power networks relates to the sparseness of the corresponding graphs, as denoted in Table 2.1. The sparse graphs, such as the underlying graph of power networks, are difficult to control as they demand a high number of driver nodes [21]. These issues justify employing symmetry as a concept independent to network size, order, and node degree distribution in order to analyze and improve the controllability of power networks.

2.5.3 Symmetry impact on controllability of power networks

The impact of symmetry on controllability has been verified outside of power networks; see, e.g., [11], [12], and [14]. To observe the impact of symmetry on controllability of power net-

Table 2.1: The specification of the sample power networks

Power Network	N_V	N_E	D	$\lvert Aut_{\mathcal{G}}\rvert$
39-Bus System	39	131	0.1768	4
49-Bus System	49	167	0.1420	144
118-Bus System	118	476	0.0689	4
US Power Grid	274	1612	0.0431	28311552
443-Bus System	443	1623	0.0165	$1.252 * 10^{13}$
685-Bus System	465	1300	0.0055	4096
662-Bus System	662	906	0.0041	16384
1176-Bus System	1176	18552	0.0268	$\sim 10^{259}$
768-Bus System	768	2943	0.0099	$1.73 * 10^{17}$
494-Bus System	494	586	0.0048	$1.80 * 10^{16}$
1138-Bus System	1138	1500	0.0024	$8.84 * 10^{37}$
US Power Grid	4941	13188	0.0010	$5.19 * 10^{152}$

works, the underlying graph is modified by adding an edge to a node that contributes to the automorphism group. After each modification, the number of driver nodes is computed using the exact controllability method proposed in [4].

Random trials have been performed on the 1176-bus system. The number of driver nodes leading to exact controllability of this network is 402. This network contains a large automorphism group which cannot be computed with existing mathematical software (only the size of automorphism group is computed in Sage, that is approximately 10^{259}). However, the building blocks of automorphisms, i.e., generators of automorphisms $Gen(\mathcal{G})$, can be derived using Sage. The 1176-bus system has 381 generators. To run a more reasonable trial, first the nodes are clustered based on their multiplicities in the generator set $Gen(\mathcal{G})$. The 1176-bus system is clustered into sets of 30, 102, 464, 400, and 180 nodes characterized by 4, 3, 2, 1, and 0 multiplicities in generators, respectively, denoted by $\mathcal{N}_j$ where $j \in \{0, 1, 2, 3, 4\}$. Then modification types are defined as adding a distinct edge in N_t trials to each cluster. All edges are added between two nearby nodes to comply with real power network scenarios.

The list of modification types, the number of trials N_t for each kind of modification, the average number of driver nodes N_d after N_t trials, and the ratio $R_{d_{av}}$ of driver nodes to the total number of nodes are presented in Table 2.2. As expected, the number of driver nodes is decreased after modifying those nodes that are contributed in generators of automorphisms. There is a correlation between the number of driver nodes and the size of automorphism group as those nodes with a higher multiplicity in generators are modified by adding an edge to them.

The statistical results presented in Tables 2.1-2.2 inductively prove the existence of certain level of symmetry in power networks which, in turn, motivate extending the symmetry-based theories to power systems. The results also indicate that the traditional measure of symmetry, i.e. $|Aut(\mathcal{G})|$, can not fully capture the correlation between symmetry and controllability. This triggers including other parameters such as orbits of automorphisms in the symmetry index.

Table 2.2: The symmetry modifications on 1176-bus system

Adding an Edge	N_t	$N_{d_{av}}$	$R_{d_{av}}$
between 2 nodes in V_{r_0}	533	403.1	0.34
between V_{r_0} and V_{r_3}	30	390	0.332
between V_{r_0} and V_{r_4}	30	379.7	0.323
between V_{r_1} and V_{r_2}	38	369.2	0.250
between V_{r_1} and V_{r_3}	18	381.5	0.324
between V_{r_1} and V_{r_4}	26	376.6	0.320
between V_{r_2} and V_{r_4}	28	361.2	0.307
between V_{r_3} and V_{r_4}	28	363.8	0.309
between 2 nodes in V_{r_4}	24	294.1	0.250

2.5.4 Simulation on power networks of various sizes

The simulation has been performed on various real and synthetic power networks. The computations related to symmetry structure of the networks such as the size of automorphism group $|\text{Aut}(\mathcal{G})|$, generator set $\text{Gen}(\mathcal{G})$, and orbits of automorphisms $\mathcal{O}(\mathcal{G})$ have been carried out in Sage. The exact controllability method is implemented in MATLAB where the number of driver nodes is attained using (3.2)) and the eigenvalue multiplicity is computed with tolerance 10^{-8}. Unlike maximum matching, the proposed approach in this chapter is not dependent on the node degree distribution. To show its independence to network size and order, the simulation results on three power networks of various sizes are presented.

Small network: 49-bus system

The exact controllability method for the 49-bus system has resulted in 7 driver nodes denoted by green rings in Figure 2.2[2]. The 49-bus system has 144 automorphisms as listed in Table 2.3. The determining set from this automorphism group can be computed from previous methods (presented in Lemma 3.1). One such set is computed as the set of 10 nodes $[9, 10, 11, 24, 25, 26, 1, 4, 47, 48]$. For this small network, the list of automorphisms can be computed, and as such, the previous approach based on automorphism group can be implemented. To modify the network symmetry, an edge is added to node 10 which has the maximum multiplicity in the automorphism group. This causes a drop in the number of automorphisms to 48 after adding an edge between nodes 4 and 10 ($\mathcal{F}_{12} \leftrightarrow \mathcal{F}_{96}$) which is equal to 33% of the $|Aut(\mathcal{G})|$ of the original network. The new determining set is $\{0, 9, 10, 23, 24, 46\}$ denoted by red circles in Figure 2.2. The list of automorphisms of the modified network is presented in Table 2.3. The number of driver nodes after modification has dropped to 5 as illustrated by dashed blue rings in Figure 2.2. This indicates a 28% decrease in the number of control inputs.

However, to illustrate how the proposed approach is effective in reducing the computation burden, we have computed the driver nodes from our proposed approach as follows: The set of

[2]In all computations/drawings by Sage, the node numbering begins with 0.

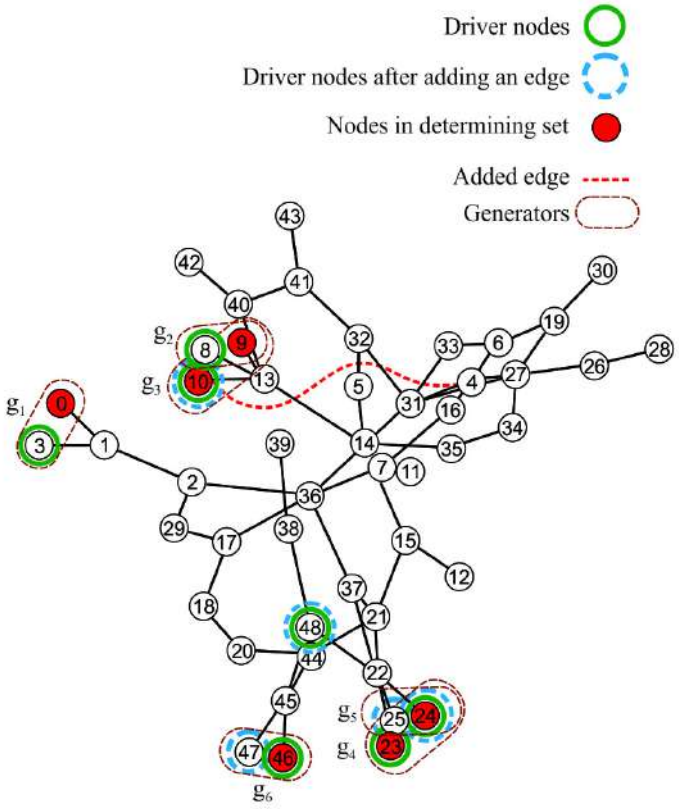

Figure 2.2: The result of exact controllability method on a 49-bus system before and after adding a link between nodes 4 and 10 ($\mathcal{F}_{12} \leftrightarrow \mathcal{F}_{96}$). The number of driver nodes is reduced by 28% following by 67% reduction in the number of automorphism.

generators of automorphisms of 49-bus network is computed in Sage which contains 6 generators as

$$[(46, 47), (24, 25), (23, 24), (9, 10), (8, 9), (0, 3)]$$

which are indicated by g_1,g_2,...,g_6 in Figure 2.2. A determining set from the above set can be computed from our proposed method in Lemma 3.2 as $[46, 24, 23, 10, 9, 3]$. After adding an edge between nodes 4 and 10, one of the generators (the generator (9,10)) will be omitted from the symmetry group leaving the set of generators with 5 generators as the set below:

$$[(46, 47), (24, 25), (23, 24), (8, 9), (0, 3)]$$

A determining set from the above set can be $[46, 24, 23, 9, 3]$. Adding an edge to this network has reduced the number of generators from 6 to 5. Clearly, computing and sweeping over the generator sets are easier than automorphism groups. However, the real impact of the proposed method can be observed in the next sections while computing the symmetry groups of the larger networks.

An interesting result is the high overlap between driver nodes, determining set, and the

generator set. A similar result is attained while examining other networks. This emphasizes the importance of symmetry on the controllability of complex networks.

Table 2.3: The automorphisms groups of 49-bus system and its modified graph

The set of automorphisms 49-bus system	The set of automorphisms 49-bus system after adding an edge between nodes 4 and 10
[(I), (23,24), (46,47), (0,3), (24,25), (9,10), (8,9), (23,24,25), (0,3)(8,9), (8,9,10), (0,3)(9,10), (9,10)(46,47), (23,25,24), (9,10)(23,24), (24,25)(46,47), (8,9)(46,47), (23,24)(46,47), (9,10)(24,25), (8,10,9), (8,9)(23,24), (8,9)(24,25), (0,3)(24,25), (0,3)(46,47), (0,3)(23,24), (0,3)(9,10)(46,47), (23,24,25)(46,47), (0,3)(9,10)(23,24), (0,3)(8,9,10), (9,10)(23,24)(46,47), (8,9)(23,24)(46,47), (8,10,9)(46,47), (0,3)(8,9)(46,47), (0,3)(23,24)(46,47), (8,10), (8,9,10)(23,24), (0,3)(8,9)(23,24), (23,25,24)(46,47), (8,9)(23,25,24), (0,3)(9,10)(24,25), (0,3)(23,25,24), (8,9)(23,24,25), (9,10)(24,25)(46,47), (8,9)(24,25)(46,47), (23,25), (8,10,9)(23,24), (8,9,10)(46,47), (9,10)(23,25,24), (8,10,9)(24,25), (0,3)(8,9)(24,25), (8,9,10)(24,25), (0,3)(24,25)(46,47), (9,10)(23,24,25), (0,3)(8,10,9), (0,3)(23,24,25), (0,3)(8,9)(24,25)(46,47), (0,3)(23,24,25)(46,47), (8,9)(23,25,24)(46,47), (8,9,10)(23,24,25), (8,10)(24,25), (8,9,10)(24,25)(46,47), (8,10,9)(23,24,25), (8,10,9)(23,24)(46,47), (9,10)(23,24,25)(46,47), (0,3)(8,10,9)(46,47), (0,3)(8,10,9)(23,24), (0,3)(8,9,10)(24,25), (0,3)(9,10)(23,24,25), (8,10,9)(23,25,24), (8,10)(46,47), (8,9,10)(23,24)(46,47), (0,3)(9,10)(24,25)(46,47), (9,10)(23,25,24)(46,47), (0,3)(9,10)(23,25,24), (0,3)(23,25,24)(46,47), (8,9)(23,25), (0,3)(8,9)(23,24,25), (0,3)(8,10)(46,47), (8,9,10)(23,25), (0,3)(8,10)(23,24), (0,3)(8,9,10)(23,24,25), (0,3)(8,9)(23,25,24)(46,47), (0,3)(23,25)(46,47), (8,10,9)(23,25), (0,3)(8,9)(23,24,25)(46,47), (0,3)(8,9,10)(23,24)(46,47), (0,3)(8,9,10)(23,25,24), (8,9,10)(23,24,25)(46,47), (0,3)(8,10,9)(23,25,24), (8,10)(23,24,25), (8,10)(24,25)(46,47), (0,3)(9,10)(23,25,24)(46,47), (0,3)(8,10,9)(23,24)(46,47), (0,3)(8,9)(23,25), (8,10)(23,24)(46,47), (0,3)(8,10,9)(23,24,25), (0,3)(8,9,10)(24,25)(46,47), (0,3)(9,10)(23,24,25)(46,47), (8,10,9)(23,25,24)(46,47), (9,10)(23,25)(46,47), (8,9)(23,25)(46,47), (0,3)(8,10,9)(24,25)(46,47), (8,10)(23,25,24), (0,3)(9,10)(23,25), (8,9,10)(23,25,24)(46,47), (0,3)(8,10)(24,25), (8,10,9)(23,24,25)(46,47), (0,3)(8,10)(23,24,25), (0,3)(8,10)(23,25,24), (0,3)(8,9)(23,25)(46,47), (8,10)(23,24,25)(46,47), (8,10)(23,25,24)(46,47), (0,3)(8,10)(24,25)(46,47), (0,3)(8,10,9)(23,24,25)(46,47), (8,10,9)(23,25)(46,47), (8,10)(23,25), (0,3)(8,10)(23,24)(46,47), (0,3)(8,10,9)(23,25), (8,9,10)(23,25)(46,47), (0,3)(8,9,10)(23,25,24)(46,47), (0,3)(8,9,10)(23,24,25)(46,47), (0,3)(8,9,10)(23,25), (0,3)(8,10,9)(23,25,24)(46,47), (0,3)(9,10)(23,25)(46,47), (0,3)(8,9,10)(23,25)(46,47), (0,3)(8,10,9)(23,25)(46,47), (0,3)(8,10)(23,24,25)(46,47), (0,3)(8,10)(23,25), (0,3)(8,10)(23,25,24)(46,47), (8,10)(23,25)(46,47), (0,3)(8,10)(23,25)(46,47)]	(I), (23,24), (46,47), (8,9), (0,3), (24,25), (23,24,25), (0,3)(8,9), (8,9)(46,47), (23,25,24), (8,9)(23,24), (23,24)(46,47), (24,25)(46,47), (8,9)(24,25), (0,3)(24,25), (0,3)(46,47), (0,3)(23,24), (8,9)(23,24)(46,47), (0,3)(8,9)(46,47), (0,3)(24,25)(46,47), (0,3)(23,25,24), (23,25,24)(46,47), (8,9)(24,25)(46,47), (23,24,25)(46,47), (0,3)(23,24)(46,47), (23,25), (0,3)(8,9)(23,24), (8,9)(23,24,25), (8,9)(23,25,24), (0,3)(8,9)(24,25), (0,3)(23,24,25), (0,3)(23,25), (0,3)(8,9)(23,24)(46,47), (8,9)(23,24,25)(46,47), (23,25)(46,47), (0,3)(8,9)(24,25)(46,47), (8,9)(23,25,24)(46,47), (0,3)(23,24,25)(46,47), (0,3)(23,25,24)(46,47), (8,9)(23,25), (0,3)(8,9)(23,25,24), (0,3)(8,9)(23,24,25), (0,3)(8,9)(23,24,25)(46,47), (0,3)(23,25)(46,47), (0,3)(8,9)(24,25)(46,47), (0,3)(8,9)(23,25), (0,3)(8,9)(23,25,24)(46,47), (8,9)(23,25)(46,47), (0,3)(23,25)(46,47), (0,3)(8,9)(23,25)(46,47)]

Table 2.4: The list of nodes with the highest multiplicities

Node	N_r	Node	N_r
8	96	23	16
9	96	24	16
10	96	25	16
23	96	8	12
24	96	9	12
25	96	46	12
0	72	47	12
3	72		
46	72		
47	72		

Medium network: 274**-bus system (US power grid)**

The graph of 274-bus system representing the US power grid with 1612 edges which contains $28,311,552$ automorphisms is shown in Figure 4.6. The number of driver nodes with exact controllability method is 16 nodes denoted by green rings. The set of generators are as below.

$$\begin{aligned} Gen(\mathcal{G}) = \{&(219,220),(212,267),(180,270),(178,179),(177,178),(166,167),(142,193),\\ &(111,112),(95,97),(74,233),(73,207),(67,66),(58,59),(58,57),(54,245),(32,222),\\ &(30,43),(29,145),(19,87),(18,142),(10,35),(7,132),(4,3)\} \end{aligned} \tag{2.27}$$

The determining set from the above set of generators can be attained, that is 19 nodes as below (red circles in Figure 4.6).

$$\{219,222,178,166,142,111,95,73,65,57,54,32,30,29,19,18,10,7,3\} \tag{2.28}$$

The nodes 58, 142, and 178 are repeated two times (which is the maximum multiplicity for this network) in generator set while the rest of nodes in generators are repeated only once. According to Table 2.1, the 274-bus system is less symmetric than the 49-bus system. Proceeding with Algorithm 4, two edges are added between nodes 147 and 178 and nodes 142 and 258 (represented by dashed red lines). These modifications cause a decrease in the size of automorphism group to $3,145,728$ which is equal to 11% of the $|Aut(\mathcal{G})|$ of the original network. Running the exact controllability method for the modified network results in 14 driver nodes as demonstrated with blue rings in Figure 2.3. This is equal to 88% of the N_d of the original network.

Large network: 1176**-bus system**

The 1176-bus system features $18,552$ edges and approximately 10^{259} automorphisms. The modification results are presented in Table 2.2. The original network 402 driver nodes. Some simulation outcomes of this network are already discussed in 2.5.2 upon which a few inferences can be deducted: (i) modifying a node with higher multiplicity in generators will usually results in lower symmetry, and in turn, lower the number of required driver nodes, (ii) there are other factors such as generators and orbits of automorphisms that affect the symmetry index.

The index of symmetry in (2.1) is used to re-evaluate the symmetry level of the network. For the original network $\mathcal{S}(\mathcal{G})$ is equal to 2.4104. The average symmetry index attained after 24 times modification of the nodes with maximum multiplicity in generators (equal to 4) is 2.1958. The minimum symmetry index computed is 1.9129 attained after adding an edge between nodes with maximum multiplicity (i.e., $\mathcal{F}_4 \leftrightarrow \mathcal{F}_4$) which resulted in 294 driver nodes, or equivalently 26% reduction in the number of required driver nodes.

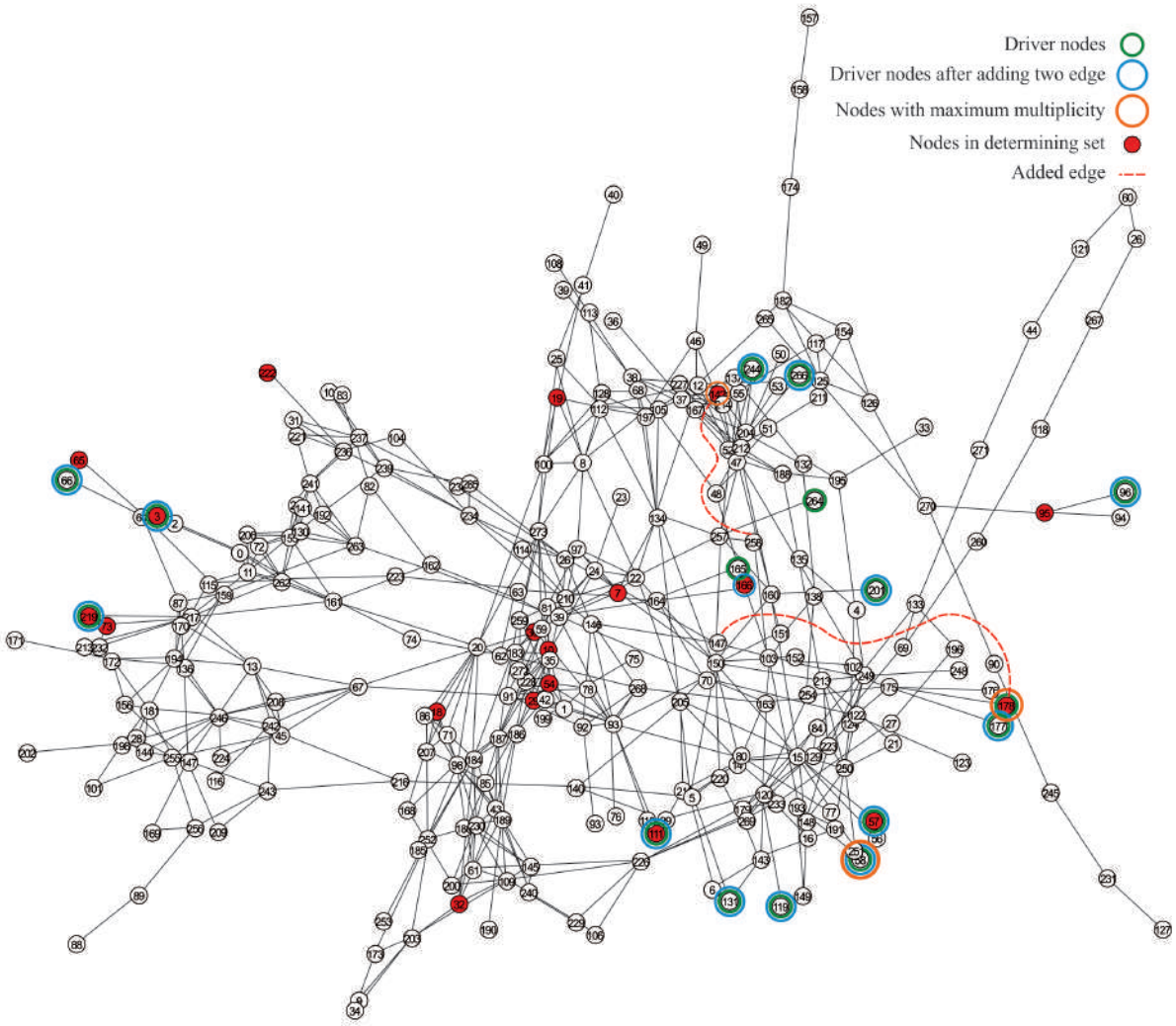

Figure 2.3: The result of exact controllability method for 274-bus system before and after adding a link between nodes 147 and 178 ($\mathcal{F}_0 \leftrightarrow \mathcal{F}_2$), and the second link between nodes 142 and 258 and ($\mathcal{F}_2 \leftrightarrow \mathcal{F}_0$). These modifications have led to 12% reduction in the number of driver nodes following by 89% reduction in following by 67% reduction in the number of automorphism.

2.5.5 Comparing the results of ECM with the set of driver nodes attained from Lemma 3.2

In this section, we investigate the overlap between the set of driver nodes attained from ECM with the set of driver nodes attained from satisfying the necessary conditions (for controllability) of Lemma 3.2. This is shown in Figure 2.2 for 49-bus system. As can be seen, the number of driver nodes for original 49-bus system is 7 which are node 3, 8, 10, 23, 24, 46, and 48. The set of nodes satisfying the conditions of Lemma 3.2 are 6 nodes including nodes 0, 9, 10, 23, 24, 46. Thus, the necessary conditions of Lemma 3.2 has led to only one driver node less than sufficient number of nodes for controllability. Also, 4 nodes are exactly at the same locations. Even if we replace node 0 with node 3 and nodes 9 with 8 (as they belong to the same generators and can act interchangeably) then 6 out of 7 nodes are exactly at the same locations. The comparison

results are presented in Table 2.5 for the three networks investigated in the previous sections. As can be seen, the majority of nodes attained from ECM are also nodes selected in the determining set satisfying the conditions of Lemma 3.2. This means that the proposed necessary conditions is very close to be also sufficient conditions for controllability.

Table 2.5: The number of driver nodes attained from ECM and Lemma 3.2 showing considerable overlap of the nodes' locations between two methods

Network	N_d	$N_{d_{ECM}}$	Overlap
49-bus system	7	6	$\%86$
274-bus system	16	9	$\%56$
1176-bus system	402	309	$\%77$

2.6 Conclusion

This chapter provides further insights into the controllability of complex networks. In particular, the impact of graph symmetry on CN controllability is analyzed and the necessity of controlling the highly symmetric networks via a high number of driver nodes is clarified. The challenge in computing the determining set based on automorphism group is highlighted and a novel and computationally effective solution is proposed which leverages on properties of generators of automorphisms instead of automorphism groups. The new proposed metric of symmetry features more correlation with controllability compared to the traditional measure of symmetry. The proposed modification algorithm is implemented on several real and synthetic networks, where it is verified that the number and locations of the driver nodes can be computed by the proposed approach based on generators of automorphisms which is computationally more effective than the previous approach based on automorphism group. Also, based on a new index of symmetry, the critical nodes of the networks, in terms of their impact on the number of required driver nodes, are identified. It is shown that adding an edge to these critical nodes can significantly reduce the symmetry in the network and, in turn, a lower number of driver nodes will be required for full controllability. Moreover, unlike the common CN modification strategies which necessitate manipulating the node degree distribution, the proposed modification strategy does not impose many modifications to the network topology.

In addition to reducing the number of driver nodes, the modification of the network based on symmetry consideration can change the locations of the driver nodes as well. The implication of this impact on the network operation is one of our future studies. Also, we are working on analytical explanation of the overlap of the results attained from ECM and the results of satisfying the proposed necessary conditions for controllability.

Bibliography

2.7 References

[1] C. C. Chu, H. H. C. Iu, "Complex Networks Theory For Modern Smart Grid Applications: A Survey," *IEEE Journal on Emerging and Selected Topics in Circuits and Systems*, vol. 7, no. 2, pp. 177-191, 2017.

[2] Y. Y. Liu and J. J. W. Slotine, and A. L. Barabasi, "Controllability of complex networks," *Nature*, vol. 473, no.7346, pp. 167-173, May. 2011, doi:10.1038/nature10011.

[3] H. Li, "H_∞ group consensus for partial-state coupled linear systems with fixed and switching topologies in the cooperation-competition networks," *Journal of the Franklin Institute*, vol. 357, no. 1, pp. 314-342, Jan. 2020, doi:10.1038/nature10011.

[4] Z. Yuan and C. Zhao, Z. Di, W. X. Wang, and Y. C. Lai, "Exact controllability of complex networks," *Nature: Communincation*, vol. 4, no.2447, Sep. 2013, DOI: 10.1038/ncomms3447.

[5] A. Farrugia and I. Sciriha, "Controllability of undirected graphs," *Linear Algebra and its Applications*, vol. 454, pp. 138-157, 2014.

[6] F. Pasqualetti, S. Zampieri, and F. Bullo, "Controllability metrics, limitations and algorithms for complex networks," *IEEE Transactions on Control of Network Systems*, vol. 1, no. 1, pp. 40-52, Mar. 2014.

[7] L. Z. Wang, Y. Z. Chen, W. X. Wang, and Y. C. Lai, "Physical controllability of complex networks," *Nature, Scientific Reports*, vol. 7, no. 40198, 2017.

[8] C. T. Lin, "Structural controllability," *IEEE Transactions on Automatic Control*, vol. 9, 2014.

[9] X. D. Gao, W. X. Wang, and Y. C. Lai, "Control efficacy of complex networks," *Nature, Scientific Reports*, vol. 6, no. 28037, Jun. 2016, DOI: 10.1038/srep28037.

[10] J. C. Nacher and T. Akutsu, "Dominating scale-free networks with variable scaling exponent: heterogeneous networks are not difficult to control," *New Journal of Physics*, vol. 14, no. 073005, Jul 2012.

[11] C. O. Aguilar and B. Gharesifard, *A graph-theoretic classification for the controllability of the laplacian leader-follower dynamics*", *53rd IEEE Conference on Decision and Control*, 2014.

[12] A. Rahmani, M. Mesbahi, M. Egersted, "Controllability of multi-agent systems from a graph-theoretic perspective," *SIAM Journal of Control and Optimization*, vol. 48, no. 1, pp. 162-186, 2009.

[13] M. Ji and Egerstedt, "A graph-theoretic characterization of controllability for multi-agent systems," *Proceedings of the 2007 American Control Conference*, 2007.

[14] A. Chapman and M. Mesbahi, "On symmetry and controllability of multi-agent systems," *53rd IEEE Conference on Decision and Control.* Los Angeles, California, USA, 2014.

[15] A. Chapman, M. Nabi-Abdolyousefi, and M. Mesbahi, "Controllability and observability of networks-of-networks via cartesian products," *IEEE Transactions on Automatic Control*, vol. 59, 2014.

[16] A. Chapman and M. Mesbahi, "State controllability, output controllability and stabilizability of networks: A symmetry perspective," *IEEE 54th Annual Conference on Decision and Control (CDC).*, 2015.

[17] A. J. Whalen, S. N. Brennan, T. D. Sauer, and S. J. Schiff, "Observability and controllability of nonlinear networks: The role of symmetry," *Physical Review*, 2015.

[18] A. J. Whalen, S. N. Brennan, T. D. Sauer, and S. J. Schiff, "Effects Of Symmetry On The Structural Controllability Of Neural Networks: A Perspective," American Control Conference, 2016.

[19] E. Capobianco, "Inference From Complex Networks: Role of Symmetry and Applicability to Images," *Front. Appl. Math. Stat.*, 2020.

[20] B. D. MacArthur, R. J. Sanchez-Garcia, and J. W. Anderson, "Symmetry in Complex Networks," *Disc. App. Math.*, vol. 156, 2018.

[21] T. H. Summers and J. Lygeros, "Optimal sensor and actuator placement in Complex Dynamical Networks", *Proceedings of the 19th World Congress The International Federation of Automatic Control.* Cape Town, South Africa. August 24-29, 2014.

[22] Y. J. Zhang, Z. J. Kang, X. F. Li, and Z. M. Lu, "The controllabilty of power grids in comparison with classical complex network models," *IEICE Transactions on Information and Systems*, vol. E99-D, 2016.

[23] S.-P. Pang and F. Hao, "Optimizing controllability of edge dynamics in complex networks by perturbing network structure," *Physica A,* vol. 470, pp. 217–227, 2017.

[24] L. Xiang, F. Chen, W. Ren, and G. Chen, "Advances in network controllability," *IEEE Circuits and Systems Magazine,* Second quarter, 2019.

[25] Y. D. Xiao, S. Y. Lao, L. L. Hou, and L. Bai, "Edge orientation for optimizing controllability of complex networks," *Physical Review E,* vol. 90, no. 4, 2014.

[26] L. L. Hou, S. Y. Lao, M. Small, and Y. D. Xiao, "Enhancing complex network controllability by minimum link direction reversal," *Physical Letters A,* vol. 379, no. 20–21, pp. 1321–1325, 2015.

[27] Y.S. Li, D.Z. Ma, H.G. Zhang, and Q.Y. Sun, "Critical Nodes Identification of Power Systems Based on Controllability of Complex Networks", *Applied Sciencce*, vol. 5, pp. 622-636, 2015.

[28] J. Li, L. Duenas-Osorio, C. Chen, B. Berryhill, and A. Yazdani, "Characterizing the topological and controllability features of U.S. power transmission networks", *Physica A: Statistical Mechanics and its Applications*, vol. 453, 2016.

[29] A. Noori, M. jafari-Shahbazadeh, and M. Eslami, "Designing of wide-area damping controller for stability improvement in a large-scale power system in presence of wind farms and SMES compensator," *International Journal of Electrical Power and Energy Systems*, vol. 119, 2020.

[30] M. Maherani, I. Erlich, and G. Krost, "Robust Centralized Fixed Order Wide Area Damping Controller for wind integrated power system," IFAC-PapersOnLine, vol. 52, 2019.

[31] C.O. Maddela and B. Subudhi, "Robust wide-area TCSC controller for damping enhancement of inter-area oscillations in an interconnected power system with actuator saturation," *International Journal of Electrical Power and Energy Systems*, vol. 105, 2019.

[32] M. Maherani, I. Erlich, and G. Krost, "Fixed order non-smooth robust H_∞ wide area damping controller considering load uncertainties," *International Journal of Electrical Power and Energy Systems*, vol. 115, 2020.

[33] J. Bhukya and V. Mahajan, "Optimization of controllers parameters for damping local area oscillation to enhance the stability of an interconnected system with wind farm," *International Journal of Electrical Power and Energy Systems*, vol. 119, 2020.

[34] A. Al-Ahmad and R. Sirjani, "Optimal placement and sizing of multi-type FACTS devices in power systems using metaheuristic optimisation techniques: An updated review," *Ain Shams Engineering Journal*, In press, 2019.

[35] E. Naderi, M. Pourakhbari-Kasmaei, and h. Abdi, "An efficient particle swarm optimization algorithm to solve optimal power flow problem integrated with FACTS devices," *Applied Soft Computing*, vol. 80, 2019.

[36] M. Ghiasi, "Technical and economic evaluation of power quality performance using FACTS devices considering renewable generations," *Renewable Energy Focus*, vol. 29, 2019.

[37] S. Gasperic and R. Mihalic, "Estimation of the efficiency of FACTS devices for voltage-stability enhancement with PV area criteria," *Renewable and Sustainable Energy Reviews*, vol. 105, 2019.

[38] B. Singh and R. Kumar, "A comprehensive survey on enhancement of system performances by using different types of FACTS controllers in power systems with static and realistic load models," *Energy Reports*, vol. 6,2020.

[39] B. Liu, T. Chu, L. Wang, and G. Xie, "Controllability of a leader-follower dynamic network with switching topology," *IEEE Transactions on Automatic Control*, vol. 53, pp. 1009-1013, 2008.

[40] E. R. Scheinerman, Mathematics: A Discrete Introduction, Thomson, 2nd Edition, 2006.

[41] D. Bonchev, *Information Theoretic Indices for Characterization of Chemical Structures,* Research Studies Press, Chichester, UK, 1983.

[42] M. Ramezani, S. Li, and Y. Sun, "DQ-reference-frame based impedance and power control design of islanded parallel voltage source converters for integration of distributed energy resources," *Electric Power Systems Research*, vol. 168, pp. 67-80, 2019.

[43] A. Bidram, F. L. Lewis, and A. Davoudi, "Distributed control systems for small-scale power networks," *IEEE Control System Magazine*, vol. 34, pp. 56-77, 2014.

[44] S. Chen, H. Jiang, B. Lu, and Z. Yu, "Exponential synchronization for inertial coupled neural networks under directed topology via pinning impulsive control," *Journal of the Franklin Institute*, vol. 357, no. 3, pp. 1671-1689, Feb. 2020.

[45] R. A. Rossi and N. K. Ahmed, "The network data repository with interactive graph analytics and visualization," *Proceedings of the Twenty-Ninth AAAI Conference on Artificial Intelligence.* 2015.

Chapter 3

Graph Automorphic Approaches to the Robustness of Complex Networks

3.1 Overview

Leveraging on graph automorphic properties of complex networks (CNs), this study investigates three robustness aspects of CNs including the robustness of controllability, disturbance decoupling, and fault tolerance against failure in a network element. All these aspects are investigated using a quantified notion of graph symmetry, namely the automorphism group, which has been found implications for the network controllability during the last few years. The typical size of automorphism group is very big. The study raises a computational issue related to determining the whole set of automorphism group and proposes an alternative approach which can attain the emergent symmetry characteristics from the significantly smaller groups called generators of automorphisms. Novel necessary conditions for network robust controllability following a failure in a network element are attributed to the properties of the underlying graph symmetry. Using a symmetry related concept called determining set and a geometric control property called controlled invariant, the new necessary and sufficient conditions for disturbance decoupling are proposed. In addition, the critical nodes/edges of the network are identified by determining their role in automorphism groups. We verify that nodes with more repetition in symmetry groups of the network are more critical in characterizing the network robustness. Further, the impact of elimination of critical network elements on its robustness is analyzed by calculating a new improved index of symmetry which considers the orbital impacts of automorphisms. The importance of all symmetry inspired findings of this chapter is highlighted via simulation on various networks[1].

[1]This chapter is published in *Control Engineering Practice*

Nomenclature

Abbreviations

PBH	Popov-Belevitch-Hautus.
CEA	Community energy association.
CN	Complex network.
CN	Complex network.
CN	Complex network.
CS	Charging station.
ECM	Exact controllability method.
ECM	Exact controllability method.
EV	Electric vehicle.
FACTS	Flexible AC transmission systems.
lcm	The lowest common multiple.
LQR	Linear quadratic regulator.
LTI	Linear time invariant.
MMP	Maximum matching principle.
PCS	Portable charging station.
PEV	Plug-in electric vehicle.
PID	proportional integrative derivative.
VSC	Voltage-source converter.
WAC	Wide area controlled.

Constants

ε Identity (or trivial) permutation.

ε Identity (or trivial) permutation.

c A complex number.

c A complex number.

Q, R, Y Arbitrary weights.

Parameters

α_{sh} Angle of shunt VSC.

β The bus voltage angles.

δ A permutation.

δ_i Maximum algebraic multiplicity of $\lambda_(i)$.

δ_i Maximum algebraic multiplicity of $\lambda_(i)$.

δ_i The angle of voltage of node i.

γ_{sh} Conversion ratio signal.

λ^M Maximum algebraic multiplicity of teh eigenvalue λ^M.

λ^M Maximum algebraic multiplicity of the eigenvalue λ^M.

λ_i The i^{th} eigenvalue.

λ_i The i^{th} eigenvalue.

ν A point (node) of permutation.

σ An automorphism or a Permutation.

σ Permutation.

σ Permutation.

$\mathcal{A}$ Adjacency matrix.

$\mathcal{A}$ Adjacency matrix.

$\mathcal{A}, A$ Adjacency matrix.

$\mathcal{D}$ Degree matrix.

$\mathcal{D}$ The degree matrix.

$\mathcal{E}$ The set of edges.

$\mathcal{E}_c$ The set of critical edges.

$\mathcal{F}$ The determining set attained from Gen($\mathcal{F}$).

$\mathcal{G}$ Graph.

$\mathcal{G}$ Graph.

$\mathcal{G}$ Graph.

$\mathcal{G}_k$ The released graph.

$\mathcal{J}$ The incidence vector of driver nodes.

$\mathcal{K}$ Optimal feedback gain vector.

$\mathcal{L}$ Laplacian matrix.

$\mathcal{L}$ Laplacian matrix.

$\mathcal{L}$ Laplacian matrix.

$\mathcal{S}$ Determining set.

$\mathcal{S}$ Determining set.

$\mathcal{V}$ Controlled invariant subspace.

$\mathcal{V}$ The set of nodes.

$\mathcal{V}_c$ The set of critical nodes.

Aut($\mathcal{G}$) Automorphism group.

Aut($\mathcal{G}$) Automorphism group.

Aut($\mathcal{G}$) Automorphism group.

dimV_{λ_i} Dimension of eigenspace associated with $\lambda(i)$.

dimV_{λ_i} Dimension of eigenspace associated with $\lambda(i)$.

Fix(σ) The set of fixed nodes by permutation.

Gen($\mathcal{G}$) Generators of automorphism.

Gen($\mathcal{G}$) Generators of automorphism.

Gen($\mathcal{G}$) Generators of automorphism.

$\text{Gen}_{dis}(\mathcal{G})$ Set of disjoint generators.

$\text{Move}(\sigma)$ The set of moved nodes by permutation.

$\text{Move}(\sigma)$ The set of moved nodes by permutation.

$\text{Mov}_{v_l}^{Gen}$ the set of generators mapping v_l.

$\mu(\lambda_i)$ Maximum geometric multiplicity of $\lambda(i)$.

$\mu(\lambda_i)$ Maximum geometric multiplicity of $\lambda(i)$.

$\rho_{\mathcal{O}}$ The orbital ratio of symmetry after node removal.

ρ_{aut} The ratio of symmetry after node removal.

σ A permutation.

ε Identity (or trivial) permutation.

φ A generator of automorphism.

ζ A permutation.

ζ_{dis} , δ_{dis} Disjoint generators.

A State matrix.

a_{ij} Element of $\mathcal{A}$.

a_{ij} Weight of ij^{th} element of $\mathcal{A}$.

B Input matrix.

B Input matrix.

B Input matrix.

C Capacitor.

C Size (or capacity) of charging station [kW].

E The set of edges.

E The set of edges.

$F(x_i)$ the individual node's dynamical equation.

F_{vl}^{Gen} The set of generators that fixes v_l.

I_{dc} Capacitor current.

I_{sh} Shunt reactive current setpoint.

I^*_{sh} Reactive current of the outer loop.

$Im\, C$ Image of C.

K The feedback gain.

k The number of distinct mappings.

k_m Conversion ration between the voltage of AC and DC sides.

$ker\, L$ Kernel or null space of L.

l_{ij} The $(i, j)^{th}$ element of the Laplacian matrix.

M A matching.

m Index of a permutation.

M^{Gen}_{vl} The set of generators that moves v_l.

N_D Number of required driver nodes.

N_D Number of required driver nodes.

P The solution of Riccati equation.

p Multiplicity of critical node in Gen($\mathcal{G}$).

P_{ac} Active power on AC side.

P_{ij} Active power flow between nodes i and j.

q The size of disjoint generators.

Q_{ij} Reactive power flow between nodes i and j.

$r^*_{\mathcal{G}}$ Normalized measure of network redundancy.

$r_{\mathcal{G}}$ Network redundancy.

S Determining set.

$s(t)$ The desired state.

$S_{\mathcal{O}}(\mathcal{G})$ Symmetry index based on orbits.

T Waiting time [min].

u Control signal (charging supply).

u Control signal.

u Control signal.

V The set of nodes.

V The set of nodes.

V Voltage.

V_m Voltage magnitude.

V_{dc} Capacitor terminal voltage.

V_{ref} Setpoint voltage.

$w(t)$ Disturbance.

Z Line impedance.

3.2 Introduction

A review on the related works is presented in this section following by motivations on the necessity for addressing CN robustness using graph symmetry. It then proceeds with the contributions and organization of the chapter.

3.2.1 Literature review and motivations

Graph theory, rooted in discrete algebra, has formed increasing applications in CN analysis during the last decade ([1]- [18]). However, in spite of these extensions of graph properties in complex networks, many other graph characteristics and their potential applications in networked systems have remained rather unknown for the community. The wealth of fundamental knowledge of graph theoretic properties that have not yet been widely studied, the significant improvement in the analysis and synthesis of CNs using the abstract network modeling facilitated by CN theory [2], and the necessity to answer many open problems related to CN analysis [3] motivate investigating the impact of other graph properties on network behavior. Among these graph properties, graph symmetry, as described by automorphism group [4], is the focus of this study.

Although the implications of graph symmetry in engineering is not investigated extensively, significant results have attained in [4]- [7] (in a general form of networks) and [8]- [10] (in power networks) explaining some emergent behaviors of complex networks by employing the underlying graph symmetry. In particular, symmetry has been employed to investigate the controllability [5] and robustness [4] of CN in general form of networked systems, and synchronization in power networks ([8]- [10]). It has been verified in [4]- [5] that symmetry is an obstruction

to controllability but it reinforces the robustness. In fact, by attributing the controllability of complex networks to the number of required driver nodes ([11]- [12]), it is shown that the more symmetric network necessitates more driver nodes to be fully controllable [5]. Conversely, a network with higher number of automorphisms has more robust characteristics [4]. These significant impacts of symmetry on fundamental network's behavior stimulate conducting further research in this direction. For this purpose, three aspects of network robustness, i.e., (i) the robustness of controllability, (ii) disturbance decoupling, and (iii) fault tolerance against node failure are discussed below and will be addressed by graph symmetry.

Serious concerns about the robustness of complex networks have been raised during the last decade ([13]- [21]) which necessitate a better understanding of influencing factors and methods for protecting the network. *Robustness* and *fault tolerance* entail wide ranges of topics in networked systems. However, here, *fault tolerance* is defined as the network's ability to tolerate failure in a network element with no significant performance degradation [22]. Also, the *robustness of controllability* is defined as the network ability to preserve the controllablity with a fixed number of driver nodes after a node failure.

It is important to know which network components are critical and if compromised can cause significant malfunctioning of the whole network. For example, a failure in a critical element of a power network can lead to cascading failure or large blackouts ([14] and [19]- [20]). *Robustness* and fault tolerance are addressed by improving the network's ability to tolerate disturbance and node elimination, respectively [22]. To this end, robustness is investigated via the impact of graph symmetry on (1), robustness of controllability (2), disturbance decoupling and (3) fault tolerance against node failure. The necessity to investigate on these issues using symmetry is discussed below.

The traditional rank of controllability is not applicable, in particular, to complex networks as the accurate system parameters are difficult to acquire ([11]- [12] and [23]- [25]). Structural controllability is proposed as a solution in [23] from the graph perspective. Then, the structural controllability problem converted to the problem of finding the minimum number of external inputs to fully control a network [24]. These external inputs are usually referred to as driver nodes ([11] and [26]- [32]) which act as the control nodes through which the control signals can be injected. They could be specified as the non-zero elements of the input matrix of the system. The external control vector is then applied to each node correspondent to each non-zero element of the input matrix. This reformulation of controllability in CNs via finding the set o required driver nodes stimulated many research studies in recent years ([26]- [32]).

Symmetry has been verified to have an important role in controllability of complex networks [5]. However, the necessary conditions of CN controllability attained in [6]- [**?**] impose a serious computation burden as it relies on computing and sweeping over a very big set of automorphisms in order to find the set of driver nodes. The cardinality of automorphism group of typical networks can be $10^{17} - 10^{159}$ (this is verified in [4] and also calculated in simulation section). As a result, it is not practical to compute and sweep over all automorphisms.

Disturbance decoupling is another characteristics of a reliable network ([33]- [36]) that is

investigated in this chapter under the impact of symmetry. To decouple the disturbance, a state feedback must be designed in such a way that the disturbance could not affect the output. Although, various aspects of disturbance rejection in complex networks are addressed in literature, the majority of the proposed approaches rely on designing a specific controller which can not be used when the disturbance or operating conditions are changed.

All the proposed approaches in literature present a method for controller design to address disturbance rejection for specific disturbance and system dynamics. The lack of a more comprehensive approach to deal with disturbance without depending to system's dynamics motivates exploring the common topological properties of the underlying networks. Symmetric structures, as verified in [4] and also in our simulation results, is present in all networks and can be used to find the set of driver nodes [6]. This study verifies that, under a controlled invariant subspace, the disturbance rejection is dependent to the selection of the set of driver nodes attained from symmetry analysis. A significant advantage of the proposed approach is that, instead of proceeding with complicated algorithms for controller design, the disturbance rejection is accomplished via a systematic selection of set of driver nodes under a controlled invariant subspace.

Ideally, we try to protect all network elements. However, this is not feasible in practice as it imposes a high cost, in particular, in physical systems such as power grids. Therefore, it is crucial to identify and protect the most important (critical) nodes of the network. Previous studies on critical node/edge identification have mostly relied on an assessment of graph centrality such as closeness, betweenness, and node degree distribution ([16], [37]- [38]). The idea is to find the set of hub nodes that have significant role in determining the network performance. Node degree is verified as a key to characterize various properties of electricity distribution networks [18]. The node degree distribution then have a critical role in the network vulnerability as nodes with higher degree are considered more critical ([16] and [37]). Therefore, a common approach to enhance the network tolerance against a node failure is to manipulate the node degree distribution. This can entail adding/eliminating lots of nodes/edges over the network ([39]- [41]) or changing the directions of some edges ([17] and [39]). As a result, the proposed modification algorithms are not cost effective.

3.2.2 Contributions

In this chapter, computation issue related to calculating the whole set of automorphism groups is resolved by proposing an alternative approach based on computing and sweeping over generators of automorphisms which are significantly smaller groups than automorphisms. The necessary conditions for full controllability can then be computed effectively by the proposed approach. Furthermore, the necessary conditions for robustness of controllability is attained in this chapter. It is verified that the network can function after a change in its topology if some conditions satisfy on its symmetry group determining the set of driver nodes.

An inherent network property, the multiplicity of a node in the network symmetry factors, called the generator set, is leveraged to find the critical components of complex networks. This

study verifies that even a node with low centrality can have significant impact on network performance if it highly contributes to the construction of the generator set. It will be shown that, using the symmetry analysis, it is enough to manipulate only one or two nodes to modify the symmetry strength of the network. A significant advantage of using symmetry is that the idea relies on an inherent characteristic of the networks, and no network synthesizing or severe structural manipulation are required. Moreover, the chapter will show that symmetry, in the context of automorphisms, is present in all networks independent of network size, order, and degree distribution.

Finally, some interesting results are observed in simulation section which further emphasises on the importance of symmetry in determining the network behaviour. For example, it is observed that the network symmetry and in turn, its robustness, can be independent to nodes degree distribution. This is not aligned with the majority of related literature where only the importance of the most central nodes or hub nodes have been highlighted. According to our symmetry analysis, even a node with low degree distribution can have significant impact on the network robustness. Also, we noticed that there is an overlap between the set of driver nodes attained from symmetry analysis and the set of driver nodes attained from another established method called exact controllability method (ECM). Such observations motivate conducting more studies in this direction.

The rest of this article is organized as follows. Section 3.3 reviews the mathematical preliminaries and definitions. The main results on network robustness using the symmetry characteristics of the underlying graph of the network are presented in Section 3.4. The simulation is carried out on various networked systems in Section 3.5. Finally, the conclusion is presented in Section 3.6.

3.3 Preliminaries

Some mathematical preliminaries and definitions are given in this section. These include some notions from linear algebra, graph theory and, in particular, graph symmetry.

Definition 3.3.1. *The column space (also called image) of a matrix A is the set of all linear combinations of its column vectors. If A is an $m \times n$ matrix where its column vectors are $\mathbf{v}_1, ..., \mathbf{v}_n$ and a linear combination of these vectors form*

$$c_1\mathbf{v}_1 + c_2\mathbf{v}_2 + ... + c_n\mathbf{v}_n,$$

where $c_1, c_2, ..., c_n$ are scalars, the image of A is the column space of all possible compositions $A\mathbf{x}$ for $\mathbf{x} \in \mathbf{c}^n$.

Definition 3.3.2. *The kernel (also called null space) of a linear map $L : V \to W$ between two vector spaces V and W is the set of all elements $\mathbf{v}$ of V for which $L(\mathbf{v}) = 0$, where $\mathbf{0}$ denotes the zero vector in W, i.e., ker $L = \{\mathbf{v} \in V \mid L(\mathbf{v}) = \mathbf{0}\}$.*

3.3.1 Graph theory

An undirected graph $\mathcal{G}$ is composed of a set of un-ordered pairs of nodes V and edges E and is denoted by $\mathcal{G}(V, E)$ or simply $\mathcal{G}$. Two nodes v_1 and v_2 are said to be adjacent if there is an edge between them. The size and order of $\mathcal{G}$ are denoted by $|V|$ and $|E|$, respectively. An *adjacency matrix*, denoted by $\mathcal{A}$, is a square $|V| \times |V|$ matrix whose element, a_{ij}, indicates whether pairs of nodes i and j are connected together or not. For a simple graph, if there is an edge from node i to node j then a_{ij} is one, otherwise it is zero. The degree matrix $\mathcal{D}$ is a diagonal matrix where d_{ii} is the number of edges attached to node i. The Laplacian matrix is a form of representing $\mathcal{G}$ and is defined as $\mathcal{L} = \mathcal{D} - \mathcal{A}$ where $\mathcal{D}$ is the degree matrix,.

Definition 3.3.3. *A subgraph of $\mathcal{G}$ is a graph $\mathcal{H}$ such that $V_{\mathcal{H}} \subset V_{\mathcal{G}}$ and $E_{\mathcal{H}} \subset E_{\mathcal{G}}$. In general, any isomorphic graph to a subgraph of $\mathcal{G}$ is also said to be a subgraph of $\mathcal{G}$.*

Definition 3.3.4. *The composition or product of two functions ζ and δ, denoted by $\zeta \circ \delta$ is the pointwise action of ζ to the result of δ which generates a third function. The notation $\zeta \circ \delta$ is read as "ζ composed with δ" and $(\zeta \circ \delta)\big|_{(i)}$ denotes the pointwise composition of ζ and δ" on point i. Intuitively, by composition of two functions, the pointwise output of the inner function becomes the input of the outer function.*

The composition of two permutations is calculated in the simple example below.

Example 3.3.1. *Let ζ and δ be given by*

$$\zeta = (1 \quad 2 \quad 3 \quad 4) \quad and \quad \delta = (1 \quad 3).$$

To compute the composition of ζ and δ, $\zeta \circ \delta$, first we have to check the commutation (represented by the symbol $\mapsto$) of element by δ and then its commutation by ζ. In this example

$$\begin{aligned} 1 \mapsto^{\delta} 3 \mapsto^{\zeta} 4 \quad &\Rightarrow \quad (\zeta \circ \delta)\big|_{(1)} = 4 \\ 4 \mapsto^{\delta} 4 \mapsto^{\zeta} 1 \quad &\Rightarrow \quad (\zeta \circ \delta)\big|_{(4)} = 1 \\ 3 \mapsto^{\delta} 1 \mapsto^{\zeta} 2 \quad &\Rightarrow \quad (\zeta \circ \delta)\big|_{(3)} = 2 \\ 2 \mapsto^{\delta} 2 \mapsto^{\zeta} 3 \quad &\Rightarrow \quad (\zeta \circ \delta)\big|_{(2)} = 3. \end{aligned}$$

Thus the composition of ζ and δ is $\zeta \circ \delta = (1 \quad 4)(3 \quad 2)$.

A *permutation* σ is defined as the act of rearranging a subset of nodes of $\mathcal{G}$. The *order of permutation*, denoted by order(σ), is the smallest positive integer m such that $\sigma_1 \circ \sigma_2 \circ \ldots \circ \sigma_m = \sigma^m = \varepsilon$ where ε is the identity (trivial) permutation.

Two permutations ζ and δ are *disjoint* if each node moved by ζ is fixed by δ, or equivalently, every node moved by δ is fixed by ζ, otherwise they are called *joint* permutations. The set of nodes that are not mapped by a permutation are *fixed* nodes, and the set of nodes that are mapped is called *moved* nodes. Also the set of permutations that map a node v_l is denoted by Mov_{v_l}.

Definition 3.3.5. *Two permutations ζ and δ commute if $\zeta \circ \delta = \delta \circ \zeta$.*

Lemma 3.3.1. *Disjoint cycles commute, i.e., if $\zeta = (u_1...u_r)$ and $\delta = (v_1...v_r)$ are disjoint cycles then $\zeta \circ \delta = \delta \circ \zeta$.*

Proposition 3.3.1. *The composition of disjoint permutations does not move an already fixed node by all of these permutations. Equivalently, the composition of disjoint permutations does not fix an already moved node by one of the permutations.*

3.3.2 Graph symmetry

Graph symmetry rooted in discrete mathematics can be revealed by automorphism groups. Automorphism is a form of symmetry in which the graph is mapped onto itself while preserving the graph structure, meaning the adjacency or Laplacian matrix of the underlying graph remains unchanged under mapping by an automorphism. This is illustrated by a simple example below.

Example 3.3.2. *Consider the simple triangle graph of Figure 3.1. The adjacency matrix of this graph is*

$$\begin{pmatrix} 0 & 1 & 1 \\ 1 & 0 & 1 \\ 1 & 1 & 0 \end{pmatrix}$$

An automorphism of this graph is $(1\,2\,3)$ which permute nodes 1, 2, and 3 to nodes 2, 3, and 1, respectively. However, the adjacency matrix of the graph remain the same as the above matrix under the act of this automorphism.

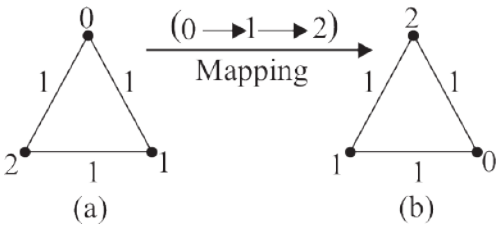

Figure 3.1: The graph of Example 2.2

Definition 3.3.6. *An automorphism of $\mathcal{G}$ is a permutation σ for which $\{i, j\} \in E(\mathcal{G})$ (where $E(\mathcal{G})$ is the set of edges of $\mathcal{G}$) if and only if $\big(\sigma(i), \sigma(j)\big) \in E(\mathcal{G})$. The automorphism group of $\mathcal{G}$ and its size are denoted by $Aut(\mathcal{G})$ and $|Aut(\mathcal{G})|$, respectively.*

Each automorphism can be attained by the multiplication of some elementary automorphisms (also called generator of of automorphisms). Throughout this chapter, automorphisms are divided into two categories: (i) generators of automorphisms, and (ii) ordinary automorphisms. Each ordinary automorphisms can be attained from the compositions of generators or other ordinary automorphisms. This is illustrated by the simple example below.

Example 3.3.3. *For the simple graph of Figure 3.1.(a), the set of generators and automorphisms are computed in Sage as*

$$Gen(\mathcal{G}) = \{(1,2),(0,1)\}$$
$$Aut(\mathcal{G}) = \{(I),(1,2),(0,1),(0,2,1),(0,1,2),(0,2)\}$$

In the above set of automorphism, (I) is identity or trivial automorphism. The second and third automorphisms are also generators of automorphisms. The last three automorphisms can be attained from the compositions of other automorphisms as:

$$(1,2)\circ(0,1) = (0,2,1)$$
$$(0,1)\circ(0,2,1) = (0,2)$$
$$(1,2)\circ(0,2) = (0,1,2).$$

No non-repetitive automorphism can be generated by any composition of the automorphisms. A permutation matrix, denoted by $\mathcal{J}$, is a square binary matrix attained by permuting the rows of an identity matrix where every permutation matrix associates to a unique permutation (here the permutation is either an automorphism or a generator).

Definition 3.3.7. *The incidence vector or indicator vector or characteristic vector of a subset T of a set S is the vector $x_T \coloneqq (x_s)_{s\in S}$ such that $x_s = \mathbf{1}$ if $s \in T$ and $x_s = 0$ if $s \notin T$.*

Lemma 3.3.2. *Let two nodes $a, b \in \mathcal{G}$ and σ be a permutation on $\mathcal{G}$. By defining $a \sim b$ if and only $b = \sigma^n(a)$ for $n \in \mathbb{Z}$, then $\sim$ is an equivalence relation on $\mathcal{G}$. This equivalence classes are called orbits of $\mathcal{G}$.*

3.3.3 The exact controllability method (ECM)

In this study, the exact controllability method ([11]) is used to compute the number of required driver nodes satisfying the full CN controllability. The approach is based on maximum multiplicity of eigenvalues to attain the number of driver nodes N_d after each modification. It has been verified in [11] that the minimum number of driver nodes can be computed by the maximum geometric multiplicity $\mu(\lambda_i)$ of the eigenvalue λ_i of the coupling matrix $\mathcal{A}$:

$$N_d = \max_i\{\mu(\lambda_i)\} \tag{3.1}$$

where

$$\mu(\lambda_i) = \dim V_{\lambda_i} = N - \text{rank}(\lambda_i I_N - A) \tag{3.2}$$

and $\lambda_i (i = 1, ..., l)$ represents the eigenvalues of A. For undirected weighted networks, the maximum algebraic multiplicity $\delta(\lambda_i)$ determine the number of driver nodes as

$$N_d = \max_i\{\delta(\lambda_i)\} \tag{3.3}$$

where $\delta(\lambda_i)$ is also the eigenvalue degeneracy of matrix A [11]. Using the elementary column transformation on the matrix $(\lambda^M I_N - A)$ a reduced row echelon form of the adjacency matrix can be attained. Subsequently, the set of linearly dependent rows corresponds to the driver nodes which is equivalent to the maximum geometric multiplicity. Consider the general form of linear time invariant system as

$$\dot{x} = A\boldsymbol{x}(t) + B\boldsymbol{u}(t) \tag{3.4}$$

where A is the coupling or (adjacency) matrix, B is the input matrix, $\boldsymbol{x}(t)$ is the state vector, and $\boldsymbol{u}(t)$ is the control vector. According to the exact controllability method, system (3.4) is controllable if and only if

$$\text{rank}(cI_N - A, B) = N \tag{3.5}$$

is satisfied for any complex number c, where I_N is the identity matrix of dimension N.

3.4 Symmetry impact on complex network robustness

This section focuses on the concept of graph symmetry to address a few issues related to the robustness of complex networks. Three aspects of network robustness are addressed. First, the network's ability to function after failure in a critical element is examined. This is attributed to the *robustness of controllability* referring to network controllability after failure. This parameter is assessed by the number of required driver nodes for full controllability before and after a node failure. The Second aspect of robustness points to the robustness of the grid against disturbance (disturbance decoupling) which is analyzed under the impact of symmetry. The third aspect of robustness deals with the identification of the most critical network elements in terms of their contributions in symmetry group and, in turn, grid robustness. *Fault tolerance* points to the network ability to preserve controllability (or tolerate failure or loss of a node) with a fixed set off driver nodes. The set of "critical" nodes/edges should be defined: A node/edge that has the most impact on the cardinality of automorphism group is considered as a *critical* element since, as will be verified, the elimination of nodes/edges with more multiplicity in the symmetry group can significantly change the number of required driver nodes. Subsequently, *controllability* means that the network can be driven from any initial state to any final state in finite time using a set of driver nodes. All findings of this chapter are attained by leveraging on the concept of symmetry.

In controlled consensus problem, the external control signal $u(t) \in \mathbb{R}^q$ should be applied to node i through input matrix $\overline{B}_i \in \mathbb{R}^q$. The individual node's dynamics can be written as

$$\dot{x}_i(t) = -\sum_{\{i,j\}\in E} (x_i - x_j) + \overline{B}_i^T u(t) \tag{3.6}$$

where $x_i(t) \in \mathbb{R}$ is the state of node $i \in V$ at time t. The network's dynamics at time t is observed by a $y(t) \in \mathbb{R}^p$ via an output matrix $C \in \mathbb{R}^{p\times n}$. The full network dynamics is then

given by

$$\begin{aligned} \dot{x}(t) &= -\mathcal{L}(\mathcal{G})x(t) + Bu(t) \\ y(t) &= Cx(t) \end{aligned} \tag{3.7}$$

where $B = [\overline{B}_1, \overline{B}_1, ..., \overline{B}_n]^T \in \mathbb{R}^{n\times q}$. For a set of input nodes or driver nodes in the graph as $S = [i_1, i_2, ..., i_q]$ for $i_1 < i_2 < ... < i_q$ the associated input matrix is given by $B(S) = [e_{i_1}, e_{i_2}, ..., e_{i_q}] \in \mathbb{R}^{n\times q}$.

The network dynamics given in (3.7) is said to be controllable if the pair $(-\mathcal{L}(\mathcal{G}), B)$ is controllable. This criterion is restated in proposition below according to the network symmetric characteristics.

Proposition 3.4.1. *[5] A graph $\mathcal{G}$ is uncontrollable from any pair $(-\mathcal{L}(\mathcal{G}), B(S))$, if there exist a nontrivial automorphism of $\mathcal{G}$ which fixes all inputs in the set S.*

In [5], the choice of driver nodes is attributed to the determining set via Corollary 4.3.1 where the state matrix is replaced by the adjacency matrix.

Corollary 3.4.1. *[5] Let $\mathcal{A}(\mathcal{G})$ represents the adjacency matrix of the graph $\mathcal{H}$. A necessary condition for controllability of the pair $(A(\mathcal{G}), B(S))$ is that S is a determining set.*

3.4.1 CN controllability and robustness of controllability based on symmetry groups

The necessary conditions for controllability (or sufficient conditions for uncontrollability) have been attained in [5] as proposition below.

Proposition 3.4.2. *[5] The system of Equations (3.4) is uncontrollable if there exists a nontrivial automorphism of $\mathcal{G}$ which fixes all inputs in the set of driver nodes S (or equivalently matrix B).*

This proposition can be restated using the concept of determining set defined as below.

Definition 3.4.1. *A set of vertices S is a determining set for a graph $\mathcal{G}$ if every automorphism of $\mathcal{G}$ is uniquely determined by its action on S. Equivalently, a subset S of the vertices of a graph G is called a determining set if whenever $g, h \in Aut(\mathcal{G})$ so that $g(s) = h(s)$ for all $s \in S$, then $g = h$.*

The above lemma implies that to find the whole set of driver nodes, one have to compute and sweep over the whole set of automorphism group $Aut(\mathcal{G})$. The typical cardinality of automorphism group for complex networks can be as big as 10^{17} (this is verified in [4] and also computed in simulation section for several networks). Obviously, computing and sweeping over this set is not computationally effective. Lemma below presents an alternative approach based on generators of automorphisms.

Lemma 3.4.1. *Let σ be an automorphism attained from the composition of some generators of automorphisms $\sigma_1, \sigma_2, ..., \sigma_r$ where their orders are $\epsilon_1, \epsilon_2, ..., \epsilon_r$, respectively. The necessary conditions for controllability of $\mathcal{G}^*$ are*

(i) if order(σ) = lcm$(\epsilon_1, \epsilon_2, ..., \epsilon_r)$ where lcm stands for the lowest common multiple, then there is at least one node n^* in the set of nodes $V^* \in \{\sigma_1 \cap \sigma_2 \cap ...\sigma_r\}$ for which $n^* \in S^*$,

(ii) if order$(\sigma) \neq$ lcm$(\epsilon_1, \epsilon_2, ..., \epsilon_r)$ then for the joint node/s n_j where $n_j \in V^*$, $n_j^* \notin S^*$,

(iii) if all nodes in V^* are joint nodes then $V^* \in S^*$, and

(iv) if a node $n_a \notin$ Gen$(\mathcal{G})$ then n_a can be excluded from S^*.

Proof. Any automorphism σ is a composition of either joint or disjoint generators and/or mediator automorphisms. If $\sigma_1, \sigma_2, ..., \sigma_r$ are disjoint, according to commuting property of permutations, one can write

$$(\sigma_1 \circ \sigma_2 \circ ...\sigma_r)^z = \sigma_1^z \circ \sigma_2^z \circ ... \circ \sigma_r^z$$

for all positive integers z. Let m be the lowest common multiple of the integers $\epsilon_1, \epsilon_2, ..., \epsilon_r$. Then

$$(\sigma_1 \circ \sigma_2 \circ ...\sigma_r)^m = \sigma_1^m \circ \sigma_2^m \circ ...\sigma_r^m$$

and clearly $(\sigma_1 \circ \sigma_2 \circ ...\sigma_r)^m = \varepsilon$. On the other hand, if $(\sigma_1 \circ \sigma_2 \circ ...\sigma_r)^m = \varepsilon$ it follows (from the permutations being disjoint) that the order of each σ_i is m or $\sigma_i^m = \varepsilon$. Therefore m is divisible by each ϵ_i which leads to

$$\text{order}(\sigma_1 \circ \sigma_2 \circ ...\sigma_r) = m = \text{lcm}(\epsilon_1, \epsilon_2, ..., \epsilon_r).$$

Then for S^* to be a determining set there should be at least one node n^* in S^* that also belongs to set of nodes in $\sigma_1 \cap \sigma_2 \cap ...\sigma_r$. Similarly, if $(\sigma_1 \circ \sigma_2 \circ ...\sigma_r)$ contain two or more joint permutations then order$(\sigma) \neq$ lcm$(\epsilon_1, \epsilon_2, ..., \epsilon_r)$. Consequently, joint nodes have to be excluded from the determining set, i.e., $n_j \notin S^*$. Finally, if all nodes in the composition $(\sigma_1 \circ \sigma_2 \circ ...\sigma_r)$ are joint nodes (which is very rare) then all nodes V^* are in S^*. Finally, condition (iv) is straightforward considering that if a node is fixed by all generators then the composition of generators or/and mediator automorphisms will not move it. □

The above lemma relates the necessary conditions of CN controllability to the selection of a set of driver nodes attained from generators of automorphisms $Gen(\mathcal{G})$. The cardinality of $Gen(\mathcal{G})$ is very smaller than $Aut(\mathcal{G})$. It is thus computationally more effective to attain the set of driver nodes from $Gen(\mathcal{G})$ instead of $Aut(\mathcal{G})$.

The network controllability (or the number of required drive nodes) can be affected once the network topology is changed following a failure in a network element. Robustness of controllability can be guaranteed if the selection of nodes in determining set are constrained to some conditions on generators of automorphisms. These conditions are formalized in the theorem below.

Theorem 3.4.1. *Assume that the adjacency matrix of $\mathcal{G}$ is diagonalizable and symmetry preserving and b is the indicator vector associated to the set S of N_d driver nodes. Let the network topology after attacks be denoted by $\mathcal{G}^*$. If the robustness of controllability of $\mathcal{G}$ in case of a successful attack manipulating the network topology to $\mathcal{G}^*$ is guaranteed then*

(i) Given g_k^* as a generator of automorphism of $\mathcal{G}^*$, if all $j \in V_{g_k^*}$ are joint nodes then all nodes of g_k^* are in S, otherwise $j \notin S$ where j is the joint node/s of the pairwise joint generators, and

(ii) there is no non-trivial generator g^* of $\mathcal{G}$ that fixes S, and

(iii) if all eigenvalues of $M = J - I - 2\mathcal{A}$, where I and J are the identity and unit matrices, be simple then $S \nsubseteq \Phi_g$ where Φ_g is the set of fixed nodes by all generators of automorphisms.

Proof. Consider the matrix W defined as

$$W = [\mathcal{J} \quad \mathcal{A}\mathcal{J} \quad ... \quad \mathcal{A}^{n-1}\mathcal{J}] \tag{3.8}$$

where $\mathcal{J}$ is the incidence vector associated with the set of driver nodes. Then W is invertible if the network is robustly controllable. Considering $\mathcal{M}_p$ as the permutation matrix associated with $Aut(\mathcal{G})$, then the set of generators that fix the driver nodes as a set need to satisfy $\mathcal{M}_p\mathcal{J} = \mathcal{J}$. Subsequently, it can be written

$$\begin{aligned} \mathcal{M}_p W &= [\mathcal{M}_p\mathcal{J} \quad \mathcal{M}_p\mathcal{A}\mathcal{J} \quad ... \quad \mathcal{M}_p\mathcal{A}^{n-1}\mathcal{J}] \\ &= [\mathcal{M}_p\mathcal{J} \quad \mathcal{A}\mathcal{M}_p\mathcal{J} \quad ... \quad \mathcal{A}^{n-1}\mathcal{M}_p\mathcal{J}] \end{aligned} \tag{3.9}$$

where along with $\mathcal{M}_p\mathcal{J} = \mathcal{J}$ one can conclude $\mathcal{M}_p W = W$. Since W is invertible then $\mathcal{M}_p$ needs to be identity matrix which, in turn, implies that the only generator of $\mathcal{G}$ that fixes the driver nodes is the identity or trivial permutation. Contrastingly, the joint nodes of generators have to be excluded from the driver nodes since the composition of joint generators may fix the joint node. Consequently, there will be an automorphism that fixes the joint node which is also a driver node. This contradicts the required conditions for controllability mentioned in Corollary 4.3.1. In the case where all nodes of a generator are joint nodes all nodes need to be included in driver nodes so that there won't be an automorphism that fixes all nodes in S except for identity. From the properties of compositions of permutations one can write

$$Mov\{\zeta_{dis}^r \circ \delta_{dis}^s\} \subset Mov\{Gen_{dis}\}$$

where ζ_{dis} and δ_{dis} are disjoint generators and r and s are the orders of generators in composition. This simply means that the compositions of disjoint generators does not move an already fixed node by all of those generators. Then the proof of part (iii) is a straightforward result of Theorem 5.8 in [44]. □

The above theorem relates the selection of driver nodes to some permutation properties of

generator set. The use of this theorem is computationally effective as it relies on sweeping over a limited number of permutations.

3.4.2 Robustness against disturbance by employing the concepts of determining set and controlled invariant subspace

In this section, a model of network with disturbance is considered as

$$\dot{x}(t) = f(x(t), u(t), w(t)) \tag{3.10}$$

where $w(t) \in \mathbb{R}^n$ is the disturbance which can possibly represent external disturbances, modeling uncertainty, parameter uncertainty, and unmodeled nonlinear dynamics, etc. The disturbance decoupling problem is thus to find a state feedback so that the outputs are not disturbed by w.

Definition 3.4.2. *In the state space model of the systems, if there is a subspace that contains the initial states then it is possible to preserve the states in that subspace at all times. This subspace is called a controlled invariant subspace. For the LTI system of (3.4), the subspace $\mathcal{V}$ is an (A, B)-invariant or controlled invariant subspace if*

$$(A + Bk)\mathcal{V} \subseteq \mathcal{V} \tag{3.11}$$

where k is the feedback gain.

In configuring the choice of determining set of automorphism group (or generator set) according to the concept of controlled invariant subspace, a new lemma is proposed below which presents the necessary and sufficient conditions for disturbance decoupling. The resulted determining set also preserves the necessary condition of controllability as verified earlier in Theorem 8.2.

The general form of LTI systems considering the disturbance can be written as

$$\begin{aligned} \dot{x}(t) &= Ax(t) + Bu(t) + Ew(t) \\ y &= Cx(t) \end{aligned} \tag{3.12}$$

where $w(t) \in \mathbb{R}^n$ is a vector of unmeasured signals which lumps the impacts of all disturbances. In a network with controlled consensus protocol of (3.7), a node's dynamics with disturbance is given by

$$\begin{aligned} \dot{x}(t) &= -\mathcal{L}x(t) + Bu(t) + Ew(t) \\ y &= Cx(t), \end{aligned} \tag{3.13}$$

where $B = [\overline{B}_1, \overline{B}_2, ..., \overline{B}_n]^T \in R^{n \times q}$.

Theorem 3.4.2. *The set of driver nodes attained from the determining set characterizes the network model of (3.13) as*

$$\begin{aligned} \dot{x}(t) &= -\mathcal{L}x(t) + \mathcal{S}u(t) + Ew(t) \\ y &= Cx(t) \end{aligned} \tag{3.14}$$

where $\mathcal{S} \in \mathbb{R}^q$ is the characteristic matrix associated to the determining set attained from the $Aut(\mathcal{G})$ or $Gen(\mathcal{G})$ such that $\mathcal{S}_{i,1} = 1$ if $v_i \in S$ otherwise $\mathcal{S}_{i,1} = 0$. Assume that the adjacency matrix of the network $\mathcal{G}$ is diagonalizable and symmetry preserving. With fixed control feedback k, the disturbance E can be decoupled if S^* satisfies

$$\textit{Im}\, E \subseteq \langle -\mathcal{L} + S^*k \,|\, \textit{Im}\, E \rangle \subseteq \textit{ker}\ C. \tag{3.15}$$

Proof. The Equation (3.13) can be written as

$$\dot{y}(t) = C(-\mathcal{L} + Sk)x(t) + ECw(t)$$

To decoupe the disturbance, the second term in the above equation must be zero, i.e., $CE = 0$. Subsequently, by assuming $C(\mathcal{L} + Sk)^{i-2}E = 0$ where $i \geq 2$, one can write

$$y^{(i)} = C(-\mathcal{L} + Sk)^i x + C(-\mathcal{L} + Sk)^{i-1}Ew.$$

Then the following conditions must be satisfied

$$\begin{aligned} CE &= 0 \\ C(-\mathcal{L} + Sk)^{i-1}E &= 0 \end{aligned} \tag{3.16}$$

where $i = \{0, 1, ..., n\}$. The above equation can be restated as

$$\begin{aligned} &\text{Im } E \subseteq \text{ker } C \\ &(-\mathcal{L} + Sk)^{i-1}\text{Im } E \subseteq \text{ker } C. \end{aligned} \tag{3.17}$$

Equivalently,

$$\langle -\mathcal{L} + S^*k \,|\, \text{Im } E \rangle \subseteq \text{ker } C \tag{3.18}$$

i.e., $\langle \mathcal{L} + S^*k \,|\, \text{Im } E \rangle \subseteq \text{ker } C$ features $(\mathcal{L}, B)$-invariant or controlled invariant property. If $E \subseteq \langle \mathcal{L} + S^*k \,|\, \text{Im } E \rangle$ then

$$\langle -\mathcal{L} + S^*k \,|\, \text{Im } E \rangle \subseteq \langle -\mathcal{L} + S^*k \rangle \subseteq \text{ker } C$$

and it is necessary that

$$\langle -\mathcal{L} + Sk \,|\, \text{Im } E \rangle \subseteq \text{ker } C.$$

Since $\langle -\mathcal{L} + Sk \,|\, \text{Im } E \rangle$ is an $(-\mathcal{L}, \mathcal{S})$ invariant subspace of ker C, then $\langle -\mathcal{L} + Sk \,|\, \text{Im } E \rangle \subseteq$

$\langle -\mathcal{L} + S^*k \,|\, \text{Im } E\rangle$. Subsequently Im $E \subseteq \langle -\mathcal{L} + Sk \,|\, \text{Im } E\rangle$ results in Im $E \subseteq \langle -\mathcal{L} + S^*k \,|\, \text{Im } E\rangle$. □

Theorem 3.4.2 presents the necessary and sufficient conditions for disturbance decoupling in the networked system of (3.14). It relates the disturbance decoupling to the appropriate selection of determining set (attained from symmetry groups, i.e., $Aut(\mathcal{G})$ and $Gen(\mathcal{G})$) and control feedback gain.

3.4.3 Critical nodes identification based on symmetry

As verified in [4], symmetry can improve the network's robustness by inducing redundancy which, in turn, provides structural backups against attacks [21]. The more often any given node is repeated in $Aut(\mathcal{G})$, the more effective it is in the structural robustness of the underlying network. However, since $|Aut(\mathcal{G})|$ for a typical network is usually a very big number ([4]) it is not cost effective to find the whole set of automorphisms (this is also verified in simulation section in Table 1). Instead, we propose another criteria to quantify the role of each node in symmetry and, in turn, in network robustness. To this end, the elementary factors of automorphisms or generators of automorphisms ($Gen(\mathcal{G})$) are used. Lemma 3.4.2 formalizes this adaption from automorphism group to the set of generators.

Lemma 3.4.2. *For a given graph $\mathcal{G}$, if the multiplicity of a node v_l in $Gen(\mathcal{G})$ is p, then the multiplicity of v_l in $Aut(\mathcal{G})$ is greater or equal to $p(1+q)$ where q is the cardinality (size) of the set of generators that fix v_l.*

Proof. Let the set of generators that map v_l be denoted by

$$\text{Mov}_{v_l}^{Gen} := \{\delta_1, \delta_2, ..., \delta_p\}$$

and the set of generators that fix v_l be denoted by $\{\sigma_1, \sigma_2, ..., \sigma_q\}$. Given the pointwise product of $\{\sigma_1, \sigma_2, ..., \sigma_q\}$ and $\{\delta_1, \delta_2, ..., \delta_p\}$ be denoted by $\Delta. \circ \Sigma$, we can write

$$|\text{Mov}_{v_l}^{Aut}| \geq |\text{Mov}_{v_l}^{Gen}| + |\text{Mov}_{v_l}^{\Delta.\circ\Sigma}|$$

where $|.|$ stands for the cardinality of the set. Clearly, the above inequality can be written as

$$|\text{Mov}_{v_l}^{Aut}| \geq (p + p.q) = p(1+q).$$

□

Lemma 3.4.2 guarantees a lower bound on the multiplicity of a node v_l in $Aut(\mathcal{G})$ as long as v_l is permuted by at least one generator. Implied by the above lemma, one can determine the most repeated nodes in $Aut(\mathcal{G})$ by only assessing $Gen(\mathcal{G})$ without imposing a large computation burden. The node multiplicity can be used as a measure of each node/edge's impact on symmetry strength of the network. In fact, it is enough to compute the size of automorphism

group $|Aut(\mathcal{G})|$ after deleting each node with maximum multiplicity. The higher increase in $|Aut(\mathcal{G})|$ after each modification means that the modified node/edge is more effective in the structural robustness of the network and, in turn, is considered as a more critical node. This is also verified by simulation on several networks and discussed in the simulation section.

3.4.4 Fault tolerance against node elimination based on a novel symmetry index

We can compute the size of automorphism group before and after node elimination. Then the consistency between the number of required driver nodes with the network's symmetry level can be investigated. We attain the ratio of the symmetry after node removal to the original network's symmetry using equation below:

$$\rho_{aut} = \%\frac{|\overline{\text{Aut}(\mathcal{G})}|}{|\text{Aut}^*(\mathcal{G})|} \times 100 \tag{3.19}$$

where $|\text{Aut}^*(\mathcal{G})|$ and $|\overline{\text{Aut}(\mathcal{G})}|$ are the size of automorphism group of original network and the average size of automorphism group of the network after removing a node. The size of the automorphism group, as the traditional measure of symmetry, provides a fair approximation of symmetry. However, to create a metric that realizes the complex structure of symmetry, a novel notion of symmetry, network redundancy, has been proposed in [4] as

$$r_{\mathcal{G}} = \frac{|\mathcal{O}| - 1}{V} \tag{3.20}$$

where $r_{\mathcal{G}}$ is a measure of network redundancy and $|\mathcal{O}|$ is the number of orbits. A normalized measure of redundancy is

$$r^*_{\mathcal{G}} = 1 - \frac{|\mathcal{O}| - 1}{V - 1} \tag{3.21}$$

presented in [42] that captures the asymmetric case as well. In (3.20) and (3.21), the presence of symmetric structures in a graph is quantified employing the orbits of automorphisms. In fact, all nodes in the same orbit are structurally equivalent. Consequently, non-trivial orbits have been associated with structural redundancy which according to [4] and [21] reinforces the robustness of the network against attacks on the nodes by providing structural backups. However, the difference between the induced symmetry by two orbits of different sizes can not be projected by (3.20) and (3.21).

Inspired by Shannon's entropy formula that provides a measure of disorder, uniformity, or randomness in networks [43], the orbits' impact on the network symmetry could be better described as

$$S_{\mathcal{O}}(\mathcal{G}) = \frac{\sum_{i=1}^{l} |\mathcal{O}_l| \text{ln} |\mathcal{O}_l|}{n} \tag{3.22}$$

where $S_{\mathcal{O}}(\mathcal{G})$ is the impact of orbits of automorphisms on symmetry level featuring the orbits' structures, $|\mathcal{O}_l|$ is the number of elements of the l^{th} orbit, and n is the number of nodes. The

Table 3.1: The symmetry specifications of various networks including the sizes of automorphism group $|Aut(\mathcal{G})|$, generator set $Gen(\mathcal{G})$, orbits of automorphisms $|\mathcal{O}|$, maximum multiplicity of nodes in generator set denoted by M_{max}, cardinality of the set of nodes with maximum multiplicity $|M_{max}|$, and the symmetry index $\mathcal{S}_{\mathcal{O}}(\mathcal{G})$ associated with the impact of orbits of automorphisms

Network Name	$\lvert V\rvert$	$\lvert E\rvert$	$\lvert Gen(\mathcal{G})\rvert$	$\mathcal{M}_{max}$	$\lvert\mathcal{M}_{max}\rvert$	$\lvert Aut(\mathcal{G})\rvert$	$\lvert\mathcal{O}(\mathcal{G})\rvert$	$\mathcal{S}_{\mathcal{O}}(\mathcal{G})$
Net. of Figure 3.2.a	101	380	53	5	42	1.27×10^{20}	7	4.22
Net. of Figure 3.2.b	273	1474	23	2	43	28×10^{6}	251	0.12
Net. of Figure 3.2.c	332	4252	54	3	2	2.5×10^{24}	276	0.30
Net. of Figure 3.2.d	47	264	2	22	2	6	44	0.07
US Power Grid	4941	13188	420	2	143	5.2×10^{152}	4466	0.15
QHPS	882	3354	82	3	52	8.5×10^{27}	336	1.08
NEPS	66	1194	35	2	52	1.7×10^{25}	7	2.25

bigger the orbit sizes, the more symmetric the underlying graph is. Computing (3.22) before and after node elimination determines how robust the network is against node elimination. We define the ratio of symmetry after a node removal to the original network's symmetry as

$$\rho_{\mathcal{O}} = \%\frac{\overline{S_{\mathcal{O}}(\mathcal{G})}}{S^{*}_{\mathcal{O}}(\mathcal{G})} \times 100 \tag{3.23}$$

where $S^{*}_{\mathcal{O}}(\mathcal{G})$ and $\overline{S_{\mathcal{O}}(\mathcal{G})}$ are the symmetry index of the original network and the average symmetry index of the network after removing a node.

3.5 Simulation

The symmetric characteristics of several networks are initially investigated to verify that the quantified form of symmetry studied in this chapter is present in all networks independent of network size and order. This is carried out on Sage with Python programming for several real and synthetic networks of various sizes and orders. The symmetry specifications of a few of these networks are presented in Table 3.1. It is observed that all networks of various sizes entail a certain level of symmetry.

The detailed simulation is accomplished on two synthetic networks with 101 nodes and 273 nodes illustrated in Figures 3.2.a-b. The symmetry specifications of these networks are presented in Table 1, rows 2-3. The network of Figure 3.2.a is selected as an illustrative example to examine the symmetry characteristics and the proposed adaption (of Lemma 4.3.1, Theorem 8.2, and Lemma 3.4.2) from automorphism to generators of automorphisms. As explained in

Section 3, nodes with more multiplicities in symmetry group are more critical for the network robustness. The 101-node network of Figure 3.2.a has 1.27×10^{20} automorphisms. According to Table 1, this can be considered as a medium cardinality for the size of automorphism group as there are networks with 10^{152} automorphisms in the Table 3.1. Since computing and sweeping over these large sets of automorphism groups is computationally inefficient, we implement the proposed adaption of this chapter, presented in Lemma 4.3.1, Theorem 8.2, and Lemma 3.4.2, in order to investigate the symmetry characteristics of the network and its impact on the network robustness.

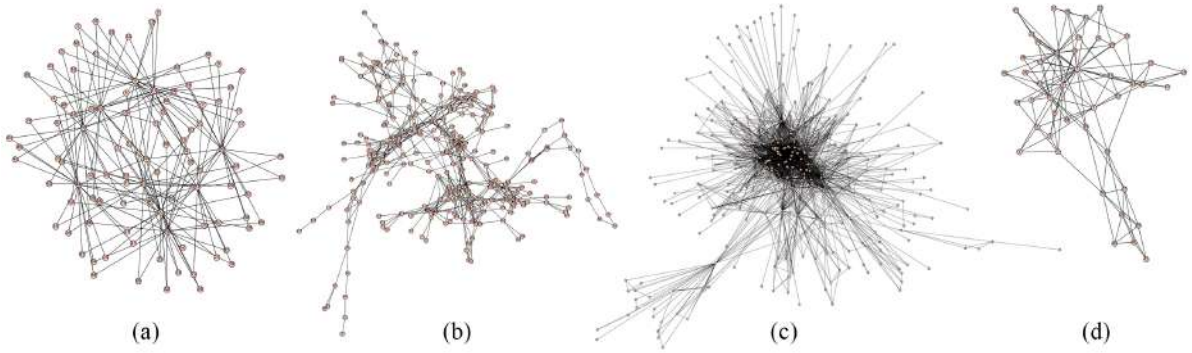

Figure 3.2: Four networks with (a) 101 nodes, (b) 273 nodes, (c) 332 nodes, and (d) 47 nodes

The set of generators of automorphism of the network of Figure 3.2.a are computed in Sage and, unlike the automorphism group, its size is small and is equal to 53. The full set of generators of automorphisms of this network is presented in Table 2, row 2. The number of required driver nodes can be attained by ECM explained in Section 2.3. The set of essential driver nodes for full controllability is attained in MATLAB and a big portion of nodes, 81 nodes which is approximately %81 percent of all nodes, are selected as drive nodes. This set of nodes are presented in Table 2, row 4 and also indicated in Figure 3.3 with green rings.

To investigate the robustness of controllability in case of failure in a network critical element, first, we determine the set of critical nodes in terms of their impact on the cardinality of the symmetry group. Since the cardinality of $\mathrm{Aut}(\mathcal{G})$ for the network of Figure 3.3 is too big, we need to implement the proposed approach of this study for finding the most critical nodes. To this end, the corresponding generator set is calculated via Python programming in Sage and 53 generators are attained (see Table 2, row 2).

The set of nodes with maximum multiplicity in the $\mathrm{Gen}(\mathcal{G})$ is computed in Sage and the results are presented in Table 2, row 5. As indicated, there are 42 nodes which are repeated 5 times (maximum multiplicity) in $\mathrm{Gen}(\mathcal{G})$. There are also 28 nodes with multiplicity 4 (Table 2, row 6), 16 nodes with multiplicity 3 (Table 2, row 7), 12 nodes with multiplicity 2 (Table 2, row 8), and 2 nodes with multiplicity 1 (Table 2, row 9). These sets of nodes are illustrated in Figure 3.3 with distinct colours.

Now, we compare the characteristics of the network symmetry after failure (removing) of nodes with different multiplicity. The cardinality of automorphism group of the modified network after removing a node is computed for nodes with different multiplicities in $\mathrm{Gen}(\mathcal{G})$ and

the average cardinality of Aut($\mathcal{G}$) is computed and the results are presented in Table 3, row 3. As can be seen, removing the nodes with more multiplicities is more effective in reducing the cardinality of Aut($\mathcal{G}$). The average cardinality of Aut($\mathcal{G}$) has reduced to 1.4×10^{18}, 1.8×10^{18}, 2.3×10^{18}, 1.3×10^{19}, and 1.5×10^{19} after removing a node with multiplicities 5, 4, 3, 2, and 1, respectively. This entail a significant reduction of $\%98.9$ in $|\text{Aut}(\mathcal{G})|$ when we remove a node with 5 times repetitions in the Gen($\mathcal{G}$). However, this dramatic change does not reflect on the number of required driver nodes after removing a nodes. As indicated in Table 3, row 5, the number of required driver nodes has remained unchanged (equal to 81) after removing a node with different multiplicities. This means that the cardinality of automorphism group, as a quantified measure of symmetry, is not consistent with the controllability requirement of the network. We investigate this proportional relation between symmetry level and the number of required driver nodes via the proposed index of symmetry in Equation (3.22).

The set of orbits of automorphisms for the network of Figure 3.3 is computed in Sage and 7 orbits are identified as listed in Table 3.2, row 3. Computing (3.22) leads to $\mathcal{S}_{\mathcal{O}} = 4.22$ which, compared to other networks in Table I, is considered a high value of symmetry. The number of nodes in the 7 orbits are 8, 32, 56, 2, 1, 1, and 1. The symmetry index has reduced to 3.76 for any node removal. This leads to the fixed ratio index equal to %88.89 after node removal. Comparing to the size of automorphism groups, this index indicates a significant lower reduction in the symmetry level which can explain why there is no reduction in the number of required driver nodes. This is in line with high robustness of strongly symmetric networks. The significance of index (3.22) could be better realized for less symmetric networks like 273-node network.

The 273-node network has the orbital symmetry index equal to $S_{\mathcal{O}} = 0.1221$ which is considered a very less symmetric network compared to 101-node network. Modifying this network by removing nodes with multiplicities 2 (maximum multiplicity) and 1 has resulted to the orbital symmetry index equal to 0.1195 and 0.1202 which means %2.13 and %1.56 reduction in the symmetry index. This reduction is in line with the reduction in the average number of required driver nodes from 16 driver nodes for original network to 13.7 and 14.6 driver nodes after removing a node with multiplicities 2 and 1, respectively. As expected, removing a node with more multiplicity in Gen($\mathcal{G}$) is more effective in reducing the number of required driver nodes attained by ECM. This consistence between the number of required driver nodes and the network symmetry level highlights the importance of (3.22) in capturing the symmetry impact on the robustness of controllability.

It should be noted that although reducing the symmetry index can reduce the number of required driver nodes but the configuration of these driver nodes after node removal might totally differ from their original configuration. Thus, after network manipulation, it might not be controllable by the fixed set of initial driver nodes.

Table 3.2: The symmetry specifications of 101-node network including the elements of generator set $Gen(\mathcal{G})$, orbits of automorphisms $|\mathcal{O}|$, the set of driver nodes N_d, set of nodes in M_i where i is the multiplicity of nodes in the generator set denoted, cardinality of the set of nodes with maximum multiplicity $|M_{max}|$, and the symmetry index $\mathcal{S}_{\mathcal{O}}(\mathcal{G})$ associated with the impact of orbits of automorphisms.

Param.	Elements of the symmetry parameter
Gen($\mathcal{G}$)	(89,98), (79,97), (78,87), (69,96), (68,86), (67,76), (59,95), (58,85), (57,75), (56,65), (49,94), (48,84), (47,74), (46,64), (45,54), (39,93), (38,83), (37,73), (36,63), (35,53), (34,43), (29,92), (28,82), (27,72), (26,62), (25,52), (24,42), (23,32), (19,91), (18,81), (17,71), (16,61), (15,51), (14,41), (13,31), (12,21), (9,90), (8,9) (18,19) (28,29) (38,39) (48,49) (58,59) (68,69) (78,79) (80,90) (81,91) (82,92) (83,93) (84,94) (85,95) (86,96) (87,97) (88,99), (8,80), (7,8) (17,18) (27,28) (37,38) (47,48) (57,58) (67,68) (70,80) (71,81) (72,82) (73,83) (74,84) (75,85) (76,86) (77,88) (79,89) (97,98), (7,70), (6,7) (16,17) (26,27) (36,37) (46,47) (56,57) (60,70) (61,71) (62,72) (63,73) (64,74) (65,75) (66,77) (68,78) (69,79) (86,87) (96,97), (6,60), (5,6) (15,16) (25,26) (35,36) (45,46) (50,60) (51,61) (52,62) (53,63) (54,64) (55,66) (57,67) (58,68) (59,69) (75,76) (85,86) (95,96), (5,50), (4,5) (14,15) (24,25) (34,35) (40,50) (41,51) (42,52) (43,53) (44,55) (46,56) (47,57) (48,58) (49,59) (64,65) (74,75) (84,85) (94,95), (4,40), (3,4) (13,14) (23,24) (30,40) (31,41) (32,42) (33,44) (35,45) (36,46) (37,47) (38,48) (39,49) (53,54) (63,64) (73,74) (83,84) (93,94), (3,30), (2,3) (12,13) (20,30) (21,31) (22,33) (24,34) (25,35) (26,36) (27,37) (28,38) (29,39) (42,43) (52,53) (62,63) (72,73) (82,83) (92,93), (2,20), (1,2) (10,20) (11,22) (13,23) (14,24) (15,25) (16,26) (17,27) (18,28) (19,29) (31,32) (41,42) (51,52) (61,62) (71,72) (81,82) (91,92), (1,10), (0,11) (2,12) (3,13) (4,14) (5,15) (6,16) (7,17) (8,18) (9,19) (20,21) (30,31) (40,41) (50,51) (60,61) (70,71) (80,81) (90,91)
$\mathcal{O}(\mathcal{G})$	[0, 11, 22, 33, 44, 55, 66, 77, 88, 99], [1, 2, 10, 3, 20, 12, 4, 30, 13, 21, 5, 40, 14, 31, 23, 6, 50, 15, 41, 24, 32, 7, 60, 16, 51, 25, 42, 34, 8, 70, 17, 61, 26, 52, 35, 43, 9, 80, 18, 71, 27, 62, 36, 53, 45, 90, 19, 81, 28, 72, 37, 63, 46, 54, 91, 29, 82, 38, 73, 47, 64, 56, 92, 39, 83, 48, 74, 57, 65, 93, 49, 84, 58, 75, 67, 94, 59, 85, 68, 76, 95, 69, 86, 78, 96, 79, 87, 97, 89, 98], [100]
N_d	5, 9, 10, 11, 14, 15, 16, 17, 18, 19, 20, 21, 22, 24, 25, 26, 27, 28, 29, 30,31,32,33,35,36,37,38,39, 40, 42, 43, 44, 46, 47, 48, 49, 50, 51, 52, 53, 54, 55, 57, 58, 59, 60, 61,62,63,64,65, 66, 68, 69, 70, 71, 72, 73, 74, 75, 76, 77, 79, 80, 82, 83, 84, 85, 86, 87, 88, 90, 92, 93, 94, 95, 96, 97, 98, 99, 101
$v \in M_5$	13, 14, 15, 16, 17, 18, 24, 25, 26, 27, 28, 31, 35, 36, 37, 38, 41, 42, 46, 47, 48, 51, 52, 53, 57, 58, 61, 62, 63, 64, 68, 71, 72, 73 , 74 , 75 , 81 , 82 , 83 , 84 , 85 , 86
$v \in M_4$	2 ,3 ,4 ,5 ,6 ,7 ,8 ,19 ,20 ,29 ,30 ,39 ,40 ,49 ,50 ,59 ,60 ,69 ,70 ,79 ,80 ,91 ,92 ,93 ,94 ,95 ,96 ,97
$v \in M_3$	9 , 12 , 21 , 23 , 32 , 34 , 43 , 45 , 54 , 56 , 65 , 67 , 76 , 78 , 87 , 90
$v \in M_2$	1 ,10 ,11 ,22 ,33 ,44 ,55 ,66 ,77 ,88 ,89 ,98
$v \in M_1$	0, 99

3.5.1 Discussing the results

Equation (3.22), as the proposed measure of symmetry impact on the number of required driver nodes, captures the importance of orbits with bigger sizes. According to Table 1, the 332-node network of Figure 3.2.c with 276 orbits has a small $S_{\mathcal{O}}$ equal to 0.30. This is because the sizes of majority of 276 orbits are 1 and, in practice, have no contribution in characterizing the network's symmetry strength. In contrast, the 101-node network of Figure 3.2.a has only 7 orbits but it has a high symmetry index equal to 4.44 because the sizes of orbits are big (as listed in Table 2. row 3). The importance of the index (3.22) is more realizable when we also compare the size of automorphism groups of these two networks. According to Table 1, the size of automorphism group of 273-node network is 19,685 times bigger than 101 node network.

Table 3.3: The impact of removing the nodes with different multiplicities (indicated by M_i where i represents the multiplicity of the deleted nodes) on the symmetry indexes and the number of required driver nodes

Network name	*101-node network*						*273-node network*		
Parameter	$\mathcal{G}$	M_5	M_4	M_3	M_2	M_1	$\mathcal{G}$	M_2	M_1
$\overline{\lvert \mathrm{Aut}(\mathcal{G}) \rvert}$	-	$1.4e18$	$1.8e18$	$2.3e18$	$1.3e19$	$1.5e19$	-	$3,545,168$	$9,437,184$
ρ_{aut}	-	$\%1.10$	$\%1.42$	$\%1.81$	$\%10.24$	$\%11.81$	-	$\%12.6$	$\%33.70$
N_d	81	81	81	81	81	81	16	13.7	14.6
$\overline{S_{\mathcal{O}}}$	-	3.76	3.76	3.76	3.76	3.76	-	0.1195	0.1202
$\% \frac{S_{\mathcal{O}}^{av}}{S_{\mathcal{O}}} \times 100$	-	$\%88.89$	$\%88.89$	$\%88.89$	$\%88.89$	$\%88.89$	-	$\%97.87$	$\%98.44$

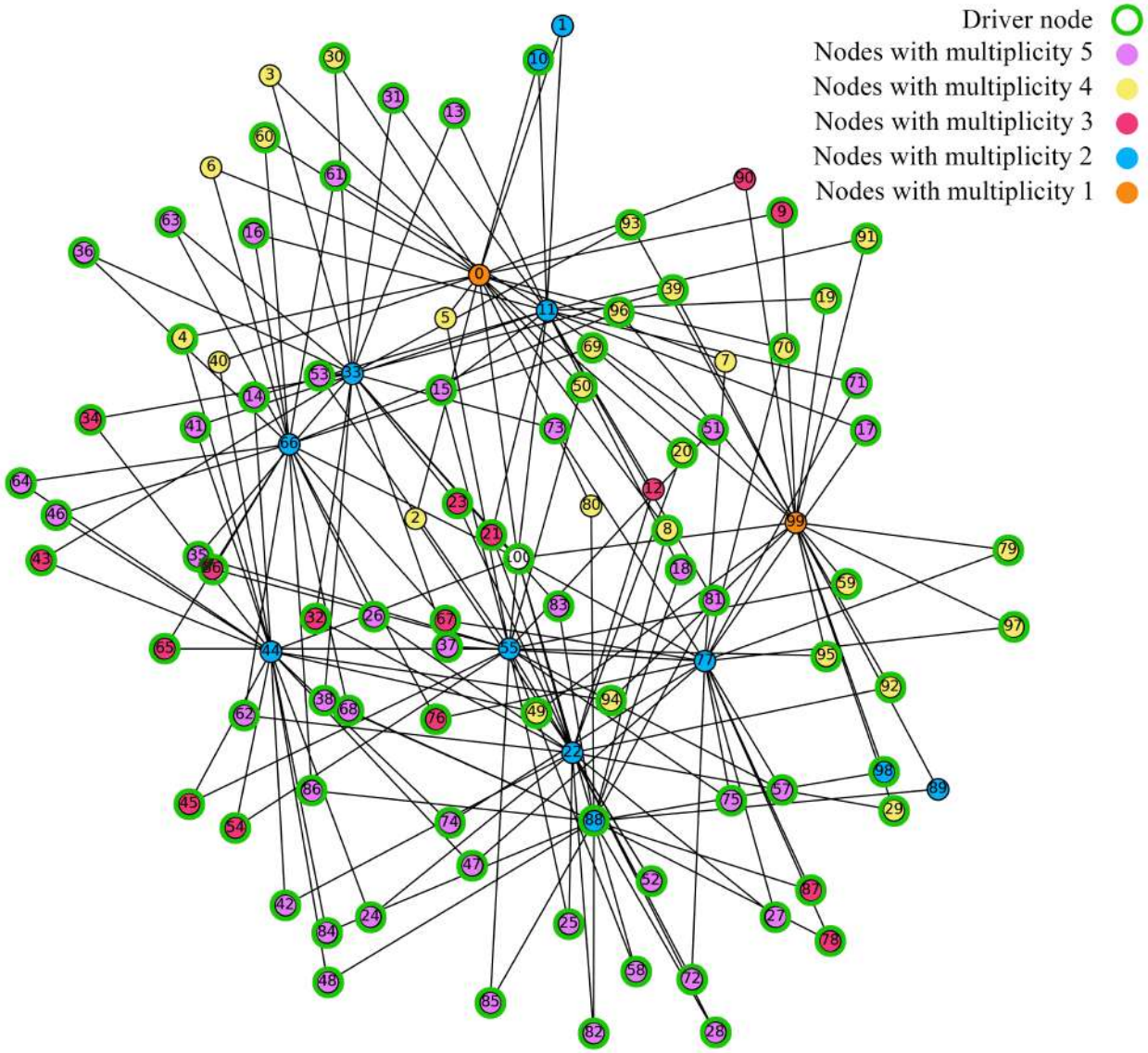

Figure 3.3: 101-node system, driver nodes (green rings), nodes with maximum multiplicity $\mathcal{M}_{max} = 96$ (red circles), nodes with $\mathcal{M}_{max} = 72$ (orange circles)

One interesting result that can be observed in most networks is that the majority of driver nodes are also nodes with maximum multiplicity in Aut($\mathcal{G}$) (or $Gen(\mathcal{G})$). This is the case, in particular, in networks with less symmetry than 101-node network. In fact, high symmetric networks necessitate to pin a big portion of nodes as driver node and, as such, it is sometimes unclear to realize this impact of symmetry on the selection of driver nodes. However, for networks with lower symmetry, such as the 273-node network, this is very common that the majority of driver nodes attained by ECM belong to the symmetry groups. To illustrate this, the 273-node network of Figure 3.2.b with 273 nodes and 1475 edges are examined. The symmetry characteristics of this network are attained in Sage and presented in Table 1, row 3. Implementing ECM (explained in Section 2.3) has resulted in 16 driver nodes. Interestingly, 10 out of 16 driver nodes belong to the set of generator set. Considering only 46 nodes are in the generator set, this means that the nodes in symmetry group are crucial for the network controllability.

Another interesting observation is that, unlike the majority of network studies which emphasise on the impact of nodes with high centrality or high degree distribution, nodes with low degree distribution may also have significant influence on network performance. As illustrated in Figures 3.3, the degree of some nodes in symmetry group is 2 while there are nodes that have higher degree but are not selected as driver nodes. For example, node 66 in Figure 3.3 with degree 19 is neither a driver node nor within the symmetry group.

The impact of symmetry on the robustness of controllability (number of driver nodes) depends on the symmetry level of the network. The highly symmetric networks are very robust against node removal but, at the same time, necessitate that a high portion of nodes be driver node. It can be concluded that symmetry reinforces the robustness of controllability meaning a network with higher symmetry index of Equation (our index) is controllable with, naturally, a fixed and bigger set of driver nodes. Moreover, the highly symmetric networks are more tolerant against node failure.

Although the number of required driver nodes can be changed by the variations in the cardinality of symmetry groups, the energy cost of control is not proportionally impacted. A bigger control signal might be required when a lower number of driver nodes are needed. A future research focus can be on a trade off between the number of driver nodes and energy cost of control.

3.6 Conclusion

This study highlights the importance of the inherent networks' symmetry in addressing three issues related to the network robustness. The robustness of controllability is guaranteed under satisfying some conditions related to the properties of the underlying symmetry group while selecting the set of driver nodes. By incorporating the concept of controlled invariant subspace and determining set, a new necessary and sufficient condition for disturbance decoupling is presented while guaranteeing a necessary condition for CN controllability. Finally, the critical nodes and edges of the network, in terms of their impact on symmetry and in turn, robustness,

are identified and the network robustness against node failure is investigated.

The proposed approach in this study is unique as it leverages on an inherent feature of complex networks, i.e., symmetry, to describe novel notions of robustness. The study shows that graph symmetry is independent of network size, order, node degree distribution or any measure of centrality. Additionally, the findings of this chapter emphasise on the necessity of considering network symmetry in the pre-design and development of networks.

Bibliography

3.7 References

[1] V. P. Tran, M. Garratt, and I.R. Petersen, "Switching time-invariant formation control of a collaborative multi-agent system using negative imaginary systems theory," *Control Engineering Practice*, vol. 95, Feb 2020.

[2] G.A. Pagani and M. Aiello, "The Power Grid as a complex network: A survey," *Physica A*, vol. 392, pp. 2688–2700, 2013.

[3] F. Dorfler, J.W. Simpson-Porco, and F. Bullo, "Electrical Networks and Algebraic Graph Theory: Models, Properties, and Applications," *Proceedings of the IEEE*, vol. 106, no. 5, 2018.

[4] B. D. MacArthur, R. J. Sanchez-Garcia, and J. W. Anderson, "Symmetry in Complex Neworks," *Disc. App. Math.*, vol. 156, 2018.

[5] A. Chapman and M. Mesbahi, "On symmetry and controllability of multi-agent systems," *53rd IEEE Conf. Dec. Con.* Los Angeles, 2014.

[6] A. Chapman, M. Nabi-Abdolyousefi, and M. Mesbahi, "Controllability and observability of networks of networks via cartesian products," *IEEE Transactions on Automatic Control*, vol. 59, 2014..

[7] A. Chapman and M. Mesbahi, "State controllability, output controllability and stabilizability of networks: A symmetry perspective," *IEEE 54th Annual Conference on Decision and Control (CDC).,* 2015.

[8] L.M. Pecora, F. Sorrentino, A. M. Hagerstorm, T.E. Murphy, and R. Roy , "Cluster synchronization and isolated desynchronization in complex networks with symmetries," *Nature, Communication*, vol. 5, 2014.

[9] F. Sorrentino, L.M. Pecora, "Approximate cluster synchronization in networks with symmetries and parameter mismatches," *Chaos: An Interdisciplinary Journal of Nonlinear Science*, vol. 26, no. 9, 2016.

[10] A.B. Siddique, L.M. Pecora, J.D. Hart, and F. Sorrentino, "Symmetry-and input-cluster synchronization in networks," *Physical Review*, vol. 97, 2018.

[11] Z. Yuan and C. Zhao, Z. Di, W. X. Wang, and Y. C. Lai, "Exact controllability of complex networks," *Nat.: Comm.*, vol. 4, Sep. 2013.

[12] Y.S. Li, D.Z. Ma, H.G. Zhang, and Q.Y. Sun, "Critical Nodes Identification of Power Systems Based on Controllability of Complex Networks," *Applied Science*, vol. 5, 2015.

[13] Z. Wang, D.J. Hill, G. Chen, and Z.Y. Dong, "Power system cascading risk assessment based on complex network theory," *Physica A*, vol. 482, pp. 532-543, 2017.

[14] R. Albert, I. Albert, and G. Nakarado, "Structural vulnerability of the north american power grid," *Physical Review E*, vol. 69, no. 2, 2004.

[15] A. Holmgren, "Using graph models to analyze the vulnerability of electric power networks," *Risk Analysis*, vol. 26, no. 4, 2006.

[16] A.B.M. Nasiruzzaman, and H.R. Pota, "Critical node identification of smart power system using complex network framework based centrality approach," *Annual North-American Power Symposium*, 2011.

[17] Y. D. Xiao, S. Y. Lao, L. L. Hou, and L. Bai, "Edge orientation for optimizing controllability of complex networks," *Phys. Rev. E,* vol. 90, no. 4, p. 042804, 2014.

[18] S. Abeysinghe, J. Wu, M. Sooriyabandara, M. Abeyskera, T. Xu, and C. Wang, "Topological properties of medium voltage electricity distribution networks," *Applied Energy*, vol. 210, pp. 1101-1112, 2018.

[19] G. Como, K. Savla, D. Acemoglu, M. D. Dahleh, and E. Frazzoli, "Robust Distributed Routing in Dynamical Networks–Part II: Strong Resilience, Equilibrium Selection and Cascaded Failures ," *IEEE Trans. Aut. Con.*, vol. 58, no. 2, 2013.

[20] D. Z. Tootaghaj, N. Bartolini, H. Khamfroush, T. He, and T. La Porta, "Mitigation and Recovery from Cascading Failures in Interdependent Networks under Uncertainty," *IEEE Trans. Con. Net. Sys.*, vol. 5, 2018.

[21] G. Tononi, O. Sporns, and G.M. Edelman, "Measures of degeneracy and redundancy in biological networks", *Proc. Natl. Acad. Sci. USA.*, vol. 96, no. 6, 1999.

[22] R. Albert, A. L. Barabasi, "Statistical mechanics of complex networks," *Rev. Modern Phys.*, vol. 74, no. 1, 2002.

[23] C. T. Lin, "Structural controllability," *IEEE Transactions on Automatic Control*, vol. 19, no. 3, pp. 201–208, 1974.

[24] Y.-Y. Liu, J. J. Slotine, and A.-L. Barabási, "Controllability of complex networks," *Nature*, vol. 473, no. 7346, pp. 167–173, May 2011.

[25] X. Wu, X. Wang, M. Gu, and G.P. Jiang, "Structural Controllability for a Class of Complex Networks with Root Strongly Connected Components," *IEEE Access*, Early Access, Feb 2020.

[26] B. Ouyang, Q. Ye, S. Patil, C. Wang, L. Lu, and Z. Yan, "The Relation Between Communication Range and Controllability of Networked Multi-Agent Systems," *IEEE Access*, vol. 6, pp. 35901–35907, Jan 2018.

[27] B. Hou, X. Li, and G. Chen, "Structural controllability of temporally switching networks," *IEEE Trans. Circuits Syst. I Regul. Pap*, vol. 63, no. 10, pp. 1771–1781, Sep 2016.

[28] A. M. Amani, M. Jalili, X. Yu, and L. Stone, "Finding the most influential nodes in pinning controllability of complex networks," *IEEE Trans. Circuits Syst. II, Exp. Briefs*, vol. 64, no. 6, pp. 685–689, Jun. 2017.

[29] Y. Lou, L. Wang, and G. Chen, "Toward stronger robustness of network controllability: A snapback network model," *IEEE Trans. Circuits Syst. I Regul. Pap.,*, vol. 65, no. 9, pp. 2983–2991, Sep. 2018.

[30] R. Zhang, X. Wang, M. Cheng, and T. Jia, "“The evolution of network controllability in growing networks," *Physica A,*, vol. 520, pp. 257–266, Apr. 2019.

[31] M. Jalili and X. Yu, "“Enhancing pinning controllability of complex networks through link rewiring," *IEEE Trans. Circuits Syst. II, Exp. Brief*, vol. 64, no. 6, pp. 690–694, Jun. 2017.

[32] L. Xiang, F. Chen, W. Ren, and G. Chen, "Advances in network controllability," *IEEE Circuits Syst. Mag.*, vol. 19, no. 2, pp. 8–32, May. 2019.

[33] S. Wang, H. Li, Y. Li, and W. Sun, "Event-triggered control for disturbance decoupling problem of mix-valued logical networks," *Journal of the Franklin Institute*, vol. 357, no. 2, pp. 796–809, Jan 2014.

[34] P. Selvaraj, O.M. Kwon, S.H. Lee, and R. Sakthivel, "Uncertainty and disturbance rejections of complex dynamical networks via truncated predictive control ," *Journal of the Franklin Institute*, vol. 357, no. 8, pp. 4901–4921, May 2014.

[35] J. Alshehri and M. Khalid, "Power Quality Improvement in Microgrids Under Critical Disturbances Using an Intelligent Decoupled Control Strategy Based on Battery Energy Storage System," *IEEE Access*, vol. 7, pp. 147314–147326, Oct 2019.

[36] L. Djilali, E. N. Sanchez, and M. Belkheiri, "Real-time Neural Input–Output Feedback Linearization control of DFIG based wind turbines in presence of grid disturbances," *Control Engineering Practice*, vol. 83, pp. 151–164, Feb 2019.

[37] G. Lawyer, "Understanding the influence of all nodes in a network," *Nature, Scientific Reports*, vol. 5:8665, 2015.

[38] Y. Koc, M. Warnier, R. E. Kooij, and M. T. Brazier, "An Entropy-based Metric to Quantify the Robustness of Power Grids against Cascading Failures," *Safety Science*, vol. 59, 2013.

[39] S.P. Pang and F. Hao, “Optimizing controllability of edge dynamics in complex networks by perturbing network structure,” *Physica A,* vol. 470, pp. 217–227, 2017.

[40] L. Xiang, F. Chen, W. Ren, and G. Chen, "Advances in network controllability," *IEEE Circuits and Systems Magazine,* Second quarter, 2019.

[41] L. Z. Wang, Y. Z. Chen, W. X. Wang, and Y. C. Lai, "Physical controllability of complex networks," *Nature, Scientific Reports*, vol. 7, no. 40198, 2017.

[42] F. Ball and A. Geyer-Schulz, "How Symmetric Are Real-World Graphs? A Large-Scale Study," *Symmetry*, vol. 10, no. 1, 2018.

[43] D. Bonchev, *Information Theoretic Indices for Characterization of Chemical Structures,* Research Studies Press, UK, 1983.

[44] A. Farrugia and I. Sciriha, "Controllability of undirected graphs," *Linear Algebra and its Applications*, vol. 454, 2014.

[45] http://www.networkrepository.com/, Available online, Last access Jun 2020.

Chapter 4

Cyber-Security Constrained Placement of FACTS Devices in Power Networks from a Novel Topological Perspective

4.1 Overview

Optimal placement of flexible AC transmission systems (FACTS) devices and the cyber-security of associated data exchange are crucial for the controllability of wide area power networks. The placement of FACTS devices is studied in this chapter from a novel graph theoretic perspective, which unlike the existing approaches, purely relies on topological characteristics of the underlying physical graphs of power networks. To this end, the maximum matching principle (MMP) is used to find the set of required FACTS devices for the grid controllability. In addition, the cyber-security of the most critical data related to the FACTS controllers is guaranteed by introducing the concept of moderated-k-security where k is a measure of data obscurity from the adversary perspective. The idea of moderated-k-symmetry is proposed to facilitate the arrangement of the published cyber graph based on a permutation of nodes within the symmetry group of the grid, called generator of automorphism. It is then verified that the published cyber-graph can significantly obscure the data exchange over the cyber graph for adversaries. Finally, a similarity is observed and demonstrated between the set of critical nodes attained from the symmetry analysis and the solution of the FACTS devices placement that further highlights the importance of symmetry for the analysis and design of complex power networks. Detailed simulations are applied to three power networks and analyzed to demonstrate the performance and eligibility of the proposed methods and results[1].

[1]This chapter is published in *IEEE Access*

Nomenclature

Abbreviations

PBH	Popov-Belevitch-Hautus.
CEA	Community energy association.
CN	Complex network.
CN	Complex network.
CN	Complex network.
CS	Charging station.
ECM	Exact controllability method.
ECM	Exact controllability method.
EV	Electric vehicle.
FACTS	Flexible AC transmission systems.
lcm	The lowest common multiple.
LQR	Linear quadratic regulator.
LTI	Linear time invariant.
MMP	Maximum matching principle.
PCS	Portable charging station.
PEV	Plug-in electric vehicle.
PID	proportional integrative derivative.
VSC	Voltage-source converter.
WAC	Wide area controlled.

Constants

ε Identity (or trivial) permutation.

ε Identity (or trivial) permutation.

c A complex number.

c A complex number.

Q, R, Y Arbitrary weights.

Parameters

α_{sh} Angle of shunt VSC.

β The bus voltage angles.

δ A permutation.

δ_i Maximum algebraic multiplicity of $\lambda_(i)$.

δ_i Maximum algebraic multiplicity of $\lambda_(i)$.

δ_i The angle of voltage of node i.

γ_{sh} Conversion ratio signal.

λ^M Maximum algebraic multiplicity of teh eigenvalue λ^M.

λ^M Maximum algebraic multiplicity of the eigenvalue λ^M.

λ_i The i^{th} eigenvalue.

λ_i The i^{th} eigenvalue.

ν A point (node) of permutation.

σ An automorphism or a Permutation.

σ Permutation.

σ Permutation.

$\mathcal{A}$ Adjacency matrix.

$\mathcal{A}$ Adjacency matrix.

$\mathcal{A}, A$ Adjacency matrix.

$\mathcal{D}$ Degree matrix.

$\mathcal{D}$ The degree matrix.

$\mathcal{E}$ The set of edges.

$\mathcal{E}_c$ The set of critical edges.

$\mathcal{F}$ The determining set attained from Gen($\mathcal{F}$).

$\mathcal{G}$ Graph.

$\mathcal{G}$ Graph.

$\mathcal{G}$ Graph.

$\mathcal{G}_k$ The released graph.

$\mathcal{J}$ The incidence vector of driver nodes.

$\mathcal{K}$ Optimal feedback gain vector.

$\mathcal{L}$ Laplacian matrix.

$\mathcal{L}$ Laplacian matrix.

$\mathcal{L}$ Laplacian matrix.

$\mathcal{S}$ Determining set.

$\mathcal{S}$ Determining set.

$\mathcal{V}$ Controlled invariant subspace.

$\mathcal{V}$ The set of nodes.

$\mathcal{V}_c$ The set of critical nodes.

Aut($\mathcal{G}$) Automorphism group.

Aut($\mathcal{G}$) Automorphism group.

Aut($\mathcal{G}$) Automorphism group.

dimV_{λ_i} Dimension of eigenspace associated with $\lambda(i)$.

dimV_{λ_i} Dimension of eigenspace associated with $\lambda(i)$.

Fix(σ) The set of fixed nodes by permutation.

Gen($\mathcal{G}$) Generators of automorphism.

Gen($\mathcal{G}$) Generators of automorphism.

Gen($\mathcal{G}$) Generators of automorphism.

$\text{Gen}_{dis}(\mathcal{G})$ Set of disjoint generators.

$\text{Move}(\sigma)$ The set of moved nodes by permutation.

$\text{Move}(\sigma)$ The set of moved nodes by permutation.

$\text{Mov}_{v_l}^{Gen}$ the set of generators mapping v_l.

$\mu(\lambda_i)$ Maximum geometric multiplicity of $\lambda(i)$.

$\mu(\lambda_i)$ Maximum geometric multiplicity of $\lambda(i)$.

$\rho_{\mathcal{O}}$ The orbital ratio of symmetry after node removal.

ρ_{aut} The ratio of symmetry after node removal.

σ A permutation.

ε Identity (or trivial) permutation.

φ A generator of automorphism.

ζ A permutation.

ζ_{dis} , δ_{dis} Disjoint generators.

A State matrix.

a_{ij} Element of $\mathcal{A}$.

a_{ij} Weight of ij^{th} element of $\mathcal{A}$.

B Input matrix.

B Input matrix.

B Input matrix.

C Capacitor.

C Size (or capacity) of charging station [kW].

E The set of edges.

E The set of edges.

$F(x_i)$ the individual node's dynamical equation.

F_{vl}^{Gen} The set of generators that fixes v_l.

I_{dc} Capacitor current.

I_{sh} Shunt reactive current setpoint.

I^*_{sh} Reactive current of the outer loop.

$Im\, C$ Image of C.

K The feedback gain.

k The number of distinct mappings.

k_m Conversion ration between the voltage of AC and DC sides.

$ker\, L$ Kernel or null space of L.

l_{ij} The $(i, j)^{th}$ element of the Laplacian matrix.

M A matching.

m Index of a permutation.

M^{Gen}_{vl} The set of generators that moves v_l.

N_D Number of required driver nodes.

N_D Number of required driver nodes.

P The solution of Riccati equation.

p Multiplicity of critical node in Gen($\mathcal{G}$).

P_{ac} Active power on AC side.

P_{ij} Active power flow between nodes i and j.

q The size of disjoint generators.

Q_{ij} Reactive power flow between nodes i and j.

$r^*_{\mathcal{G}}$ Normalized measure of network redundancy.

$r_{\mathcal{G}}$ Network redundancy.

S Determining set.

$s(t)$ The desired state.

$S_{\mathcal{O}}(\mathcal{G})$ Symmetry index based on orbits.

T Waiting time [min].

u Control signal (charging supply).

u Control signal.

u Control signal.

V The set of nodes.

V The set of nodes.

V Voltage.

V_m Voltage magnitude.

V_{dc} Capacitor terminal voltage.

V_{ref} Setpoint voltage.

$w(t)$ Disturbance.

Z Line impedance.

4.2 Introduction

The imbalance between reactive power at the generating side and the network demand causes voltage instability. The wide area active compensation devices, collectively known as flexible AC transmission systems (FACTS) devices ([1]- [9]) are power electronic based equipment which play a vital role in enhancing the power system controllability and power flow capability. The importance of FACTS devices for the grid operation raises serious concerns about the cyber-security of data exchange over these controllers as the false data injection to one of the critical FACTS devices can lead to cascading failure in the grid [10]. In this chapter, these two problems are addressed from a novel topological perspective.

4.2.1 State of the art

The optimal placement of FACTS devices is a common yet important research topic in literature and has been investigated via various approaches. These include (1) conventional methods (such as indexing [11], controlling [12], residue analysis [13], numerical optimization [14], sensitivity [15], and eigenvalue [16]), (2) optimization methods (such as optimal power flow [17], linear programming [18], dynamic programming [19], mixed integer programming [20], stochastic load flow [21], and adaptive control law [22]), (3) artificial intelligence techniques (such as Monte Carlo simulation [23], artificial bee colony [24], artificial neural network [25], symbiotic organism search algorithm [26], fuzzy systems [27], and particle swarm optimization [28]), (4) hybrid techniques (such as hybrid of bee colony and neural networks [29], hybrid of genetic algorithm and fuzzy systems [30], mixed optimal power flow and particle swarm optimization [31], mixed bee colony and optimal power flow [32], and hybrid of fuzzy systems and

Lyapunov theory [33]), and (5) other approaches (such as energy approach [34], active control [35], graph search algorithms [36], whale optimization [37], Gray Wolf optimizer [38], salp swarm optimizer [39], Grasshooper optimization [40], ant lion optimization [41], and spider monkey optimization [42]).

At the same time, cyber-security has been one of the hot topics related to the management, operation, and control of power systems [49]- [52]. The reliability of wide area controlled (WAC) power systems highly depends on the security of the underlying communication networks. Information exchange via cyber graph is one of the underpinning platforms of all networks including power networks and smart grids that has significant role in grid control and operation. The interplay between power systems and the underlying communication platforms raises various security concerns about attacks from adversary agents. Thus the important grid information such as the data associated with the critical transmission lines, generation units, and the locations of FACTS devices must be hidden or obscured for adversary agents.

Due to its significant impacts on various aspects of network, graph topology has drawn the attention of engineering communities including power system community during the last two decades. The role of network topology is investigated for a few power system problems such as synchronization [44], flexibility of transmission lines for day-ahead scheduling [45], and the patterns of attacks to power networks [46]. Recently, graph symmetry, described by automorphism groups, has been leveraged in literature to address important network behaviors such as its controllability [62], robustness [59], and synchronization [47]. It has been verified that symmetry is an obstruction to controllability [62] meaning that systems with larger number of automorphisms require more driver nodes to satisfy the network controllability. In contrast, network robustness can be improved by increasing the network symmetry (or the size of automorphism group) [59]. Also, power networks with high symmetry are more resilient towards desynchronization propagation [48].

Early applications of symmetry in security emerged in the computer science community targeting the cyber-security of social networks ([53]- [55]) by proposing the concepts of k-symmetry, k-isomorphic, and k-automorphic. In fact, these studies found that releasing a permuted graph by an automorphism or isomorphism instead of original cyber graph makes it difficult for adversary agents to distinguish their targets. During the last decade, the applications of automorphisms in cyber-security, categorized under the concept of "security via obscurity", have been the main focus when implementing the symmetry characteristics for investigating the networks' cyber-security. However, the use of symmetry gives rise to some practical challenges. Computing and sweeping over all automorphisms to find the set of nodes with maximum multiplicities for a large network is a computationally challenging task. Moreover, important questions arise when identifying priorities for design and protection: Which cyber components, if compromised, can lead to significant power delivery disruption? What grid topologies are inherently robust to classes of cyber attack? Is the information available through advanced cyber infrastructure worth the increased security risk?

k-isomorphic graphs can be attained only by adding/deleting many edges through some

modification algorithms (for example see [53]- [56]). Satisfying k-automorphism for a real world network imposes many modifications on the original network which compromises its cost efficiency. In k-symmetry it is enough that k distinct mappings exist where for each node the set of k automorphisms may be different. In practice, it is not computationally efficient to impose such modifications. Furthermore, for k automorphisms, the same set of k automorphisms have to be applied to all nodes. This makes k-automorphism an even more difficult property to satisfy. In k-isomorphism, in addition to the above issues, connections among sub-graphs are deleted in the released graph. This, in turn, causes the loss of data utility in the published graph.

4.2.2 Research gaps and contributions

Although the placement of FACTS controllers has been widely studied during the last decade, no study has considered the possible impacts of network topology on the solutions. Moreover, the majority of the existing approaches have computational issues such as intractable nature of optimization techniques [17]- [25] which is caused by the lack of an analytical, non-heuristic, or systematic approach for finding the solution. In addition, the cyber-security of FACTS devices have not been investigated in literature. In this chapter, an analytical approach for the placement of FACTS controllers is proposed based on the topological characteristics of the network which does not suffer from the computational issues. To this end, the maximum matching principle is implemented which is a mechanism to find the set of unmatched nodes that are considered as the set of driver nodes which are able to drive the states of system from any initial state to any desired state in reasonable time (network controllability). The controllability of the complex networks (CNs) is then attributed to the number of required driver nodes for full state controllability [43].

In this chapter, the placement of FACTS controllers is constrained to the controllability of the power grid. By realizing the power grid as a complex network, the grid controllability is attributed to the number of required driver nodes for full state controllability. The FACTS controllers act as these driver nodes which can be found by performing the maximum matching principle on the physical graph of power systems. To overcome the computational issues related to computing the whole set of automorphisms, we adapt a symmetry benchmark according to a set of elementary automorphisms, known as generators of automorphisms. It will be verified that all essential symmetry characteristics can be realized via this set which has a significantly smaller size than automorphism groups and it is computationally effective to calculate and sweep over them. In addition, the graph symmetry is implemented to find the most critical components of power system in terms of their impact on the network controllability. Nodes with bigger multiplicities in the automorphism group, or in generators of automorphisms, are considered as the most critical nodes. The computation of the symmetry groups and the associated computation complexity are discussed in details. Throughout simulation, it is observed that the set of critical nodes identified by symmetry analysis is a subset of unmatched nodes corresponding to the locations of FACTS controllers. This overlap further reveals the importance of symmetry in power network analysis and synthesis.

This study proposes an approach to secure the critical elements of power networks via obscuring the published graph of the grid and, in turn, reducing the chance of distinguishing and manipulating the critical data of FACTS devices by adversaries. This has been accomplished via introducing a new concept, namely moderated-k-security, which provides new necessary and sufficient conditions for obscuring the network critical data.

The rest of the chapter is organized as follows. In Section 4.3, a topology-based solution to the placement of FACTS controllers is presented using the maximum matching principle. The cyber-security of the critical data of the network including the data exchange between FACTS controllers is addressed in section 4.4 using the concept of symmetry groups. The simulation is carried out on the 49-bus, 274-bus, and $1,176$-bus systems in section 4.5 and the effectiveness of the proposed approaches are verified.

4.3 A topological approach to the placement and control of FACTS devices in power networks

In this section, we look at the placement of FACTS devices from a controllability perspective. To this end, the problem of FACTS placement is transformed to the problem of finding the number and locations of the required FACTS devices that can structurally control the system. First, some preliminaries on graph theory and symmetry are reviewed and then the main result of this section is presented.

4.3.1 Preliminaries on graph theory and symmetry groups

A graph $\mathcal{G}$ is a composition of a set of nodes $\mathcal{V}$ and edges $\mathcal{E}$ denoted by $\mathcal{G}(\mathcal{V}, \mathcal{E})$. Two nodes are *adjacent* if there is an edge between them. The size and order of $\mathcal{G}$ are denoted by $|\mathcal{V}|$ and $|\mathcal{E}|$, respectively. An *adjacency matrix* $\mathcal{A}$ is a square $|\mathcal{V}| \times |\mathcal{V}|$ whose elements a_{ij} indicate the connection between every pair of nodes within the graph. $a_{ij} = 1$ if there is an edge between nodes i and j, otherwise $a_{ij} = 0$. The *degree matrix* $\mathcal{D}$ is a diagonal matrix whose diagonal elements d_{ii} is equal to the number of nodes connected via an edge to node i. The *Laplacican matrix* $\mathcal{L}$ is defined as $\mathcal{L} = \mathcal{D} - \mathcal{A}$. A *permutation* σ of a set of ordered nodes $\mathcal{V}$ is a rearrangement of its members into a sequence. The order of σ is the smallest positive integer m such that $\sigma^m = \varepsilon$ where ε is the identity (also known as trivial) permutation. The composition of two permutations σ_1 and σ_2, denoted by $\sigma_1 \circ \sigma_2$ is the point-wise product of them. If a node is rearranged by a permutation it is called a *moved* node by that permutation, otherwise it is a *fixed* node. The set of all permutations that rearrange a node v_l is denoted by Mov_{v_l}. Two permutations σ_1 and σ_2 are *disjoint* if each moved node by σ_1 is fixed by σ_2, or equivalently, every moved node by σ_2 is fixed by σ_1, otherwise, σ_1 and σ_2 are *joint* permutations.

Proposition 4.3.1. *If a node is rearranged by a permutation σ on $\mathcal{G}$, it can not be fixed by the composition of σ and its disjoint permutations on $\mathcal{G}$.*

Proposition 4.3.2. *If a node is fixed by a set of disjoint permutations, it can not be moved by the compositions of these disjoint permutations.*

Automorphism group is a quantified notion of symmetry. Under the act of an automorphism, a graph can be mapped to itself without changing the graph adjacency or Laplacian matrices. It can be mathematically described as a permutation σ for which $\{i, j\} \in \mathcal{E}(\mathcal{G})$ if and only if $\sigma(i), \sigma(j) \in \mathcal{E}(\mathcal{G})$. The set of all automorphisms of $\mathcal{G}$ and its size are denoted by $\text{Aut}(\mathcal{G})$ and $|\text{Aut}(\mathcal{G})|$. Automorphism groups can be built up from a set of elementary automorphisms called generators of automorphisms $\text{Gen}(\mathcal{G})$ (See Appendix A). Once the whole set of generators are determined, the automorphism group can be constructed from the compositions of all generators and automorphisms of order m up to generating unique permutations. Throughout this chapter, σ and φ are used to indicate an automorphism and a generator of automorphism, respectively. The symmetry elements, including $\text{Aut}(\mathcal{G})$ and $\text{Gen}(\mathcal{G})$, are computed in Sage (System for Algebra and Geometry Experimentation).

4.3.2 CN Controllability implications for placement of facts devices

The above preliminaries on graph theory and symmetry will be used later in this chapter. Now, the necessary conditions for controllablity by means of a set of FACTS devices are presented using the maximum matching principle which can be implemented for finding the number of required FACTS devices in the next section. The necessary conditions for uncontrollability of a pair of system matrices $(\mathcal{A}, B)$ is related to a the determining set [58] which can be attained from the symmetry group.

Definition 4.3.1. *A subset S of the vertices of a graph $\mathcal{G}$ is called a determining set if whenever $g, h \in$ Aut$(\mathcal{G})$ so that $g(s) = h(s)$ for all $s \in S$, then $g = h$. Equivalently, a subset of nodes of a graph $\mathcal{G}$ is called a determining set $\mathcal{S}$ if every automorphism of $\mathcal{G}$ can be uniquely determined by its action on the nodes of $\mathcal{S}$.*

Corollary 4.3.1. *[62] A necessary condition for controllability of the pair $(\mathcal{A}(\mathcal{G}), B(S))$ is that S is a determining set.*

Lemma 4.3.1 adapts the necessary conditions for controllability attained in [62] to the context of power networks where the FACTS controllers act as the so called driver nodes.

Lemma 4.3.1. *[58] Assume that the adjacency matrix $\mathcal{A}$ of the graph of power network $\mathcal{G}$ is diagonalizable and symmetry preserving. Then the pair of system matrices $(\mathcal{A}, \mathcal{S})$, where $\mathcal{S}$ and $|S|$ are the associated determining set and its size, respectively, is uncontrollable if $\mathcal{G}$ admits a nontrivial automorphism σ which fixes the input set $\mathcal{S}$, i.e., $\sigma(i) = i$ for all $i \in \mathcal{S}$.*

A straightforward result of the Lemma 4.3.1 is stated in the proposition 4.3.3.

Proposition 4.3.3. *The necessary condition for controllability of $(\mathcal{A}, \mathcal{S})$ is that for all $\sigma_i \in$ Aut$(\mathcal{G})$ there is at least one node v_l where $v_l \in$ Mov(Aut$(\mathcal{G})$).*

The above proposition simply means that at least one moved node of each automorphism must belong to the determining set $\mathcal{S}$ in order to satisfy the controllability of $(\mathcal{A}, \mathcal{S})$. Although Lemma 4.3.1 or Proposition 4.3.3 can theoretically be used to examine the controllability of power networks, in practice, checking the whole set of automorphisms for medium and large networks is not computationally effective. In [59], the size of automorphism group of US power grid is computed which is equal to 5.1851×10^{152}. Clearly, this is a big computation burden to calculate the determining set S by computing all automorphisms and sweeping over them. In contrast, if we attain the determining set from the generators of automorphisms, which is significantly a smaller set than automorphism group, then the determining set can be effectively computed using the conventional processing tools.

Lemma 4.3.2. *Assume that $\mathcal{A}$ is diagonalizable and symmetry preserving, $\mathcal{F}$ is a determining set (for which if the generators of automorphisms $\varphi_1, \varphi_2 \in Gen(\mathcal{G})$ so that $\varphi_1(f) = \varphi_2(f)$ for all $f \in \mathcal{F}$ then $\varphi_1 = \varphi_2$), and $\mathcal{J}$ is the set of all possible unique compositions of generators of order m with at least one joint node. The pair of system matrices $(\mathcal{A}, \mathcal{F})$ is uncontrollable if there exists at least one generator of automorphism φ_j, where $\varphi_j \neq \varepsilon$, for which $\varphi_j(i) = i$ for all $i \in \mathcal{S}$. Moreover, the necessary conditions for controllability of the power system using the FACTS devices corresponding to the nodes in $\mathcal{F}$ are*

1. *$\forall \mathcal{J}_J,\ J = 1, ..., |\mathcal{J}|,\ i = 1, ..., |\mathcal{F}|,\ \mathcal{F}(i) \neq j$ where j is a joint node of $\mathcal{J}_J$,*
2. *If $\forall v_l \in \varphi_g \Rightarrow v_l$ is a joint node, then $\mathcal{F}(v_l) \neq v_l$,*
3. *$\forall i \in \mathcal{F} \Rightarrow \varphi_g(i) \neq i$ where $g = 1, ..., h$ and $h = |Gen(\mathcal{G})|$.*

Proof. Using the proof by contradiction, we assume that if there is a generator φ_j for which $\varphi_g(i) = i$ for all $i \in \mathcal{S}$ then the pair $(\mathcal{A}, \mathcal{F})$ is controllable. This means

$$\exists\, \sigma,\ \sigma \in \text{Aut(G)}\ \&\ \sigma(i) = i$$

since all $\varphi \in \text{Aut}(\mathcal{G})$. This contradicts the condition of Lemma 4.3.1. For the second part of the proof, we have to verify that the determining set or the locations of FACTS devices attained in $\mathcal{F}$ must satisfy the conditions 1-3. The composition of joint generators may fix an unfixed node by one or some of them. Condition 1 thus excludes the joint nodes from $\mathcal{F}$ as it might be fixed in a composition and does not emerge in the resulted automorphisms. Hence, another node in those generators containing joint nodes must be included in $\mathcal{F}$. On the other hand, if all moved nodes of a generator are joint nodes, then all nodes must be included in $\mathcal{F}$, i.e., $\forall v_l \in \varphi_g,\ \mathcal{F}(v_l) \neq v_l$, as some of these nodes might be fixed by the composition (condition 2). Condition 3 considers the case where the composition is a product of disjoint generators. In this case, selecting one node from each generator will generate a set of nodes that necessarily satisfies the condition of being a determining set for the corresponding set of automorphisms. This is because the composition of disjoint generators does not fix a moved node by each of generators. This verifies that $\mathcal{S} \subset \mathcal{F}$ which means the determining set attained from generator set contains all moved nodes by $\mathcal{S}$. □

Lemma 4.3.2 facilitates using generators of automorphisms instead of automorphism group in order to find the determining set. According to Lemma 4.3.2, the whole set of FACTS devices can be attained effectively from the set of generators of automorphisms. However, Lemma 4.3.2 only provides the necessary conditions for controllability. To attain the sufficient condition for controllability of power systems, we use the maximum matching principle.

Definition 4.3.2. *A matching, M, of $\mathcal{G}$ is a subset of edges of E such that no node in V is adjacent to more than one edge in M, or intuitively, no two edges in M share a common node. A matching M is called maximum matching if for any other matching M', $|M| \geq |M'|$.*

In [57], the CN controllability is addressed by maximum matching principle where the set of all unmatched nodes are considered as driver nodes. In our problem setup, the set of FACTS devices can be considered as the set of required driver nodes for full controllability of power network. Once the maximum matching algorithm is implemented, all unmatched nodes must be considered as the locations of FACTS devices.

Using the maximum matching principle, the set of required FACTS devices for full controllability of power network can be attained. The simulation results on 49-bus and 274-bus systems in section IV confirm the effectiveness of using maximum matching principle for the placement of FACTS devices. Lemma 4.3.2 is also assessed in the simulations where it is observed that the number and locations of FACTS devices attained from MMP and Lemma 4.3.2 are very similar.

4.3.3 Modeling of the shunt FACTS devices in power networks

Once the number and locations of the required FACTS devices are determined, a dynamic control strategy can be implemented to improve the power flow capabilities. Note that there are various types of FACTS devices which we do not intend to explore as the main focus of this chapter is on the proposed approaches for placement of FACTS devices (Section 4.3) and securing them (Section 4.4) from the novel topological perspectives.

The power flow equations can be written as

$$P_{ij} = \frac{V_i V_j}{X_{ij}} sin(\delta_i - \delta_j) \tag{4.1}$$

$$Q_{ij} = \frac{1}{X_{ij}} (V_i^2 - V_i V_j cos(\delta_i - \delta_j)) \tag{4.2}$$

where V_i and V_j are the voltage magnitudes at buses i and j, X_{ij} is the reactance of the line between buses i and j, and $\delta_i - \delta_j$ is the angle difference between phasor voltages V_i and V_j. We have used the shunt voltage-source converter (VSC) FACTS devices in two control modes: voltage magnitude control mode and var control mode. The dynamic model of a shunt VSC FACTS devices is shown in Figure 4.1.a and its balanced positive sequence model is shown in Figure 4.1.b where V_i, $i = 1, 2, 3$ is the bus voltage, and Z_1 and Z_2 are the line impedances. Also, γ_{sh} and α_{sh} are conversion ratio signal to control the shunt converter voltage magnitude and the angle of the shunt VSC measured with respect to β of the shunt bus voltage

phasor V. The dynamic model of shunt VSC with PID (proportional integrative derivative) controller in voltage magnitude mode and VAR control mode are shown in Figure 4.2.a and 4.2.b, respectively. The voltage magnitude V_m and the angle of the VSC voltage are determined

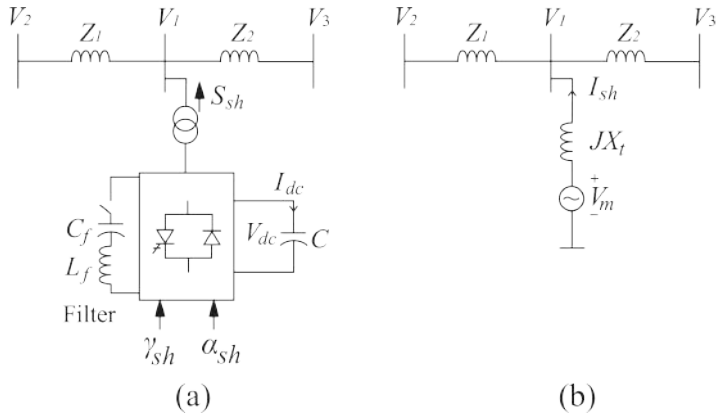

Figure 4.1: Shunt VSC converter. (a) The schematic diagram, (b) The balanced positive-sequence model.

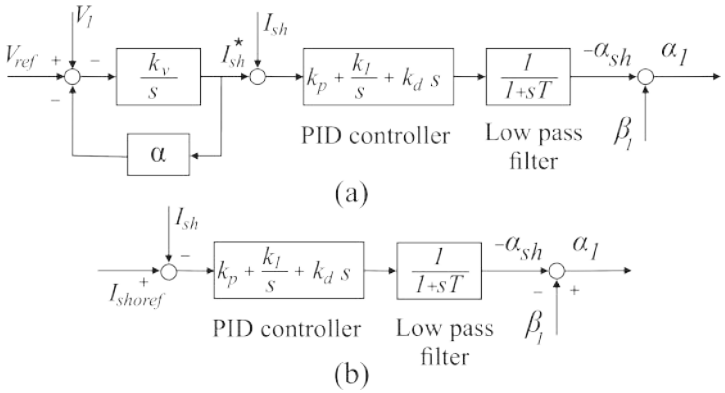

Figure 4.2: Schematic control diagram of a shunt VSC in (a) voltage control mode, (b) VAR control mode.

from the control signal generated by a PID controller. In voltage magnitude control mode, by fixing k_{dc} to a constant, the VSC voltage magnitude changes in response to changing the capacitor voltage. The bus voltage V_1 is regulated compared to setpoint voltage V_{ref} using outer control loop consisting an integrator with a gain which results in a droop α. The outer loop generates a reactive current I_{sh}^* which acts as the setpoint for the inner control loop. Finally, the shunt reactive current I_{sh}^* is compared to real I_{sh} via the inner PID loop and a low-pass filter. The VSC voltage angle α can then be computed from the bus voltage angle β. In VAR control mode, the shunt reactive current setpoint I_{sh} is directly determined (without an outer loop) and compared with real I_{sh} to trigger the PID controller.

The inserted voltage by VSCs can be approximated as

$$V_m = k_m V_{dc} e^{j(\alpha_{sh}+\beta)} \tag{4.3}$$

where V_{dc} and k_m are the capacitor terminal voltage and the conversion ratio between the dc-side and ac-side voltages, respectively. From Figure 4.1.b, the line current I_s can be written as

$$I_{sh} = \frac{V_m - V_1}{jX_t} \tag{4.4}$$

and the active power that can be injected to the system is

$$P_{sh} = -\frac{V_1 V_m sin(\beta - \alpha_{sh})}{X_t} \tag{4.5}$$

and the reactive power injected to the system is equal to

$$Q_{sh} = \frac{V_1(V_m cos(\beta - \alpha_{sh}) - V_1)}{X_t}. \tag{4.6}$$

When the system is oscillating, the control signal is not zero and the capacitor C will exchange reactive power with the power system which results in increasing or decreasing the capacitor voltage V_{dc} following the equation

$$C\frac{dV_{dc}}{dt} = I_{dc} \tag{4.7}$$

where I_{dc} is the capacitor current. After transition time, the control signal converges to zero and, as a result, the energy exchange between the capacitor and power system converges to zero. With an ideal VSC model, the active power on its ac and dc sides are equal ($P_{ac} = V_{dc}I_{dc}$). Thus we can write

$$\frac{dV_{dc}}{dt} = \frac{1}{CV_{dc}}P_{ac}. \tag{4.8}$$

The dynamic model of power system can then be constructed by interfacing the dynamic model of FACTS device with other network components attained from the Kirchhoff electrical equations in order to analyze the power flow.

4.4 The moderated k-security approach for obscuring the critical network data for adversaries

In this section, the cyber-security of critical elements of power grid is addressed using a graph theoretic property, i.e., graph symmetry. In discrete algebra, the graph symmetry is quantified using the automorphism group. It is verified that graph symmetry has a significant role in determining the controllability of the underlying network [62]. In fact, symmetry is an obstruction to controllability. The higher the number of automorphisms, the more symmetric is the network and, in turn, more driver nodes are required for full state controllability. These driver nodes, in the context of power networks, are the well known FACTS devices ([8]- [9], [16], and [18]) or wide area controllers ([65]- [66]).

4.4.1 Definitions and the proposed theorems

A notion of symmetry, k-symmetry, is leveraged here to make the critical nodes/edges indistinguishable by adversary agents. Necessary and sufficient conditions for security are attained and a novel algorithm is proposed for cyber-security constrained placement of FACTS devices. The bigger the symmetry group, the more symmetric the underlying graph is. On the other hand, symmetry is an obstruction to controllability [62] meaning a bigger number of FACTS devices are required when the network is more symmetric. We compute the symmetry index (Aut($\mathcal{G}$) or Gen($\mathcal{G}$)) before and after removing a node possessing a FACTS device as a measure of how critical is this node. This index is computed in simulation section for 49-bus and $1,176$-bus systems.

Now, we leverage on the concept of k-security to obscure the identification of critical elements of power grid.

Definition 4.4.1. *[56] Let $\mathcal{G}_k$ be the released version of $\mathcal{G}$. The set of critical nodes $\mathcal{V}_c$ of $\mathcal{G}$ is k-secure if the adversary cannot distinguish it from $\mathcal{G}_k$ with a probability greater than $1/k$. The set of critical edges $\mathcal{E}_c$ of $\mathcal{G}$ is k-secure if the adversary cannot distinguish them from $\mathcal{G}_k$ with a probability greater than $1/k$.*

Now, we introduce the concept of moderated-k-symmetry which will be used in Theorem 4.4.1 to adapt an approach for securing the most critical elements of the power grid.

Definition 4.4.2. *A graph $\mathcal{G}$ satisfies moderated-k-symmetry if for the finite set of nodes v_l there exists $k-1$ distinct automorphisms $\sigma_{i,1}(v_l), \sigma_{i,2}(v_l), ..., \sigma_{i,k}(v_l)$ that satisfy*

(i) $\sigma_{i,m}(v_l) \neq \sigma_{i,n}(v_l)$ *if* $m \neq n$, *and*

(ii) $\sigma_i(v_l) \neq v_l$ *for* $l = 1, ..., n$.

Theorem 4.4.1. *The critical nodes/edges of $\mathcal{G}$ are k-secure if $\mathcal{G}$ satisfies moderated-k-security for the finite set of nodes $v_c = \{v_1, ..., v_i\}$.*

Proof. If $\mathcal{G}$ is moderated-k-symmetric, then for every critical node v_c there are $k-l$ distinct mappings that preserve the network structure after permuting v_c. For any accessible structural information $\mathcal{G}_k$ for the adversary targeting node v_c there are at least k distinct nodes that act the same structural role as v_c. Hence, the adversary cannot distinguish v_c with a probability greater than $1/k$. Subsequently, for a successful attack on an edge, the adversary needs to identify the end nodes of the targeted edge. Hence the probability of identifying an edge is equal to $1/k \times 1/k = 1/k^2$. □

Theorem 8.2 can be used to secure the cyber graph of the power network by releasing a permuted graph to the public. However, the approach is not optimal as usually not all critical nodes are permuted by the k number of automorphisms in Aut($\mathcal{G}$). We have improved this approach by relating the concept of moderated-k-security to the case where only the critical nodes are needed to be secured. Moreover, the automorphism groups typically have a gigantic

size for medium and large networks [59] and it is not possible to compute and sweep over all of them. Theorem 4.4.2 resolves these issues by leveraging on the symmetric characteristics of generators of automorphisms.

Theorem 4.4.2. *Assume that the adjacency matrix of $\mathcal{G}$ is diagonalizable and symmetry preserving, b is the indicator vector associated to the set $\mathcal{F}$ containing $|\mathcal{F}|$ number of FACTS devices, and $\mathcal{G}_P$ is the published network to the public. Having access to $\mathcal{G}_P$, the adversary cannot distinguish the critical nodes and edges of the network with the probabilities greater than $1/(p(1+q)-1)$ and $1/(p(1+q)-1)^2$, respectively, where p and q are the multiplicities of the critical node/s in Gen$(\mathcal{G})$ and the size of disjoint generators denoted by $|Gen_{dis}(\mathcal{G})|$.*

Proof. Assume $\mathcal{A}'$ is the adjacency matrix associated with $\mathcal{G}_P$. Since $\mathcal{G}_P$ is the permuted graph of $\mathcal{G}$ under an automorphism σ_l, and $\sigma_l \in \text{Aut}(\mathcal{G})$, we can write $\mathcal{A}' = \mathcal{A}$ which simply means that the adjacency matrix of the published graph is preserved under mapping that generates $\mathcal{G}$. Given $F_{v_l}^{Gen}$, $M_{v_l}^{Gen}$, and $F. \circ M$ as the set of generators that fixes v_l, the set of generators that moves v_l, and the pointwise composition of $F_{v_l}^{Gen}$ and $M_{v_l}^{Gen}$, respectively, we can write

$$|M_{v_l}^{Aut}| \geq |M_{v_l}^{Gen}| + |M_{v_l}^{F.\circ M}|. \tag{4.9}$$

The above equation can be written as

$$|M_{v_l}^{Aut}| \geq p + p.q. \tag{4.10}$$

Therefore the multiplicity of critical nodes in Gen$(\mathcal{G}_P)$ is at least $p(1+q)$. Then the immediate result, according to Theorem 4.4.1, is that the network is moderated-k-secure where $k = p(1+q)-1$. □

4.4.2 Proposed algorithm for locating and securing critical FACTS devices

Associating the cyber-security to p and q in Theorem 4.4.2 guarantees conservative bounds on the probabilities of recognizing the critical elements. The reason for this is that conditions of Theorem 4.4.2 are derived assuming that all compositions of automorphisms moving a critical node with joint generators and mediators will fix the joint nodes, which, in practice, is a very rare possibility. In fact, since the size of automorphism group is very big compared with generator set, the probabilities of recognizing the critical nodes and edges are far less than $1/(p(1+q)-1)$ and $1/(p(1+q)-1)^2$, respectively. This means that the probability of recognizing the critical elements is lower than the bounds guaranteed by Theorem 4.4.2. The proposed symmetry-based approach for identifying and protecting the critical data of the cyber networks is summarized in the Algorithm 2.

Algorithm 2 An algorithm for finding and securing the critical FACTS devices

Input: The graph $\mathcal{G}$ of the power network

Output: The number and locations of FACTS devices and the cyber-secured topology of the power network

1: Perform the maximum matching procedure on the graph of power network to attain the set of unmatched nodes.
2: Assign a FACTS device to each unmatched node.
3: Compute the adjacency matrix $\mathcal{A}$ of the network
4: Compute Gen($\mathcal{G}$) from $\mathcal{A}$ using Sage.
5: Find the set of FACTS devices $\mathcal{F}$ with maximum multiplicity in Gen($\mathcal{G}$).
6: **for** i=1:$|\mathcal{F}|$ **do**
7: Remove the FACTS device number i.
8: Compute the symmetry index (Aut(G) or Gen($\mathcal{G}$)) after removing the FACTS device number i.
9: **end for**
10: Sort all values of |Aut(G)| or |Gen($\mathcal{G}$)| attained in steps 6-9 from the highest to the lowest value in a vector z which will be correspondent to the critical FACTS devices from highest to the lowest critical device.
11: The lowest amount of |Aut(G)| or |Gen($\mathcal{G}$)| corresponds to the most critical node identified in Step 1.
12: Order the critical elements in a vector e_r from maximum critical to the minimum critical element.
13: Determine the generator φ that moves the most critical nodes.
14: Attain the cyber-secured graph under the act of φ attained in Step 13.

4.4.3 Discussions

In this chapter, the placement of FACTS devices is pursued using the network topology. The physical parameters of the power systems are then used to analysis the power flow with fixed FACTS controllers. As the network size increases, the proposed approach is more effective since the typical network symmetry group is bigger and the nodes with maximum multiplicities in generators of automorphisms are more effective in determining the number of required FACTS devices. Furthermore, for large symmetry sizes, the associated vast obscurity can be realized by further reducing the probability of distinguishing the most critical nodes of the grid. In a similar manner, the proposed approach for identifying the critical nodes can be used to

Table 4.1: Parameters of the modified 49-bus system [67] for power flow analysis: Bus number, bus voltage magnitude $|V|$ in volts, angle of bus θ, net active power of the bus P_n in MW, and the net reactive power of the bus Q_n in MVar.

Bus	|V|	θ	P_n	Q_n	Bus	|V|	θ	P_n	Q_n
1	380	0	-35	-12	26	347	-12	-33	-17
2	366	-10	45	12	27	338	-11	127	45
3	372	-5	-39	45	28	358	-9	212	67
4	361	2	-73	-27	29	349	4	-37	-17
5	353	0	-87	-42	30	376	-14	-22	-15
6	383	-1	-63	-28	31	359	-1	-39	-13
7	345	-4	-22	-9	32	366	-10	-47	-19
8	347	-8	-52	-24	33	330	6	237	121
9	369	5	-45	-19	34	369	-9	-78	-33
10	346	-7	-39	-21	35	354	7	-49	-18
11	338	5	-27	-11	36	357	-11	256	79
12	339	-8	-56	-21	37	347	-12	-56	-26
13	339	-5	-37	-14	38	327	-10	-67	-17
14	349	-7	-68	-34	39	337	-12	-44	-15
15	353	-11	-65	-13	40	347	-13	-32	-14
16	345	-8	277	101	41	369	-9	255	98
17	349	6	-55	-23	42	350	-7	-43	-19
18	350	8	284	121	43	352	2	-61	-27
19	354	3	-45	-22	44	357	-7	-27	-13
20	351	-12	-37	-17	45	352	-3	-83	-36
21	334	-11	189	82	46	323	-6	302	143
22	336	-5	-64	-34	47	341	-9	-45	-21
23	354	3	-12	8	48	339	-6	-74	-31
24	337	-11	-43	-19	49	350	-5	-64	-25
25	355	-12	-32	-8					

identify the critical edges. We do this by (a) removing the edges with at least one end connected to a FACTS controller with maximum multiplicity in Gen($\mathcal{G}$), and (b) following steps 3-12 for edges instead of FACTS devices.

A novel advantage of the proposed methodology is that the symmetry concept is inherent in the graph of the network; therefore, no manipulation is required as we only leverage on an intrinsic property of the network. The impacts of symmetry on the number and locations of FACTS devices and their roles in the security of the underlying cyber graph motivate the consideration of symmetry characteristics of the grid in developing the existing networks or constructing new networks. Embedding the asymmetrical structures makes the system more controllable which, in turn, reduces the number of required FACTS devices which leads to more security realization.

The critical elements of the grid can be identified using the proposed symmetry analysis. It will be observed in simulations of section IV that these critical nodes are usually the same nodes that are selected as the locations of FACTS controllers. This is quite interesting as the locations of FACTS controllers are at the unmatched nodes attained from the maximum matching principle while the critical nodes are attained from a totally different technique, i.e. nodes with maximum multiplicities in the symmetry groups are identified as critical nodes. This re-emphasizes the role of symmetry for explaining the emergent behavior of a complex power network.

The proposed cyber-security approach is implemented after placement of the FACTS devices. It obscures identifying the data associated to FACTS devices by leveraging on the symmetry characteristics of the grid. In fact, the proposed security approach only deals with the cyber graph and has no compromising implication for the physical graph of power network. Thus the approach does not compromise the original functionalities of the FACTS devices. However, the placement result can, to some extent, impact on the level of cyber-security. This is because the symmetry characteristics of the set of FACTS devices might be slightly different for different configurations of FACTS devices in the grid. This difference is not significant since the majority of FACTS devices are placed at the locations of driver nodes identified from symmetry analysis.

4.5 Implementation of the proposed cyber constrained placement of FACTS controllers on three power networks

The proposed topology-based approach for placement, control, and securing FACTS devices is implemented for the small 49-bus, moderate 274-bus, and a large 1,176-bus systems of references [67], [68], and [69], respectively. For the 274-bus and 1,176 bus systems, the emphasis is on the effectiveness of the proposed approach for obscuring the critical data for moderate/large networks.

4.5.1 Simulation and analyses of 49-bus system

The physical graph of the 49-bus system with 59 transmission lines is shown in Figure 4.3. There are 9 generation buses where all of them are load buses as well. The rest of buses are

considered as load buses. The physical parameters of 49-bus system including the voltage magnitude and angle, active, and reactive power of all 49 busses are presented in Table 4.1. The line parameters for each of 59 transmission lines are presented in Tables 4.2 where $|V|$, θ, R, X and B are the bus voltage magnitude in volts, angle of bus voltage in degree, line resistance in ohms (Ω), line reactance in ohms (Ω), and capacitive susceptance in siemens (s), respectively. The conductance is considered zero at all lines. The maximum matching principle

Table 4.2: Parameters of the modified 49-bus system [67] for power flow analysis: line number as "$l : i - j$" where l is the line number and i and j are the the nodes at two ends of the line number l, line resistance R in ohms (Ω), reactance X in ohms (Ω), and capacitive susceptance B in siemens (s).

line	R (Ω)	X (Ω)	B (s)	line	R (Ω)	X (Ω)	B (s)
1:1-2	0.40	0.23	0.213	31:6-33	0.23	0.15	0.034
2:2-3	0.10	0.04	0.124	32:32-33	0.35	0.31	0.042
3:2-4	0.12	0.03	0.154	33:7-34	0.54	0.24	0.635
4:9-14	0.40	0.33	0.163	34:32-34	0.51	0.34	0.122
5:10-14	0.05	0.23	0.017	35:28-35	0.5	0.38	0.210
6:11-14	0.39	0.06	0.213	36:15-36	0.23	0.34	0.045
7:6-15	0.43	0.28	0.143	37:35-36	0.34	0.04	0.030
8:12-15	0.10	0.36	0.013	38:3-37	0.04	0.09	0.027
9:14-15	0.23	0.33	0.123	39:8-37	0.45	0.41	0.037
10:13-16	0.25	0.29	0.114	40:18-37	0.03	0.08	0.028
11:15-16	0.32	0.35	0.026	41:32-37	0.12	0.25	0.033
12:7-17	0.23	0.14	0.118	42:22-38	0.34	0.33	0.015
13:8-17	0.24	0.18	0.216	43:23-38	0.04	0.13	0.035
14:18-19	0.03	0.07	0.028	44:37-38	0.45	0.04	0.035
15:7-20	0.32	0.04	0.238	45:39-40	0.03	0.08	0.043
16:19-21	0.24	0.03	0.018	46:41-14	0.12	0.01	0.123
17:16-22	0.09	0.04	0.118	47:42-33	0.34	0.03	0.145
18:22-23	0.10	0.24	0.219	48:41-42	0.43	0.03	0.136
19:23-24	0.03	0.32	0.173	49:43-41	0.45	0.04	0.120
20:23-25	0.05	0.07	0.133	50:44-42	0.43	0.02	0.040
21:23-26	0.23	0.04	0.115	51:45-21	0.02	0.05	0.179
22:5-28	0.34	0.03	0.266	52:45-22	0.04	0.13	0.220
23:20-28	0.10	0.23	0.326	53:46-45	0.06	0.08	0.040
24:27-28	0.03	0.05	0.246	54:47-46	0.04	0.24	0.254
25:27-29	0.05	0.28	0.166	55:48-46	0.34	0.04	0.074
26:3-30	0.23	0.01	0.226	56:49-23	0.33	0.03	0.135
27:18-30	0.13	0.08	0.216	57:49-39	0.43	0.11	0.255
28:20-31	0.04	0.09	0.173	58:49-45	0.45	0.13	0.130
29:5-32	0.03	0.05	0.046	59:49-46	0.05	0.03	0.220
30:44-28	0.05	0.24					

is implemented on the graph of the 49-bus system and the matched edges are illustrated with red lines in Figure 4.4. Implementing the MMP has resulted in 7 unmatched nodes at locations

4, 9, 10, 24, 25, 47 and 48 which, according to the maximum matching principle adapted in Section III, can be considered as the locations of FACTS devices. Therefore, seven series VSC FACTS controllers with 100-MVA rating at a voltage of 1 p.u. are located at the determined locations (Figure 4.4). The power flow transmission is analysed in MATLAB using Newton Raphson algorithm to solve for a vector of bus voltage magnitudes and angles. The parameters of PID controller are selected after trial and error. The proportional coefficient is $k_p = 0.3$, the integrator coefficient is $k_i = 0.5$, and the derivative parameter is $k_d = 0.05$. The power flow analysis of 49-bus system is performed in MATLAB by interfacing the 7 shunt VSC-FACTS devices with the network. The network parameters including the line/bus voltage, angle, and apparent power before and after adding the FACTS controllers are presented in Figure 4.5.

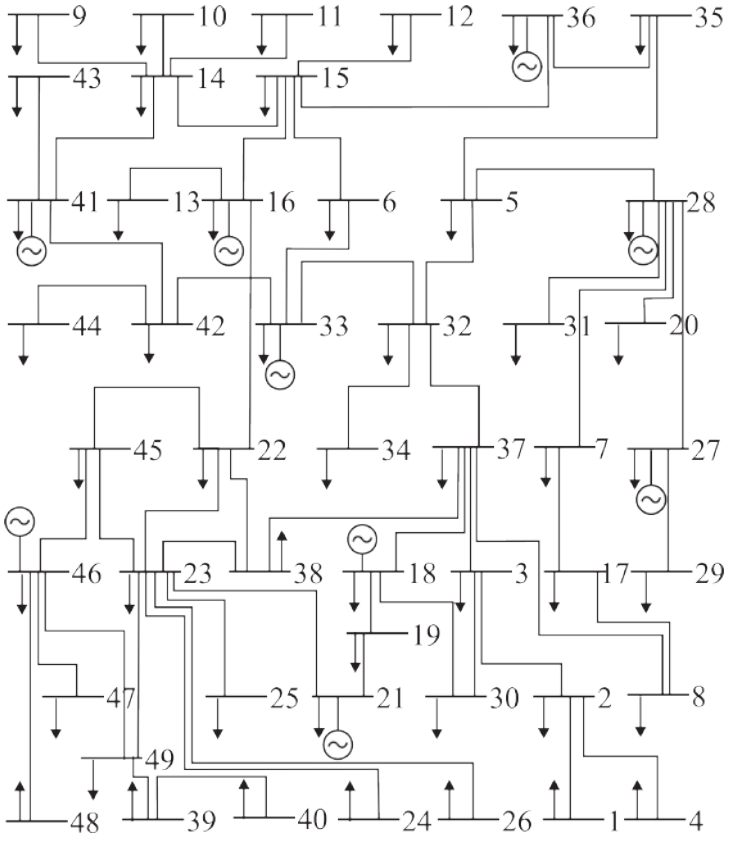

Figure 4.3: The schematic diagram of the modified 49-bus system [67].

The Newton Raphson algorithm has reached the solution after 28 iterations. The bus voltage magnitudes of all busses before and after using the FACTS controllers are illustrated in Figure 4.5.a. The voltage drop from the voltage base of 1 p.u. has significantly reduced after using the FACTS controllers. The average magnitude voltage of all 49 buses before and after using FACTS devices are 0.9233 p.u. and 0.9947 p.u., respectively, that means over %7.7 increase in the average of bus voltage magnitudes. The active power flow transfer of all 59 lines are compared and demonstrated in Figures 4.5.b. The sums of active power flow before and after using FACTS controllers are 3,052 MW and 3,153 MW, respectively. Equivalently, there is 101 MW power flow increase with using FACTS controllers. Also the line power losses for all 59 transmission lines before and after placing the FACTS controllers are shown in Figure 4.5.c.

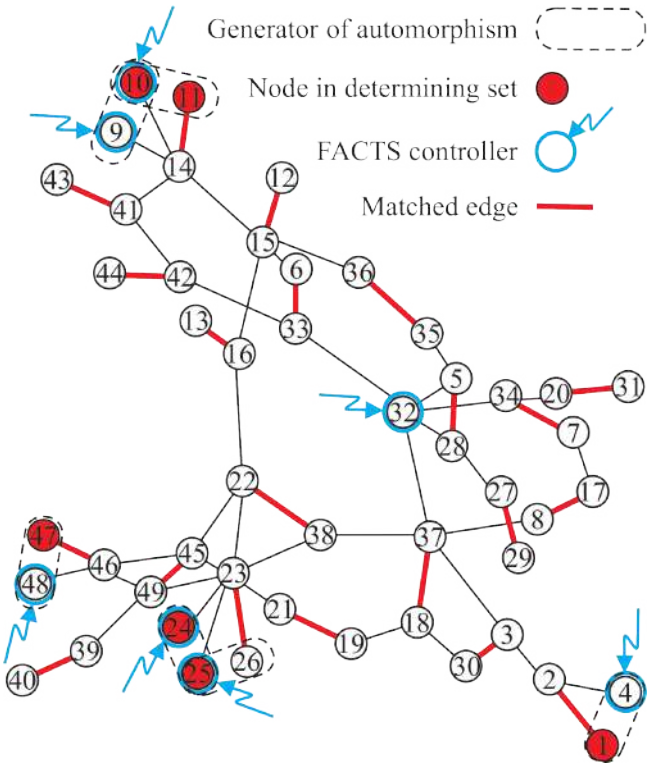

Figure 4.4: The duplicated topology of the network shown in Figure 4.3 generated in Sage. Red nodes are the set of nodes in determining set, red transmission lines are the matched edges attained from MMP, nodes inside the dashed loops are the set of nodes in Gen($\mathcal{G}$), and the blue rings with arrows represent the FACTS controllers which are positioned at the unmatched nodes attained from MMP.

The sum of power losses has been reduced from 8.65 MW to 7.08 MW indicating an overall improvement of over $\%18$.

To secure the data exchange between FACTS controllers using the proposed topological approach, first the cyber graph of the 49-bus system is adapted from its physical graph as shown in Figure 4.4. The size of Aut($\mathcal{G}$) for this network is computed in Sage and is equal to 144 (More explanation about computing the symmetry characteristics of the graph is presented in Appendix A). Although this is not a significantly large number and we can effectively compute the determining set by sweeping over all automorphisms, but we proceed with Gen($\mathcal{G}$) instead to adhere to the proposed approach of this chapter. Later, for larger networks (274-bus and $1,176$-bus systems), it will be shown that we can not sweep over the corresponding automorphism groups due to their gigantic sizes. The generators of automorphisms Gen($\mathcal{G}$) of 49-bus system are computed in Sage as

$$\text{Gen}(\mathcal{G}) = \{\varepsilon, (1,4), (9,10), (10,11), (24,25), (47,48)\}$$

and illustrated inside the dashed loops in Figure 4.4 (See Appendix A for calculating Gen($\mathcal{G}$)). The necessary conditions of controllability in Lemma 4.3.2 are tested and the determining set over Gen($\mathcal{G}$) is determined as $\mathcal{F} = \{1, 10, 11, 24, 25, 47\}$. Interestingly, it can be observed that

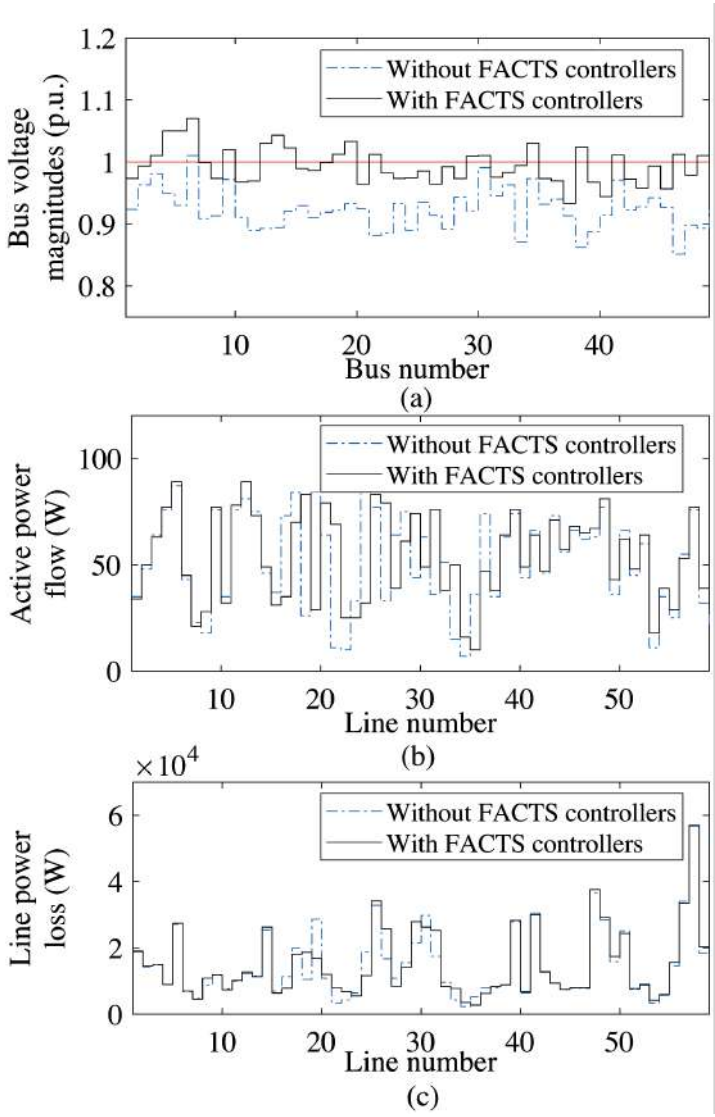

Figure 4.5: The power flow analysis of 49-bus system before and after using FACTS controllers. (a) The average of bus voltage magnitude has increased from 0.9233 p.u. to 0.9947 p.u. that means $\%0.0774$ p.u. increase. (b) The active power flow, which shows the overall 101 MW (or $\%3$) addition of active power transfer throughout the transmission lines. (c) The line power loss, which indicates $\%18$ reduction in power loss in the 59 transmission lines after using FACTS controllers.

the set of determined locations for FACTS devices attained from MMP is a subset of locations of generators of automorphisms. This verifies the importance of symmetry in controllability of power networks.

To investigate the cyber-security of FACTS devices, we first construct the cyber-graph of the network based on the available physical graph. The cyber graph is illustrated in Figure 4.4. The cyber-security of the most critical nodes of 49-bus system can be investigated using Theorem 4.4.2. The maximum multiplicity of the critical nodes in $\text{Gen}(\mathcal{G})$ is 2, i.e., $p = 2$, and the number of disjoint generators is 4. Therefore, by publishing a permuted network instead of the original network, the probability of the critical nodes and edges being recognized by an adversary is

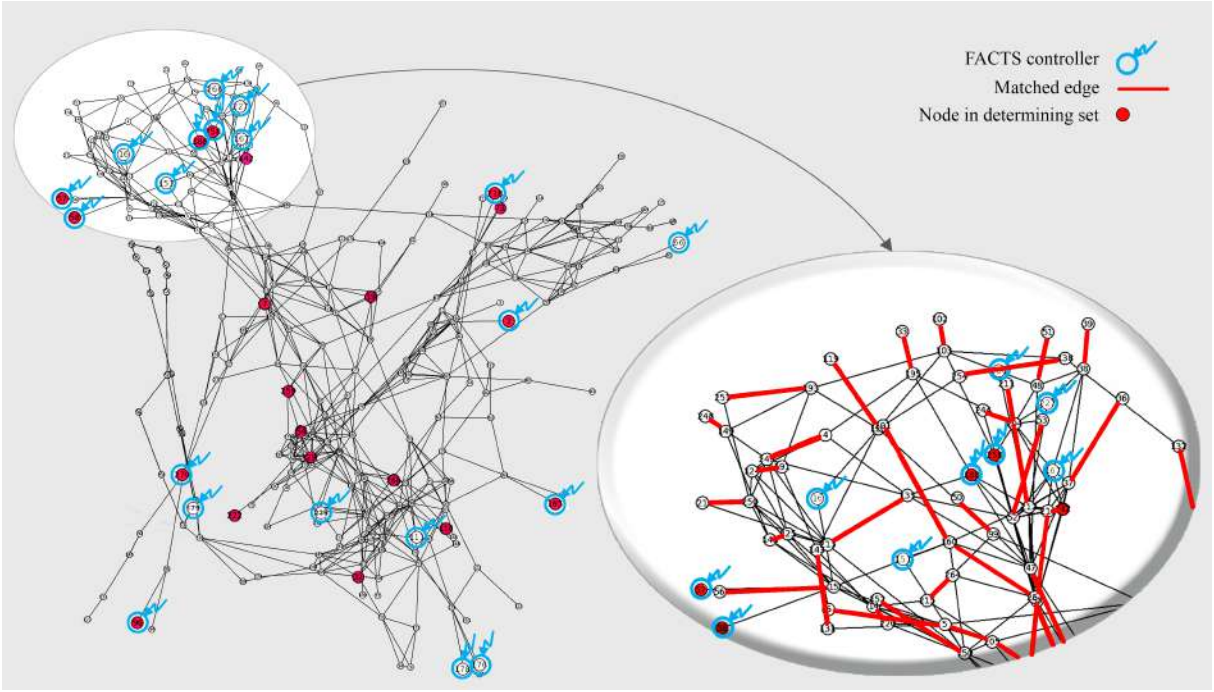

Figure 4.6: The MMP performed on the graph of 274-bus system. The unmatched nodes are considered as the locations of FACTS controllers. For clarification, a portion of matched edges is magnified on the right side of the figure. In total, 253 out of all 1338 edges are matched edges.

not greater than $1/9$ and $1/81$, respectively. It should be noted that under this permutation, the actual obscurity for adversary agent is even more than these values. This is because the maximum multiplicities of nodes in $\mathrm{Aut}(\mathcal{G})$ is 96 and the number of disjoint automorphisms is 4. Thus the actual probability of distinguishing the FACTS devices is less than $1/385$. However, for networks with bigger sizes, it is not feasible to compute the whole set of automorphisms and we have to rely on generators of automorphisms. This is verified via the simulation results on the next two networks, 274-bus and $1,176$-bus systems.

4.5.2 Simulation and analyses of 274-bus system

We perform simulations for the 274-bus system to better clarify the advantages of the proposed approaches for larger networks. Since the networks' parameters such as the impedances of the lines are not available for these two networks, we have not investigated the impacts of the proposed FACTS placement. We only determine the locations of FACTS controllers, the cyber-security, and the symmetry analysis for these networks. The FACTS placement impacts can be investigated in the same way as performed on the 49-bus system.

The 274-buss system is the equivalenced representation of US power grid [68] which has 274 nodes and $1,338$ edges as illustrated in Figure 4.6. The number of automorphisms of this network is $28,311,552$. Therefore, it is not computationally effective to sweep over this huge number of automorphisms. However, the size of $\mathrm{Gen}(\mathcal{G})$ for this network is very small compared to automorphism group and is equal to 23. The maximum matching principle is im-

plemented on this network and matched edges are identified (A portion of these matched edges are denoted by red lines in Figure 4.6). This has resulted in 20 unmatched nodes that are selected as the locations of FACTS devices. Since it is not possible to compute the maximum multiplicities of nodes in Aut($\mathcal{G}$) we compute the multiplicities of nodes in Gen($\mathcal{G}$). The maximum multiplicity of nodes in Gen($\mathcal{G}$) for 274-bus system is 1 and the size of disjoint generators is 21. It follows from Theorem 8.2 that $p = 1$ and $q = 21$. Correspondingly, the probabilities of the critical nodes being recognized when the adversary has access only to a permuted version of 274-bus network is no greater than $1/(1.(1 + 21) - 1) \simeq 0.047$. Similarly, the probability of identifying the critical edges, assuming one end at the critical node, is not greater than $1/(1.(1 + 21) - 1)^2 \simeq 0.002$.

4.5.3 Simulation and analyses of 1,176-bus system

We also examine the security of the $1,176$-bus system [69] which has $1,176$ nodes and $18,552$ edges. The number of automorphisms of this network is approximately 10^{259}. Clearly, it is computationally prohibitive to generate the whole set of automorphisms and then compute the maximum multiplicities of nodes within the set. However, the size of Gen($\mathcal{G}$) for this graph is 377. We performed the MMP on this network and identified 437 unmatched nodes which are then considered as the locations of FACTS devices. The maximum multiplicity of the most repeated nodes in Gen($\mathcal{G}$) is 4 and the size of disjoint generators is 237. Following the conditions of Theorem 8.2, the probability of recognizing the data associated to the FACTS devices and the critical edges in $1,176$-bus system are 10^{-3} and 10^{-6}, respectively. Due to space limitations, it is not possible to illustrate the graph of $1,176$-bus system.

The simulation results are summarized in Tables 3-4. As can be observed in Table 4, there is an overlap between the nodes in determining set and the set of nodes that are considered as the locations of FACTS controllers by MMP. For the 49-bus, 274-bus, and $1,176$-bus systems, these overlaps are $\%66$, $\%38$, and $\%42$, respectively. Although all nodes in determining set are not selected as the locations of FACTS controllers, yet it is inline with Lemma 4.3.2 since for every node in determining set which is not selected as a FACTS controller there is an alternative node belonging to $\mathcal{F}$ and within the same generator of automorphism which plays a same structural role in the network and, as such, can be alternatively selected as the location of FACTS controllers. For example, in 49-buss system, node 1 is in determining set but is not in $\mathcal{F}$. As demonstrated in Figure 4.4, nodes 1 and 4 belong to a same generator of automorphism and, according to Lemma 4.3.2, a necessary condition for controllability is that only one of these nodes must be included in the set of FACTS controllers. This further highlights the importance of symmetry in explaining some aspects of the network behavior.

Table 4.3: The results of FACTS placement and cyber-security of critical data using moderated-k-security indicating the number of nodes $|\mathcal{V}|$, edges $|\mathcal{E}|$, matched edges $\mathcal{M}$, number of required facts controllers $|\mathcal{F}|$, the average voltage of all buses in p.u. without FACTS controller $|\mathcal{V}_0|$ and with FACTS controllers $|\mathcal{V}^*|$, the total power flow in lines without FACTS controllers $|\mathcal{P}_0|$ and with FACTS controllers $|\mathcal{P}^*|$, the total line power losses without FACTS controllers $\mathcal{P}_{L0}$ and with FACTS controllers $\mathcal{P}_L^*$, the size of automorphism group |Aut| and generators of automorphism |Gen|, the size of determining set $|\mathcal{S}|$, maximum multiplicity of nodes in generators of automorphisms p, the number of disjoint generators q, the probability of distinguishing the data associated to the critical nodes $\mathcal{P}_\mathcal{V}$ and edges $\mathcal{P}_\mathcal{E}$ by adversary. The results of FACTS placement on the voltage and power flow and power loss of 274-bus and $1,176$-bus systems are not computed since these networks' information are not available. "NC" stands for "Not computed".

Simulation task			**MMP**		**FACTS placement on the physical graph**						**Symmetry results**			**Security of critical data**			
System	$\|\mathcal{V}\|$	$\|\mathcal{E}\|$	$\mathcal{M}$	$\|\mathcal{F}\|$	$\|\mathcal{V}\|_0$	$\|\mathcal{V}\|^*$	$\mathcal{P}_0$	$\mathcal{P}^*$	$\mathcal{P}_{L0}$	$\mathcal{P}_L^*$	|Aut|	|Gen|	$\|\mathcal{S}\|$	p_A	q_G	$\mathcal{P}_\mathcal{V}$	$\mathcal{P}_\mathcal{E}$
49-bus [67]	49	59	21	7	0.92	0.99	3052	3153	8.65	7.08	144	6	4	2	6	0.11	0.01
274-bus [68]	274	1338	253	20	NC	NC	NC	NC	NC	NC	28m	23	21	1	21	0.047	0.002
1,176-bus [69]	1176	18552	1121	53	NC	NC	NC	NC	NC	NC	$10E259$	377	33	4	237	0.001	$10E-6$

4.6 Conclusion

The placement of FACTS devices in power systems with the consideration of cyber-security of associated data exchange is addressed from a CN controllability perspective based on advanced topological techniques which, unlike the conventional methods, has no computational impediments. The proposed solution is attained using: i) the concepts of MMP and moderated-k-security to guarantee the cyber-security of the most critical data related to the FACTS controllers., ii) the idea of moderated-k-symmetry to arrange the published cyber graph based on generators of automorphisms that will significantly obscure the data exchange over the cyber graph for adversaries , and iii) the similarity between the set of critical nodes attained from the symmetry analysis to enhance the FACTS placement solution. The proposed solution procedure is implemented on the modified small 49-bus, moderate 274-bus, and large 1,176-bus systems. The power flow analysis of 49-bus system shows that the voltage magnitudes of all buses have increased by reaching to near 1 p.u. and the active power flow over the transmission lines has increased by $\%3$ while the total power losses has decreased by $\%18$ due to reactive compensation by FACTS controllers. In addition, the most critical data of the cyber graph is attributed to data exchange between FACTS controllers. This is in line with the verified importance of these controllers for the whole network performance. The cyber-security of these controllers are then addressed by obscuring the data exchange throughout the nodes assigned as the locations of these controllers. To this end, the network symmetry is leveraged to identify the set of permutations within the symmetry group for which the most critical nodes corresponding to the locations of FACTS controllers are permuted. It is verified in the chapter that publishing any of the graphs associated to the network structure mapped by one of these permutations can

Table 4.4: The determining set attained from symmetry analysis and the locations of FACTS controllers attained from MMP. The overlap between the set of FACTS locations attained from MMP and the determining set underscores an important impact of symmetry on networked systems. The number of 4 out of 6 nodes of determining set of 49-bus system, 8 out of 21 nodes of the determining set of 274-bus system, and 14 out of 33 nodes of determining set of $1,176$-bus are also selected as the locations of facts controllers by MMP.

System	**Determining set $\mathcal{S}$ attained from symmetry analysis**	**The locations of FACTS controllers $\mathcal{F}$ attained from MMP**
49-bus [67]	$\{1, 10, 11, 24, 25, 47\}$	$4, 9, 10, 24, 25, 47, 48$
274-bus [68]	{2, 16, 17, 18, 28, 30, 32, 54, 57, 65, 73, 95, 111, 142, 166, 178, 219, 222, 259, 268, 271}	3, 7, 58, 59, 67, 97, 112, 142, 166, 168, 177, 179, 180, 189, 219, 222, 236, 259, 267, 271
1,176-bus [69]	{5, 25, 55, 76, 129, 131, 188, 241, 276, 288, 308 , 366, 376, 455, 465, 475, 516, 547, 627, 668, 670, 695, 712, 734, 746, 765, 777, 805, 824, 849, 852, 931, 948}	5, 24, 40, 54, 70, 73, 92, 107, 112, 129, 132, 147, 152, 154, 172, 189, 212, 241, 276, 286, 296, 306, 307, 331, 346, 356, 366, 376, 386 , 396, 426, 455, 465, 476, 515, 549, 627, 668, 680, 694, 711, 732, 746, 765, 771, 787, 803, 824, 835, 851, 937, 948, 1031

significantly obscure the source of critical data for adversaries.

Throughout the simulations, an overlap is observed between the set of nodes in determining set and the set of nodes assigned as the locations of FACTS controllers by MMP. This further reveals the importance of symmetry in power network analysis. Therefore, another novel contribution of this chapter is that finding the set of driver nodes for a power system can be translated to finding the set of nodes with highest repetitions in the symmetry group. Potential forthcoming research directions may be on: i) considering the network topology while addressing future expansions of the existing networks or constructing a new network, and ii) expanding the proposed approach to also address sizing of FACTS devices.

4.7 Appendix: computational clarification

In this appendix, the computation process of the proposed approaches are explained. First, we clarify how to compute MMP in MATLAB and then the symmetry analysis is discussed in Sage.

4.7.1 Computing the matched edges and unmatched nodes of MMP

The required data for performing MMP is the adjacency matrix of the network. Once the adjacency matrix of the underlying graph of the network is constructed in MATLAB, we can attain the full set of matched edges using the command

$$>> maximal\_matching(A)$$

which uses a matching function in MATLAB. In all our case studies, MATLAB was able to compute the whole set of matched edges and unmatched nodes in a few seconds. Thus finding the locations of FACTS devices (or unmatched nodes) does not impose a big computation burden.

4.7.2 Calculating the symmetry group

The previous studies (for example [62]) rely on computing the automorphism group to identify the determining set (which can be used to find the set of driver nodes) while the proposed approach of this chapter is based on computing the generators of automorphisms. The computational advantage of the proposed approach can be distinguished simply by comparing the size of automorphism groups with the size of generators of automorphisms. For the small grid of 49-bus system, it is shown in section IV.A that there are only 144 automorphissms and it is possible to compute and sweep over this range. However, for the moderate 274-bus system, and the large $1,176$-bus system, it is shown that the sizes of the corresponding automophism groups are $28,311,552$ and 10^{259}, respectively. Therefore, it is not computationally effective to compute these sets and sweep over them. In addition, the large number of automorphisms makes it very difficult, if not impossible, to find the critical nodes as it needs to compute all automorphisms and then sweep over them to find the set of nodes with maximum multiplicities in Aut$(\mathcal{G})$. However, the novel approach of this chapter addresses these computational issues by adapting generators of automorphisms instead of automorphism groups. As indicated in sections IV.B and IV.C, the number of generators of automorphisms for 274-bus is 23, and for $1,176$-bus systems it is equal to 381. Clearly sweeping over these small sets of generators is more computationally effective than sweeping over the very large number of automorphisms associated with theses systems. There are effective algorithms, such as those in [64] for computing the automorphism group but, in general, the algorithms for calculating automorphism group and elementary automorphisms are well-known and rather trivial. These algorithms are built in some commands in SageMath or similar computing tools. Once the underlying graph is constructed in Sage, computing the automorphism group and the elementary automorphisms can be easily done using the following commands:

$$> \mathcal{G}.automorphismgroup().list() \#Computing \text{ Aut}(\mathcal{G})$$

$$> \mathcal{G}.gens() \quad \#Computing \text{ Gen}(\mathcal{G}).$$

However, for moderate/large scale networks, the first command will not result in the list of automorphisms. Only the cardinality of automorphism group can be computed using the following commands:

$$> \mathcal{A} = \mathcal{G}.automorphismgroup()$$

$$> \mathcal{A}.cardinality().$$

Bibliography

4.8 References

[1] J. Bhukya and V. Mahajan, "Optimization of controllers parameters for damping local area oscillation to enhance the stability of an interconnected system with wind farm," in *Int. J. Elec. Power Energy Sys.,* vol. *119*, Jul, 2020, DOI. 10.1016/*j.ijepes*.2020.105877.

[2] A. H. Elmetwaly, A. A. Eldesouky, and A. A> Sallam, "An Adaptive D-FACTS for Power Quality Enhancement in an Isolated Microgrid," in *IEEE Access* Early Access, 2020, DOI. 10.1109/ACCESS.2020.2981444.

[3] A. Al-Ahmad and R. Sirjani, "Optimal placement and sizing of multi-type FACTS devices in power systems using metaheuristic optimisation techniques: An updated review," in *Ain Shams Eng. J.,* In Press, Dec, 2019, DOI. 10.1016/*j.asej*.2019.10.013.

[4] A.M. Shiddiq Yunus, A. Abu-Siada, M.A.S. Masoum, F. El-Naggar, J.X. Jin, "Enhancement of DFIG LVRT Capability during Extreme Short-Wind Gust Events using SMES Technology," in *IEEE Access,* vol. *8,* pp. *47264–47271,* 2020, DOI. 10.1109/ACCESS.2020.2978909.

[5] M. Moghbel, M. A. S. Masoum, A. Fereidouni and S. Deilami, "Optimal Sizing, Siting and Operation of Custom Power Devices With STATCOM and APLC Functions for Real-Time Reactive Power and Network Voltage Quality Control of Smart Grid," in *IEEE T. Smart Grid,* vol. *9, no*. 6, pp. *5564–5575,* Nov, 2018, DOI. 10.1109/TSG.2017.2690681.

[6] A.M. Shiddiq Yunus, M.A.S. Masoum, A. Abu-Siada, "Application of SMES to Enhance the Dynamic Performance of DFIG during Voltage Sag and Swell," in *IEEE T. App. Superconductivity,* vol. *22, no*. 4, pp. *1–9,* 2012, 10.1109/TASC.2012.2191769.

[7] A.M. Shiddiq Yunus, A. Abu-Siada, M.A.S. Masoum, "Sag and Flicker Reduction using Hysteresis-Fuzzy Control Based SMES Unit," in *Canadian Journal of Electrical and Computer Engineering Measurement,* vol. *42, no*. 1, pp. *52–57,* Nov, 2019, DOI. 10.1109/CJECE.2019.2891272.

[8] E. Naderi, M. Pourakhbari-Kasmaei, and h. Abdi, "An efficient particle swarm optimization algorithm to solve optimal power flow problem integrated with FACTS devices," in *Applied Soft Computing,* vol. *80*, pp. *243–262,* Jul, 2019, DOI. 10.1016/*j.asej*.2019.10.013.

[9] M. Ghiasi, "Technical and economic evaluation of power quality performance using FACTS devices considering renewable generations," in *Renewable Energy Focus,* vol. *29*, pp. *49–62,* Jun, 2019, DOI. 10.1016/*j.ref*.2019.02.006.

[10] M. M. Eladany, A. A. Eldesouky and A. A. Sallam, "Power System Transient Stability: An Algorithm for Assessment and Enhancement Based on Catastrophe Theory and FACTS Devices," in *IEEE Access,* vol. *6*, pp. *26424–26437,* 2018, DOI. 10.1109/ACCESS.2018.2834906.

[11] G. Carpinelli, P. Caramia, A. Russo, and P. Varilone, "Voltage stability in unbalanced power systems: a new complementarity constraints-based approach," in *IET. Gen. Trans. Dist.,* vol. *9, no*. 14, pp. *2014-2023,* 2015 DOI. 10.1049/*iet-gtd*.2014.0990.

[12] J. Zhu, K. Cheung, D. Hwang, and A. Sadjadpour, "Operation strategy for improving voltage profile and reducing system loss," in *Applied Soft Computing,* vol. *25, no*. 1, pp. *390–397,* Jan, 2010, DOI. 10.1109/ *TPWRD*.2009.2033968

[13] M. Adnan, M. Tariq, M. Zhou, Z. Vincent, and H. Poor, "Load flow balancing and transient stability analysis in renewable integrated power grids," in *Elec. Power Energy Sys.,* vol. *104*, pp. *744–771,* Jan, 2019, DOI. 10.1016/*j.ijepes*.2018.06.037

[14] S.W. Monod and V. Mohan, "A STATCOM-control scheme for grid connected wind energy system for PQ improvement," in *IEEE SYS. J.,* vol. *4, no*. 3, pp. *346–352,* 2010, DOI. 10.1109/*JSYST*.2010.2052943

[15] N.A. Bakar and K.M. Mohd, "Optimal Placement of TCSC in Transmission Network using Sensitivity Based Method for Multi objective Optimization ," in IEEE Sys. Conf. Energy Conversion, pp. *321–329,* Kuala Lumpur, Malaysia, 2017 DOI. 10.1109/*CENCON*.2017.8262484.

[16] Y. Li, C. Rehtanz, S. Ruberg, L. Lhuo, and Y. Chao, "Assessment and choice of input signals for multiple HVDC and FACTS wide-area damping controllers," in *IEEE Trans. Power Delivery,* vol. *27, no*. 4, pp. *1969–1977,* Jul, 2012, DOI. 10.1109/*TPWRS*.2012.2189865.

[17] F. Hu, K. Sun, A.D. Rosso, E. Farantatos, and N. Bhatt, "Measurement-based real-time voltage stability monitoring for load areas," in *IEEE Trans. Power Sys.,* vol. *31, no*. 4, pp. *2787–2798,* Jul, 2016, DOI. 10.1109/*TPWRS1*.2015.2477080

[18] A.L. Ara, A. Kazemi, and S.A. Niaki, "Multi objective optimal location of FACTS shunt-series controllers for power system operation planning," in *IEEE Trans. Pow. Del,* vol. *27, no*. 2, pp. *481–490,* Jul, 2019, DOI. 10.1109/TPWRD.2011.2176559.

[19] N. Khalesi, N. Rezaei, and M.R.D.G. Haghifam, "Allocation with application of dynamic programming for loss reduction and reliability improvement," in *Int. J. Elec. Pow. Energy Sys.,* vol. *33, no*. 2, pp. *243–262,* Feb, 2011, DOI. 10.1016/j.ijepes.2010.08.024.

[20] M. Nojavan, H. Seyedi, B. Mohammadi-Ivatloo, "Voltage stability margin improvement using hybrid non-linear programming and modified binary particle swarm optimization algorithm considering optimal transmission line switching," in *IET Gen. Trans. Dist.,* vol. *12, no*. 4, pp . *815-823,* Feb, 2018, DOI. 10.1049/iet-gtd.2016.1895.

[21] M. Jadidbonab, M.J. Vahid-pakdel, H. Seyedi, and B. Mohammadi-Ivatloo, "Stochastic assessment, enhancement of voltage stability in multi carrier energy systems considering wind power," in *Int. J. Elec. Pow. Energy Sys.,* vol. *106,* pp . *572–584,* Mar, 2019 DOI. 10.1016/j.ijepes.2018.10.028.

[22] R. Muzzammel, M. Ahsan, and W. Ahmed, "Non- linear analytic approaches of power flow analysis and voltage profile improvement," in Power Gen. Sys. Ren. Energy Tech. (PGSRET) Islamabad, Pakistan, 2015, DOI. 10.1109/PGSRET.2015.7312232.

[23] G. Blanco, F. Olsina, F. Garces, and C. Rehtanz, "Real option valuation of FACTS investments based on the least square Monte Carlo method," in *IEEE Trans. Pow. Sys.,* vol. *26, no*. 3, pp . *1389–1398,* Aug, 2011, DOI. 10.1109/TPWRS.2010.2094211.

[24] J.H. Shyh and Z.L. Xian, "Application of artificial bee colony-based optimization for fault section estimation in power systems," in *Int. J. Elec. Pow. Energy Sys.,* vol. *44, no*. 1, pp . *210–218,* Jan, 2013, DOI. 10.1016/j.ijepes.2012.07.012.

[25] B. Mozhgan, "Using neural network to control STATCOM for improving transient stability," in *J Artificial Intelligence in Elec. Eng.,* vol. *1, no*. 1, pp . *26–31,* 2012.

[26] R.K. Pandey and D.K. Gupta , "Integrated multi-stage LQR power oscillation damping FACTS controller," in *CSEE J Pow. Energy Sys.,* vol. *4, no*. 1, pp . *83–92,* Mar, 2018, DOI. 10.17775/CSEEJPES.2016.00510.

[27] L.J. Cai and I. Erlich, "Fuzzy coordination of FACTS controllers for damping power oscillations," in *IEEE Trans Pow. Sys.,* vol. *28, no*. 5, pp . *23–30,* 2006.

[28] H. Shayeghi, H. Shayanfar, S. jalilzadeh, and A. Safari, "Design of output feedback UPFC controller for damping of electromechanical oscillations using PSO," in *Energy Conv. Mang.,* vol. *50, no*. 10, pp . *2554–2561,* Oct, 2009, DOI. 10.1016/j.enconman.2009.06.005.

[29] A. Satheesh and T. Manigandann, "Maintaining power system stability with FACTS controllers using artificial bee algorithm and ANN," in *J. Theo. Appl. Inf. Tech.,* vol. *49, no*. 1, pp . *38–47,* Mar, 2013.

[30] y. Li, C. Rehthanz, S. Rubherg, L. Lhuo, and Y. Chao, "Assessment and choice of input signals for multiple HVDC and FACTS wide-area damping controllers," in *IEEE Trans. Pow. Sys.,* vol. *27, no*. 4, pp . *1969–1977,* Nov, 2012, DOI. 10.1109/TPWRS.2012.2189865.

[31] T. Niknam, M.R. Narimani, J. Aghaei, and A.R. Azizipanah, "Improved PSO for multiobjective OPF considering the cost, loss, emission and voltage stability index," in *IET Gen. Trans. Dist.,* vol. *6, no*. 6, pp . *515–527,* Jun, 2012, DOI. 10.1049/iet-gtd.2011.0851.

[32] A.M. rezaei and A. Karimi, "Artificial bee colony algorithm for solving multiobjective optimal power flow problem," in *Int. J. Elec. Pow. Energy Sys.,* vol. *53*, pp . *219–230,* Dec, 2013, DOI. 10.1016/j.ijepes.2013.04.021.

[33] P. Kumkhratug, "Application of lyapunov theory and fuzzy logic to control shunt FACTS devices for enhancing transient stability in multi machine system," in *J. Elec. Eng. Tech,* vol. *7, no*. 5, pp . *672–680,* Sep, 2012, DOI. 10.5370/JEET.2012.7.5.672.

[34] J. Aghaei, M. Zarei, M. Asban, S. Ghavidel, A. Heidari, and V.G. Agelidis, "Determining potential stability enhancements of flexible ac transmission system devices using corrected transient energy function," in *IET Gen. Trans. Dist,* vol. *10, no*. 2, pp . *470–476,* Feb, 2016, DOI. 10.1049/iet-gtd.2015.0849.

[35] C. Guo, Z. Wen, and C. Zhao, "Small-signal instability and supplementary coordinated damping-control of LCC-HVDC system with STATCOM under weak AC grid conditions," in *Elec. Pow. Ener. Sys.,* vol. *104*, pp . *246–254,* Jan, 2019, DOI. 10.1016/j.ijepes.2018.06.055.

[36] C. Madhtharad, S. Premrudeepreechacharn, N. Watson, and R. Saeng-Udom, "An Optimal Measurement Placement Method for Power System Harmonic State Estimation,," in *IEEE Trans. Pow. Del.,* vol. *20, no*. 2, pp . *1514–1521,* May, 2005, DOI. 10.1109/TPWRD.2004.841309.

[37] P.R. Sahu, P.K. Hota, and S. Panda, "Whale optimization algorithm for fuzzy lead–lag structure SSSC damping controller design," in IEEE India Council Int. Conf. (INDICON), Roorkee, India, 2017

[38] D.P. Ladhumaor, N.T. Indrajit, R.H> Bhesdadiya, and P. jangir, "Optimal Power Flow with shunt Flexible AC Transmission system (FACTS) device using Grey Wolf Optimizer," in Int. Conf. Adv. Elec. Electronics, Info. Comm. Bio-Info. (AEEICB), Chennai, India, 2017, DOI. 10.1109/AEEICB.2017.7972338.

[39] Y.C. Kuyu and F. Vatansever, "Real Loss Minimization in Power Systems via Recent Optimization Techniques," in Int. Symp. Multidisciplinary Studies and Innovative Techno. (ISMSIT), Oct, 2018.

[40] H. hamour, S. Kamel, H.A. Mawgoud, A. Korashy, and F. Jurado, “Distribution Network Reconfiguration Using Grasshopper Optimization Algorithm for Power Loss Minimization,” in Int. Conf. Smart Ener. Sys. Tech. (SEST), Sevilla, Spain, 2018, DOI. 10.1109/SEST.2018.8495659.

[41] T. George, A.R. Youssef, M. Ebeed, and S. Kamel, “Ant Lion Optimization Technique for Optimal Capacitor Placement Based on Total Cost and Power Loss Minimization,” in Int. Conf. Innov. Trends in Comp. Eng. (ITCE), pp . *350–356,* Aswan, Egypt, 2018, DOI. 10.1109/ITCE.2018.8316649.

[42] T.K. Behera, M.K. Behera, and N. Nayak, “Spider Monkey Based Improve P & O MPPT Controller for Photovoltaic Generation System,” in Int. Conf. on Tech. for Smart-City Ener. Secu. and Pow. (ICSESP-2018), Mar, 2018. DOI. 10.1109/ICSESP.2018.8376735.

[43] F. Pasqualetti, S. Zampieri, and F. Bullo, "Controllability metrics, limitations and algorithms for complex networks," *IEEE Transactions on Control of Network Systems*, vol. 1, no. 1, pp. 40-52, Mar. 2014.

[44] B. Siddique, L.M. Pecora, J.D. Hart, and F. Sorrentino “Symmetry-and input-cluster synchronization in networks,,” in *Phys. Rev.,* vol. *97,* Mar, 2018, DOI. 10.1103/PhysRevE.97.042217.

[45] Y. Lin, B. Hu, K. Xie, L. Wang, Y. Xiang, R. Xiao, and D. Kong, “Day-Ahead Scheduling of Power System Incorporating Network Topology Optimization and Dynamic Thermal Rating,” in *IEEE Access,* vol. *7,* 2019, pp . *35287–35301,* DOI. 10.1109/ACCESS.2019.2904877.

[46] L. Wang, Z. Qu, Y. Li, K. Hu, J. Sun, and K. Xue, “Method for Extracting Patterns of Coordinated Network Attacks on Electric Power CPS Based on Temporal–Topological Correlation,” in *IEEE Access,* vol. *8,* pp . *57260–57272,* 2020, DOI. 10.1109/ACCESS.2020.2982057.

[47] F. Sorrentino, L.M. Pecora, “Approximate cluster synchronization in networks with symmetries and parameter mismatches,” in *Chaos: An Interdisciplinary J. Nonlin Sci.,* vol. *26, no*. 9, Sep, 2016, DOI. 10.1063/1.4961967.

[48] L.M. Pecora, F. Sorrentino, A. M. Hagerstorm, T.E. Murphy, and R. Roy, “Cluster synchronization and isolated desynchronization in complex networks with symmetries,” in *Nat. Comm.,* vol. *5,* Jun, 2014.

[49] B. Li, Y. Chen, S. Huang, R. Yao, Y. Xia, and S. Mei, “Graphical Evolutionary Game Model of Virus-Based Intrusion to Power System for Long-Term Cyber-Security Risk Evaluation,” in *IEEE Access,* vol. *7*, pp . *178605–178617,* 2019, DOI. 10.1109/ACCESS.2019.2958856.

[50] C.C. Sun, A. Hahn, and C.C. Liu, "Cyber security of a power grid: State-of-the-art," in *Int. J. Elec. Pow. Energy Sys.,* vol. *99*, pp . *45–56,* Jul, 2018, DOI. 10.1016/j.ijepes.2017.12.020.

[51] S. Poudel, Z. Ni, and N. Malla, "Real-time cyber physical system testbed for power system security and control," in *Int. J. Elec. Pow. Energy Sys.,* vol. *7*, pp . *124–133,* Sep, 2017, DOI. 10.1016/j.ijepes.2017.01.016.

[52] M.Z> Gunduz and R. Das, "Cyber-security on smart grid: Threats and potential solutions," in *Comm. Net.,* vol. *169*, Mar, 2020, DOI. 10.1016/j.comnet.2019.107094.

[53] L. Zou, L. Chen, and T. M. Ozsu, "K-automorphism: a general framework for privacy preserving network publication," in *Proc. VLDB Endow.,* vol. *2, no*. 1, Aug, 2009, DOI. 10.14778/1687627.1687734.

[54] J. Yang, B. Wang, X. Yang, H. Zhang, and G. Xiang, "A secure K-automorphism privacy preserving approach with high data utility in social networks," in *Sec. Comm. Net,* vol. *7, no*. 9, Sep, 2013, DOI. 10.1002/sec.840.

[55] Z. Lin, "From Isomorphism-Based Security for Graphs to Semantics-Preserving Security for the Resource Description Framework (RDF)," M.S. thesis, University of Waterloo, Canada, 2016.

[56] J. Cheng, A. W. C. Fu, and J. Liu, "K-isomorphism: privacy preserving network publication against structural attacks," in Proc. ACM SIGMOD Int. Conf. Manag. Data, SIGMOD 2010, Indianapolis, Indiana, USA, June 6-10, 2010, DOI. 10.1145/1807167.1807218.

[57] Y. Liu, J.J. Slotine, and A.L. Barabasi, "Controllability of complex networks," in *Nature,* vol. *437*, pp . *167–173,* May, 2011.

[58] A. Chapman, M. Nabi-Abdolyousefi, and M. Mesbahi, "Controllability and observability of networks-of-networks via cartesian products," in *IEEE Trans. Aut. Cont.,* vol. *59, no*. 10, pp . *2668-2679,* Oct, 2014, DOI. 10.1109/TAC.2014.2328757.

[59] B. D. MacArthur, R. J. Sanchez-Garcia, and J. W. Anderson, "Symmetry in Complex Neworks," in *Disc. App. Math.,* vol. *156, no*. 18, pp . *3525–3531,* Nov, 2008, DOI. 10.1016/j.dam.2008.04.008.

[60] W. Wu, Y. Xiao, Z. He, And Z. Wang, "K-symmetry model for identity anonymization in social networks," in Proc. 13th Int. Conf. Extending database Tech. (ACM) Lausanne, Switzerland, March 22-26, 2010, DOI. 10.1145/1739041.1739058.

[61] H. Parastvand, A. Chapman, O. Bass, and S. Lachowicz, "Graph Automorphic Approaches to Robustness of Complex Networks," in *Control Engineering Practice,* To be Published, 2020.

[62] A. Chapman and M. Mesbahi "On symmetry and controllability of multi-agent systems," in 53rd Conf. Dec. Con. Los Angeles, USA, 2014, DOI. 10.1109/CDC.2014.7039451.

[63] A. Farrugia and I. Sciriha, "Controllability of undirected graphs," in *Lin. Algeb. and Its Applications,* vol. *454,* pp. *138–157,* Aug, 2014, DOI. 10.1016/j.laa.2014.04.022.

[64] J. J. Cannon, D.F. Holt, "Automorphism group computation and isomorphism testing in finite groups," in *J. Symb. Comp.,* vol. *35, no*. 3, pp. *241–267,* Mar, 2003, DOI. 10.1016/S0747-7171(02)00133-5.

[65] M. Maherani, I. Erlich, and G. Krost, "Robust Centralized Fixed Order Wide Area Damping Controller for wind integrated power system," in *IFAC-PapersOnLine,* vol. *52, no*. 3, 2019,

[66] A. Noori, M. jafari-Shahbazadeh, and M. Eslami, "Designing of wide-area damping controller for stability improvement in a large-scale power system in presence of wind farms and SMES compensator," in *Int. J. Elec. Pow. Ene. Sys.,* vol. *119*, 2020.

[67] S. Aziz, H. Wang, Y. Liu, J. Peng, H. Jiang, "Variable Universe Fuzzy Logic-Based Hybrid LFC Control With Real-Time Implementation," in *IEEE Access* vol. *7*, 2019.

[68] B. Dembart and J. Lewis, "Symmetric structure equivalenced presentation of US power network," in *SuitSparse Matrix Collection* Available Online: https://sparse.tamu.edu/HB/bcspwr04, Access Date: May, 2020.

[69] A. Erisman, "SYMMETRIC PATTERN OF ERISMAN, SUMMER 1973," in *SuitSparse Matrix Collection* Available Online: https://sparse.tamu.edu/HB/eris1176, Access Date: May, 2020.

Chapter 5

A Graph Automorphic Approach for Placement and Sizing of Charging Stations in EV Network Considering Traffic

5.1 Overview

This chapter proposes a novel graph-based approach with automorphic grouping for the modelling, synthesis, and analysis of electric vehicle (EV) networks with charging stations (CSs) that considers the impacts of traffic. The EV charge demands are modeled by a graph where nodes are positioned at potential locations for CSs, and edges represent traffic flow between the nodes. A synchronization protocol is assumed for the network where the system states correspond to the waiting time at each node. These models are then utilized for the placement and sizing of CSs in order to limit vehicle waiting times at all stations below a desirable threshold level. The main idea is to reformulate the CS placement and sizing problems in a control framework. Moreover, a strategy for the deployment of portable charging stations (PCSs) in selected areas is introduced to further improve the quality of solutions by reducing the overshooting of waiting times during peak traffic hours. Further, the inherent symmetry of the graph, described by graph automorphisms, are leveraged to investigate the number and positions of CSs. Detailed simulations are performed for the EV network of Perth Metropolitan in Western Australia to verify the effectiveness of the proposed approach[1].

[1]This chapter is published in *IEEE Transaction on Smart Grids*

Nomenclature

Abbreviations

PBH	Popov-Belevitch-Hautus.
CEA	Community energy association.
CN	Complex network.
CN	Complex network.
CN	Complex network.
CS	Charging station.
ECM	Exact controllability method.
ECM	Exact controllability method.
EV	Electric vehicle.
FACTS	Flexible AC transmission systems.
lcm	The lowest common multiple.
LQR	Linear quadratic regulator.
LTI	Linear time invariant.
MMP	Maximum matching principle.
PCS	Portable charging station.
PEV	Plug-in electric vehicle.
PID	proportional integrative derivative.
VSC	Voltage-source converter.
WAC	Wide area controlled.

Constants

ε Identity (or trivial) permutation.

ε Identity (or trivial) permutation.

c A complex number.

c A complex number.

Q, R, Y Arbitrary weights.

Parameters

α_{sh} Angle of shunt VSC.

β The bus voltage angles.

δ A permutation.

δ_i Maximum algebraic multiplicity of $\lambda_(i)$.

δ_i Maximum algebraic multiplicity of $\lambda_(i)$.

δ_i The angle of voltage of node i.

γ_{sh} Conversion ratio signal.

λ^M Maximum algebraic multiplicity of teh eigenvalue λ^M.

λ^M Maximum algebraic multiplicity of the eigenvalue λ^M.

λ_i The i^{th} eigenvalue.

λ_i The i^{th} eigenvalue.

ν A point (node) of permutation.

σ An automorphism or a Permutation.

σ Permutation.

σ Permutation.

$\mathcal{A}$ Adjacency matrix.

$\mathcal{A}$ Adjacency matrix.

$\mathcal{A}, A$ Adjacency matrix.

$\mathcal{D}$ Degree matrix.

$\mathcal{D}$ The degree matrix.

$\mathcal{E}$ The set of edges.

$\mathcal{E}_c$ The set of critical edges.

$\mathcal{F}$ The determining set attained from Gen($\mathcal{F}$).

$\mathcal{G}$ Graph.

$\mathcal{G}$ Graph.

$\mathcal{G}$ Graph.

$\mathcal{G}_k$ The released graph.

$\mathcal{J}$ The incidence vector of driver nodes.

$\mathcal{K}$ Optimal feedback gain vector.

$\mathcal{L}$ Laplacian matrix.

$\mathcal{L}$ Laplacian matrix.

$\mathcal{L}$ Laplacian matrix.

$\mathcal{S}$ Determining set.

$\mathcal{S}$ Determining set.

$\mathcal{V}$ Controlled invariant subspace.

$\mathcal{V}$ The set of nodes.

$\mathcal{V}_c$ The set of critical nodes.

Aut($\mathcal{G}$) Automorphism group.

Aut($\mathcal{G}$) Automorphism group.

Aut($\mathcal{G}$) Automorphism group.

dimV_{λ_i} Dimension of eigenspace associated with $\lambda(i)$.

dimV_{λ_i} Dimension of eigenspace associated with $\lambda(i)$.

Fix(σ) The set of fixed nodes by permutation.

Gen($\mathcal{G}$) Generators of automorphism.

Gen($\mathcal{G}$) Generators of automorphism.

Gen($\mathcal{G}$) Generators of automorphism.

$\text{Gen}_{dis}(\mathcal{G})$ Set of disjoint generators.

$\text{Move}(\sigma)$ The set of moved nodes by permutation.

$\text{Move}(\sigma)$ The set of moved nodes by permutation.

$\text{Mov}_{v_l}^{Gen}$ the set of generators mapping v_l.

$\mu(\lambda_i)$ Maximum geometric multiplicity of $\lambda(i)$.

$\mu(\lambda_i)$ Maximum geometric multiplicity of $\lambda(i)$.

$\rho_{\mathcal{O}}$ The orbital ratio of symmetry after node removal.

ρ_{aut} The ratio of symmetry after node removal.

σ A permutation.

ε Identity (or trivial) permutation.

φ A generator of automorphism.

ζ A permutation.

ζ_{dis} , δ_{dis} Disjoint generators.

A State matrix.

a_{ij} Element of $\mathcal{A}$.

a_{ij} Weight of ij^{th} element of $\mathcal{A}$.

B Input matrix.

B Input matrix.

B Input matrix.

C Capacitor.

C Size (or capacity) of charging station [kW].

E The set of edges.

E The set of edges.

$F(x_i)$ the individual node's dynamical equation.

F_{vl}^{Gen} The set of generators that fixes v_l.

I_{dc} Capacitor current.

I_{sh} Shunt reactive current setpoint.

I^*_{sh} Reactive current of the outer loop.

$Im\, C$ Image of C.

K The feedback gain.

k The number of distinct mappings.

k_m Conversion ration between the voltage of AC and DC sides.

$ker\, L$ Kernel or null space of L.

l_{ij} The $(i, j)^{th}$ element of the Laplacian matrix.

M A matching.

m Index of a permutation.

M^{Gen}_{vl} The set of generators that moves v_l.

N_D Number of required driver nodes.

N_D Number of required driver nodes.

P The solution of Riccati equation.

p Multiplicity of critical node in Gen($\mathcal{G}$).

P_{ac} Active power on AC side.

P_{ij} Active power flow between nodes i and j.

q The size of disjoint generators.

Q_{ij} Reactive power flow between nodes i and j.

$r^*_{\mathcal{G}}$ Normalized measure of network redundancy.

$r_{\mathcal{G}}$ Network redundancy.

S Determining set.

$s(t)$ The desired state.

$S_{\mathcal{O}}(\mathcal{G})$ Symmetry index based on orbits.

T Waiting time [min].

u Control signal (charging supply).

u Control signal.

u Control signal.

V The set of nodes.

V The set of nodes.

V Voltage.

V_m Voltage magnitude.

V_{dc} Capacitor terminal voltage.

V_{ref} Setpoint voltage.

$w(t)$ Disturbance.

Z Line impedance.

5.2 Introduction

Electric vehicles (EVs) powered by electricity from low carbon emission grids can provide significant benefits by reducing transportation impact on climate and grid's reliance on oil-based fuels. EVs provide a quiet and cleaner environment while reducing the operation and maintenance costs [1]. Plug-in electric vehicles (PEVs) which are an integration of battery and plug-in hybrid electric vehicles are key innovations to attain low-carbon transportation [2].

As the expectations for future EV sales increase, there is a growing number of researches focusing on the development of charging infrastructure indicating their importance in the early stage of EV market [3]. According to community energy association (CEA), the charging infrastructure is broadly divided into three categories based on the EV charging speeds. The standard levels of PEVs charging are AC level 1, AC level 2 and DC Charging. The AC level 1 typically takes 10-20 hours to charge ([4]- [5]). The long charging time makes Level 1 chargers mostly suitable for home usage. The AC Level 2 typically takes 4-5 hours to charge and can be used for both commercial and home charging. The DC charging (also called fast charging) is the fastest option and can achieve full charge in 10 to 15 minutes ([4]- [5]). Additionally, portable charging stations (PCSs) have recently emerged as an alternative for charging stations to deliver extra capacity during peak hours or in emergency occasions [6]. Unlike fixed stations, PCSs do not impose much construction and maintenance cost, and are not constrained with power grid capacity or the size of the site based on control [7]. The trunks equipped with battery storage feature either the lightweight lithium battery or the electric double-layer capacitor technologies ([8]- [9]). Both technologies can supply all charging levels. Throughout this chapter, fast charging is assumed at all EV charging stations (CSs).

To increase the uptake rate of EVs, governments and automotive industries in most developed countries have been working together, and have undertaken projects to deploy a network of electric CSs, commonly known as EV networks [10]. EV networks are anticipated to play a critical role in coming decades as the forecast for PEV market growth looks very promising [11]. This is mainly due to increasing supports from governments and automotive industries.

The bulk of EV charging demand is synchronized with daily driving patterns. The anticipated challenges associated with the increasing number of EVs are long waiting times at public CSs with impacts on actual road traffic patterns and the electricity demand from utility networks. To resolve these challenges, researchers have been investigating various aspects of EV charging including PEV load shifting to address the so called duck curve challenges associated with the rapid increase in demand at sunset ([12]- [13]).

Recently, there has been a growing attention to use graph theory in many engineering applications (see [13]- [16]). This stimulates leveraging on the wealth of the fundamental graph related theories in modeling and synthesis of EV networks. Although EV community has recently utilized some aspects of graph theory in synthesizing EV networks ([17]- [23]), these works are not leveraging on substantial concepts of graph theory. In fact, previous studies have used graph topology for only visualizing the map of EV network. After constructing a graph-like EV network, they implement optimization techniques in different frameworks to address route planning [6]- [18], placement [19], and sizing [22] as well as simultaneous placement and sizing [23]- [25]. In [19], the locations of fast charging stations are attained according to the spatio-temporal requirements of the planners. Grasshopper optimization technique is implemented in [25] to address the placement and sizing of CSs where the EV battery load models are developed for load flow analysis. In [23], a real case optimal CS placement and sizing is addressed using five integer linear programs based on weighted set covering models of the CSs locations. Using a two stage optimization technique, the provision and dimension of DC fast charging stations are investigated with particular attention for maintaining the voltage stability by adding a minimum number of voltage stabilizers. A multi-objective particle swarm optimization method is used in [20] for the planning of charging stations. Similar to these studies, the majority of CS placement and sizing approacehs rely on an optimization tool. However, these computational tools are always subject to computationally interactable solutions [8]. The lack of an analytical approach to CS placement and sizing motivates leveraging on the potential of graph theoretic properties to establish a systematic method which is less affected by the computational burden. In this chapter, we will show that graph theory can be used for modelling EV networks upon which the EV problems can be reformulated based on control frameworks where there are useful theories that can be adapted for placement and sizing of CSs.

This study proposes a new graph-based approach to modeling, synthesis, and analysis of EV networks that considers the impacts of traffic and is demonstrated for the placement and sizing of CSs based on the following steps: i) The EV network is modeled by a graph where the nodes are potential locations of CSs and edges represent the traffic (e.g., number of vehicles between the nodes). A model of network synchronization [27] is assumed as the EV network protocol.

This model is then developed into a pinning framework ([28]- [29]) featuring actual CSs as the driver nodes. ii) The placement problem is mapped to the problem of finding a set of driver nodes for a CN representing the EV network. We verify that this set act as charging stations and can reduce the waiting time below a threshold level. Further, the problem of CSs sizing is reformulated as a problem of finding an optimal regulator gain. iii) The proposed approach is then elaborated by introducing a deployment strategy for portable charging stations (PCSs). This will compensate small mismatches between the generation and EV demand particularly during peak traffic hours. iv) Finally, the impacts of graph symmetry (or automorphism groups) on the graph of EV network are investigated. In particular, the role of symmetry in determining the number and location of charging stations is highlighted.

The proposed graph-based EV model facilitates addressing the EV network problems using various analytical approaches originated from control theories. The novel graph theoretic approach to EV network placement and sizing is relying on reformulation of these problems in a control framework. The study verifies that the charging stations can be considered as the driver nodes of a complex network. Then the set of driver nodes (or CSs) and their control inputs (size of CSs) can be identified using established control theories. Inspired by the similarity of the structural dynamics of two nodes in the same automorphism (or generator of automorphism), this study verifies that these nodes can be alternatively selected as the charging spot. This feature is notable as the selected spots by placement approaches are subject to practical constraints.

As a comprehensive case study, the proposed method and all results are examined on the EV network of Perth in Western Australia. The main contributions and advantages of the proposed graph-based method for modelling, placement and sizing of CSs within EV networks are:

- Reformulating the problems of CSs placement and sizing to a control framework which facilitate using fundamental control and graph theories.
- Consideration of traffic flow and its impacts on EV network controllability, number, locations and sizes of CSs such that vehicle waiting times at all CSs are limited below a desirable threshold level.
- Investigating the graph symmetry of EV network and verifying its impact on number and locations of the CSs as well as providing alternative spots for CSs.
- A strategy for the deployment of PCSs in selected areas (subgraphs) is introduced and tested to further improve the quality of solutions by reducing the overshooting of the waiting times during peak traffic.

The rest of the chapter is organized as follows. Section 5.3 presents some mathematical preliminaries on graph theory and graph symmetry. Section 5.4 discusses the main idea of the chapter, introduces the proposed approach for placement and sizing of CSs and investigates the impacts of EV graph symmetry on the solutions. Simulations results are presented and analyzed in Section 5.5 followed by the conclusion.

5.3 Preliminaries

A complex network can be abstracted by a graph $\mathcal{G}(V, E)$ where V and E characterize the set of nodes and edges, respectively. An edge exists between nodes i and j if $(i, j) \in E$. The graph is called undirected if the edges have no orientation. The adjacency matrix $\mathcal{A}$ of an undirected graph is a square $|V| \times |V|$ matrix whose element $[\mathcal{A}_{ij} = 1]$ if there is an edge between nodes i and j, and $[\mathcal{A}_{ij} = 0]$ when there is no edge. The $order$ and the $size$ of $\mathcal{G}$ are the cardinalities of its vertex set V and its edge set E, respectively.

A $permutation$ σ on a set of nodes V is a bijection from V to itself, i.e., $\sigma : V \to V$. Through a permutation, the node sequence or order will be changed. The *order of permutation*, denoted by order(σ), is the smallest positive integer m such that $\sigma_1 \circ \sigma_2 \circ ... \circ \sigma_m = \sigma^m = \varepsilon$ where ε is the identity (trivial) permutation.

Definition 5.3.1. *The composition or product of two functions ζ and δ, denoted by $\zeta \circ \delta$ is the pointwise action of ζ to the result of δ which generates a third function. The notation $\zeta \circ \delta$ is read as "ζ composed with δ". Intuitively, by composition of two functions, the pointwise output of the inner function becomes the input of the outer function. As an example, Appendix A explains how to compute the composition of two functions.*

Graph symmetry is originated from discrete mathematics and can be revealed by automorphism groups. Automorphism is a permutation of graph to itself that preserves the graph structure, meaning the adjacency matrix of the underlying graph remains unchanged. As a result, nodes in the same automorphism have the same structural role in the graph. This type of symmetry has important implications for the controllability and robustness [30] of the underlying network ([20]- [16], [31], and [35]- [36]). A formal definition of automorphism is as below.

An automorphism of $\mathcal{G}$ is a permutation σ for which $\{i, j\} \in E(\mathcal{G})$ if and only if $(\sigma(i), \sigma(j)) \in E(\mathcal{G})$. The automorphism group of $\mathcal{G}$ and its size are denoted by $Aut(\mathcal{G})$ and $|Aut(\mathcal{G})|$, respectively. Also, all automorphisms can be identified from a set of elementary automorphisms or generators of automorphisms $Gen(\mathcal{G})$. There are well known algorithms to compute graph automorphisms. There are also computing tools such as Sage (System for Algebra and Geometry Experimentation) and GAP (Graph Analytics Platform) for attaining $Aut(\mathcal{G})$ and $Gen(\mathcal{G})$.

Definition 5.3.2. *The graph $\mathcal{G}$ is symmetric if $Aut(\mathcal{G})$ contains at least one non-identity automorphism, otherwise it is called asymmetric. Identity permutation is also called trivial automorphism or trivial generator.*

A set of nodes S of graph $\mathcal{G}$ is called determining set if every automorphism of $\mathcal{G}$ can be uniquely determined by its action on S. An element $s \in S$ is a fixed point of σ if $\sigma(s) = s$ where $\sigma : S \to S$ is a permutation of a set S. The permutation σ moves the point v if $\sigma(v) \neq v$. The fixed and moved points by the permutation σ are denoted by Fix(σ) and Move(σ), respectively. More details about graph symmetry can be found in [37].

5.4 EV network graph and proposed solution for placement and sizing of charging stations

This section establishes the main ideas of the chapter upon reformulating the CS placement and sizing into a networked control problem which facilitates implementing control and graph theories. The CS placement is transformed to the problem of finding the set of driver nodes that will guarantee the full controllability of the EV network graph. CS sizing is then mapped to the problem of finding a set of optimal feedback gain in LQR (Linear Quadratic Regulator) framework. Also, a strategy for deploying of PCSs is proposed that will further improve the quality of the solution. Further, the symmetry of EV graph and its impact on the number and positions of CSs as well as its role in providing alternative spots for selected charging stations are verified.

5.4.1 EV network modeling and problem formulation

The EV network is modeled as a graph where nodes are positioned at the potential locations for CSs and the edges represent the number of vehicles in the area between the two corresponding nodes. A few spots along the roads are specified as the primary potential places for CSs. To determine the number of vehicles on the main roads, some edges are assumed between nearby nodes according to the traffic flow. The edges are weighted based on the number of vehicles in the area. The waiting times at potential stations are considered as the system states. The dynamic equation of EV network can thus be formulated as

$$\dot{T}_i = -\sum_{j=1}^{n}(T_i - T_j) \quad (i = 1, ..., n) \tag{5.1}$$

where T is the system state and represents the waiting time. T_i is the state of i^{th} node. The above equation features typical synchronization protocol. Considering the control inputs as the charging supply in charging stations, the dynamic equation of the network can be written as below.

$$\dot{T}_i = -\sum_{j=1}^{n}(T_i - T_j) + Bu(t) \quad (i = 1, ..., n) \tag{5.2}$$

where B is the input matrix and $u(t)$ is the control signal or charging supply injected through the CSs. Equation (8.2), which renders a general pinning protocol, provides a framework suitable for applying control theories.

Given the above formulation, CS placement and sizing problem can be restated as below.

Problem 1: Given the mathematical model of EV network in (8.2), find the set of driver nodes that can fully control the dynamic of (8.2).

Problem 2: Find the optimal control $u = -\mathcal{K}T$ for the set of driver nodes attained from the solution of *Problem 1*.

5.4.2 Proposed CS placement formulation and solution

Based on the formulation presented in the previous section, the CS placement problem can be transformed to the problem of finding the required driver nodes that can fully control the complex network of (8.2). Then the attained driver nodes are correspondent to the positions of the required CSs.

The network dynamic in (8.2) can be rewritten as below

$$\dot{T}_i = -L(\mathcal{G})T_i + Bu(t) \quad (i = 1, ..., n) \tag{5.3}$$

where $L(\mathcal{G})$ is the Laplacian matrix and is given by

$$L(\mathcal{G}) = \Delta(\mathcal{G}) - \mathcal{A}(\mathcal{G}) \tag{5.4}$$

where $\Delta(\mathcal{G})$ and $\mathcal{A}(\mathcal{G})$ are the degree and adjacency matrices, respectively. Also, $T = (T_1, ..., T_N)^T$ represents the waiting time at each node, $\mathcal{A} \in \mathbb{R}^{N\times N}$ stands for the coupling or adjacency matrix of the system where its elements a_{ij} denote the weight of the link between i and j. B is the $N \times m$ control matrix where m stands for the number of controllers in the control vector $u = (u_1, ..., u_m)^T$. The dynamics in (7.2) is controllable if the pair $(-L(\mathcal{G}), B)$ is controllable [31].

To find the required driver nodes, the exact controllability method (ECM) is implemented [16]. The method is based on Popov-Belevitch-Hautus (PBH) rank criterion upon which the minimum number of driver nodes is equal to the maximum geometric multiplicity of all eigenvalues of the network matrix. Based on PBH theorem, the system (7.2) is fully controllable (meaning that the waiting time can be reduced to the desired values in finite time) if and only if

$$\text{rank}\big(cI_N - L(\mathcal{G}), B\big) = N \tag{5.5}$$

is guaranteed for any complex number c, where I_N is the identity matrix. In [16], it is proven that the minimum number of driver nodes N_D can be calculated by the maximum geometric multiplicity $\mu(\lambda_i)$ of the eigenvalue λ_i of $L(\mathcal{G})$, that is

$$N_D = \text{max}_i\{\mu(\lambda_i)\} \tag{5.6}$$

where

$$\mu(\lambda_i) = \text{dim}V_{\lambda_i} = N - \text{rank}(\lambda_i I_N - \mathcal{L}). \tag{5.7}$$

The minimum number of driver nodes for undirected networks can be determined by the maximum algebraic multiplicity $\delta(\lambda_i)$ of λ_i as

$$N_D = \text{max}_i\{\delta(\lambda_i)\} \tag{5.8}$$

The control matrix B can be calculated from

$$\text{rank}[\lambda^M - L(\mathcal{G}), B] = N \tag{5.9}$$

where λ^M is the maximum geometric multiplicity of the eigenvalue λ^M. Here, the attained non-zero entries of B imply on the necessity of injecting control input for those entries in order to fully control the network.

To find the minimum set of driver nodes, ECM implements elementary column transformation on the matrix $\lambda^M I - L(\mathcal{G})$ leading to a set of linearly independent rows. Eliminating all linear relations via B guarantees the full controllability with the minimum number of driver nodes. The minimum set of driver nodes attained by ECM characterizes the number and locations of CSs. These approaches are successfully implemented in Section IV for the EV network of Perth metropolitan and the results are presented in Figs. 5.2-5.5 and Table 1.

5.4.3 Proposed CS sizing formulation and solution

Once the CS placements are accomplished, the required capacity for each station must be determined. First, the EV network graph is partitioned into N_D subgraphs with only one charging station (determined in the previous section) in each subgraph. The partitioning algorithm, based on [33], decomposes the graph into N_D sub-graphs which will be refined later by making the final decomposition with as fewer interconnections as possible (see [33] for further details on the partitioning approach). Once the graph is partitioned, an adaption of Linear Quadratic Regulator (LQR) problem is implemented on each subgraph. The attained regulator will lead to the required capacity of the corresponding CSs.

For a dynamic system represented by the linear differential equations of (5.10), an optimal cost can be defined by the quadratic function of (5.11):

$$\dot{x} = Ax(t) + Bu(t), \tag{5.10}$$

$$J = \int_0^\infty (x^T Q x + u^T R u + 2x^T Y u) dt \tag{5.11}$$

where

$$u = -\mathcal{K}x \tag{5.12}$$

is the optimal feedback law and $\mathcal{K}$ is given by

$$\mathcal{K} = R^{-1}(B^T P + Y^T). \tag{5.13}$$

In (5.13), P is the solution of the following Riccati equation:

$$A^T P + PA - (PB + Y)R^{-1}(B^T P + Y^T) + Q = 0 \tag{5.14}$$

where Q, R, and Y are arbitrary symmetric and positive semi-definite matrices. In addition,

(A, B) is stabilizable and $(Q - YR^{-1}Y^T, A - BR^{-1}Y^T)$ has no unsolvable modes on the imaginary axis. The relative importance of reducing and saving the control energy can be determined by the appropriate selections of Q and R. A higher R penalizes on the cost function demanding higher energy costs while a higher Q penalizes on the cost entailing higher settling time for the network.

Given the EV network model of (8.2), the problem of CS sizing can be transformed to the problem of finding the optimal control gain of (5.12). The following proposition facilitates this transformation.

Proposition 5.4.1. *The required capacity $\mathcal{C}$ of the charging station located by applying ECM to CS placement is equal to*

$$\mathcal{C} = \mathcal{K}T \tag{5.15}$$

where $\mathcal{K} = [k_1, k_2, ..., k_{n_s}]$ and $T = [T_1, T_2, ..., T_{n_s}]$ and n_s is the number of nodes in the graph. Further, $\mathcal{K}$ is given by (5.13) and P is the solution of the following Riccati equation

$$\mathcal{L}(\mathcal{G})^T P + P\mathcal{L}(\mathcal{G}) - PBR^{-1}B^T P + \mathcal{Q} = 0 \tag{5.16}$$

where

$$\mathcal{L}(\mathcal{G}) = L(\mathcal{G}) - BR^{-1}Y^T$$

$$\mathcal{Q} = Q - YR^{-1}Y^T.$$

Proof. In the LQR framework of the dynamic (7.2), parameter $\mathcal{K}$ attained from (5.13) minimizes the cost function of (5.11). By rewriting (5.12) as $u = \mathcal{C} = \mathcal{K}T$ and replacing matrix A with $\mathcal{L}$, P is the solution of the Riccati equation in (5.16). □

The proposed EV placement and sizing transformations are illustrated in Figure 5.1. The Algorithm 3 summarizes the procedure for CS placement and sizing. In steps 1-9, we apply the exact controllability method to find the number of required CSs. Then to find the size of each CS, the whole graph is partitioned into N_D subgraphs where there is only one CS in each subgraph (steps 10-12). To attain an optimized balance between the sizes of CSs and reducing the peak of waiting times, the traffic models at 17 instances between 6 am and 10 pm have to be attained. in our case study, we attained this information (the number of vehicles) from the traffic map of Western Australia [17]. In practice, T is a dynamic variable. Thus, in this chapter, the attained capacity at each hour is weighted by a factor ρ_i where i represents the instant i (see steps 16-17 of Algorithm 1). For any small mismatch between the supplied capacity and charging demand, a portable charging station can be deployed. This means that given $\mathcal{K}_{it}$ and T^*_{it} as the optimal gain and waiting time of node i at hour t, a portable charging station will be deployed at the area covered by subgraph i if

$$C_i < q\mathcal{K}_{it}T^*_{it} \tag{5.17}$$

where C_i is the size (or capacity) of station i in kW and $0 < q < 1$ is an arbitrary weighting factor.

Note that the arbitrary weights R, Q, and Y can be selected accordingly to set the importance of either optimal size or the settling times of the system. The settling times are the amount of time it takes to reach to the desired system state. By selecting a big matrix Q the system reaches to the desired state rapidly in the cost of increased control signal $u(t)$. Similarly, selecting a big matrix R leads to much smaller $u(t)$ but the system response will be much slower. Equivalently, selecting a big enough Q leads to non-optimal sizes for the CS while selecting a bigger matrix R reduce the capacity in the cost of increased time response to reach to the desired waiting time. Therefore a trade off is necessary while selecting theses weights. This illucidates how the waiting time and the size are affected by the solution of LQR.

Algorithm 3 A graph-based solution to the CS placement and sizing problem in EV networks

Input: The traffic flow of the underlying area from 6 am to 10 pm (17 traffic flow models, one at every hour)

Output: Locations and sizes of CSs

while maximum iteration is not met **do**
  Calculate the matrix B from rank$[\lambda^M - L(\mathcal{G}), B] = N$.
  Assign $N_D = 0$.
  for i=1 to N **do**
    if $B(i)$=1 **then**
      Assign a charging station to node i.
      $N_D = N_D + 1$.
    end if
  end for
  Apply partitioning algorithm to EV network to drive N_D subgraphs featuring one driver node per partition.
  for i=1 to N_D **do**
    Augment the subgraph by adding the detailed dynamics of the underlying area.
    for t=1 to 17 **do**
      Compute P from the Riccati equation $\mathcal{L}(\mathcal{G})^T P + P\mathcal{L}(\mathcal{G}) - PBR^{-1}B^T P + \mathcal{Q} = 0$.
      Compute $\mathcal{K}_{it}$ from $\mathcal{K}_{it} = R^{-1}(B^T P + Y^T)$.
      Assign the weighting factor ρ_i.
      Compute $C_{it} = \rho_i \mathcal{K}_{it} T^*_{it}$.
    end for
    Compute $C_i = \frac{(C_{i1}+C_{i2}+...+C_{i17})}{17}$
  end for
  Assign the weighing parameter q.
  for i=1 to N_D **do**
    for t=1 to 17 **do**
      if $C_i < q\mathcal{K}_{it} T^*_{it}$ **then**
        Assign a portable charging station (PCS).
      end if
    end for
  end for
end while

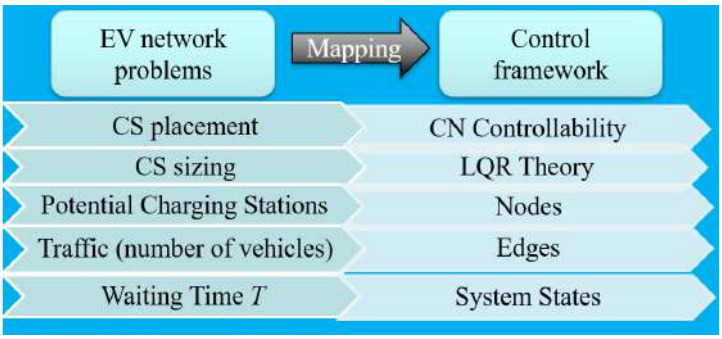

Figure 5.1: Transformation of EV placement and sizing into control frameworks.

5.4.4 Impact of graph symmetry on CS placement solution

Symmetry, described by graph automorphisms, plays an important role in the controllability of complex networks ([31], [34], and [35]). Symmetry is an obstruction to controllability, meaning a big automorphism group necessitates a high number of driver nodes [35]. Therefore, the possible impacts of EV network symmetry on the number and positions of the required charging stations can be investigated by mapping the CS placement problem to the CN controllability problem. The placement of CSs is affected by the automorphism groups. The cardinality (size) of automorphism group determines the symmetry strength of a graph. It is verified in [35] that the symmetry is an obstruction to controllability, meaning a higher number of driver nodes (or in our case, charging stations) are required to fully control the network when the size of automorphism group is big. Lemma 5.4.1 relates CN controllability to automorphism group.

Lemma 5.4.1. *Assume that $A(\mathcal{G})$ is diagonalizable and symmetry preserving ([36]), then the pair $(A(\mathcal{G}), B(S))$ is uncontrollable if $\mathcal{G}$ admits a nontrivial automorphism σ which fixes the input set S, i.e., $\sigma(i) = i$ for all $i \in S$.*

In practice, due to difficulty of listing and sweeping all automorphisms of medium/large networks such as the EV networks, the above lemma is not computationally effective. In [13], an alternative approach based on generators of automorphisms is presented which impose less computation burden.

Lemma 5.4.2. *[13] Assume that $A(\mathcal{G})$, the adjacency matrix of the underlying network, is diagonalizable and symmetry preserving and B is the input matrix applied to set S of N_d driver nodes. Then, the necessary conditions for controllability of the pair $(A(\mathcal{G}), B(S))$ are*

(i) $\sigma_{g_t}(i) \neq i$ and for all $i \in S$ and $t = 1, 2, ..., h$, where $\sigma_{g_t}(i)$ represents for the set of generators and $h = |Gen(\mathcal{G})|$,

(ii) $S(i) \neq j$ for the set of pairwise joint generators with joint node j where $i = 1, 2, ..., N_d$,

(iii) If all nodes of generators g_k are joint nodes then all of its joint nodes are in S.

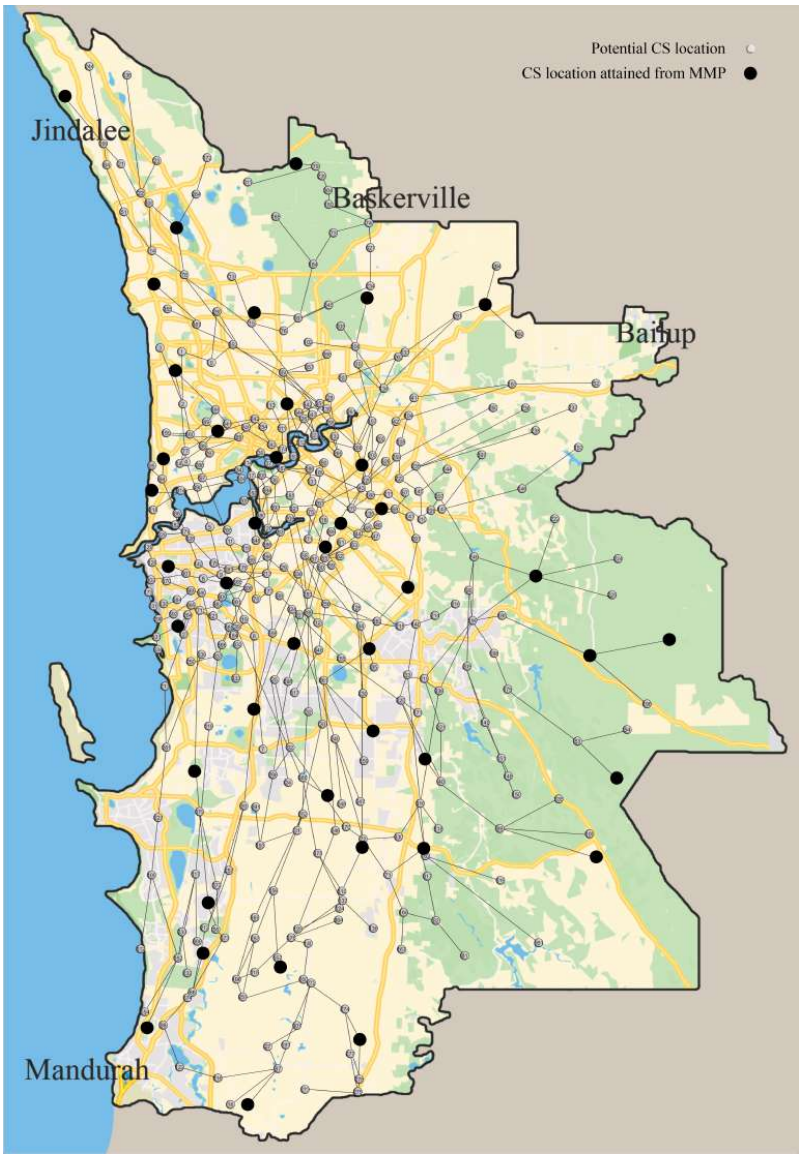

Figure 5.2: Map of Perth metropolitan in Western Australia with 400 virtual nodes representing the potential candidate locations for CSs. The magnified area represents the augmented dynamics of the selected subgraph featuring node 389 as its charging station (driver node). There are 39 more subgraphs that are not shown due to space limitations.

The above lemma leverages on some properties of permutation products to find the determining set of a graph. Then by mapping the Lemma 5.4.1 to CS placement problem, a set of necessary conditions for finding the number and positions of charging stations can be attained. This lemma is used in the simulations of Section IV to investigate the impact of symmetry on EV network of Perth, Western Australia.

An important feature of Lemma 5.4.2 for EV networks is that it provides alternative locations for the charging stations. This fortunate feature is attained since the determining set is not unique. Therefore, it is possible to replace one node in S with another node that has the same structural role in the EV network graph. Two (or more) nodes in a given generator can have the same dynamic in the graph meaning that replacing the entire corresponding to these two nodes

in the graph adjacency (or Laplacian) matrix will not change the adjacency (or Laplacian) matrix. This feature is important for EV networks due to geographical limitations on selecting a spot for CS as the selected spot by ECM or other approaches might not be authorized for constructing a charging station.

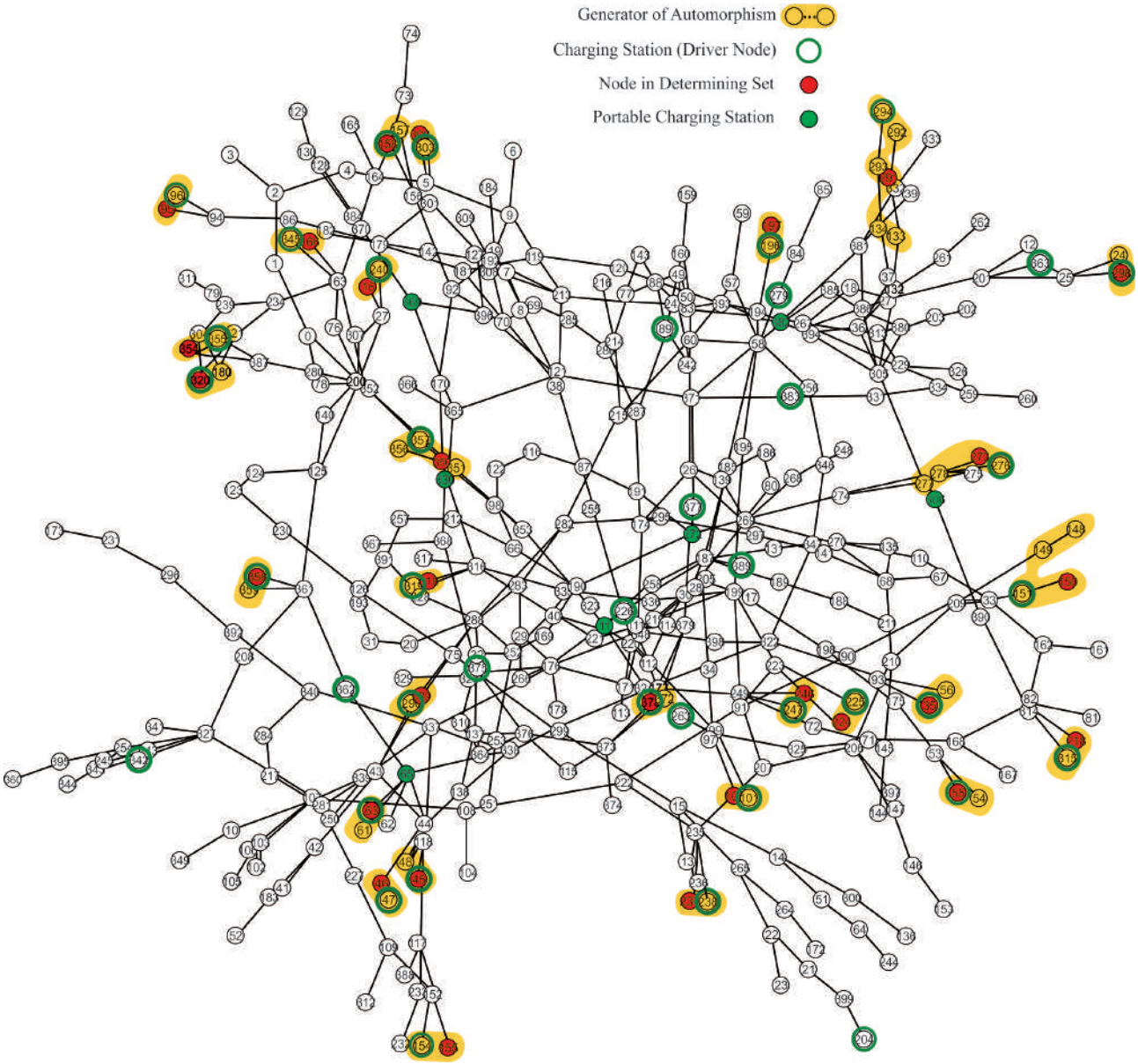

Figure 5.3: Generated graph of Perth EV network showing locations of the 40 CSs or driver nodes (green rings), the 28 generators of automorphisms (black circles in yellow highlighted areas), the 7 PCS nodes (green circles), and the 28 nodes in the determining set (red circles). There are 400 virtual nodes (Figure 5.2). The 28 nodes in determining set are also in CSs set.

5.5 Case study: EV network of the Perth metropolitan in Western Australia

The proposed graph-based approaches for the modeling of EV networks and finding locations/sizes of the CSs and PCSs are implemented and tested on the EV network of Perth Metropolitan in Western Australia (Figure 5.2) and the results are provided in Figure 5.3-5.5 and Table 1. This section provides detailed explanation and analyses of the generated simulation results.

5.5.1 Graph and parameters of Perth EV network

The graph of Figure 5.2 is generated based on the traffic information of Perth metropolitan taken from the Traffic Map of Western Australia [17] which measures the number of vehicles on the main roads. The nodes (potential locations for CSs) are selected using the actual traffic map between areas with known traffic where the number of vehicles in each area represents the weight of the edge connecting two nearby areas. The Perth EV network is bordered to the north by city of Wanneroo, to the east by City of Swan, Kalamunda, and Armadale, and is bordered to the south by Mandurah and to the west by Indian Ocean.

For the simulations and analysis of this chapter, we have made a number of assumptions including 1) there are $10,000$ vehicles in Perth metropolitan, WA with an average vehicle power consumption of 0.173 kW/km [17], 2) all CSs are equipped with the standard DC fast chargers with the service time of $10-15$ minutes ([17]), 3) the desired waiting time is the same at all CSs and is limited to the threshold of 15 minutes, 4) the maximum and minimum battery state of charge for EVs are SoCmax $= 80\%$ and SoCmin $= 20\%$, 5) EVs arriving at the CSs have uniform SoC distribution in the range of 20% to 80%. Considering the characteristics of the existing commercial vehicles, the upper and lower boundaries of SoC are fixed at ideal level, which are currently 80% for the maximum level and 20% for the minimum level [39].

5.5.2 Number, locations and sizes of CSs of Perth EV network

To find the number and locations of CSs, the set of driver nodes that can fully control the EV network (represented by (2)) must be determined. To this end, the exact controllability method is implemented (Equations (7.3)-(7.3.2)) in MATLAB which resulted in a set of 40 driver nodes as illustrated in Figure 5.3 with green rings. The ECM relates the controllability of complex networks to the maximum geometric multiplicity of eigenvalues of the matrix A, and in turn, to the corresponding Laplacian matrix $L(\mathcal{G})$. This matrix, in the context of EV network, is the adjacency matrix representing the traffic flow between nearby nodes. According to Section III.B, the driver nodes that can fully control a complex network are mapped into the charging stations that can fully supply the charging demand of EV network. Due to analogy between driver nodes and charging stations, these driver nodes can thus be selected as the locations of

the CSs. Therefore, using the Algorithm 1, the number and locations of charging stations can be attained from steps 2-9.

To find the size of each CS, first the 400-node graph in Figure 5.2 is partitioned into 40 sub-graphs with minimum edge cuts. The graph partitioning is accomplished according to step 10 of Algorithm 1. This is constrained by the consideration of only one CS in each subgraph. The LQR approach is then implemented in MATLAB for each subgraph after subgraph augmentation (steps 12-15). Due to space limitation, only one of the subgraphs corresponding to the CS at node 389 is augmented in Figure 5.2. The arbitrary weights R, Q, and Y for each subgraph are selected after a few trials and errors. Once these arbitrary weights are selected, the Riccati equation in step 14 can be solved where B in step 14 has only one non-zero element at the entry corresponding to the driver node (or charging station) and L corresponds to the Laplacian matrix of traffic flow in the subgraph. The solution of the Riccati Equation (in step 16) is the matrix P which is then substituted in step 15 to attain $\mathcal{K}$. Finally, according to Proposition III.1, the required capacity for the corresponding CS in the subgraph can be computed from step 19. Note that the augmented area contains more nodes (not shown in Figure 5.2) that are used to accurately model the traffic flow of the area. The corresponding subgraph to the CS at node 389 is magnified in Figure 5.2 to illustrate the detailed dynamics of the underlying area. According to Algorithm 1, the LQR approach is implemented for this subgraph for 17 instances corresponding to 17 traffic models between 6 am and 10 pm. These models are each investigated to attain the required capacity at each hour (steps 13-17 of Algorithm 1). Solving the LQR for 17 instances has resulted in the following capacities at each hour (ordered form 6 to 10 pm, respectively).

$$\begin{aligned} C_{it} = [&339, 391, 472, 498, 475, 455, 431, 411, 440, 465, 457, \\ &432, 398, 372, 341, 299, 273] \end{aligned} \tag{5.18}$$

Steps 18-28 of Algorithm 1 facilitate attaining an optimized charging capacity via choosing an appropriate parameter ρ. The arbitrary weighting parameter ρ (where $0 < \rho_i < 1$) determines the balance between reducing the overshoot in the waiting time at peak hours and increasing the charging capacity. In fact, if for all values of i we assume $\rho_i = 1$ then the overshoot at peak hours will be zero at the cost of significant increase in charging capacity. According to the magnitude difference between the charging demand at peak hours and the rest of instances, we selected the variable values for ρ_i (e.g., $\rho_i \approx 1$ at peak hours). This has resulted to the required charging capacity of 371 kW at node 389. Similarly, the required charging capacities of other CSs are calculated and provided in Table 1 (row 5).

5.5.3 Waiting times of Perth EV network without portable charging stations

To find the waiting times, the EV network is simulated with the 40 allocated CSs (driver nodes) of Figure 5.3 and the calculated CS capacities of Table 1 (row 5). The EV network dynamic

taken from (3) is modeled by selecting initial waiting times at each station while matrix B and the capacities (corresponding to control signal $u(t)$ in (3)) are computed in the previous section. Equation (3) is simulated in MATLAB and the network states (waiting time T_i at each station) over the 17 instants models between 6 am and 10 pm are calculated as illustrated in Figure 5.4. As indicated in this figure, the waiting time diagrams undergo two overshoots near the peak hours. This is caused by selecting different ρ_i for different hours. Although the waiting time has increased at peak hours, the network capacity is optimized. For example, if $\rho_i = 1$ for all values of i then the charging capacity at node 389 must be 495 kW which is 124 kW more than the computed capacity (371 kW) in the previous section.

5.5.4 Introduction of PCSs in Perth EV network

As illustrated in Figure 5.4, there are some overshoots during peak traffic hours around 9 am and 3 pm (e.g., the waiting times are longer than the designated threshold of 15 minutes). These overshoots are mainly due to the selected weighting factor (ρ_i; Algorithm 1: Step 17). This chapter proposes deployment of PCSs to reduce the overshoots. The deployment of PCSs can be scheduled by i) updating the waiting time vector every hour, ii) checking inequality (5.17), and iii) proceeding with Steps $21 - 28$ of Algorithm 1. For the EV network of Figure 5.2, seven PCSs are assigned and located in an hourly basis (Table 1, row 6). Adding these PCSs modifies the network dynamics by changing the entries of matrix B associated to the nodes corresponding to the locations of the added PCSs. Running the EV network model of (3) in MATLAB and measuring the new waiting times at the 40 charging stations has resulted in shorter waiting times at peak hours as illustrated in Figure 5.5. Compared with the results of Figure 5.4, there are notable reductions in the frequency and magnitudes of the overshoots.

5.5.5 Analyses of simulation results for Perth EV network

A symmetry analysis of the EV network of Perth is performed with Sage software package. Having the network Laplacian matrix L, the number of automorphisms of the EV network can be attained in Sage in less than a minute by simply typing a one line command (i.e., by typing "*G.automorphism_group()*" where G is the simulated network by its Laplacian). This has resulted in approximately 268 million automorphisms. Obviously, it is not computationally effective to sweep over all automorphisms. Instead, the generators of automorphisms are calculated using the command "*gens(G)*" which is resulted in 28 generators listed in Table 1 (row 4) and illustrated in Figure 5.3. As indicated in Figure 5.3, there is at least one CS in each generator set. This verifies the adaption of Lemma 5.4.1 to EV networks where driver nodes represent the charging stations. According to Lemma 8.2, a determining set can be calculated by sweeping over the set of 28 generators and selecting one node in each generator. The determining set thus contains 28 nodes (Figure 5.3; red circles) that are listed in Table 1, row 7.

The concept of determining set characterizes an important feature for the CS placement

Table 5.1: Summary of simulation results for the Perth EV network of Figure 5.2-5.3.

Parameter	**Value**	**Figure number and/or Descriptions**
Virtual Nodes	400	Figure 5.2, yellow highlighted groups of nodes.
Aut($\mathcal{G}$)	268 m	The 268 million automorphisms are identified with the Sage software package.
Gen($\mathcal{G}$)	28	Figure 5.2, yellow highlighted groups of nodes; $Gen(\mathcal{G})$ =[(372,378), (358,359), (350,351)(356,357), (318,319), (302,303), (289,290), (273,276), (277,278), (246,247),(237,238), (224,225), (218,315),(196,197), (180,320), (166,345), (157,158), (154,155), (100,101), (35,56), (148,150)(149,151), (95,96), (354,355), (133,134)(291,293)(292,294), (61,63), (54,55), (46,47), (45,48), (24,298), (16,240)].
CSs	40	Figure 5.3, green rings at nodes 35 (275 kW), 45 (128 kW), 47 (213 kW), 55 (349 kW), 63 (72 kW), 89 (200 kW), 96 (173 kW), 101 (362 kW), 151 (252 kW), 154 (393 kW), 158 (234 kW), 196 (336 kW), 204 (188 kW), 225 (218 kW), 226 (72 kW), 238 (254 kW), 240 (385 kW), 247 (214 kW), 263 (192 kW), 276 (317 kW), 279 (87 kW), 290 (352 kW), 294 (52 kW), 298 (205 kW), 303 (271 kW), 315 (226 kW), 319 (191 kW), 320 (128 kW), 342 (241 kW), 345 (365 kW), 355 (273 kW), 357 (379 kW), 358 (90 kW), 362 (204 kW), 363 (94 kW), 375 (218 kW), 377 (276 kW), 378 (59 kW), 383 (311 kW), and 389 (371 kW).
PCSs	7	Figure 5.3, green circles, nodes 11, 65, 272, 306, 330, 369, and 382 (PCSs have the same capacity of 250 kW).
Determining Set $\mathcal{S}$	28	Figure 2, red circles at nodes 16, 35, 45, 46, 55, 63, 95, 100, 150, 155, 158, 166, 197, 218, 224, 237, 246, 273, 289, 291, 298, 302, 318, 320, 350, 354, 358, and 372.
Nodes in both sets of S and CSs	28	Figure 5.3, 28 nodes in the determining set that are also in the set of CSs.
Waiting Times at CSs without PCSs	-	Figure 5.4, the family of 40 curves with a daily average of 12 minutes and two peaks of 19.3 minutes and 17 minutes. The average waiting times at peak hours, 9 am and 4 pm, are 17.7 and 17.1 minutes, respectively.
Waiting Times at CSs with PCSs	-	Figure 5.5, the family of 40 curves with a daily average of 12 minutes. Two peaks of Figure 5.4 have reduced to 16.6 minutes and 16.5 minutes. Also, the average waiting times at peak hours have reduced to 15.4 and 15.35 minutes.

problem. Since the determining set of an automorphism group is not unique, there are alternatives for the majority of driver nodes to act as the charging stations. For example, node 378 in the determining set (Figure 5.3) can be replaced with nodes 372 because the set of nodes $\{372, 378\}$ is a generator in $Gen(\mathcal{G})$ (Table 1, row 4) and as a result they can play the same structural role in the EV network.

The set of driver nodes together with the generators of automorphisms are illustrated in Figure 5.3. Also the set of nodes belonging to the determining set is highlighted in Figure 5.3. There is an overlap between the set of driver nodes and determining set meaning that all nodes in the determining set also belong to the set of driver nodes. This implies the importance of symmetry in the structure of EV network. In practice, all locations selected as driver nodes may not be suitable for the installation of charging stations. Fortunately, the determining set provides alternative options/locations for the installation of charging station.

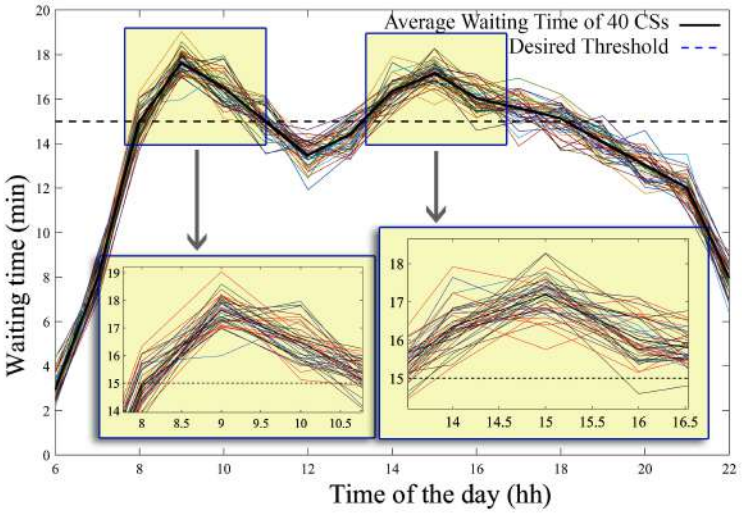

Figure 5.4: Waiting time at the allocated 40 CSs (Table 1; row 5) without the deployment of PCSs. The thick black curve shows the average waiting time of the 40 CSs from 6 am to 10 pm.

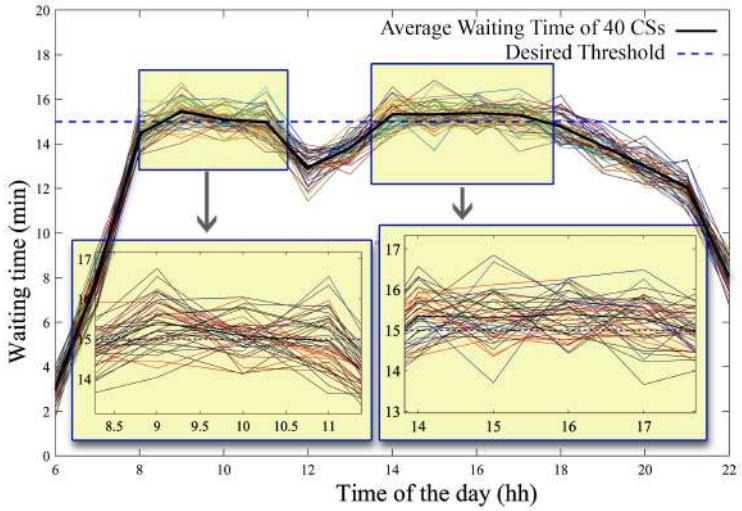

Figure 5.5: Waiting time at the allocated 40 CSs (Table 5.1; row 5) with the deployment of PCSs (Table 5.1, row 6) according to Steps 21-28 of Algorithm 1. The thick black curve shows the average waiting time of the 40 CSs from 6 am to 10 pm.

5.6 Conclusion

A graph-based method is proposed and implemented for the placement and sizing of CSs that considers traffic and limits the vehicle waiting times at all stations below a desirable threshold level (e.g., 15 minutes). The research reveals the analogies between (i) the CS placement and controllability of the underlying network and (ii) the CS sizing and optimal controller design. In addition, a strategy for deployment of PCSs is introduced to further improve the quality of solutions by reducing the overshooting of waiting times during peak traffic hours. Although further study is required to analytically explain the symmetry impacts of EV networks on the

solutions of CS placement and sizing, our results verifies that the EV graph symmetry, in the context of graph automorphism, can significantly change the number and locations of the CSs while suggesting alternative locations for CSs.

The new proposed framework to reformulate CS placement and sizing using control and graph theories facilitates adapting many other concepts from control as well as graph theory. Our future work will be on the development of robust control methods to EV networks under dynamic pricing and uncertain traffic. Another interesting research direction would be pursuing an analytical explanation for the overlap between the determining set (attained with symmetry analysis of the underlying network) and the set of driver nodes (or charging stations). Finally, the impact of the proposed charging network design on the power grid is not considered in this chapter and will be addressed in our further research.

5.7 Appendix: composition of permutations

The method of calculating the product or composition of two permutations is described below through an example. *Example A.1:* Let ζ and δ be given by

$$\zeta = (1 \quad 2 \quad 3 \quad 4 \quad 5) \quad and \quad \delta = (1 \quad 4 \quad 3).$$

To compute the composition of ζ and δ, $\zeta \circ \delta$, first we have to check the commutation (represented by the symbol $\mapsto$) of element by δ and then its commutation by ζ. In this example

$$\begin{aligned}
1 \mapsto^{\delta} 4 \mapsto^{\zeta} 5 \quad &\Rightarrow \quad \zeta \circ \delta(1) = 5 \\
5 \mapsto^{\delta} 5 \mapsto^{\zeta} 1 \quad &\Rightarrow \quad \zeta \circ \delta(5) = 1 \\
4 \mapsto^{\delta} 3 \mapsto^{\zeta} 4 \quad &\Rightarrow \quad \zeta \circ \delta(4) = 4 \\
3 \mapsto^{\delta} 1 \mapsto^{\zeta} 2 \quad &\Rightarrow \quad \zeta \circ \delta(3) = 2 \\
2 \mapsto^{\delta} 2 \mapsto^{\zeta} 3 \quad &\Rightarrow \quad \zeta \circ \delta(2) = 3.
\end{aligned}$$

Thus the composition of ζ and δ is $\zeta \circ \delta = (1 \quad 5)(3 \quad 2)$.

Bibliography

5.8 References

[1] N. Daina and J. W. Polak, Hazard based modelling of electric vehicles charging patterns, in Transportation Electrication Asia-Pacifc (ITEC AsiaPacific), 2016 IEEE Conference and Expo., 2016.

[2] E. Daramy-Williams, J. Anable, and S. Grant-Muller, "A systematic review of the evidence on plug-in electric vehicle user experience," *Transportation Research Part D: Transport and Environment*, vol. 71, pp. 22-36, 2019.

[3] S. Ou, Z. lin, X. He, S. Przesmitzki, and J. Bouchard, "Modeling charging infrastructure impact on the electric vehicle market in China," *Transportation Research Part D: Transport and Environment*, vol. 81, pp. 2020.

[4] Community Energy Association. [Online]. Available: http://communityenergy.bc.ca/.

[5] S. Huang, L. He, Y. Gu, K.Wood, and S. Benjaafar, "Design of a mobile charging service for electric vehicles in an urban environment," *IEEE Trans. Intel. Trans. Sys.*, vol. 16, 2018.

[6] Z. Moghaddam, "Smart charging strategies for electric vehicle charging stations," PhD Thesis, Edith Cowan University, WA, Australia, 2019.

[7] Q. Liu, J. Li, X. Sun, P. Xu, J. Wang, W. Zheng, J. Li, and H. Liu, "Planning mobile charging vehicles based on user charging behavior," ACM, pp. 37-42, 2018.

[8] S.N. Yang, H.W. Wang, C.H. Gan, and Y.B. Lin, "Mobile charging information management for smart grid networks," *Int. J. of Info. Man.*, vol. 33, no. 2, pp. 245-251, 2013.

[9] S. F. Tie and C. W. Tan, "A review of energy sources and energy management system in electric vehicles," *Ren. and Sus. Ene. Rev.*, vol. 20, pp. 82-102, 2013.

[10] J. Li, J. Jiao, and Y. Tang, "An evolutionary analysis on the effect of government policies on electric vehicle diffusion in complex network," *Energy Policy*, vol. 129, pp. 1-12, 2019.

[11] B. N. E. Finance, Electric vehicle outlook 2017, Tech. Rep., 2017, [Online]. Available: https://about.bnef.com/ electric-vehicle-outlook.

[12] H. Zhang, C. J. R. Sheppard, T. E. Lipman, T. Zeng, and S. J. Moura, "Charging infrastructure demands of shared-use autonomous electric vehicles in urban areas," *Transportation Research Part D: Transport and Environment*, vol. 78, 2020.

[13] Y. Huang and K. M. Kockelman, "Electric vehicle charging station locations: Elastic demand, station congestion, and network equilibrium," *Transportation Research Part D: Transport and Environment*, vol. 78, 2020.

[14] H. Parastvand, A. Chapman, O. Bass, and S. Lachowicz, "A Symmetry Perspective on Complex Network Controllability with Applications to Power Systems," *Power Electric Systems Research*, under review.

[15] B. D. MacArthur, R. J. Sanchez-Garcia, and J. W. Anderson, "Symmetry in Complex Neworks," *Disc. App. Math.*, vol. 156, 2018.

[16] L. M. Pecora, F. Sorrentino, A. M. Hagerstorm, T. E. Murphy, and R. Roy , "Cluster synchronization and isolated desynchronization in complex networks with symmetries," *Nature, Communication*, vol. 5, 2014.

[17] Z. Moghaddam, I. Ahmed, D. Habibi, and M. Masoum, "A coordinated dynamic pricing model for electric vehicle charging stations," *IEEE Trans. on Intel. Trans. Sys.*, vol. 5, 2019.

[18] M. Baum, J. Dibbelt, T. Pajor, and D. Wagner, "Dynamic TimeDependent Route Planning in Road Networks with User Preferences,"In Proceedings of the 15th International Symposium on Experimental Algorithms (SEA'16), vol. 9685, Springer, 2016.

[19] I. Morro-Mello, A. Padilha-Feltrin, J. D. Mello, and A. Calvino, "Fast charging stations placement methodology for electric taxis in urban zones," *Energy*, vol. 188, 2019.

[20] Y. Zhang, Q. Zhang, A. Farnoosh, S. Chen, and Y. Li, "GIS-Based Multi-Objective Particle Swarm Optimization of charging stations for electric vehicles," *Energy*, vol. 169, pp. 844-853, 2019.

[21] B. Moritz, S. Jong, W. Dorothea, and Z. Tobias, "Consumption Profiles in Route Planning for Electric Vehicles: Theory and Applications,"16th International Symposium on Experimental Algorithms (SEA 2017), 2017.

[22] S. D. Gaikwad and P. C. Ghosh, "Sizing of a fuel cell electric vehicle: A pinch analysis-based approach," *International Journal of Hydrogen Energy*, In Press, 2020.

[23] S. Boug and S. Layeb, "Determining Optimal Deployment of Electric Vehicles Charging Stations: Case of Tunis City, Tunisia,"Case Studies on Transport Policy 7(3):628-642, 2019.

[24] M. E. Kabir, C. Assi, H. Alameddine, J. Antoun, and J. Yan, "Demand Aware Deployment and Expansion Method for an Electric Vehicles Fast Charging Network,"IEEE International Conference on Smart Grid Communications (SmartGridComm), 2019.

[25] S. R. Gampa, K. Jasthi, P. Goli, D. Das, and R. C. Bansal, "Grasshopper optimization algorithm based two stage fuzzy multiobjective approach for optimum sizing and placement of distributed generations, shunt capacitors and electric vehicle charging stations,"Journal of Energy Storage, 2020.

[26] Y. Chen, S. Kar, and and Jose M. F. Moura, "Optimal Attack Strategies Subject to Detection Constraints Against Cyber-Physical Systems," *IEEE Trans. on Cont. Net. Sys.*, vol. 5, no. 3, 2018.

[27] C. Chen, K. Xie, F. L. Lewis, S. Xie, And A. Davoudi, "Fully Distributed Resilience for Adaptive Exponential Synchronization of Heterogeneous Multiagent Systems Against Actuator Faults," *IEEE Trans. on Aut. Con.*, vol. 64, no. 8, pp. 3347-3355, 2019.

[28] N. Ma, Z. Liu, and L. Chen, "Synchronisation for complex dynamical networks with hybrid coupling time-varying delays via pinning adaptive control," *Int. J. of Sys. Sci.*, vol. 50, 2019.

[29] Y. L. Huang and S. X. Wang, "Synchronisation in an array of spatial diffusion coupled reaction diffusion neural networks via pinning control," *Int. J. Sys. Sci.*, vol. 49, no. 5, 2018.

[30] H. Parastvand and M.J. Khosrowjerdi, "A New Data Driven Approach to Robust PID Controller Synthesis," *International Journal of Systems Science*, vol. 46, no. 7, 2015.

[31] A. Chapman and M. Mesbahi, "On symmetry and controllability of multi-agent systems," *53rd IEEE Conf. on Dec. and Cont.*, USA, 2014.

[32] Z. Yuan and C. Zhao, Z. Di, W. X. Wang, and Y. C. Lai, "Exact controllability of complex networks," *Nature: Comm.*, 2013.

[33] C. Ocampo-Martinez, S. Bovo, and V. Puig, "Partitioning approach oriented to the decentralised predictive control of large-scale systems," *J. Process Control*, vol. 21, no. 5, 2011.

[34] C. O. Aguilar and B. Gharesifard, *A graph-theoretic classification for the controllability of the laplacian leader-follower dynamics*", *53rd IEEE Conf. Dec. and Cont.* Los Angeles, California, USA, 2014.

[35] A. Rahmani, M. Mesbahi, M. Egersted, "Controllability of multi-agent systems from a graph-theoretic perspective," *SIAM J. of Con. and Opt.*, vol. 48, no. 1, pp. 162-186, 2009.

[36] A. Chapman, M. Nabi-Abdolyousefi, and M. Mesbahi, "Controllability and observability of networks-of-networks via cartesian products," *IEEE Trans. on Aut. Cont.*, vol. 59, pp. 2668-2679, 2014.

[37] L. W. Beineke and R. J. Wilson, "Topics in algebraic graph theory," *Encyclopedia of mathematics and its applications*, 2007.

[38] https://www.trafficmap.mainroads.wa.gov.au/map.

[39] del Razo, Victor and Jacobsen, Hans-Arno, "Smart Charging Schedules for Highway Travel With Electric Vehicles", *IEEE Transactions on Transportation Electrification*, vol. 2. no. 2. pp. 160-173, 2016.

Chapter 6

Robust Placement and Sizing of Charging Stations from a Novel Graph Theoretic Perspective

6.1 Overview

This paper proposes analytical approaches to extend the capacity of existing networks of electric vehicles (EVs) by placement of additional charging stations (CSs) as well as determining the sizes of existing and new CSs in order to handle future expansions of EVs. The EV flow at CSs is modeled by a graph where nodes are potential locations for CSs and edges are uncertain parameters representing the variable EV flow at CSs. The required extra CS locations are explored by transforming the CS placement problem into a controllability framework addressed by maximum matching principle (MMP). To find the sizes of each CS, the graph of CS network is partitioned featuring only one CS in each subgraph. The size of CS in each subgraph is then determined by transforming the problem into the problem of robust stability of a system with uncertain parameters where each parameter is associated with an edge of subgraph. The zero exclusion principle is then tested for the related Kharitonov rectangles and polygonal polynomials of closed loop system with selected feedback gain as CS capacity. The proposed analytical approach is tested on the existing Tesla CS Network of Sydney. The locations of extra required CSs as well as the sizes of existing and new CSs are determined to maintain the waiting times at all stations below the threshold level[1].

[1]This chapter is published in *IEEE Access*

6.2 Introduction

As a response to the greenhouse gases emissions, the internal combustion vehicles have been replacing rapidly by electrically powered vehicles. As such, the charging infrastructures, mainly charging stations (CSs), have always been expanded in order to supply the ever increasing demand of new EVs added to the network.

The optimization techniques are the focal point of methodologies related to EV problems (for example see [1]- [13]). Some of the most frequently used optimization techniques in literature addressing various EV related problems include Monte Carlo simulation [3]- [4], Grasshooper optimization algorithm [5], particle swarm optimization (PSO) [6]- [7], CPLEX [8]- [9], genetic algorithm [10], active-set algorithm [11], and K-means cluster [12]. The Markov and Monte Carlo simulation are used in [3] and [4] to model the urban driving cycle and to simulate the EV travel patterns and charging demand, respectively. Grasshopper optimization is used in [5] to address the sizing of CSs while the optimal placement of distributed generations and shunt capacitors are also investigated. In [6], a multi-objective PSO and geographic information system are used for the planning of CSs with a focus on the underlying economic impacts. PSO is also used in [7] for dynamic economic emission dispatch with load demand management where a large penetration during crest-and-valley is considered. The CPLEX solver is used in [8] to construct an integer linear program in order to address the EV salesman problem constrained to a predefined windows of waiting times. CPLEX is also implemented in [9] to attain a mixed-integer linear program model for stochastic scheduling of plug-in electric vehicles (PEVs) aggregator in day-ahead and reserve market. A review on energy management and optimization of EVs based on genetic algorithm is presented in [10]. Using active-set algorithm in [11], a framework is proposed to optimally deploy various types of CSs where a heuristic algorithm is implemented for solving the model. The EV network of China is divided into 31 provinces by k-means cluster [12] to investigate the impact of EVs on the greenhouse gas emissions.

One of the main focus of studies related to EV networks during the last few years has been the Optimal placement and sizing of CSs in order to maintain the waiting time below a threshold level ([5]- [6], and [12]- [14]) where a sort of optimization technique is used in almost all of the proposed approach. The optimization techniques implemented for EV problems usually suffer from computational issues such as complexity and intractable solution [13]. On the other hand, almost all (if not all) previous studies have addressed the CS placement problems for regions where there are no existing CSs. However, as the EV networks are rapidly growing, there is a need for placement and sizing of new stations while also the existing CSs must be re-sized.

A novel approach to CS placement and sizing is proposed in [14] which, unlike the majority of current approaches based on optimization techniques, relies on graph theoretic properties of the graph of EV networks. It transforms the CS placement to the problem of finding the set of required driver nodes for CN controllability using the exact controllability method (ECM). Similarly, the CS sizing problem is transformed to the problem of finding a linear quadratic

regulator (LQR) for each partition of EV network. However, there are some limitations for this approach. It lacks the consideration of dynamic traffic flow during the day and only relies on 17 instances of traffic flow. Moreover, the proposed CS placement approach can not be applied for networks where there are some pre-existing CSs.

To address the above challenges, we have developed the control framework first introduced in [14] in order to address the CS placement and sizing for a network with existing CSs and variable flow of EVs. Firstly, the mathematical model of the underlying graph of EV network is improved by separating the traffic flow at individual node from the trafic flow between nodes. The proposed approach then transforms the placement and sizing problems to controllability and feedback gain design problems where the system states are the waiting times at CSs and control inputs are the charging capacity supplied via driver nodes acting as CSs. A model of underlying EV network is constructed using a graph where nodes are the potential locations of CSs and edges link two nearby nodes where the weights of edges represent the number of EVs in the area. The ECM implemented in [14] is not applicable for CS placements in networks with existing CSs. Thus we use another graph theoretic property, known as maximum matching principle, by modifying it to a case where there are some pre-set unmatched nodes, and then the locations of new CSs are determined by finding the remaining unmatched nodes on the graph of CS network. Moreover, the proposed approach in [14] determines the locations and sizes of CSs according to a static EV flow corresponding to few traffic instances during the day, while in this paper, the control framework and the graph theoretic approach of [14] are adapted to a more general and practical case that considers variable traffic flow. Throughout the paper, the term "traffic flow" refers to the flow of EVs at the charging stations. It is represented by uncertain parameters with known maximum and minimum values assigned to the weight of each edge.

To locate the number and locations of additional CSs, we determine the driver nodes for the associated graph of EV network based on the maximum matching principal while considering the weights of edges as an interval uncertain parameter. To address the sizing problem of existing and new CSs, we first partition the graph of EV network featuring only one CS (from the set of CSs located from the solution of CS placement) in each subgraph. Then, we use the Kharitanov theorem and zero exclusion condition [15] to transform the CS sizing problem to zero exclusion of the Kharitonov rectangles or polygonal polynomials of the closed loop system attained from the sub-graphs (or the problem of robust stability of plants with uncertain parameters [16]). Detailed simulations and analyses of the Tesla CS network of Sydney verify that the proposed approach has significant impact on reducing the waiting times at CSs in Year 2025 assuming 500% increase in EV traffic [19]. The main contributions of this paper (in general and compared to [14]) are:

1. Unlike the usual optimization methods, the proposed approaches are analytic, computationally effective, and rely on established concepts from graph/control theories.

2. The mathematical model of the EV network proposed in [14] is improved by separating the impacts of traffic flows at nodes and between nodes.

3. We consider the CS placement and sizing for expanding EV networks with existing CSs. As the best of authors' knowledge, there is no analytic approach to placement of new CSs for an expanding network considering the future traffic.

4. The ECM method used in [14] is not applicable to CS placement for expanding networks. Here, we modify the MMP so that it can be used for placement of CSs when there are some pre-existing CSs.

5. We consider and model the dynamic of traffic flow using interval uncertain parameters.

6. The proposed approach is able to maintain the waiting times at CSs below a threshold level in the presence of variable traffic.

7. The proposed approach in this paper can be easily implemented to any EV network with variable traffic. The only required data is the model of the underlying graph and the maximum/minimum number of EVs arriving at CSs during operation.

The rest of the paper is organized as follows. Section 6.3 develops an EV network model based on graph theory followed by new approaches for robust CS placement and sizing of existing and new CSs. Section 6.4 presents and analyzes comprehensive simulation results for the existing Tesla CS network of Sydney, Australia, followed by conclusions.

6.3 CS placement and sizing for expanding EV networks with variable traffic flow at CSs

In this section, the modeling of the CS network based on graph theory is explained followed by a new approach for the placement and sizing of existing and new CSs that considers the variable traffic flows of the EV network.

6.3.1 Graph-theoretic modeling of EV network

Graph theory [17] is one of the bases of the mathematical analysis in this study. Here, the terms graph or network are reserved for the abstract mathematical model of the composition of nodes and edges of CS network where nodes are the potential locations of CSs and edges are the traffic flow between nearby nodes. The weights of edges represent the traffic or the number of vehicles. A graph is defined as the pair $\mathcal{G} = (V, E)$ where V and E are the finite set of nodes and edges of the graph, respectively.

The worldwide locations and sizes of the existing charging stations are accessible through various CS networks and maps such as the Tesla CS, Plug In America, Go Electric Stations, Open Charge Map, Plug Surfing, EV Charger Maps, LEMnet, POP Point, Sun Country Highway and PlugShare. For the molding, formulation, simulations and analyses of this paper, we use the Tesla CS Map of Sydney, Australia [18]. Assuming 500% increase in Sydney EV traffic

by Year 2025 [19], this model is augmented by adding some virtual candidate locations (nodes) for additional CSs at various spots across the map to construct the graph of the whole network. Although, the simulation is performed for this specific network, it can be easily implemented to all EV networks with variable traffic.

Considering the waiting times at all potential and existing locations of CSs as the states of system and assuming that there is an online tool presenting the instance waiting times to the drivers and the majority of drivers prefer a CS with a low waiting time in nearby area, the dynamic equation

$$T_i = T_{i_0} + \int_0^t W_{ch} T_{ch} q_{ii}(t) dt + \sum_{j=1}^{n} q_{ij} a_{ij} T_j,\ i = 1, ..., n \tag{6.1}$$

governs the dynamics of waiting times at all nodes. In 8.2, T_i is the state of i^{th} node, T_{i0} is the initial state of node i, W_{ch} is the ratio of charge to full charge, T_{ch} is the full charging time, $q_{ii}(t)$ is the uncertain flow of EVs at node i, q_{ij} is the uncertain flow of EVs between nodes i and j, a_{ij} is the outer coupling matrix in which $a_{ij} = 1$ if there is an edge between nodes i and j but $a_{ij} = 0$ otherwise, T_j represents the adjacent nodes to node i, and n is the number of nodes. Given $\int_0^t q_{ii}(t)dt = Q_{ii}(t)$, we can write

$$\begin{aligned} \dot{T}_i &= W_{ch} T_{ch} Q_{ii} dt + \sum_{j=1}^{n} q_{ij} a_{ij} T_j,\ i = 1, ..., n \\ \dot{Q}_{ii} &= q_{ii}. \end{aligned} \tag{6.2}$$

Equation 6.2 governs the dynamics of waiting times T_i at all nodes since when the drivers are consciously choose a target CS, then all states T_i, $i = 1, 2, ..., n$, incrementally converge to nearly equal final states. Equation (6.2) simulates the waiting times when no CS exists and thus the waiting times increase constantly. To maintain all waiting times reasonably below a threshold level, a controlling term must be added to (6.2) which pins a few nodes to act as CSs in order to inject the control signal (charging supply) to the network. Considering the sizes of CSs as the values of control inputs of the system, the governing equation of CS network can be written as

$$\dot{T}_i = T_i + \sum_{j=1}^{n} q_{ij} a_{ij} H T_j - \delta B u_i,\ i = 1, ..., n \tag{6.3}$$

where u_i is the control signal or charging supply injected through the CS at node i, B is the input matrix, and $\delta_i = 1$ if node i is selected as a CS and $[\delta_i] = 0$ otherwise. Equation (8.1) facilitates transforming the CS sizing problem to a control framework in which finding the control signal is equivalent to finding the charging capacity required to maintain the state of system (8.1) or waiting times below a threshold level.

6.3.2 Graph-theoretic CS placement in EV networks with existing CSs and variable traffic

As verified in [14], the problem of CS placement can be transformed to the problem of finding the required driver nodes for the underlying graph of EV network where nodes are the potential places for CSs and edges represent the traffic flow (the flow of EVs at CSs) between two nearby nodes. System states are also defined as the waiting times T_i at each node i. The set of driver nodes are located in [14] by the exact controllability method which is based on the maximum geometric multiplicity of all eigenvalues of the system matrix. However, this method is not applicable here as a set of predetermined CSs are already placed. We use and modify an alternative method, known as maximum matching principle, to find the set of required driver nodes. Throughout the paper, the terms driver node, charging station, and CS have been used interchangeably, but they convey the same meaning.

Definition 6.3.1. *For a graph $\mathcal{G}(V, E)$, a matching M in $\mathcal{G}$ is a set of pairwise non-adjacent edges, none of which are loops, that is, there is no shared endpoints for none of edges or, equivalently, no two edges share a common node. A node is matched if it is an endpoint of one of the matching set, otherwise, it is unmatched. Maximum matching M_{max} of the graph $\mathcal{G}$ is a matching of maximum size among all matchings in the graph.*

The relation between maximum matching and controllability is first revealed in [22] where the Controllability of complex networks is attributed to the number of required driver nodes. Once the maximum set of matched nodes are identified, all unmatched nodes are considered as the set of driver nodes [22] needed to completely control the entire network. Considering (8.1) as a complex network with a set of pre-existing CSs, the objective is to place a set of extra CSs to address future network expansion. Thus, here, the EV network is called "controllable" if we can drive the the states (waiting times) of (8.1) below a threshold level using a set of pre-existing and extra CSs. We first set the existing CSs as unmatched nodes and then attain the number and locations of extra CSs for (8.1) by modifying the maximum matching principle as summarized in proposition below.

Proposition 6.3.1. *A given expanded graph $\mathcal{G}$ of a CS network with V nodes and existing set of driver nodes S^0_{CS} is controllable if the set of driver nodes is*

$$S_{CS} = \{V|\ (V \in S^0_{CS}) \cup (V \in S^E_{SC})\} \tag{6.4}$$

where

$$S^E_{SC} = \{V|\ (V \notin M_{max})\,\&\,(V \notin S^0_{CS})\}. \tag{6.5}$$

Proof. The proof is a straightforward result of computing the extra set of nodes S^E_{SC} using the maximum matching principle on the graph assuming that the set of nodes in S^0_{CS} are reserved as unmatched. □

Using the above proposition and the control framework of placement problem, the set of extra CSs can be found. Example below clarifies the implementation of the modified MMP for EV network.

Example 6.3.1. *Figure 6.1 illustrates the implementation of the modified MMP on a subgraph of an EV network. It represent an existing CS at node 3 in Figure 6.1.a which is set as an unmatched node. The modified MMP has resulted in two matched edges indicated by red lines and one unmatched node (node 5) indicated by the red location symbol in Figure 6.1.b. Thus, the subgraph will have two CSs, one pre-existing and one added.*

In Section 8.3, the placement of required extra CSs for the expanded Tesla CS network of Sydney, Australia is performed using this method.

6.3.3 Graph-theoretic sizing of new and existing CSs in EV networks with variable traffic

To find the sizes of all CSs, first, we partition the CS graph into N_D subgraphs where there is only one CS (from the set of CSs attained from the solution of CS placement) in each subgraph. The partitioning algorithm decomposes the graph into N_D subgraphs which will be refined later by aiming at the final decomposition with as fewer interconnections as possible (see [20] for further details on the partitioning approach). Once the graph is partitioned, the corresponding dynamic of each subgraph similar to (8.1) is calculated in which B has only one non-zero entry corresponding to a node where a CS is placed. The state space representation of each subgraph can then be written as:

$$\dot{\mathbf{T}} = \mathcal{L}\mathbf{T} + B\mathbf{u} \ , y = CT \tag{6.6}$$

where $\mathcal{L} = \mathcal{D} - \sum_{j=1}^{n_s}(T_i - T_j)$, $i = 1, ..., n_s$, n_s is the number of nodes within the subgraph, $\mathcal{D}$ is the degree matrix, and $C = \mathbf{1}$. The state space representation of the subgraph in (6.6) can then be written as the transfer function

$$G(s) = C(SI - L)^{-1}B \tag{6.7}$$

which is the Laplacian form of system (6.6).

The dynamic equation (7.2) for each subgraph is a transfer function $G(s) = \frac{N(s)}{D(s)}$ where both $N(s)$ and $D(s)$ are affine-linear uncertain polynomials. This is clarified by the following example.

Example 6.3.2. *Consider the simple graph of Figure 6.2 with three nodes and one CS at node* 2*. The number of vehicles on the three edges are defined as* $1 \leq q_1 \leq 10$*,* $1 \leq q_2 \leq 15$*, and* $1 \leq q_3 \leq 20$*. Let* $q_{ii} = 0$ *and* $q_{ij} = q_{ji}$ *for* $i = 1, 2, 3$*. The Laplacian matrix of this network can be written as:*

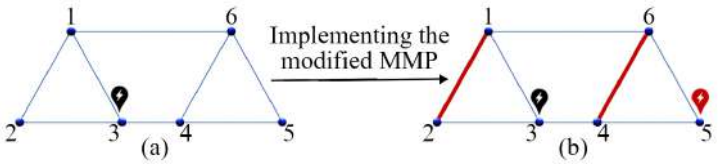

Figure 6.1: (a) A subgraph of EV network with an existing CS at node 3 and, (b) the implementation of the modified MMP which has resulted to two matched edges indicated by red lines and one added CS at node 5.

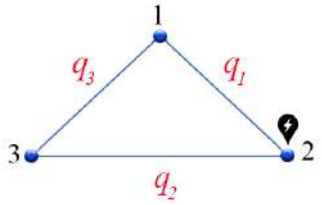

Figure 6.2: A graph with three uncertain edges and one CS.

$$\mathcal{L} = \begin{bmatrix} 2 & -q_1 & -q_3 \\ -q_1 & 2 & -q_2 \\ -q_3 & -q_2 & 2 \end{bmatrix}, \quad C = \mathbf{1}, \quad B = [0\ 1\ 0]^T$$

The closed loop transfer function (7.2) with fixed controller k can then be written as

$$H(s) = \frac{k.N(s)}{D(s) + k.N(s)}$$

where $N(s) = s^2 + (-4 - q_1 - q_2)s + 4 + 2q_1 + q_2^2 - q_3^2 + 2q_2 + q_1q_3$ *and*

$$\begin{aligned} D(s) + k.N(s) = s^3 + (-6 - kq_1 - 4k - kq_2)s^2 + s(4 - q_1^2 \\ - q_2^2 + 2kq_1 + kq_2^2 + 4k - kq_3^2 + 2kq_2 + kq_1q_3) + 2q_1^2 + 4q_2^2. \\ - 8 + 2kq_1 + kq_2^2 + 4k - kq_3^2 + 2kq_2 + kq_1q_3 \end{aligned}$$

The uncertainties of this non-linear polynomial can be over-bounded to construct an affine-linear uncertain polynomial. By defining new variables $Q_1 = kq_1$, $Q_2 = kq_2$, $Q_3 = q_1^2$, $Q_4 = q_2^2$, $Q_5 = kq_2^2$, $Q_6 = kq_3^2$ *and* $Q_7 = kq_1q_3$, *the over-bounding polynomial can be written as*

$$\begin{aligned} D(s) + k.N(s) = s^3 + (-6 - Q_1 - 4k - Q - 2)s^2 + s(4- \\ Q_3 - Q_4 + 2Q_1 + Q_5 + 4k - Q_6 + 2Q_2 + Q_7) + 2Q_3 + 4Q_4 \\ - 8 + 2q_1 + Q_5 + 4k - Q_6 + 2Q_2 + Q_7 \end{aligned}$$

which has an affine-linear uncertainty structure with uncertainty bounds $k \leq Q_1 \leq 10k$, $k \leq Q_2 \leq 15k$, $1 \leq Q_3 \leq 100$, $1 \leq Q_4 \leq 225$, $k \leq Q_5 \leq 225k$, $k \leq Q_6 \leq 400k$, *and* $k \leq Q_7 \leq 150k$.

As explained, the subsequent subgraphs of the CS network have affine-linear uncertain polynomials in the nominator and denominator of the related transfer functions. Each subgraph with an associated CS can be seen as a control system with unity feedback and a fixed compensator k that represents the charging capacity. The closed loop polynomial with fixed k can thus be seen as an affine-linear uncertain polynomial with interval uncertainty. The proposed control framework of this study facilitates implementing the controller design theories to find the appropriate feedback gain that can guarantee reaching to the desired system states. This can be translated as finding the sizes of CSs that can keep the waiting time (system state) below a threshold level.

A few definitions and preliminary results are reviewed first to demonstrate the transforming of EV sizing problem to the problem of analysing the robust stability of an interval uncertain polynomial. The Kharitanov theorem is the bedrock of the analysis in this paper. It deals with the robust stability of interval uncertain polynomials. Two solutions will be presented for CS sizing based on i) zero exclusion condition for Kharitonov polynomials, and 2) zero exclusion condition for a polytop of closed loop polynomials.

Definition 6.3.2. *A family of uncertain polynomials given by $\mathcal{P} = \{p(.,q) : q \in Q\}$ is said to have invariant degree if for any $q^1, q^2 \in Q$ it follows that deg $p(s,q^1) =$ deg $p(s,q^2)$.*

Definition 6.3.3. *A set $C \subseteq \mathbf{R}^k$ is convex if the line joining any two points it contains the whole line segment joining them. Mathematically, for any given $c_1, c_2 \in C$ and $\lambda \in [0,1]$ we have $\lambda C_1 + (1-\lambda)c_2 \in C$. The convex hull of a shape denoted by $conv\{.\}$ is the smallest convex set that contains it.*

Definition 6.3.4. *A family of polynomials $\mathcal{P} = \{p(.,q) : q \in Q\}$ is an interval polynomial family if p has an independent uncertainty structure, meaning that each coefficient of p continuously depends on q and Q is a convex box.*

Definition 6.3.5. *Given a family of polynomials $\mathcal{P} = \{p(.,q) : q \in Q\}$, the value set at $z \in \mathbf{C}$ is the image of Q under $p(z,.)$ and is given by $p(z,Q) = \{p(z,q) : q \in Q\}$.*

Theorem 6.3.1. *[15] For the interval polynomial family $\mathcal{P} = \{p(.,q) : q \in Q\}$ with $p(s,q)$ where its coefficients continuously depend on q, there exists a second interval polynomial family $\tilde{\mathcal{P}} = \{\tilde{p}(.,\tilde{q}) : \tilde{q} \in \tilde{Q}\}$ with $\tilde{p}(.,\tilde{q})$ in the form of $\tilde{p}(.,\tilde{q}) = \sum_{i=0}^{n} q_i s^i$ and, moreover, $\tilde{\mathcal{P}} = \mathcal{P}$.*

Using the above theorem, known as lumping theorem, the uncertain polynomial can be written as $p(s,q) = \sum_{i=0}^{n} q_i s^i$ and subsequently, the interval family can be described by $p(s,q) = \sum_{i=0}^{n} [q_i^-, q_i^+] s^i$ where q_i^- and q_i^+ denote the extreme points of the bound of uncertainty q_i.

Definition 6.3.6. *[15] The four Kharitonov polynomials associated with the interval polynomial $p(s,q) = \sum_{i=0}^{n} [q_i^-, q_i^+] s^i$ are the four fixed polynomials*

$$K_1(s) = q_0^- + q_1^- s + q_2^+ s^2 + q_3^+ s^3 + q_4^- s^4 + q_5^- s^5 + q_6^+ s^6 + ...$$

$$K_2(s) = q_0^+ + q_1^+ s + q_2^- s^2 + q_3^- s^3 + q_4^+ s^4 + q_5^+ s^5 + q_6^- s^6 + ...$$

$$K_3(s) = q_0^+ + q_1^- s + q_2^- s^2 + q_3^+ s^3 + q_4^+ s^4 + q_5^- s^5 + q_6^- s^6 + ...$$

$$K_4(s) = q_0^- + q_1^+ s + q_2^+ s^2 + q_3^- s^3 + q_4^- s^4 + q_5^+ s^5 + q_6^+ s^6 + ...$$

Now, we present the Kharitonov Theorem on robustness of interval polynomials.

Theorem 6.3.2. *[15] An interval polynomial family $\mathcal{P}$ with invariant degree is robustly stable if and only if its four Kharitonov polynomials, or Kharitonov rectangles, are stable.*

The above theorem can be graphically tested using the zero exclusion condition as stated below.

Lemma 6.3.1. *Given an interval family $\mathcal{P} = \{p(., q) : q \in Q\}$ with invariant degree and at least one stable member $p(s, q^0)$, $\mathcal{P}$ is robustly stable if and only if $z = 0$ is excluded from the kharitonov rectangle at all non-negative frequencies; i.e., $0 \notin p(j\omega, Q)$ for all frequencies $\omega \geq 0$.*

The calculation of the value set for the whole range of frequencies is computationally inefficient. However, there is a cutoff frequency $\omega_c > 0$ such that $0 \notin p(j\omega, Q)$ for all $\omega \geq \omega_c$. This means that the computation of the value set can be terminated at ω_c. The existance of ω_c is established in [15] using the invariant degree condition. It follows that the cutoff frequency can be calculated from

$$\omega_c = 1 + \frac{\max\{q_0^+, q_1^+, ..., q_{n-1}^+\}}{q_n^-} \tag{6.8}$$

Theorem 6.3.2 and Lemma 6.3.1 can be used to find the solution of CS sizing problem. As indicated in example 2, the closed loop polynomial of each subgraph of the CS network is an interval uncertain polynomial which can be over-bounded to attain an affine-linear uncertain polynomial. Proposition below summarize the result using the Kharitonov rectangle and zero exclusion condition.

Proposition 6.3.2. *(First Proposed Solution to CS Sizing). For a given subgraph $\mathcal{S}_i$ attained from partitioning of the CS network featuring only one CS with capacity k, the states T of the associated transfer function computed from (7.2) can reach the desired waiting time in finite time if $z = 0$ is excluded from the the kharitonov rectangles of the affine-linear polynamial $D(s) + k.N(s)$ with invariant degree for $0 \leq \omega \leq \omega_c$.*

Proof. The proof simply follows from the results of Theorem 6.3.2 and lemma 6.3.1 with the closed loop poynomial of the subgraph attained from $D(s) + k.N(s)$. □

The proposition above is tested for the Tesla CS network of Sydney, Australia and satisfactory results are attained in Section 8.3. Now, we proceed with the second solution to CS sizing using a more general form of uncertainty.

Definition 6.3.7. *A set $X \subseteq R^k$ is said to be pathwise connected if for any two points $x_0, x_1 \in X$, there is a continuous function $\Phi : [0, 1] \to X$ such that $\Phi(0) = x_0$ and $\Phi(1) = x_1$.*

Every convex set of uncertainty is thus pathwise connected. Obviously, the uncertainty in the traffic map is also pathwise connected as it is a convex set.

Theorem 6.3.3. *[15] Let the family of invariant degree polynomials $\mathcal{P} = \{p(.,q) : q \in Q\}$ with cutoff frequency ω_c and uncertainty bounding set Q, which is pathwise connected, have continuous coefficient functions $a_i(q)$ for $i = 0, 1, 2, ..., n$ and at least one stable member $p(s, q^0)$. Then $\mathcal{P}$ is robustly stable if and only if the origin $z = 0$ is excluded from the value set $p(j\omega, Q)$ at all frequencies $\omega \geq 0$; i.e., $\mathcal{P}$ is robustly stable if and only if $0 \notin p(j\omega, Q)$ for all frequencies $\omega \geq 0$.*

Now the value sets for a polytop of polynomials can be defined. It is argued in [15] that the related value sets are polygons in the complex plane. A polygonal property of value sets for a plytop of polynomials is presented below which facilitates testing the zero exclusion condition.

Lemma 6.3.2. *[15] Given a polytop of polynomials $\mathcal{P} = \{p(.,q) : q \in Q\}$ with uncertainty bounding set $Q = conv\{q^i\}$, for fixed $z \in \mathbf{C}$, the value set $p(z, Q)$ is a polygon with generating set $\{p(z, q^i)\}$ or $p(z, Q) = conv\{p(z, q^i)\}$. In addition, all edges of the polygon $p(z, Q)$ are obtained from the edges of Q so that if z_0 is a point on an edge of $p(z, Q)$, then $z_0 = p(z, q^0)$ for some q^0 is on an edge of Q.*

The second solution to EV sizing problem is summarized in the proposition below.

Lemma 6.3.3. *(Second Proposed Solution to CS Sizing) For a given subgraph $\mathcal{S}_i$ of the graph of CS network with capacity k, the states T of the associated transfer function computed from (7.2) can reach to the desired waiting time in finite time if $z = 0$ is excluded from the value set $D(j\omega, Q) + k.N(j\omega, Q)$ for all frequencies $\omega \geq 0$.*

Proof. The proof is a straightforward result of theorem 6.3.3 and lemma 6.3.2 with the closed loop polynomial of the subgraph attained from $D(s) + k.N(s)$. □

The above proposition gives a solution to the sizing of each CS in each subgraph. A clear cut solution to the CS placement and sizing is presented in Algorithm 1.

6.4 Implementation of proposed CS placement and sizing strategy in Tesla CS network of Sydney

The proposed approaches of this paper (summarized in Algorithm 1) are applied on the Tesla CS network of Sydney [18] illustrated in Figure 6.3. The 48 existing Tesla charging stations are demonstrated in Figure 6.3 with black location icons. All CSs are equipped with the standard DC fast chargers with the service time of $10-15$ minutes. According to Energeia Analysis, with current uptake rate of EVs, the number of EVs in Sydney by the year 2025 will be increased by about $\%500$ [19]. The graph of this network is augmented in Figure 6.3 considering the variable traffic flow in 2025. The number of connectors and sizes of existing CSs are indicated

Algorithm 4 The proposed graph-based solutions to the robust CS placement and sizing problem in EV networks

Input: The maximum and minimum number of EVs arriving at each CS during its operation.
Output: The locations of extra required CSs and sizes of all (existing and new) CSs.

1: **while** maximum iteration is not met **do**
2: Calculate S_{CS} from (6.4).
3: Apply partitioning algorithm to EV network to drive N_D subgraphs featuring one driver node per partition.
4: **for** i=1 to N_D **do**
5: Compute the cutoff frequency ω_c^i from (6.8).
6: Investigate the zero exclusion condition of Lemma 6.3.1 for $0 \leq \omega \leq \omega_c^i$ and a fixed k using one of the Proposition 6.3.2 or Lemma 6.3.3.
7: **if** the zero exclusion condition is satisfied **then**
the size of CS is k.
8: **else**
Increase k and go to step 6.
9: **end if**
10: **end for**
11: **end while**

in Table I. The extra required CSs (S_{CS}) are calculated by following the modified maximum matching (Lemma 6.3.1) principle as explained in Lemma 6.3.3. Since the result of maximum matching is a set of unmatched nodes that must be considered as CSs, we have performed it on a modified map where the nodes are selected in locations where it is practical to construct CS infrastructure. This has led to a set of 12 unmatched nodes (indicated by red location symbol in Figure 6.3) in addition to 48 existing CSs which are pre-set as unmatched. The resulted extra CSs are illustrated in Figure 6.3. Having the set S_{CS}, we can proceed with computing the size of each CS after constructing the graph of CS network and partitioning it into $|S_{CS}|$ subgraphs. Due to space limitation, here the simulation results for only one of the subgraphs (the area separated with a dashed rectangle in Figure 6.3) are presented. The weights on the edges of this subgraph represent the variable traffic flow q_i between two nodes. The system has 16 nodes and 20 edges. The number of nodes and edges indicate the order of subgraph and the number of uncertainties, respectively. The order of system is 16 and as such, it is a big transfer function with very long coefficients $a_i(q)$ depending on Q. Here, only the state space representation of

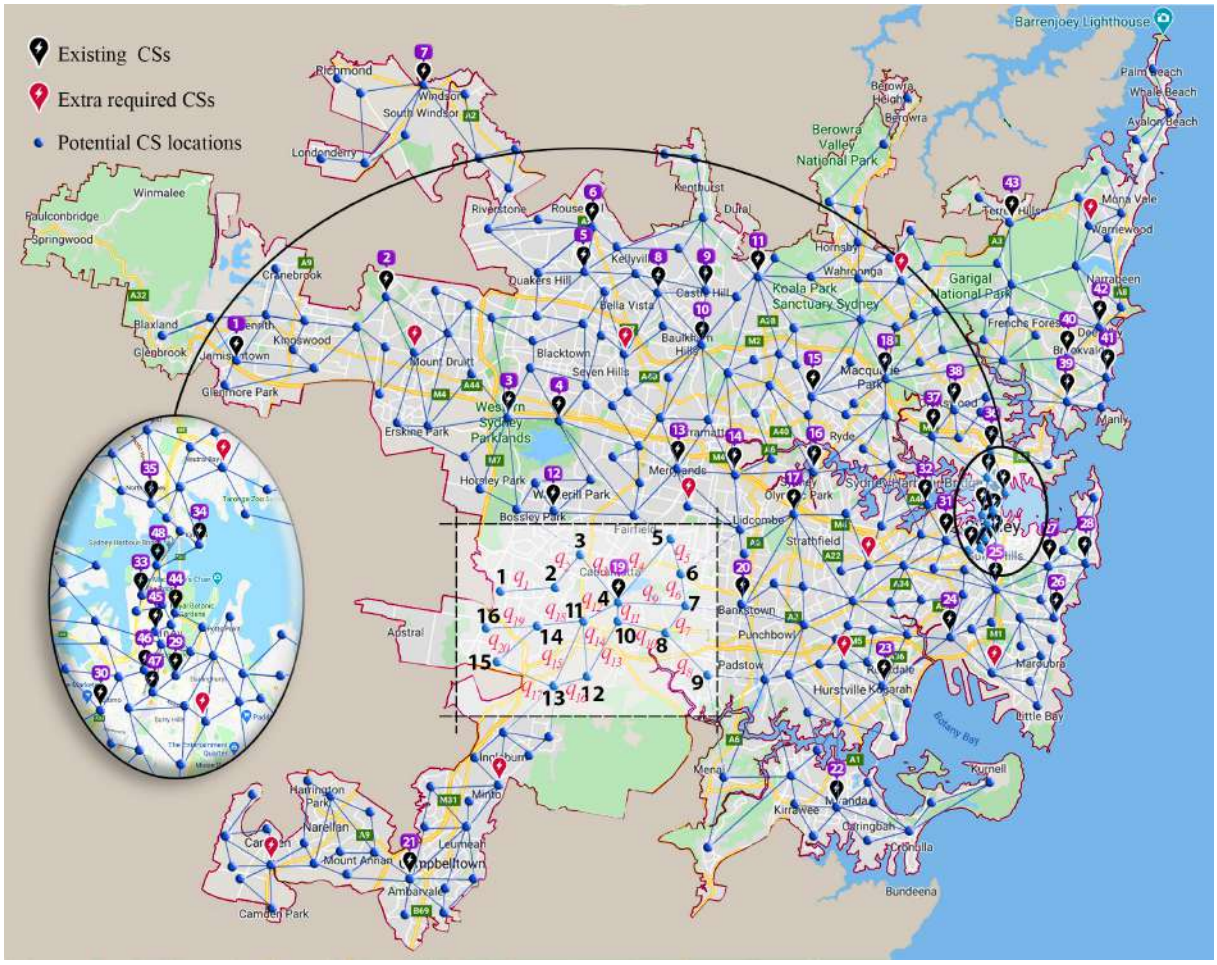

Figure 6.3: Tesla CS map of Sydney, Australia [18] used for simulations. The black, red, and blue location icons correspond to the nodes with existing CSs, new CSs (determined in this paper), and the potential CS locations, respectively.

Figure 6.4: The Kharitonov rectangles for the subgraph shown in Figure 6.3.

the subgraph is presented. The adjacency matrix $\mathcal{A}$ for the subgraph is

$$\begin{bmatrix}
q_{ii} & q_1 & . & . & . & . & . & . & . & . & . & . & . & . & . & . \\
q_1 & q_{ii} & q_2 & . & . & . & . & . & . & . & . & . & . & . & . & . \\
. & q_2 & q_{ii} & q_3 & . & . & . & . & . & . & . & . & . & . & . & . \\
. & . & q_3 & q_{ii} & q_4 & . & q_9 & . & . & q_{11} & q_{12} & . & . & . & . & . \\
. & . & . & q_4 & q_{ii} & q_5 & . & . & . & . & . & . & . & . & . & . \\
. & . & . & . & q_5 & q_{ii} & q_6 & . & . & . & . & . & . & . & . & . \\
. & . & . & q_9 & . & q_6 & q_{ii} & q_7 & . & . & . & . & . & . & . & . \\
. & . & . & . & . & . & q_7 & q_{ii} & q_8 & q_{10} & . & . & . & . & . & . \\
. & . & . & . & . & . & . & q_8 & q_{ii} & . & . & . & . & . & . & . \\
. & . & . & q_{11} & . & . & . & q_{10} & . & q_{ii} & . & q_{13} & . & . & . & . \\
. & . & . & q_{12} & . & . & . & . & . & . & q_{ii} & q_{14} & q_{15} & q_{18} & . & . \\
. & . & . & . & . & . & . & . & . & q_{13} & q_{14} & q_{ii} & q_{16} & . & . & . \\
. & . & . & . & . & . & . & . & . & . & q_{15} & q_{16} & q_{ii} & . & q_{17} & . \\
. & . & . & . & . & . & . & . & . & . & q_{18} & . & . & q_{ii} & q_{20} & q_{19} \\
. & . & . & . & . & . & . & . & . & . & . & . & q_{17} & q_{20} & q_{ii} & . \\
. & . & . & . & . & . & . & . & . & . & . & . & . & q_{19} & . & q_{ii}
\end{bmatrix}$$

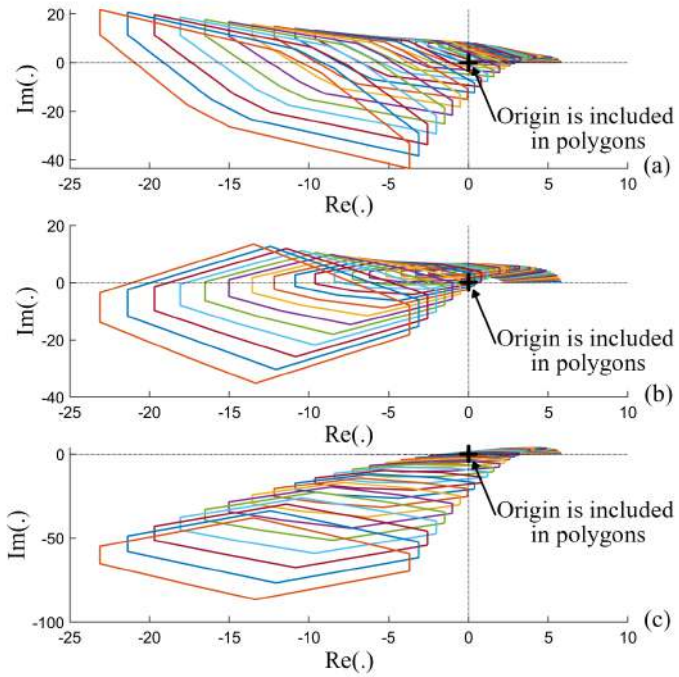

Figure 6.5: The zero exclusion condition for the polygonal polynomials of subgraph shown in Figure 6.3 for (a) $k = 65$, (b) $k = 75$, (c) and $k = 85$.

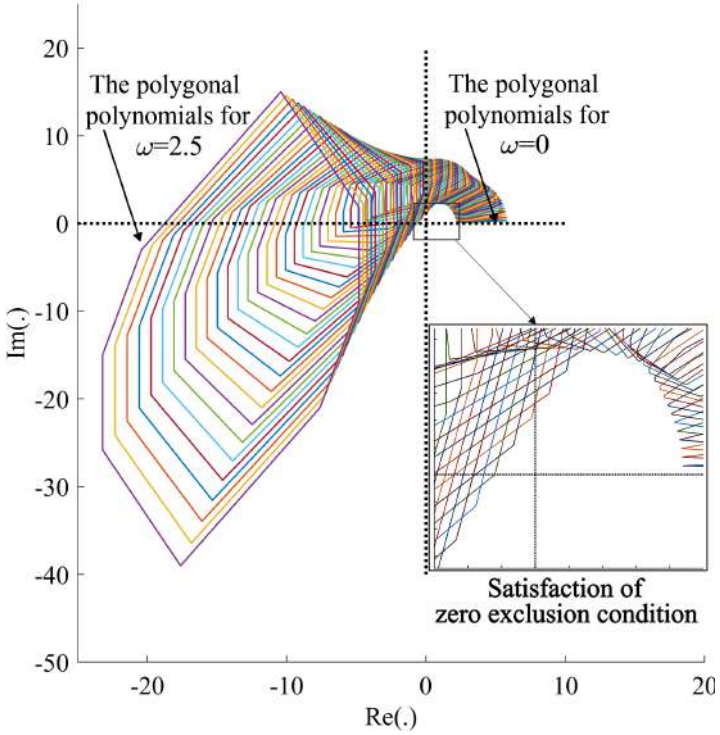

Figure 6.6: The zero exclusion condition for the polygonal polynomials of subgraph shown in Figure 6.3 for $k = 95$.

where the zeros are represented with dots for clarity. The input matrix is

$$B = [0 \quad 0 \quad 0 \quad 1 \quad 0 \quad 0 \quad 0 \quad 0 \quad 0 \quad 0 \quad 0 \quad 0 \quad 0 \quad]^T$$

Table 6.1: Number of connectors N_C, the size of each existing CS $|S_{SC}|_i$ in kW, and the size of each CS in kW after expansion $|S_{SC}|_i$ of Tesla CS network of Sydney.

CS	N_C	$\|S^0_{CS}\|_i$	$\|S_{CS}\|_i$	CS	N_C	$\|S^0_{CS}\|_i$	$\|S_{CS}\|_i$
Existing CSs with Present and Calculated New Sizes							
1	2	22	138	2	1	22	84
3	4	44	79	4	1	22	93
5	3	22	84	2	6	22	142
7	2	6	118	8	1	5	162
9	3	22	98	10	2	27	145
11	2	22	89	12	2	22	126
13	2	22	122	14	4	44	75
15	2	7	110	16	5	44	96
17	4	44	120	18	2	3	123
19	3	22	95	20	4	26	143
21	2	22	120	22	2	22	78
23	2	6	117	24	4	29	86
25	4	44	116	26	2	22	145
27	4	22	68	28	2	22	128
29	2	4	126	30	3	22	98
31	2	22	78	32	3	22	129
33	5	44	93	34	2	22	136
35	3	22	85	36	1	22	124
37	3	5.2	110	38	1	6	96
39	4	44	158	40	4	22	85
41	4	22	103	42	1	22	73
43	2	22	134	44	2	22	79
47	2	22	106	48	4	28	112
Additional CSs with Calculated Sizes							
49	-		94	50	-		129
51	-		87	52	-		85
53	-		115	54	-		95
55	-		134	56	-		113
57	-		105	58	-		93
59	-		84	60	-		138
Summary and Comparison of Results							
Existing Tesla CSs				**Upgraded Tesla CSs**			
Total Number of CSs: 48				Total Number of CSs: 60			
Total S Size: 1054.4 kW				Total S Size: 5025 kW			

and $C = \mathbf{1}$. By computing the transfer function of this subgraph and constructing $D(s) + k.N(s)$, the two proposed methods for calculating the size of the CS at node 4 are implemented by graphical examining of zero exclusion condition (Figures 6.4-6.7 and Table 6.1). Note that node 19 in the subgraph is re-numbered as node 4.

The cutoff frequency for this subgraph is calculated using (6.8) as $\omega_c = 2.5$. The zero exclusion condition for $k = 95$ and $0 \leq \omega \leq 2.5$ is investigated in MATLAB and the result

is demonstrated in Figure 6.4 for 125 equally spaced frequencies. Clearly, the origin of the complex plane is excluded from the rectangles of Kharitonov and, as such, the associated CS can handle the demand by increasing its capacity to 95kW.

Proceeding with Lemma 6.3.3 will lead to the similar results as Kharitanov rectangles. To this end, we have examined the zero exclusion condition of Lemma 6.3.3 for three values of k less than 95. The results are shown in Figures 6.5.(a)-(c). As indicated in these figures, the origin of complex plane is included in the polygons for all three values of k. The subgraph is re-examined with $k = 95$ and, as shown in Figure 6.6, zero is excluded from the polygons. There are 20 uncertainties but the attained polygons are not 20-sided as most of extreme points fall inside the convex hull of the polynomial for extreme points. The capacity of the rest of CSs are computed in a same way and the results are presented in Table I. Finally, the waiting time of node 19 is calculated in MATLAB for the variable traffic during 24 hours (as shown in Figure 6.7.(a)) and the result indicated in Figure 6.7.(b) shows that the waiting time is maintained near or lower than the 15 minutes threshold at all times.

6.5 Conclusion

This study proposes novel graph theoretic solutions from the lens of control theories to address the CS placement and sizing in EV networks with dynamic traffic flow. The new CS placement approach considers the placement of required extra CSs for an expanding EV network with existing stations. It is accomplished by modifying the maximum matching principle to find the set of extra required CSs. Subsequently, the CS sizing is addressed by resizing the existing stations in addition to the sizing of new required CSs. The sizing is performed by transforming the problem of CSs sizing for a network with dynamic traffic to the problem of robust stability of a family of polynomials with affine-linear interval uncertainties where each uncertain parameter represents an uncertain interval number of EVs in the zone between two nearby nodes. In addition to dynamic traffic flow consideration, the approach is unique as it relies on more analytical methodologies compared with the conventional solutions to CS placement and sizing problem that often suffer from computational issues such as conservative responses or intractable solutions. On the other hand, the fast growing of electric vehicles (EVs) deployment necessitates expanding the current charging stations (CSs) networks. Nearly all previous studies on CS placement and sizing are focused on the planning and design of EV networks with no existing stations. The proposed approach of this study, however, addresses the placement of new and extra required CSs as well as re-sizing of existing CSs for expanded network.

The proposed graph theoretic approaches are implemented and verified on the existing Tesla CS Network of Sydney, Australia assuming an increase of 500% in EV traffic by year 2025. Detailed simulation results indicate that the average waiting times during peak hours at CSs are kept near 15 minutes for upgraded EV network with $+500\%$ increase in EV traffic, 60 CSs, and total charging capacity of 5.025 MW.

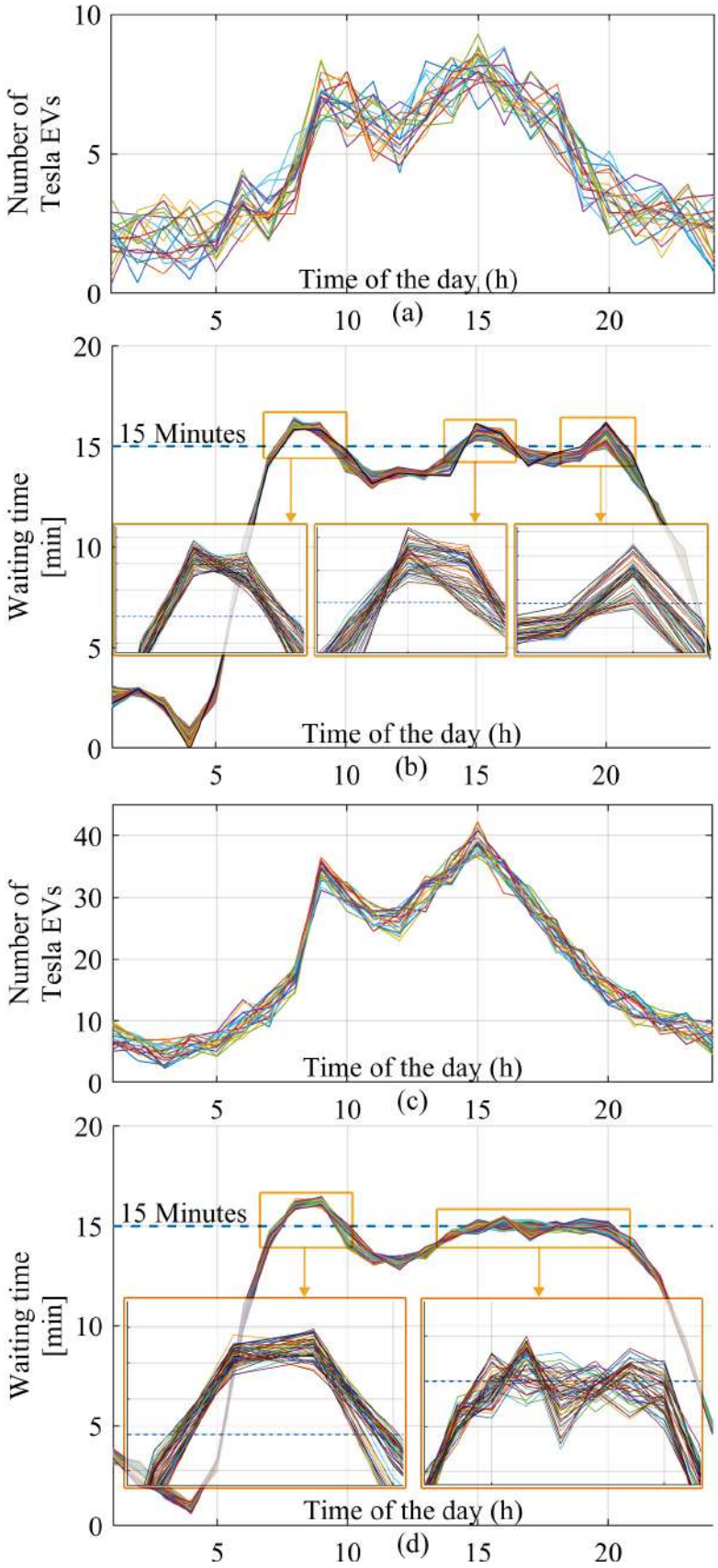

Figure 6.7: (a) The traffic flow of the existing network with 48 CSs (represented by black icons in Figure 6.3), (b) the corresponding waiting time of the existing 48 CSs, (c) The traffic flow of the expanded network (in year 2025), and (d) The corresponding waiting times of 48 pre-existing and 12 extra added CSs (represented by red icons in Figure 6.3)

Bibliography

6.6 References

[1] Y. Li, C. Rehthanz, S. Rubherg, L. Lhuo, and Y. Chao, "Assessment and choice of input signals for multiple HVDC and FACTS wide-area damping controllers," in *IEEE Trans. Pow. Sys.,* vol. *27, no*. 4, pp . *1969–1977,* Nov, 2012, DOI. 10.1109/TPWRS.2012.2189865.

[2] Z. Moghaddam, I. Ahmed, D. Habibi, and M. Masoum, "A coordinated dynamic pricing model for electric vehicle charging stations," in *IEEE Trans. Transportation Electrification,* vol. *5, no*. 1, pp . *226–238* Nov, 2019, DOI. 10.1109/TTE.2019.2897087.

[3] X. Zhao, X. Zhao, Q. Yu, Y. Ye, and M. Yu, "Development of a representative urban driving cycle construction methodology for electric vehicles: A case study in Xi'an," in *IEEE Trans. Transport. Res. Part D: Transport and Environment,* vol. *81,* Apr, 2020, DOI. 10.1016/j.trd.2020.102279.

[4] M.P. Anand, B. Bagen, and A. Rajapakse, "Probabilistic reliability evaluation of distribution systems considering the spatial and temporal distribution of electric vehicles," in *Int. J. Elec. Pow. Ene. Sys,* vol. *117,* May, 2020, DOI. 10.1016/j.ijepes.2019.105609.

[5] S.R. Gampa, K. Jasthi, P. Goli, D. Das, and R.C. bansal, "Grasshopper optimization algorithm based two stage fuzzy multiobjective approach for optimum sizing and placement of distributed generations, shunt capacitors and electric vehicle charging stations," in *J. Ene. Storage,* vol. *27,* Feb, 2020, DOI. 10.1016/j.est.2019.101117.

[6] Y. Zhang, Q. Zhang, A. Farnoosh, S. Chen, and Y. Li, "GIS-Based Multi-Objective Particle Swarm Optimization of charging stations for electric vehicles," in *Energy,* vol. *169,* pp . *844–853* Feb, 2019, DOI. 0.1016/j.energy.2018.12.062.

[7] L. T. Al-Bahrani, B. Horan, M. Seyedmahmoudian, and A. Stojcevski, "Dynamic economic emission dispatch with load demand management for the load demand of electric vehicles during crest shaving and valley filling in smart cities environment," in *Energy,* vol. *195,* Mar, 2020, DOI. 0.1016/j.energy.2020.116946.

[8] C. Doppstadt. A. Koberstein, and D. Vigo, “The Hybrid Electric Vehicle—Traveling Salesman Problem with time windows," *European Journal of Operational Research,*” in *Energy,* vol. *253, no*. 3, pp . *675–692* 2020, DOI. 10.1016/j.ejor.2016.03.006.

[9] M.W. Tian, S.R. Yan, X.X. Tian, M. Kazemi, S. Nojavan, K. Jermsittiparsert, “Risk-involved stochastic scheduling of plug-in electric vehicles aggregator in day-ahead and reserve markets using downside risk constraints method," *Sustainable Cities and Society,*” vol. *55*, Apr, 2020, DOI. 10.1016/j.scs.2020.102051.

[10] MX. Lu, Y. Wu, Y. Zhang, C.Chen, P. Wang, and L. Meng, “Energy management of hybrid electric vehicles: A review of energy optimization of fuel cell hybrid power system based on genetic algorithm," *Energy Conversion and Management,*” vol. *205*, Feb, 2020, DOI. 10.1016/j.enconman.2020.112474.

[11] H.X. Liu and D.Z.W. Wang “Analysis of greenhouse gas emissions from electric vehicle considering electric energy structure, climate and power economy of ev: A China case," *Atmospheric Pollution Research,*” vol. *11, no.*, 6, pp . *1–11* Jun, 2020, DOI. 10.1016/j.apr.2020.02.019.

[12] J. Li and B. yang, “Locating multiple types of charging facilities for battery electric vehicles," *Trans. Research: Part B,*” vol. *103,* pp . *30–55* Sep, 2017, DOI. 10.1016/j.trb.2017.01.005.

[13] M. E. Kabir, C. Assi, H. Alameddine, J. Antoun, and J. Yan, “Demand Aware Deployment and Expansion Method for an Electric Vehicles Fast Charging Network,” in *IEEE Int. Conf. Smart Grid Communication,* 2019, DOI. 10.1109/SmartGridComm.2019.8909746.

[14] H. Parastvand, Z. Moghaddam, O. Bass, M.A.S. Masoum, A. Chapman, S. Lachowicz, “A Graph Automorphic Approach for Placement and Sizing of Charging Stations in EV Network Considering Traffic,” in *IEEE Trans. Smart Grid, Early Access,* Apr, 2020, DOI. 10.1109/TSG.2020.2984037.

[15] B. R. Barmish,, “New tools for robustness of linear systems,” in *Macmillan Coll Div; 1st Edition edition,* 1993, ISBN-13: 978-0023060557.

[16] H. Parastvand and M.J. khosrowjerdi, “Parameterised controller synthesis for SISO-LTI uncertain plants using frequency domain information," in *In. J. Sys. Sci,* vol. *47, no.*, 1, pp . *32–44* 2016, DOI. 10.1080/00207721.2015.1022026.

[17] G. Agnarsson, R. Greenlaw, “Graph Theory: Modeling, Applications, and Algorithms ," *Atmospheric Pollution Research,*” *1st Edition, Pearson,* 2006, ISBN-13: 978-0131423848.

[18] https://www.tesla.com/en_AU/findus, Available online May 2020.

[19] Energeia, "Australian Electric Vehicle Market Study," Prepared by ENERGEIA for ARENA and CEFC, 2018.

[20] C. Ocampo-Martinez, S. Bovo, and V. Puig, "Partitioning approach oriented to the decentralised predictive control of large-scale systems," in *J. Process Contro,* vol. *21, no.*, 5, pp . *775–786* Jun, 2011, DOI. 10.1016/j.jprocont.2010.12.005.

[21] Y. Yang and G. Xie, "Mining maximum matchings of controllability of directed networks based on in-degree priority," 2016 35th Chinese Control Conference (CCC), Chengdu, pp . *1263-126* 2016, DOI. 10.1109/ChiCC.2016.7553261.

[22] Y. Liu, J.J. Slotine, and A.L. Barabasi, "Controllability of complex networks," in *Nature,* vol. *437*, pp . *167–173,* May, 2011.

Chapter 7

Graph Theoretic Sitting and Robust Sizing of EV Charging Stations from a Novel Control Framework

7.1 Overview

This study addresses the problems of sitting and sizing of charging stations (CSs) by implementing some tools from graph and control theories which facilitates attaining the solutions that, unlike optimization approaches, are analytically supported. First, the problem of CS placement is investigated using centrality and k-means clustering and then the results are compared with two other control theoretic methods known as Exact Controllability Method (ECM) and Maximum Matching Principle (MMP). The results are compared in terms of their impact on reducing the waiting time at CSs. The set of CSs with best results, attained from MMP, is then used in a transformed CS sizing problem to find the optimal sizes of each CS in a novel control theoretic framework. The CS sizing problem is transformed into a robust control problem where the size of each CS is attained from a modified DK-iteration approach. The simulation results on the EV network of Perth metropolitan area in Australia verifies the impacts of the proposed approach in reducing the waiting time and optimal sizing of CSs[1].

Chapter 7 is not available in tis version of the thesis

Chapter 8

Placement and Sizing of EV Charging Stations According to Centrality of the Underlying Network

Overview EV placement and sizing are the subject of ever increasing studies in the last decade mostly relying on optimization approaches. This study looks at the EV network as a complex network where the nodes are the potential locations of charging stations (CSs) and edges (links) represent the traffic flow. It then investigates the impacts of some graph properties on the solutions of the CS placement problem. In fact, the graph centrality and its variants are used to find the locations of CSs to reduce the average waiting times at the stations. It is shown that the centrality based analysis can lead to promising results for small and medium EV networks leaving the large networks to be addressed by more complicated approaches. Simulations are performed on the central (downtown) part of Perth City EV network, Western Australia scaled down by the real traffic information[1].

Chapter 8 is not available in tis version of the thesis

Chapter 9

Summary and Future Works

9.1 Summary of the thesis findings

This thesis has succeeded to develop new theories based on control and graph theories to address important questions regarding the controllability and robustness of complex networks. Power networks, smart grids, and EV network of charging stations has been used to implement the proposed approaches. Although the main theoretical development was around the concept of graph symmetry other graph and control theoretic properties such as graph centrality, clustering, and controlled invariant property is also adapted to address the targeted applications of this study. The contribution of the thesis can be summarized as

- Proposing novel necessary conditions for CN controllability based on graph symmetry which are computationally more effective than previous method.
- Proposing a novel index of symmetry is proposed upon which a more meaningful understanding of symmetry impact on CN controllability can be comprehended.
- Proposing a modification strategy aiming to satisfy CN controllability with a lower number of driver nodes with a reasonable computational complexity.
- Identifying the critical components of complex networks in terms of their impact on the number of required driver nodes.
- Proposing novel necessary conditions for network robust controllability.
- Proposing new necessary and sufficient conditions for disturbance decoupling using a symmetry related concept called determining set and a geometric control property called controlled invariant.
- Identifying the role of nodes with more multiplicity in the set of symmetry group on the network robustness.

- Identifying the impact of elimination of critical network elements on its robustness by calculating a new improved index of symmetry which considers the orbital impacts of automorphisms.
- Optimal placement of flexible AC transmission systems (FACTS) devices using a novel graph theoretic perspective, which unlike the existing approaches, purely relies on topological characteristics of the underlying physical graphs of power networks.
- Establishing the idea of moderated-k-symmetry to address the cyber-security of the most critical data related to the FACTS controllers.
- Demonstrating the similarity between the set of critical nodes attained from the symmetry analysis and the solution of the FACTS devices placement that further highlights the importance of symmetry for the analysis and design of complex power networks.
- Proposing a novel framework for modeling the network of CSs as a graph of the underlying network which facilitates implementing fundamental notions of control and graph theories.
- Novel solutions for CS placement and sizing via transforming them into a control framework which facilitates implementing various robust and optimal control theories and lead to reducing the waiting times at CSs and optimal sizing of CSs.
- Highlighting the role of symmetry in the number and positions of CSs.
- Extending the capacity of existing networks of electric vehicles (EVs) by placement of additional charging stations (CSs) as well as determining the sizes of existing and new CSs in order to handle future expansions of EVs.
- Proposing a strategy for the deployment of portable charging stations (PCSs) in selected areas to further improve the quality of solutions by reducing the overshooting of waiting times during peak traffic hours.
- Investigating the problem of CS placement using centrality and k-means clustering and then comparing the results with two other control theoretic methods known as Exact Controllability Method (ECM) and Maximum Matching Principle (MMP). The results are compared in terms of their impact on reducing the waiting time at CSs.

9.2 Conclusion and Future Works

This study has revealed some significant aspects of symmetry impact on emergent behaviour of complex networks which highlights the necessity of conducting more research in this direction. These include the following results:

- Clarifying the impacts of graph symmetry in the controllability of complex power networks;
- Establishing a theoretical framework for the relation between the number of required driver nodes for controllability and the network's symmetry level;
- Revealing the role of graph symmetry in improving the network robustness against disturbance;
- Using graph symmetry in improving the network cyber security via the concept of "security by obscurity";
- Implementing the findings of the thesis on graph of EV charging stations and reducing the waiting times;
- Placement and sizing of EV charging stations using the symmetry implications for the network

In this section, potential avenues for delving into symmetry is summarized.

9.2.1 Restoration: the impact of post-fault topology

Any fault in power lines should be treated by detection, isolation, and restoration, respectively. The first two tasks could be performed using over-current relays and reclosers. The last step, restoration, is for re-configuring the system to a post-fault topology. Finding an optimal topology after a fault occurrence is a decision making problem under constraints such as the power balance and line limits. The restoration comprises two steps. First, the optimal post-fault grid topology should be determined. This new topology is subjected to some constraints like power balance and line limits. In the second step, a switching sequence after obtaining the post-fault topology must be determined ([1]). In [2], a graph-based load restoration after natural disasters is proposed which relies on sectionalizing the switches to exploit improved electricity supply continuity. Using master-slave control method integrated in the optimization problem multiple DGs are coordinated in one microgrid. The proposed approach has shown better results on both the IEEE 33-bus and the modified 615-bus test systems. Different restoration approaches have been implemented in literature for complex power networks. For example, see [3], [4], [5], and [1], [6].

In [1], a multi agent system is proposed for an efficient and fast switching operation of an electric power distribution network to isolate fault, restore power to the de-energized area, and secure critical loads. The fast topology reconfiguration of the proposed approach leads to high reliability and resiliency of the local distribution network. The automatic restoration of a power system is realized in [6] by embedding a multi agent system in a hardware on a Java platform. The paper mostly considers the communication issues while determining a post-fault topology. In [5], a multi agent system is proposed for power system management and restoration. The bus

agents have been used to control each bus, while the coordination agents manage the behavior of bus agents. The changeable multi agent system could be modified according to power system status. A multi agent system consisting of several substation agents and line agents has been considered in [4] to analyze the power grid restoration. It is shown that implementing one of the substation agents as the management agent to control the restoration process will lead to promising results on restoring the de-energized area using the local information only. A mixed integer second order cone programming is implemented in [3] to reduce the complexity of the optimization while the optimal solution is also guaranteed. The experimental setup consists of a microgrid with several DGs. The formulation and reconfiguration of microgrid have been synthesized by sectionalizing the switches to attain better flexibility. Two restoration strategies for islanded-like power systems of a navy ship board has been implemented in [7]. The fault location is identified by the power electronic blocks, and then it is isolated from the rest of network.

Though all of these papers consider the restoration problem for a complex power grid, none of them has examined the grid restoration for a symmetric or asymmetric system. If a fault happens in a highly symmetric or highly asymmetric systems, the post-fault topology might not represent the same characteristics in terms of controllability, robustness, etc. As a result, all the features induced by symmetry or asymmetry might not be maintained. In this study, the effect of line failure on graph symmetry will be assessed. Line failure could change the number of graph automorphisms in the network rendering a different symmetry level which can cause different level of controllability, and robustness. Hence, a new constraint should be added to the optimization problem of restoration upon which a certain level of symmetry associated to fault-free topology should be maintained for post-fault topology.

9.2.2 The impact of symmetry on power grid restoration

There are many papers considering the restoration of a power grid using a multi agent framework (for example see [3], [4], [5], and [1], and [6]). However, none of existing approaches deals with the symmetry characteristic of the power network. A fault occurrence in a symmetric system gives raise to some question about the post-fault topology. As mentioned earlier, the symmetry induces some feature to the network that might vanish after a fault occurrence or as a result of post-fault topology. Hence, here the lack of analysis of the power network restoration under the constraints like keeping the symmetry (or asymmetry) or maintaining a certain level of symmetry in the network could be realized. Also, the critical lines and units, in terms of their effectiveness strength on the structural symmetry, could be identified using graph automorphisms upon which a more reliable protection strategy can be determined.

9.2.3 The impact of symmetry on energy cost of control

The controllability of complex networks has been investigated in the context of structural controllability using the maximum matching principle and the minimum dominant set. Through

these two approaches, the number of driver nodes leading to realize fully control of the network could be attained. The energy cost of control is highly affected by the number of required control nodes.

In the mathematical discipline of graph theory, a matching or independent edge set in a graph is a set of edges without common vertices. The unmatched nodes could be considered as the driver nodes and the number of unmatched nodes could be considered as the system's controllability. Using maximum matching method one can calculate the minimum number of required driver nodes to control the network, providing a benchmark to test the structural controllability of complex networks ([8]). It is shown that the minimum number of driver nodes could be computed by the degree distribution of the network ([9]). Plus, the driver nodes tend to deviate from high-degree nodes ([8]). Based on maximum matching, some studies have been conducted implementing control centrality ([10]), exact controllability ([11]), and target control ([15]).

The minimum dominating set (MDS) is another tool that has been used to test the controllability of complex networks ([12] and [13]). It is shown that the system is controllable if the driver nodes are selected from the nodes in the MDS. In [9], the MDS based model is extended to the identification of the crucial structure in the control of the network from a microcosmic perspective. A new framework is developed which defines a graph from a low to a high level of abstraction. It is concluded that each non-driver node is controllable if it is at least adjacent to a meta-structure, and all the nodes in a meta-structure are obliged to be driver nodes. One expectation of the symmetry analysis is to attain a modification strategy for the microgrid topology so that the modified network will need a lower number of driver nodes compared to the number of driver nodes obtained from maximum matching or MDS.

However, those techniques could not consider the cost effectiveness of the required control signals. Although, they can theoretically realize a framework to steer the networked system from any initial state to any final state in a given time, the energy consumption via the control signals is likely too large to be affordable ([14]). On the other hand, symmetry analysis can provide a framework to modify the network so that the post-topology guarantees an improved level of controllability. This motivates elaborating the existing structural controllability criteria by integrating them with a modification step exploited from the symmetry analysis.

9.2.4 Other impacts of symmetry

It is desirable to estimate some of the dynamic states of the system instead of measuring them directly. Kalman filter is the main tool for state estimation. One of the conditions to attain the desired performance from Kalman filter is that the underlying system be uncontrollable from the noisy inputs. This justifies breaking the symmetry in the system by manipulating the control input matrix in order to have an asymmetric graph which is resistant to noise inputs (robust system). This, in turn, gives raise to another conflict between robustness and satisfying the state estimation purpose.

Two drawbacks in most of current papers are that they consider the network as a determin-

istic system with similar agents while the real world systems are stochastic systems with non-identical nodes and edges. This makes room for modifying symmetry concept based on nodes performance, meaning a generating node with $10GW$ generation index can supply a bunch of load nodes with overall demand of $10GW$. In such case, there is no structural symmetry but there is symmetry in terms of each partition performance.

For CN-based control applications, a survey on swarm behaviour might draw a guideline on modelling the network behaviour. Swarm modelling has been categorized into two levels. The first level corresponds to modelling based on the dynamics of individual agents and interaction among them, the microscopic level. However, the higher level of swarm abstraction, macroscopic level, is usually more helpful since it entails the key properties of the entire swarm. Applying control approaches on macroscopic models allows for decreasing computation burden in cost of imposing more conflict of interests between agents and losing some details on swarm behaviors. Developing both levels of abstraction for swarm is an ongoing challenge for researchers.

Bibliography

9.3 References

[1] W. Khampanchai, M. Pipattanasomporn, and S. Rahman, "A Multi-Agent System for Restoration of an Electric Power Distribution Network with Local Generation," Power and Energy Society General Meeting, 2012 IEEE, 2012.

[2] T. Ding, Y. Lin, Z. Bie, and C. Chenu, "A resilient microgrid formation strategy for load restoration considering master-slave distributed generators and topology reconfiguration," *Applied Energy*, vol. 199, 2017.

[3] T. Ding, Y. Lin, Z. Bie, and C. Chen, "A resilient microgrid formation strategy for load restoration considering master-slave distributed generators and topology reconfiguration," *Applied Energy*, vol. 199, 2017.

[4] S. Fukunagaa and T. Nagata, "A Decentralized Power System Restoration by means of Multi-agent Approach," *Energy Procedia*, vol. 14, 2012.

[5] F. Ren, M. Zhang, D. Soetanto, and X. D. Su, "Conceptual Design of A Multi-Agent System for Interconnected Power Systems Restoration," *IEEE TRANSACTIONS ON POWER SYSTEMS*, vol. 27, 2012.

[6] R. Sampaio, L. Silveira-Melo, R. P. S. Leao, G. C. Barroso, and J. R. Bezerra, "Automatic restoration system for power distribution networks based on multi-agent systems," *IET Generation, Transmission & Distribution*, vol. 11, 2017.

[7] C. L. Su, C. K. Lan, T. C. Chou, and C. J. Chen , "Performance Evaluation of Multiagent Systems for Navy Shipboard Power System Restoration," *IEEE TRANSACTIONS ON INDUSTRY APPLICATIONS*, vol. 51, 2015.

[8] Y. Liu, J.J. Slotine, and A.L. Barabasi, “Controllability of complex networks,” in *Nature,* vol. *437*, pp . *167–173,* May, 2011.

[9] P. G. Sun and X. Mu, "Understanding the controllability of complex networks from the microcosmic to the macrocosmic," *New Journal of Physics*, vol. 19, 2017.

[10] Y. Y. Liu, J. J. Slotine, A. L. Barabasi, "Control centrality and hierarchical structure in complex networks," *PLoS ONE 7*, 2012.

[11] Z. Yuan and C. Zhao, Z. Di, W. X. Wang, and Y. C. Lai, "Exact controllability of complex networks," *Nature: Communincation*, vol. 4, no.2447, Sep. 2013, DOI: 10.1038/ncomms3447.

[12] J. C. Nacher and T. Akustu, "Analysis of critical and redundant nodes in controlling directed and undirected complex networks using dominating sets," *Journal of Complex Networks*, vol. 2, pp. 394-412, 2014.

[13] J. C. Nacher and T. Akustu, "Structurally robust control of complex networks," *Physical Review E*, vol. 91, no. 2015.

[14] L. Z. Wang, Y. Z. Chen, W. X. Wang and Y. C. Lai, "Physical controllability of complex networks," *Nature, Scientific Reports*, 2017.

[15] J. Gao, Y. Y. Liu, R. M. D'Souza, A. L. Barabasi, "Target control of complex networks," *Nature Communication*, vol. 5, no. 2014.

Bibliography

[1] L. Z. Wang, Y. Z. Chen, W. X. Wang, and Y. C. Lai, "Physical controllability of complex networks," *Nature, Scientific Reports*, vol. 7, no. 40198, 2017.

[2] J. Sun and A. E. Mptter, "Controllability transition and non-locality in network control," *Phys. Rev. Lett.*, vol. 110, 2013.

[3] R. Gutierez, I. Sendina-Nadal, M. Zanin, D. Papo, and S. Boccaletti, "Targeting the dynamics of complex networks," *Sci. Rep.*, vol. 12, 2012.

[4] R. Gutierez, I. Sendina-Nadal, M. Zanin, D. Papo, and S. Boccaletti, "Targeting the dynamics of complex networks," *Sci. Rep.*, vol. 12, 2012.

[5] L. Z. Wang, Y. Z. Chen, W. X. Wang, and Y. C. Lai, "Physical controllability of complex networks," *Nature, Scientific Reports*, vol. 7, no. 40198, 2017.

[6] A. Rahmani and Mesbahi, "On the Controlled Agreement Problem,"Proceedings of the 2006 American Control Conference Minneapolis, Minnesota, USA, June 14-16, 2006.

[7] Q. Li, C. Peng, M. Chen, F. Chen, W. Kang, J. M. Guerrero, and D. Abbott, "Networked and Distributed control Method With Optimal Power Dispatch for Islanded Microgrids," *IEEE TRANSACTIONS ON INDUSTRIAL ELECTRONICS*, vol. 64, 2017.

[8] J. Lai, X. Lu, W. Yao, J. Wen, and S. Cheng, "Robust distributed cooperative control for DC mircogrids with time delays, noise disturbances, and switching topologies," *Journal of the Franklin Institute*, vol. 354, 2017.

[9] Z. Feng and G. Hu, "Distributed Tracking Control for Multi-Agent Systems Under Two Types of Attacks," Proceedings of the 19th World Congress The International Federation of Automatic Control Cape Town, South Africa. August 24-29, 2014.

[10] J. M. G. de Durana, O. Barambones, E. Kremers, and L. Varga , "Agent based modeling of energy networks," *Energy Conversion and Management*, vol. 82, 2014.